



<https://theses.gla.ac.uk/>

Theses Digitisation:

<https://www.gla.ac.uk/myglasgow/research/enlighten/theses/digitisation/>

This is a digitised version of the original print thesis.

Copyright and moral rights for this work are retained by the author

A copy can be downloaded for personal non-commercial research or study,
without prior permission or charge

This work cannot be reproduced or quoted extensively from without first
obtaining permission in writing from the author

The content must not be changed in any way or sold commercially in any
format or medium without the formal permission of the author

When referring to this work, full bibliographic details including the author,
title, awarding institution and date of the thesis must be given

Enlighten: Theses

<https://theses.gla.ac.uk/>
research-enlighten@glasgow.ac.uk

**AN ULTRASTRUCTURAL AND ELECTRON PROBE X-RAY
MICROANALYTICAL STUDY OF SWEAT GLAND FUNCTION.**

by

Scott Alexander McWilliams B.Sc.

A Thesis submitted to the University of Glasgow for the Degree of
Doctor of Philosophy

Institute of Physiology
Glasgow University
November 1986

ProQuest Number: 10995542

All rights reserved

INFORMATION TO ALL USERS

The quality of this reproduction is dependent upon the quality of the copy submitted.

In the unlikely event that the author did not send a complete manuscript and there are missing pages, these will be noted. Also, if material had to be removed, a note will indicate the deletion.



ProQuest 10995542

Published by ProQuest LLC (2018). Copyright of the Dissertation is held by the Author.

All rights reserved.

This work is protected against unauthorized copying under Title 17, United States Code
Microform Edition © ProQuest LLC.

ProQuest LLC.
789 East Eisenhower Parkway
P.O. Box 1346
Ann Arbor, MI 48106 – 1346

"If you are sure you understand everything that is going on, you are hopelessly confused".

Walter Mondale.

CONTENTS

	Page
SUMMARY	1
ACKNOWLEDGEMENTS	iii
CHAPTER 1 SWEAT GLANDS.	1
CHAPTER 2 ULTRASTRUCTURE OF THE RAT FOOTPAD SWEAT GLAND BEFORE AND AFTER PILOCARPINE STIMULATION.	13
CHAPTER 3 SPECIMEN PREPARATION AND THE PHYSICAL BASIS OF ELECTRON PROBE X-RAY MICROANALYSIS (EPXMA).	31
CHAPTER 4 DEVELOPMENT OF A CRYOULTRAMICROTOME.	60
CHAPTER 5 EPXMA OF THE INTRACELLULAR ELEMENTS IN THE RAT FOOTPAD SWEAT GLAND BEFORE AND AFTER PILOCARPINE STIMULATION.	81
CHAPTER 6 EPXMA OF THE INTRACELLULAR ELEMENTS IN THE HUMAN AND HORSE SWEAT GLANDS BEFORE AND AFTER THERMAL STIMULATION.	91
CHAPTER 7 GENERAL DISCUSSION.	104
CHAPTER 8 MECHANISM OF ACTION OF ALUMINIUM-CONTAINING ANTIPERSPIRANTS.	111
REFERENCES	130
APPENDICES	157
LIST OF PUBLICATIONS	178

SUMMARY

This thesis was undertaken to determine the ultrastructure of the rat footpad sweat gland before and after pilocarpine stimulation and to assess whether it undergoes the same morphological changes on activation as have been described for other species. A second objective was to measure, by electron probe X-ray microanalysis (EPXMA), the intracellular concentrations of K, Na and Cl in the human and rat atrichial and the horse epitrichial sweat glands before and after stimulation. The final objective was to determine the site and possible mechanism of action of aluminium-containing antiperspirants in the human sweat gland by comparing the ultrastructural and elemental changes before and after a course of antiperspirant treatment.

The ultrastructural changes in the rat footpad sweat gland after pilocarpine stimulation included narrowing of the lumen, dilatation of the intercellular spaces, contraction of the myoepithelial cells, exocytosis and the loss of cytoplasmic material from the secretory cells. In general, these changes are qualitatively the same as have been reported in other species after thermal stimulation and it was concluded that the rat gland conforms to the model suggested by Montgomery *et al* (1985).

Although a successful method was developed for cutting ultrathin cryosections of biological material this was found to be unsuitable for the EPXMA study of sweat glands in skin samples. Using a method of bulk freeze-drying and resin embedding the results from the glands of the three species studied by EPXMA are shown below in mM/kg total dry weight of specimen analysed i.e. biological tissue and embedding medium.

In man and horse stimulation was produced by thermal stress and the samples were obtained by high speed biopsy punch. For the rat the samples were obtained by autopsy after pilocarpine stimulation.

Fundus	Na	Resting			Na	Active		
		K	Cl	n		K	Cl	
Human	n=11	151	159	110	n=8	229*	112*	114
Horse	n=3	151	198	71	n=4	238*	167*	102*
Rat	n=4	49	211	44	n=4	117*	130*	38

Duct	Na	K	Cl	n	Na	K	Cl	
								Human
Horse	n=4	204	145	66	n=4	290*	87*	107 *

* significantly different from the control value.

These results, the first of their kind from sweat glands stimulated *in vivo*, indicate that in the fundus the changes on activation are, in general, similar. There is a decrease in intracellular K, an increase in intracellular Na and little, if any, change in Cl. With reference to the fluid secreted by the fundus of each species two models are presented to explain these findings. In the duct the data are consistent with its known lack of function in both the horse and human.

Pretreatment with aluminium-containing antiperspirants had no effect on the ultrastructural changes which occur after stimulation in the human sweat gland duct and fundus. Although aluminium was not detected in the fundus the normal intracellular elemental changes after stimulation were not seen in treated glands. Taken together with the finding of aluminium-containing obstructions within the upper duct a dual mechanism of action of such compounds is proposed, namely ductal obstruction, most likely in the upper stratum corneum, and interference with the secretory function of the fundus.

ACKNOWLEDGEMENTS

To acknowledge the help and encouragement of colleagues and friends must be one of the more pleasant aspects of any thesis. I would, therefore, like to particularly thank Drs. Hugh Y. Elder and David McEwan Jenkinson for their supervision and suggestions throughout the duration of this project. I would also like to take this opportunity to offer my thanks to Prof. O. F. Hutter for allowing me to use the research facilities of the Institute of Physiology and to Beecham Products, Weybridge for financial support. The advice, and aid with statistical analysis, of Dr. Stuart Wilson are gratefully acknowledged. I am indebted to Mr. W. H. Biddlecombe for his patient guidance in the use of the electron microscope, without which this project would have been considerably more difficult. It is also a pleasure to acknowledge the expert technical assistance of Messrs. I. Montgomery, J. Pediani and C. Loney. My thanks must also go to Dr. Anne Sutton for performing the human biopsies and to the numerous volunteers who willingly gave their time and skin for the advancement of science. Finally, I would like to thank Pauline, my family and friends for their unstinting support over the years.

CHAPTER 1 SWEAT GLANDS.

1.1. INTRODUCTION

1.1.1. Control of Sweating

1.2. ULTRASTRUCTURE

1.2.1. The Human/Primate Sweat Glands

1.2.1.a. Fundus

1.2.1.b. Duct

1.2.2. Enzyme Distribution

1.3. ISOLATED GLANDS

1.4. OBJECTIVES

1.1. INTRODUCTION

Sweat glands are among the smallest mammalian exocrine glands, typically for man averaging 6–8 mm in length and 40–50 μm in diameter (Quinton, 1981). The glands are divided into two broad groups based on whether they are associated with a hair follicle (epitrichial) or not (atrichial) (Bligh, 1967; Jenkinson, 1973; Montgomery *et al.* 1984). The sweat glands on the general body surface of man and those of the footpads of rodents, cats and dogs are examples of the latter, and are often referred to in the literature as eccrine, whilst the sweat glands of most other mammals are epitrichial, often called apocrine in the literature (Jenkinson, 1973). In man the estimated number of sweat glands ranges between 1.6–4 million (Weiner & Hellman, 1960; Thaysen, 1978; Quinton, 1981) distributed unevenly over the body surface. The highest densities are found on the palms and soles (upto $2000/\text{cm}^2$, Weiner & Hellman, 1960) and the density becomes progressively lower on the forehead, cheeks, trunk and extremities ($100\text{--}200/\text{cm}^2$ on the limbs, Weiner & Hellman, 1960; Quinton, 1981) with minor individual, sexual and racial differences (Thaysen, 1978).

The function of these glands varies from species to species and also with body location. Sweat glands may be considered, in general, as protective organs: i) against thermal extremes, although a thermoregulatory role seems to be important only in man, equidae and the ungulates (Jenkinson, 1973); ii) against frictional damage in the eyelids and palms; iii) as excretory routes; iv) by exerting an antibacterial effect, either directly or by aiding the flow of sebum across the skin surface; v) against extinction of species by acting as scent organs (Jenkinson, 1973). Weiner & Hellman (1960) suggest that palmar and footpad glands increase the tactile sensitivity in these regions. In all species the glands are composed of a secretory portion (fundus), which may be sac-like, serpentine or coiled, and a relatively straight duct. The fundus is composed of a single inner layer of secretory cells supported by an outer network of myoepithelial cells and is located in the deep dermis of the skin. From the limited information currently available it seems to produce, in most instances, an isotonic plasma-like fluid and this secretory epithelium is thought to be comparable to “leaky” epithelia

such as frog skin and urinary bladder (Sato, 1982) which also produce isotonic secretions and are known to be very permeable to fluid movement (Fromter & Diamond, 1972). This initial sweat is "propelled" by hydrostatic pressure from the fundus to the duct and eventually to the skin surface. The myoepithelium does not actively expel the fluid from the fundus by contraction but is most likely involved in providing structural support to the secretory epithelium to allow the development of a high hydrostatic pressure (Sato, Nishiyama & Kobayashi, 1979). With the exception of the cat (Munger & Brusilow, 1961) and rat (Sato, 1977) footpad glands, modification of this primary fluid occurs in the duct (Slegers, 1963; Schulz, 1969) which is composed of a variable number of cell layers. The duct is thought to behave like a "tight" epithelium (Quinton, 1981) and absorbs ions in excess of water to produce a final sweat composition which varies from species to species (Table 1.1).

1.1.1 Control of Sweating

There is considerable contradictory evidence concerning the neural control of sweat glands (Vaalasti, Tainio & Rechartd, 1985) and in most species the glands are not directly innervated (Jenkinson, 1973); only those in man, some primates, the horse and the footpads of dog, cat and rodents have closely associated nerves. Although originating in the sympathetic chain these nerves are cholinergic in nature (Dale & Feldberg, 1934) and act through muscarinic receptors. Specific cholinesterases have been demonstrated histochemically in nerve endings around the secretory coil (Hurley, Shelley & Koelle, 1957; Hashimoto, Ogawa & Lever, 1962) and also possibly the coiled duct but not the straight duct (Thaysen, 1978) and the stimulatory effects of cholinergic and parasympathomimetic agents on sweating are well known (Schwartz & Thaysen, 1956; Foster & Weiner, 1970; Sato, 1977). An additional feature of these cholinergic nerve endings is the presence of vasoactive intestinal polypeptide (VIP)-like immunoreactivity which has been demonstrated in human sweat glands (Vaalasti *et al.* 1985) cat (Lundberg *et al.* 1982) and rat (Landis, 1983) footpad sweat glands. It appears that VIP and acetylcholine (ACh) coexist in the nerve terminals, although the function of the former remains unclear. The possible roles of the VIP

include vasodilatation, direct stimulation of glandular activity (Vaalasti *et al.* 1985) or, as in the cat submandibular salivary gland, enhancement of the affinity of the muscarinic receptor to ACh (Lundberg, Hedlund & Bartfai, 1982). With the possible exception of the rat, it is also well known that sweat glands, including those of man (Chalmers & Keele, 1951; Foster, Ginsberg & Weiner, 1970) respond to intradermal or intra-arterial adrenaline (Sato, 1977), although the effect in intact human skin is only $1/5$ to $1/10$ of that observed for cholinergic stimulation (Sato, Burgers & Sato, 1973). This less sensitive response to adrenergic agents is thought to occur as a result of vasoconstriction and subsequent ischaemia of the gland (Sato *et al.* 1973) and this is supported by the finding that in isolated monkey palm sweat glands adrenaline produces 45% of the sweat output of pilocarpine (Sato & Sato, 1981a). Indeed, in some species, particularly the horse (Robertshaw & Taylor, 1969) and primates (Robertshaw, Taylor & Mazzia, 1973), circulating adrenaline, secreted from the adrenal medulla, can increase exercise, but not thermally, induced sweating by 50%. However, with the exception of the Macaque monkey (Uno & Montagna, 1975) and the human (Uno, 1977), catecholaminergic nerve fibres have not been observed close enough to exert a direct effect on glandular activity and are usually associated with adjacent blood vessels. This finding led Jenkinson, Montgomery & Elder (1978) to suggest that the effect of noradrenaline released from sympathetic nerve terminals is to increase the permeability of the blood vessels to circulating catecholamines or to release catecholamines from cellular stores which then diffuses to the sweat gland. They propose that this process is common to all species but that it is less important in those species where the nerves are in close proximity to the gland. The effects of cholinergic and adrenergic stimulation seem to be the same both in terms of ultrastructural changes and in composition of the final sweat (Sato *et al.* 1973).

1.2. ULTRASTRUCTURE

Study of the sweat glands from various species has long been recognised as essential for a full understanding of the general mechanism of sweating in mammals (Weiner & Hellman, 1960; Jenkinson, Montgomery

& Elder, 1979). Although the ultrastructure of unstimulated sweat glands from a variety of species is well documented it is only recently that the appearance of glands after stimulation has been described in detail: man (Montgomery *et al.* 1984; 1985), cow sheep and goat (Jenkinson *et al.* 1979; Montgomery, Jenkinson & Elder, 1982b), and horse (Montgomery, Jenkinson & Elder, 1982a). Two consistent findings emerged from these ultrastructural studies: firstly that there appears to be a common secretory mechanism involving i) secretion including fluid transport and exocytosis and ii) cell death and secondly that the original light microscopical classification of sweat glands as apocrine and eccrine (Schiefferdecker, 1917) is no longer valid. The classification used throughout this thesis is thus based on the anatomical association of the glands with a hair follicle i.e. epitrichial ("by the hair") or atrichial ("without hair") (Bligh, 1967; Montgomery *et al.* 1984).

1.2.1. The Human / Primate Atrichial Gland

These glands have been, and will continue to be, the most extensively studied among the sweat glands of the various species. To date they have been studied *in vivo* using thermal and pharmacological stimulation and *in vitro* using skin biopsies and isolated glands. The human atrichial sweat gland is composed of a fundus and a duct with two distinct regions: a coiled portion (proximal duct) and a straight portion (distal duct).

1.2.1.a Fundus

The fundus consists of a secretory and a myo-epithelium, surrounded by a fibrocyte sheath, as in all species. The secretory epithelium is composed of two morphologically distinct cell types, the granular and the more frequent non-granular, which correspond to the dark and light cells, respectively, of light microscopical studies (Montagna, Chase & Lobitz, 1953). The processes of granule production and secretion and of fluid transport appear to have been separated in human atrichial glands into two distinct cell types whilst in other species they are performed in one cell. The basolateral membranes of adjacent

non-granular cells form extensive interdigitations and intercellular canaliculi are often observed between them. The granular cells are shaped like "tops" which are broader at the lumen than the base and although the granules are distributed throughout the cytoplasm they are more concentrated towards the luminal surface. Granular cells also possess basolateral interdigitations although these are less pronounced than those between the non-granular cells. All secretory cells are joined to their neighbours at the apical surface by tight junctions which have been shown to prevent the passage of lanthanum from the intercellular space to the lumen in the cow, sheep, goat and horse (Jenkinson *et al.* 1983). After thermal stimulation the lumen initially decreases in size but after prolonged sweating it appears to dilate again. Prominent features of activity in the secretory epithelium are the dilatation of intercellular spaces, particularly between non-granular cells, and dilatation of the canaliculi. The cytoplasm of the non-granular cells contains less glycogen and cytoplasmic vesiculation is pronounced near the lumen and adjacent to the canaliculi. The granular cells exhibit granule accumulation at the luminal surface and granule loss occurs mainly by exocytosis, although a microapocrine process is involved in some species. Prolonged sweating causes a continuation of these processes and frequently results in secretory cell death. The myoepithelial cells are contracted during stimulation.

1.2.1.b Duct

The duct was often thought to be composed of two cell layers throughout its length (Ellis, 1962; Thaysen, 1978; Kurosumi, Shibasaki & Ito, 1984) but, whilst there may be regional variation, Montgomery *et al.* (1985) have shown clear evidence that in sweat glands from the human loin the number of cell layers decreases with increasing depth into the dermis, from approximately 8 cell layers in the epidermis and upper dermal duct to 2-3 layers in the coiled portion. Myoepithelial cells are not present in the duct although there is conflicting evidence concerning their presence in the short transition zone between the coiled duct and the fundus (Kurosumi *et al.* 1984; Montgomery *et al.* 1985). In the epidermal and upper dermal regions, which are thought unlikely to be

major sites of electrolyte or water reabsorption (Kurosumi, Kurosumi & Tosaka, 1982; Montgomery *et al.* 1985), the only signs of activity after thermal stimulation are i) a widening of the intercellular spaces, ii) increased cytoplasmic vesiculation and iii) the presence of much more particulate material in a narrower lumen. The function and direction of movement of the cytoplasmic vesicles is not clear since signs commensurate with both exocytosis and pinocytosis are seen. The most marked changes in morphology after sweating are seen in the coiled duct which is composed of a single layer of columnar luminal cells and two layers of flattened basal cells. After stimulation the apical membranes of the luminal cells exhibit varying degrees of extension which, in some instances, is so extreme as to fill the luminal space. Montgomery *et al.* (1985) believed that this extension is caused by the filtering of cell fluid through a well-developed terminal web which exists in these cells and they concluded, on the basis of the presence of similar membranous configurations in the luminal contents of the duct, that the coiled duct may be involved in secretory as well as reabsorptive processes.

1.2.2. Enzyme Distribution

Attempts have been made to determine the enzymatic basis for the secretory and reabsorptive mechanisms in the sweat gland, since the location of the sites of active transport are a prime concern to any theory on fluid transport (Quinton & Tormey, 1976). To date these studies have centred on the activity of Na/K ATPase. This enzyme has been located over the basolateral surface of both the reabsorptive and secretory portions of the human atrichial gland but not on the luminal membrane or next to canaliculi (Quinton & Tormey, 1976). This distribution is similar to that seen in other epithelia (Poulsen, Bundgaard & Møller, 1975; Bundgaard, Møller & Poulsen, 1979). For the reabsorptive duct this led Quinton & Tormey (1976), Sato (1977) and Quinton (1981) to postulate that sodium reabsorption occurred by "classical" means (Ussing, Erlj & Lassen, 1974) with passive entry across the luminal membrane by an amiloride sensitive (Quinton, 1981) sodium specific conductance channel (Welsh, Smith & Frizzell, 1982). According to this theory the sodium is then actively expelled across the basal membrane by Na/K ATPase. The

situation in the fundus is more complicated since Na/K ATPase has the same basolateral location as in the duct yet sodium transport is in the opposite direction. Quinton & Tormey (1976) postulated that in the secretory epithelium Na/K ATPase is not directly involved in the active transport step but is important in maintaining electrochemical gradients and metabolic requirements which may become stressed during activity. A similar theory was proposed by Welsh *et al.* (1982) who suggested that changes in Na/K ATPase activity are associated with parallel changes in basolateral permeability so that "several fold" alterations in the rate of transepithelial transport do not lead to marked alterations in cell composition. Silva *et al.* (1977), in their model for active chloride transport by shark rectal gland, suggested that the basolateral Na/K ATPase acts to maintain a sodium gradient (out-in) which is needed for the co-transport of chloride. It is this indirect role that seems to be the function of basolateral Na/K ATPase in secretory epithelia. Sato & Dobson, (1970) and Sato, Dobson & Mali, (1971) measured the total amounts of Na/K ATPase in the three regions of the gland: duct, coiled duct and fundus. They found that the levels were virtually the same in the coiled duct and fundus, although the fundus had a greater total amount by virtue of its larger size. The straight duct, however, had only $1/10$ the level of the other zones and this suggests that the distal duct does not have a major role in active transport.

1.3. ISOLATED GLANDS

Despite the simplicity of structure the sweat gland has not been extensively studied. This is due to the inherent difficulties associated with its small size (Quinton, 1981; Sato, 1982) and the difficulties in accurately assessing the periglandular environment *in vivo* (Sato, 1973; Sato, 1977). Following the earlier cryoscopic technique of Slegers (1963) and the micropuncture work of Schulz (1969), Sato (1973) developed a technique for isolating glands which has been primarily responsible for increasing the knowledge of sweating at the glandular level (Sato, 1973; Sato, 1977; Sato & Sato, 1981a, b & c; Sato & Sato, 1983; Sato & Sato, 1984; Quinton & Tormey, 1976; Quinton, 1981) and this has been further developed by Lee, Jones & Kealey (1984). These studies have done much to

improve our understanding of sweat gland function and should, in the future, help to narrow the gap between our knowledge of sweat gland physiology when compared with other exocrine organs.

In the isolated gland, Sato & Sato (1981a) found that sweating occurred in response to cholinergic (muscarinic), α and β adrenergic agents acting through separate receptors characterised by the effectiveness of the appropriate antagonists. The order in decreasing stimulatory effect is ACh > β > α . In their subsequent papers they attempted to determine the subcellular intermediates between receptor occupation and secretion. The α adrenergic and the cholinergic mechanism have an absolute dependence on extracellular calcium (a situation which is similar to that found in the rat parotid gland; Schramm & Selinger, 1975) but, although there is a gradual decline, secretion stimulated by β receptor mechanisms is considerably resistant to the removal of extracellular calcium. Stimulation via the β receptor causes a rise in cAMP levels and there is strong evidence that the elevated cAMP acts as a second messenger (Sato & Sato, 1981b). An elevated cAMP level after β stimulation is a common response in many tissues e.g. cardiac muscle (Krause & Wollenberger, 1977) and parotid gland (Schramm & Selinger, 1975).

Sato & Sato (1981c) extrapolated the results from other exocrine glands and proposed the following theory for sweat gland stimulation: i) for α and ACh mechanisms calcium enters the cell after the agonist/receptor interaction and the raised free intracellular calcium activates membrane potassium channels (Peterson & Maruyama, 1984) which trigger stimulus secretion coupling in a manner similar to that in the rat salivary gland (Putney, 1979). There is evidence in the salivary gland that phosphatidic acid formation may have a role in the mechanism of calcium channel formation after cholinergic receptor activation (Putney, 1979; Putney *et al.* 1980); ii) the β adrenergic stimulation causes an increase in cAMP in the secretory cell which then mobilises calcium from an intracellular pool to the critical site in the cell. An intracellular calcium release in the β effect seems likely in view of the resistance to removal of extracellular calcium and a similar system has

been proposed for amylase secretion in the salivary gland, which is also mediated by β mechanisms (Young & Van Lennep, 1979). Whether the calcium has a function as a second messenger in this system is not clear (Berridge, 1975). In view of the fact that the ACh effect is mediated through muscarinic receptors, which have been shown to produce their effects through elevated cGMP in several tissues (Young & Van Lennep, 1979), Sato & Sato (1981b) attempted to correlate the ACh effect with an increase in cGMP in a manner similar to the β adrenergic and cAMP effect. Although a parallelism between sweating and cGMP accumulation existed in the first few minutes there was no correlation beyond this time and they concluded that their evidence "taken together does not firmly support the role of cGMP in cholinergic sweat secretion but does not refute it". However, in view of the conflicting and confusing reports of cGMP involvement in physiological responses (Goldberg & Haddock, 1977) it is possible for cGMP to have a role in the secretory process and the overall control mechanisms for secretion may be similar to those proposed for the salivary gland by Berridge, (1975; Fig.1 .1) with the difference that β stimulation will produce relatively more secretion than β stimulation in salivary glands. The subcellular consequences of an elevated internal calcium beyond those described above have not been studied and remain unclear in sweat glands (Sato & Sato, 1981b) although the eventual effect, in most instances, is production of an isotonic fluid in the lumen of the fundus. Various models have been put forward to explain fluid and electrolyte transport in other secretory epithelial systems and these will be discussed later (Chapter 7) with reference to work in this thesis.

1.4. OBJECTIVES

Jenkinson and co-workers have proposed that the sweating mechanism is basically the same in all species. This conclusion was based on ultrastructural studies of glands, before and after thermal stimulation, in species with (man; Montgomery *et al.* 1984; and horse; Montgomery *et al.* 1982a) and without (cow, sheep and goat; Jenkinson *et al.* 1979) direct innervation. To test the hypothesis that there is a common secretory mechanism, the ultrastructure of the rat footpad

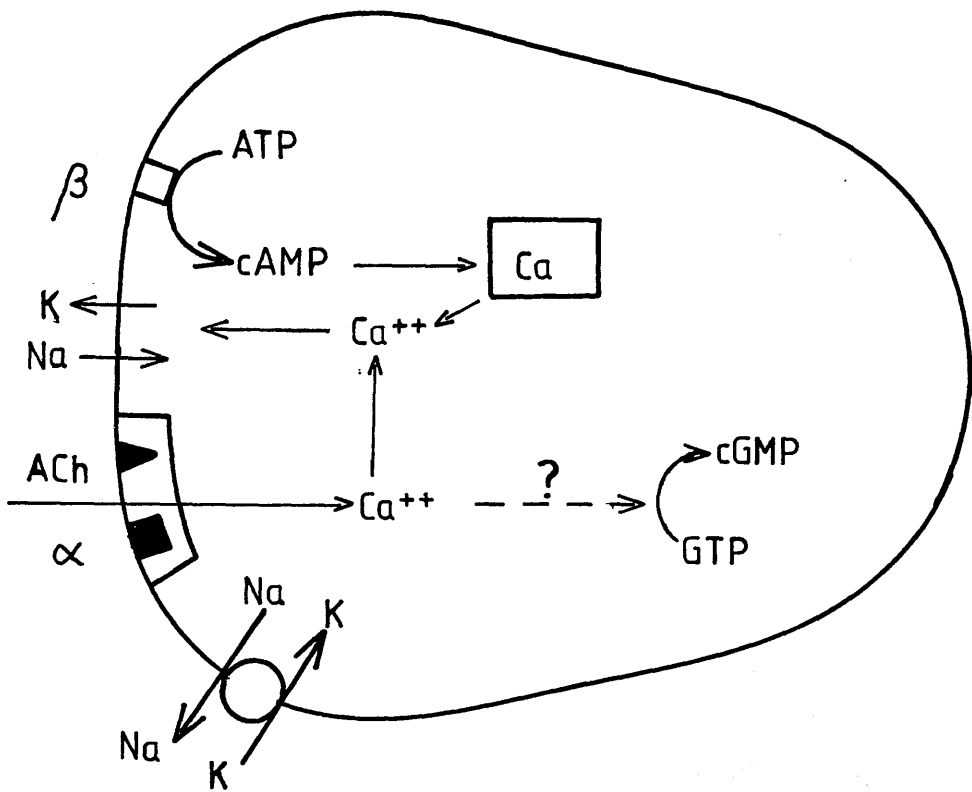
sweat gland, which is an example of a thermally unresponsive cholinergically innervated gland, was studied before and after stimulation. In addition to testing this proposal a sound knowledge of the ultrastructural appearance of the rat gland was essential for further study of glandular function by electron probe X-ray microanalysis (EPXMA). A second objective was to compare the intracellular elemental concentrations and distributions in the sweat glands of various species using EPXMA to investigate whether a common mechanism of fluid transport also exists. The glands studied were the rat footpad sweat gland (stimulated by pilocarpine injection), the human atrichial and the horse epitrichial sweat glands (stimulated by exposure to heat). These data were then used to assess sweat gland function in diseased states e.g. cystic fibrosis and after treatment of skin with sweat inhibitors. The final objective was to assess the mechanism of action of aluminium containing antiperspirants. To tackle this project it was proposed to compare the ultrastructural appearance of glands from untreated and antiperspirant treated skin before and after stimulation. A similar comparison of the intracellular elemental concentrations using EPXMA was also undertaken to determine whether antiperspirants affect the distributions in the duct and fundus. The information gained in achieving the first two objectives was, therefore, essential in answering this question.

Table 1.1. Electrolyte composition of the primary and surface sweat from various species.

SPECIES	SURFACE SWEAT			PRIMARY SWEAT		
	Na	K	Cl	Na	K	Cl
Human	hypo(F)	4-24	hypo(F)	147	?	122
Monkey palm	hypo(F)	5-19	hypo(F)	140	5.5	?
Cat paw	135-160	25-45	80-120	?	?	?
Dog paw	10-200(F)	2-25	30-150(F)	?	?	?
Rat paw	4-25	150-200	85	25	160	?
Mouse paw	60	160	?	60	>100	?

Values are given in mM hypo : hypotonic with respect to plasma. F : flow rate dependent.

Fig.1.1. Model to account for the effects of catecholaminergic and cholinergic agonists on the sweat glands. Catecholamines, released either from capillaries or adrenergic nerves, acting on basolateral β receptors stimulate adenylate cyclase and this results in an increase in intracellular cAMP. The elevated cAMP stimulates the release of Ca^{++} from intracellular reservoirs and there is a subsequent increase in free intracellular Ca^{++} concentration. Catecholamines acting on α receptors and ACh, released from cholinergic nerves, acting on muscarinic receptors produce similar effects. There is an increase in membrane conductance to Ca^{++} which leads to an increase in intracellular Ca^{++} . For all three agonists the elevated intracellular Ca^{++} activates basolateral cation channels and there is an influx of Na^+ and an efflux of K^+ . cGMP may be involved in the mechanism by which α adrenergic and cholinergic agonists produce this effect. (Adapted from Berridge, 1975)



**CHAPTER 2 ULTRASTRUCTURE OF THE RAT FOOTPAD SWEAT
GLAND BEFORE AND AFTER PILOCARPINE
STIMULATION.**

2.1. INTRODUCTION

2.2. METHODS

2.2.1. Transmission Electron Microscopy

2.3. RESULTS

2.3.1. Unstimulated Glands

2.3.2. Glands after Pilocarpine Injection

2.3.3. Glands after Anaesthesia, Saline and Sham Injection

2.4. DISCUSSION

2.1. INTRODUCTION

The rat footpad sweat gland is an example of an atrichial gland. It does not, however, respond to thermal stimulation (Ring & Randall, 1947) as do those in the species previously examined (Jenkinson *et al.* 1979; Montgomery *et al.* 1982, 1984) and it produces a hyperosmotic sweat containing high amounts of potassium (Brusilow, Ikai & Gordes, 1968; Quatralo & Laden, 1968; Sato & Sato, 1978). In view of the hypothesis of Montgomery *et al.* 1984; 1985) that the sweating mechanism is basically the same in all species it was decided to test whether this gland exhibited similar ultrastructural changes (and presumably a similar sweating mechanism) to those found in other species after stimulation.

Although rat sweat glands are not activated by heat they are nonetheless innervated by cholinergic sympathetic nerve fibres and can therefore be stimulated either by direct nerve stimulation (Ring & Randall, 1947) or by subcutaneous injection of cholinergic agents (Munger & Brusilow, 1971; Quatralo & Laden, 1968).

The morphology of the rat footpad sweat gland was studied at rest and after nervous stimulation by Ring & Randall (1947) using the light microscope and before and after pilocarpine injection by Munger & Brusilow (1971) with the electron microscope. The latter study, however, was based on results from only one stimulated rat and, in view of the variability in response of sweat glands to stimulation, even within the same skin region (Ring & Randall, 1947; Hayashi & Nakagawa, 1963; Thaysen, 1978), further work is needed to determine the full range of ultrastructural changes within the gland upon activation. The duct of the rat sweat gland undergoes no ultrastructural alteration after stimulation and shows no signs of glycogen depletion (Wechsler & Fisher, 1968) and is therefore thought to play no active role in the formation of the final sweat product (Sato, 1977). This study was, therefore, restricted to the ultrastructure of the fundus (secretory coil).

The aims were firstly to determine the ultrastructural appearance of the rat footpad sweat gland before and after pilocarpine stimulation and to compare them with the known information on secretory function and, secondly, to become familiar with the appearance of the gland prior to electron probe X-ray microanalytical studies of it in unfixed and

unstained sections in which location is difficult.

2.2. METHODS

Five groups of four 6-8 week old, male Wistar rats, (200-250g) were used.

Those in group I received one subcutaneous injection of 0.3ml pilocarpine (8mg/ml in 0.9% NaCl in distilled water) in the lumbar skin fold. Group II were given two such injections of pilocarpine, the second after a 6min interval. Group III received three injections of the pilocarpine solution at 6min intervals and Group IV were similarly injected three times subcutaneously with 0.3ml of 0.9% NaCl.

All animals in Groups I-IV and those in Group V, which were untreated, were killed by cervical dislocation, the former 6min after the final injection.

Six additional male Wistar rats were treated as follows: 2 were anaesthetised with diethyl ether and killed by cervical dislocation after 18min; 2 were anaesthetised with "Sagatal" (35mg/kg i.p.) and killed after 18min; 2 received three sham injections, which consisted of inserting the hypodermic needle into the lumbar skin fold but injecting no fluid, at 6min intervals and were killed 6min after the final needle insertion.

In both experiments, immediately after death the interdigital and metatarsal plantar pads were removed from each animal and processed by one of two routes.

2.2.1. Transmission Electron Microscopy

Small blocks of tissue, approximately 2-3 mm³, from either the left or right plantar pads were fixed for 3h in 2% glutaraldehyde in 0.1M sodium cacodylate buffer at pH 7.3 then washed in 0.1M sodium cacodylate buffer (pH 7.3) for a minimum of 4h. The tissues were then post-fixed in 1% osmium tetroxide in cacodylate buffer for 1h, dehydrated through graded concentrations of acetone, cleared in propylene oxide and embedded in epon araldite. Sections were cut from each block,

stained in alcoholic uranyl acetate followed by lead citrate, and examined in an AEI EM6B electron microscope at an accelerating voltage of 60kV.

Na/K ATPase localisation was performed by the method of Ernst (1972).

The other footpad was processed for EPXMA as described in Chapter 5.

2.3. RESULTS

2.3.1. Unstimulated Glands

The entire glandular fundus consisted of two cell types, an inner secretory epithelium and an outer myoepithelium, surrounded by dense connective tissue contained within a fenestrated fibrocyte sheath (Fig.2.1.).

The secretory epithelium was composed of cuboidal cells with differing cytoplasmic densities (Figs.2.1.& 2.4.). The basolateral membranes of adjacent secretory cells formed numerous interdigitations or plications which were occasionally arranged as parallel columns reaching to the basal lamina through gaps in the myoepithelial layer (Figs.2.1., 2.4.& 2.6.). The intercellular spaces between these plications were narrow and this region was confirmed as the site of Na/K ATPase (Fig.2.7.).

The myoepithelial cells, which formed a wide-meshed net, were crenated and attached to the basal lamina by hemidesmosomes. In the present study the connections between myoepithelial cells were not observed.

Desmosome connections were present between adjacent secretory cells and between them and the myoepithelium (Fig.2.2.). Adjacent secretory cells were also joined at their apical membranes by junctional complexes, including desmosomes and zonulae occludentes (Fig.2.3.), and gap junctions were also present between them (Fig.2.5.).

The cytoplasm of the secretory cells contained large amounts of rough endoplasmic reticulum and abundant free ribosomes. Variable numbers of short microvilli and vesicles were present at the apical

surface (Figs.2.1., 2.3.& 2.4.) and a terminal web composed of randomly arranged microfilaments was found in the apical cytoplasm.

On the basis of their cytoplasmic density and mitochondrial appearance the secretory cells belonged to one of two categories viz. 1) cells with a less dense cytoplasm, round nuclei and large pale-staining mitochondria with dilated cristae (Figs.2.1.& 2.5.) or 2) those with a darker staining cytoplasm, irregularly shaped nuclei and smaller, more dense, well-preserved mitochondria which contained numerous matrix granules (Fig.2.5.).

The myoepithelial cells were composed largely of contractile elements although nuclei, mitochondria, caveolae and rough endoplasmic reticulum were also present (Figs.2.1.& 2.5.).

2.3.2. Glands Stimulated by Pilocarpine

It was impossible to distinguish any consistent differences between the effects of one, two or three pilocarpine injections on glandular ultrastructure. In general, the glands after any one of these treatments showed a range of ultrastructural changes from mild stimulation to near fatigue.

In what were assumed to be the early stages of activity the secretory epithelium was more columnar, the lumen appeared narrower and the basolateral plications were slightly dilated (Fig.2.8.).

The most noticeable feature of stimulation was the presence of large quantities of a homogeneous, membrane-bound material, with an appearance similar to secretory cell cytoplasm without subcellular organelles, which, in some instances, completely filled the lumen (Fig.2.8.). The limiting membrane around the material was derived from the apical membrane of the secretory cell which had "ballooned-out", either from individual microvilli (Fig.2.9.) or from the expansion of the entire membrane (Fig.2.10.). Although expanded the apical membrane never appeared broken, the junctional complexes and gap junctions between secretory cells were still intact (Figs.2.9.& 2.10.). The terminal web was more opaque in those cells which were apparently extruding their cytoplasm into the lumen as described above (Fig.2.12.).

During pilocarpine stimulation there was no noticeable increase in the number of vesicles in the secretory cells and no indication of vesicle exocytosis.

After prolonged stimulation there were fewer signs of luminal cellular material and the apical membranes were seen "pinching-off" the remains of the cytoplasmic "secretion" (Fig.2.12.). The later stages of stimulation were marked by a dilation of the lumen, which frequently contained the remnants of the cellular "secretion", and a pronounced disorganisation of the basolateral membranes (Fig.2.11.). At this stage, the secretory epithelium was again low-cuboidal and contained "morbid" cells which appeared to have little cytoplasm and few remaining cytoplasmic organelles (Fig.2.13.). However, the nuclei of these cells were ovoid and regular in shape and there were no signs of cell death within the epithelium of the fundus. The differences in density of the cell cytoplasm, noted at rest, remained after three pilocarpine injections (Fig.2.14.) and were more pronounced in some instances with the pale-staining cells more frequently seen in an "exhausted" state.

The myoepithelial cells of the fundus were contracted throughout stimulation and this was most marked during the early stages of activity.

2.3.3. Glands after Anaesthesia, Saline & Sham Injection

No significant qualitative differences were seen between glands from animals in these groups. The glands exhibited basolateral dilatation of the intercellular spaces and the secretory cells were more columnar than in unstimulated glands. These changes were associated with pronounced contraction of the myoepithelium. The luminal space was narrower (Fig.2.15.) than in either the unstimulated or pilocarpine stimulated glands, other than those in which the lumen was obscured by the cytoplasmic "ballooning".

Apical microvesicles were very numerous (Fig.2.15.) and there were signs of possible exocytosis along the luminal membrane. In contrast to glands examined after pilocarpine stimulation there was no sign of cellular material within the lumen and secretory cells were never seen extruding their cytoplasmic contents.

2.4. DISCUSSION

The appearance of cells with different cytoplasmic densities is not unique and appears to be common to rodent footpad sweat glands (Munger & Brusilow, 1971; Matsuzawa & Kurosumi, 1963; Kurosumi & Kurosumi, 1970), although the last group only found the difference in mouse plantar sweat glands after double fixation with glutaraldehyde and osmium. In the rat footpad sweat gland the limited information is conflicting i.e. Matsuzawa & Kurosumi (1963) reported that the appearance of cells with different cytoplasmic densities was age dependent and was present in 10 day old rats but absent in 3 day old and adult rats, whereas Munger & Brusilow (1971) and myself used rats older than 6 weeks and still observed cytoplasmic differences. Wechsler & Fisher (1968) reported different cytoplasmic densities in cells of the rat fundus in pathological states of water imbalance and Kurosumi *et al* (1984) concluded that these differences may be brought about by differences in water content at an early stage of development or after experimentally induced imbalance in water content.

Similarly, the differences in mitochondria found in this study have been reported by Munger & Brusilow (1971). These authors likened the appearance of the rat sweat gland mitochondria with the isolated mitochondria described by Hackenbrock (1966, 1968) who described two forms. The first were condensed mitochondria (equivalent to the smaller, electron-opaque mitochondria in this study) which were indicative of inactive cells and the second were orthodox mitochondria (equivalent to the larger, paler mitochondria in this study) which were found in active cells. This agrees well with the appearance of the cell cytoplasm in that cells with dark cytoplasm, which were never positively identified expelling cytoplasmic material, contained dark mitochondria and *vice versa* for the paler cells. Munger & Brusilow (1971) found that both the cytoplasmic and mitochondrial differences disappeared after pilocarpine stimulation, with all the darker cytoplasm cells converting to the paler cells. In this study, however, the differences persisted even after a 40-fold larger dose of pilocarpine. This raises the possibility that all the cells in the secretory epithelium may not be involved in the secretory response or that they may contribute to different processes cf. the light

and dark cells of the human gland.

These findings are in general agreement with the previous study on a single stimulated gland by Munger & Brusilow (1971). The unique feature of a sweat gland fundus reported in this study is the "ballooning" of the apical membrane and the presumed filtration of the cytoplasmic material through the well-developed terminal web. Although blebbing of apical membranes has been noted as an artefact of fixation (Shelton & Mowezko, 1978) the fact that such an appearance is seen only after pilocarpine stimulation strongly suggests that this is a true feature of glandular activity in this species. The coiled duct of the human atrichial sweat gland exhibits a similar appearance at the apical membrane after thermal stimulation (Montgomery *et al.* 1985) and it may be that, functionally, this region of the human gland and the rat fundus are comparable. Matsuzawa & Kurosumi (1963) reported a "microapocrine" secretion in their study of the unstimulated rat gland which is similar to the appearance of glands in this study after prolonged stimulation which were "pinching-off" the remains of the cytoplasmic secretion.

The effects of ether and pentobarbitone anaesthesia and the sham injections, although studied in only two animals per group, collectively formed a larger group in which the fundus consistently exhibited an ultrastructure different from glands either before or after pilocarpine stimulation. In these glands there were definite signs of secretory activity including exocytosis, an increase in the number of apical vesicles and extreme contraction of the myoepithelial cells. "Ballooning" of the apical membrane was never seen after any of these treatments. The active appearance of the glands in rats after these treatments is probably caused by a combination of two factors. The first is that it is due to the action of adrenaline, released as a result of the traumatic experimental procedure in a reaction similar to the "fight-flight" syndrome. The second is that the appearance is related to the known occurrence of sweating during the excitatory phase of anaesthesia (Cohen, 1975). It seems highly probable then, that there is an adrenergic component of sweating in the rat footpad although Sato (1977) stated that this gland was not responsive to adrenaline. The ultrastructural differences between pilocarpine stimulated and anaesthesia/sham injection stimulated glands may, therefore, be due either to adrenergic and

cholinergic agonists stimulating two distinct secretory processes or to adrenaline stimulating the same process as cholinergic agonists but more mildly. However, if, as in the human sweat gland, the activation of different receptors leads to the same end result (Sato, 1984) the latter explanation seems more likely. This is further supported by the finding that the ultrastructure of the animals in the anaesthetic/sham injection group resembles that reported by Munger & Brusilow (1971), after a less severe pilocarpine ($1/40$) dose than was used in this study and it seems likely that the appearance of glands in these animals is qualitatively the same as after pilocarpine and probably represents the earliest stages of activity. Caution is needed in reaching this conclusion since Munger & Brusilow do not give the anaesthetic used in their study. Similarly, the fact that anaesthetics stimulate activity in the sweat glands indicates that in studies using anaesthetised animals as "controls" (Sampson & Bowers, 1982) care must be taken to assess the degree of activity induced by the anaesthetic.

In comparing the effects of stimulation on the ultrastructure of the rat footpad sweat glands with the differences observed in the fundus of other species by Jenkinson *et al.* (1979) and Montgomery *et al.* (1982a; 1984) there are several points to note. Firstly, no dead cells were seen in either the secretory epithelium or the lumen of the fundus of the rat gland, although it is possible, as in the horse (Montgomery *et al.* 1982a) that examination of the duct would reveal evidence of cell death. Cells with extremely pale-staining cytoplasm and few intracellular organelles were often seen after prolonged stimulation but it is not clear whether necrobiosis is a component of sweating in the rat. Secondly, the "ballooning" of the apical membrane is not seen in the fundus of any other species although it has been reported in the human coiled duct (Montgomery *et al.* 1984). The dilatation of the intercellular spaces and contraction, both of the myoepithelial cells and of the lumen, are common features of all the species studied after stimulation although only the human (Montgomery *et al.* 1984) and rat lumen appears to dilate after prolonged activity. If it is assumed that the effect of the adrenaline release induced by anaesthesia and sham injection is to stimulate the same secretory process as pilocarpine then, apart from cell death, all the other components of sweating detailed by Montgomery *et al.* (1984) were

found in the rat footpad sweat gland. These include water transport, exocytosis and loss of cytoplasmic material. Whether the "ballooning" of the apical membrane represents a form of microapocrine secretion or some form of apocrine secretion it is inconsistent with the definition of an eccrine gland as described by Schlefferdecker (1917). The stages involved in secretion in the rat gland after pharmacological stimulation appear, in general, to be similar to those previously reported for other species after thermal stimulation.

The results also provide the basis for an EPXMA study of the rat footpad sweat gland before and after pilocarpine stimulation. However, various methods of preparing specimens for the measurement of diffusible elements in thin sections had first to be developed.

M₁ - large dense granule formation

M₂ - small electron dense granule formation

R - Rhoatoma

EC - eccrine cell

EC - eccrine cell

EC - eccrine cell

EC - eccrine cell

Abbreviations Used

BI - basolateral interdigitations
BL - basal lamina
CM - cytoplasmic material
CT - connective tissue
D - desmosome
DSC - dark secretory cell
FS - fibrocyte sheath
GJ - gap junction
L - lumen
LM - limiting membrane
LSC - light secretory cell
MG - matrix granules
Mic - microvesicles
MV - microvilli
Myo - myoepithelial cell
M₁ - large pale mitochondrion
M₂ - small electron-opaque mitochondrion
R - ribosomes
SC - secretory cell
TJ - tight junction
TW - terminal web
ZO - zonula occludens

Fig.2.1. An electron micrograph of the fundus of the unstimulated rat footpad sweat gland illustrating the paler form of secretory and the myoepithelial cells, the basal lamina and the surrounding connective tissue. The secretory cells form a single layer, with extensive interdigitation of the basolateral membranes, surrounded by basal myoepithelial cells which form a loose supporting network. Luminal microvilli and two forms of mitochondria are present in the secretory cells. (bar = 1 μ m)

Fig.2.2. (Left) High power view of the basal region of the fundus showing the desmosome connections between adjacent secretory cells. Abundant free ribosomes are also present in the cytoplasm of these cells. (bar = 0.5 μ m)

Fig.2.3. (Right) High power view of the apical region of the secretory cells of the fundus. Adjacent secretory cells are connected by a junctional complex which includes a desmosome and zonula occludens. Microvilli projecting into the lumen are also visible. (bar = 0.5 μ m)

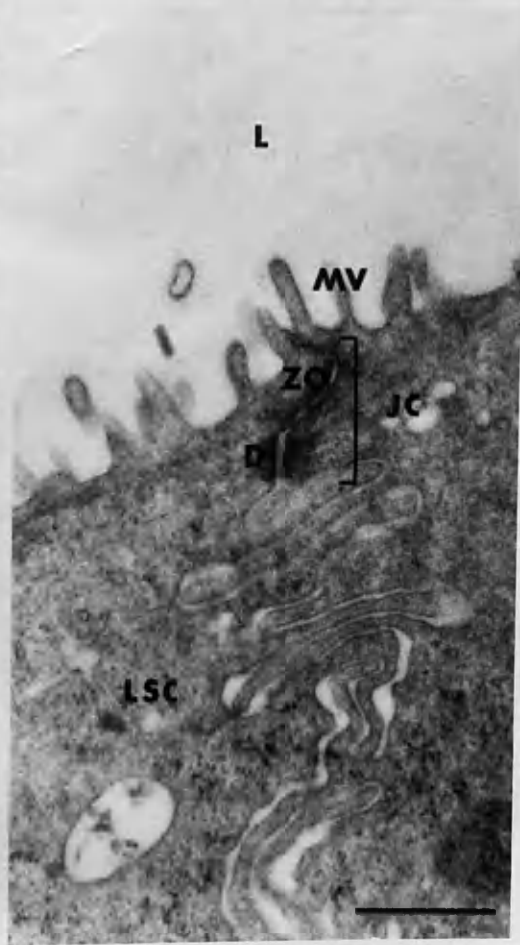
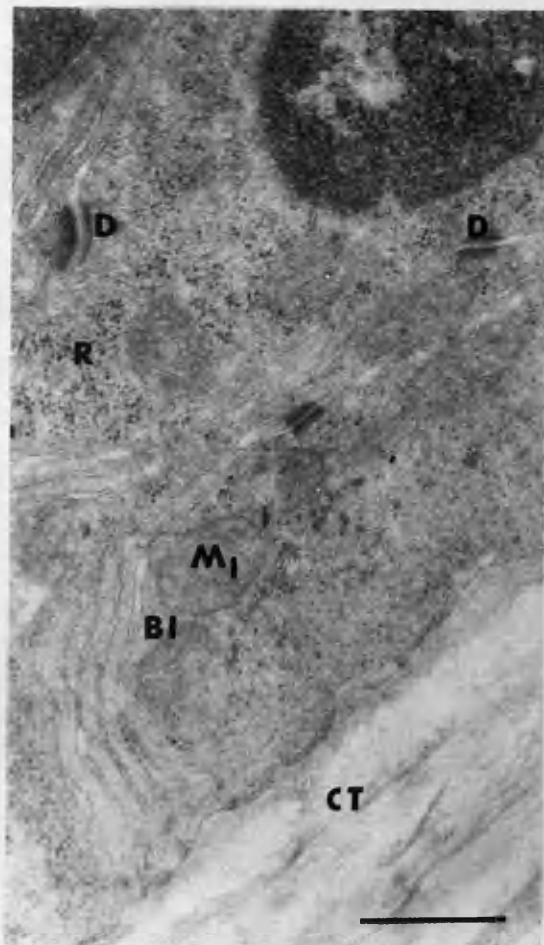
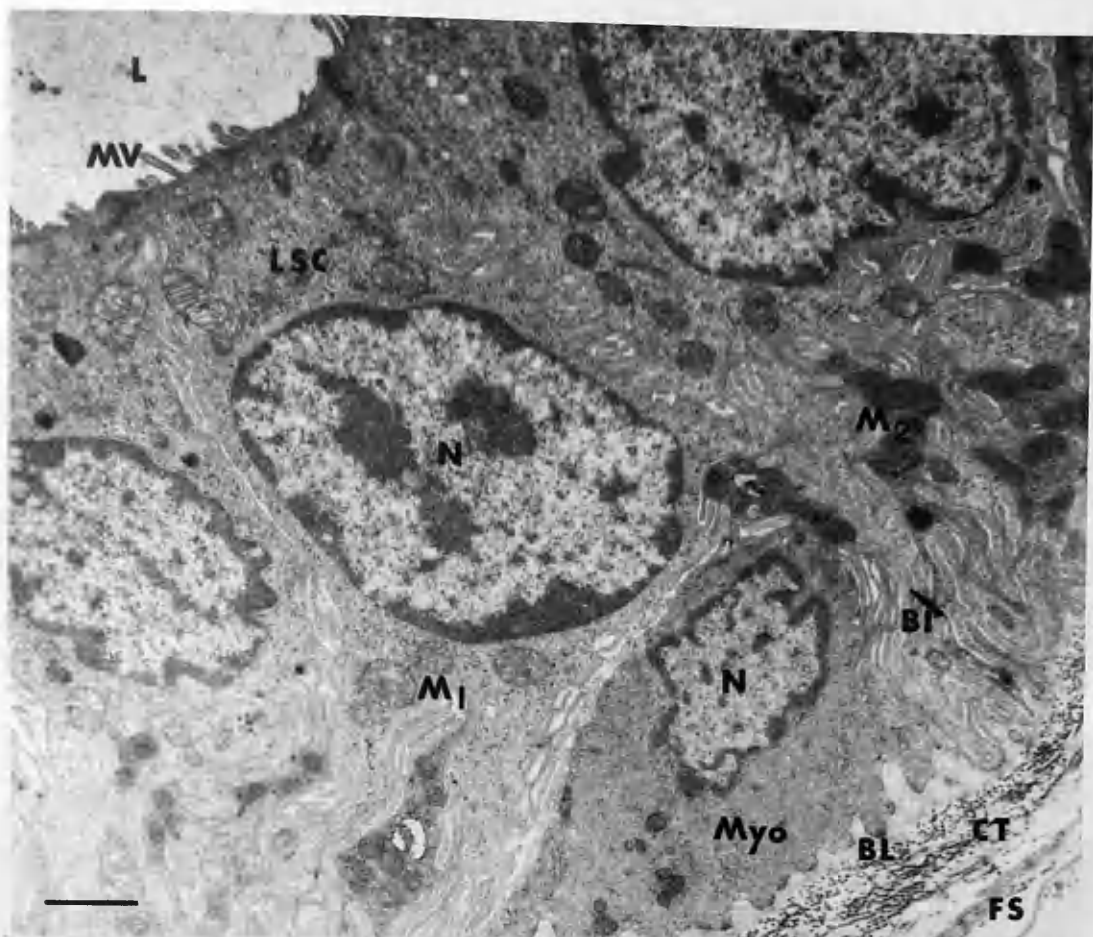


Fig.2.4. Electron micrograph of the fundus of the unstimulated rat gland illustrating the second form of the secretory cell. These cells have a darker cytoplasm, less round nuclei and are less common than the paler form of the cell. The basolateral interdigitations reach the basal lamina between the myoepithelial cells. (bar = 1 μ m)

Fig.2.5. Higher power of the basolateral interdigitations between secretory cells showing the narrow intercellular spaces and gap junctions between adjacent cells. The two types of mitochondria are clearly visible and matrix granules are more frequent in the smaller, electron-opaque variety. (bar = 1 μ m)

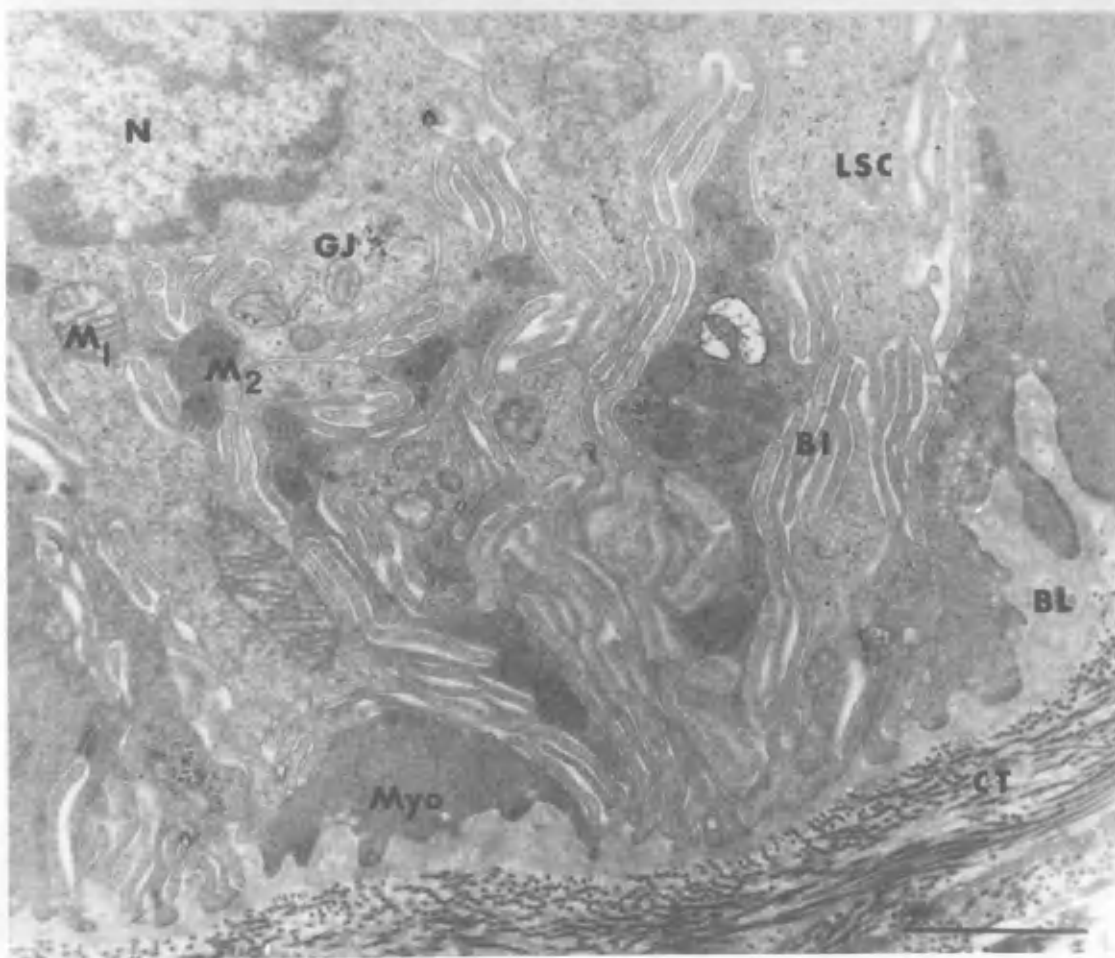
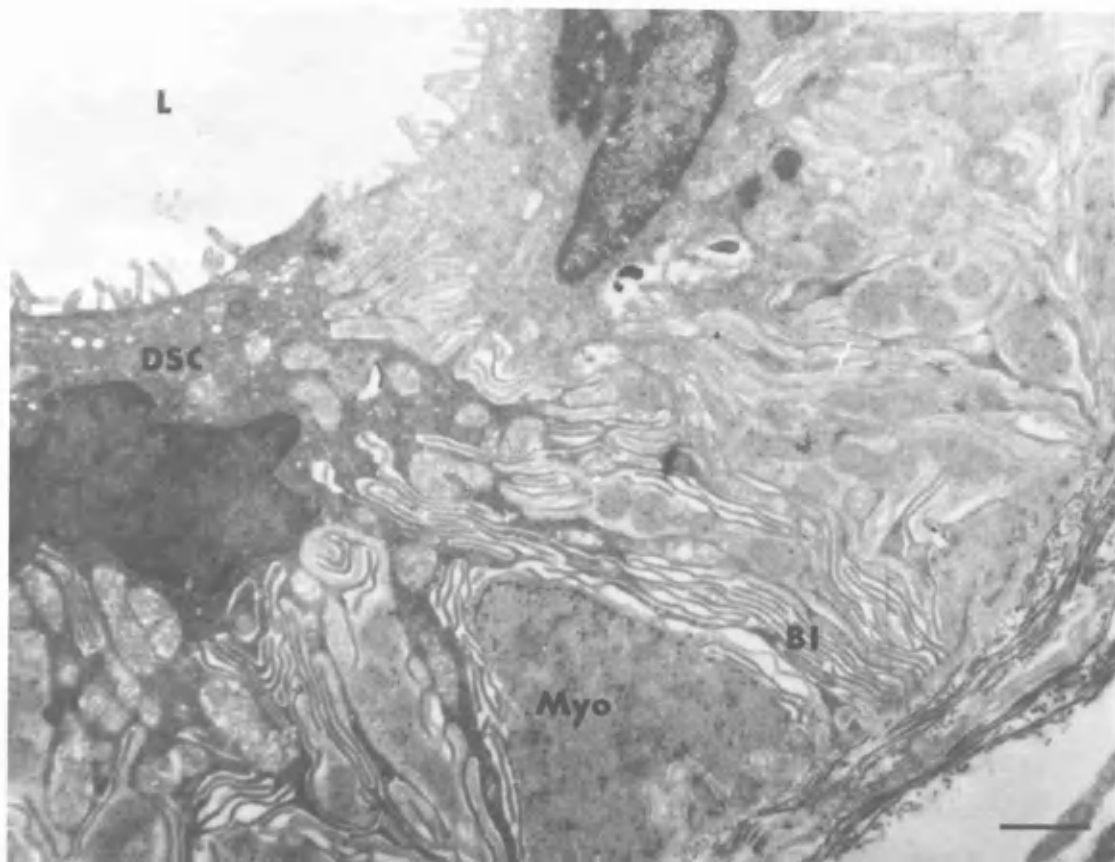


Fig.2.6. The basal region of the fundus of the unstimulated gland showing the basolateral interdigitations forming parallel columns and the narrow intercellular spaces between them. Mitochondria were often found in the secretory cell cytoplasm in this region. (bar = 1 μ m)

Fig.2.7. An electron micrograph of a comparable region to that shown in Fig.2.6. Na/K ATPase is localised along the surface of the basolateral interdigitations. (bar = 1 μ m)

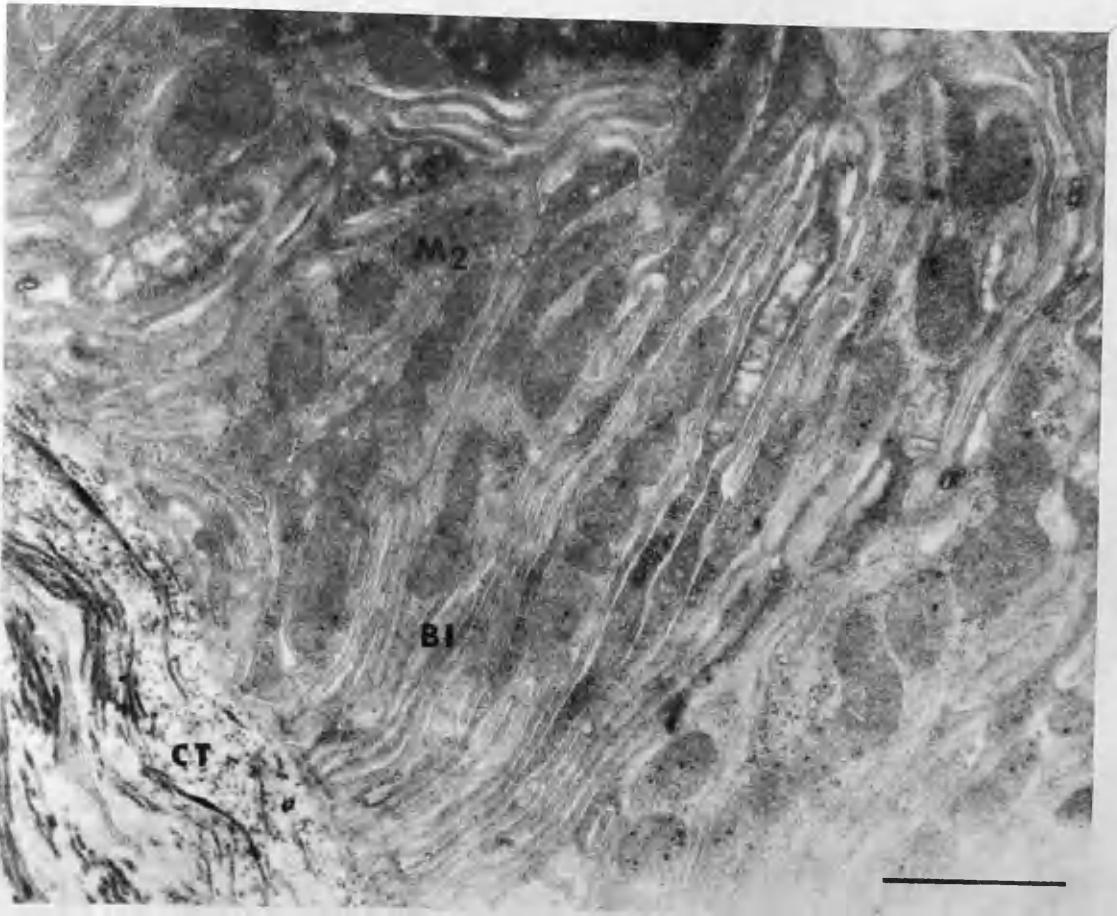
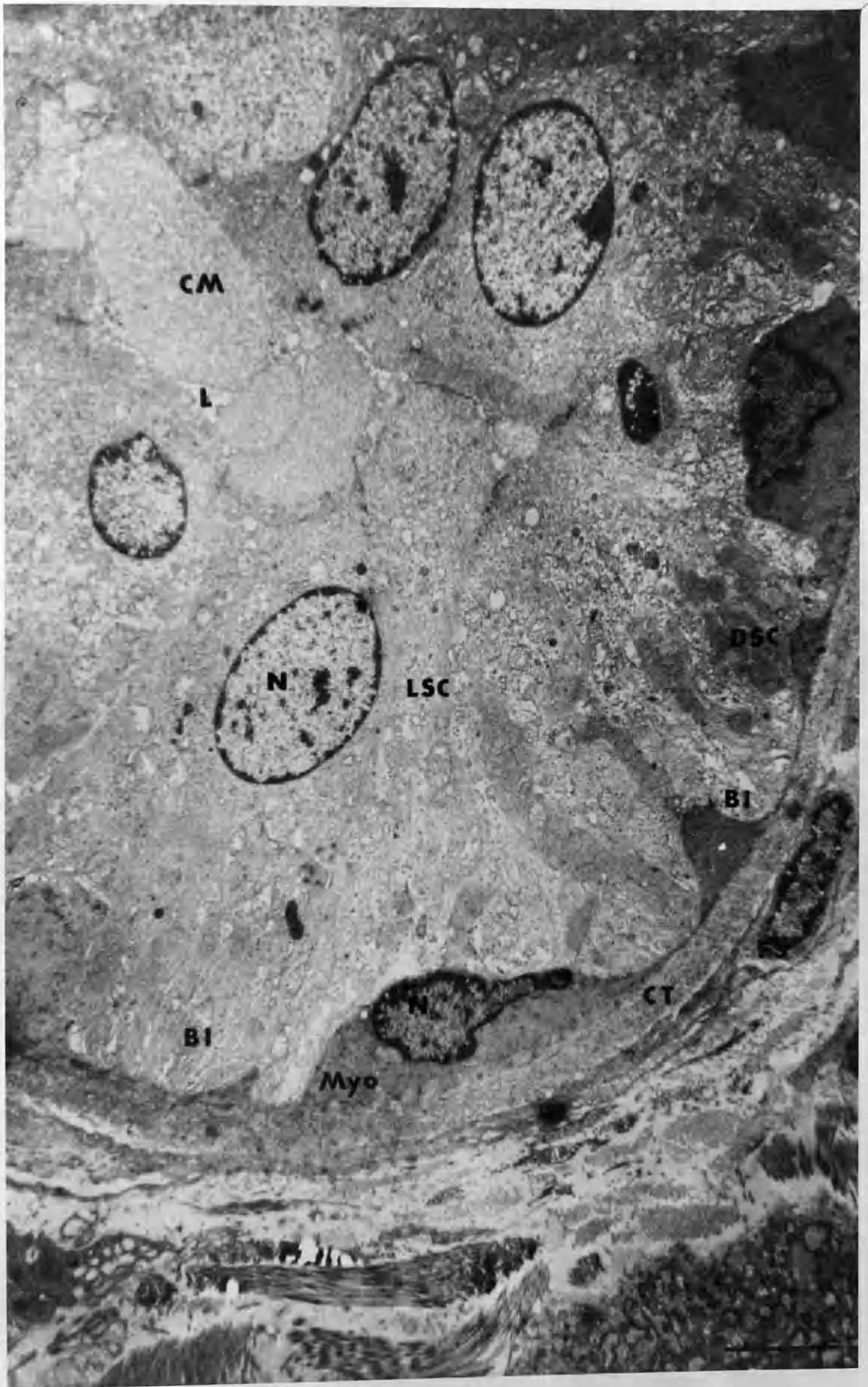


Fig.2.8. An electron micrograph of the rat footpad sweat gland after pilocarpine stimulation. The secretory cells are more columnar, the myoepithelial cells are contracted and the spaces between the basolateral interdigitations are occasionally dilated. The lumen is narrower than in control glands and is almost totally filled with membrane-bound cytoplasmic material extruded from the secretory cells. (bar = 4 μ m)



Figs. 2.9 & 2.10. Higher power views of the apical regions of the secretory cells after pilocarpine stimulation. The cytoplasmic material within the lumen is extruded either from individual microvilli (2.9.) or by the expansion of the entire apical membrane (2.10.). The junctional complexes are still present between adjacent secretory cells undergoing these processes. (bars = 1 μ m)

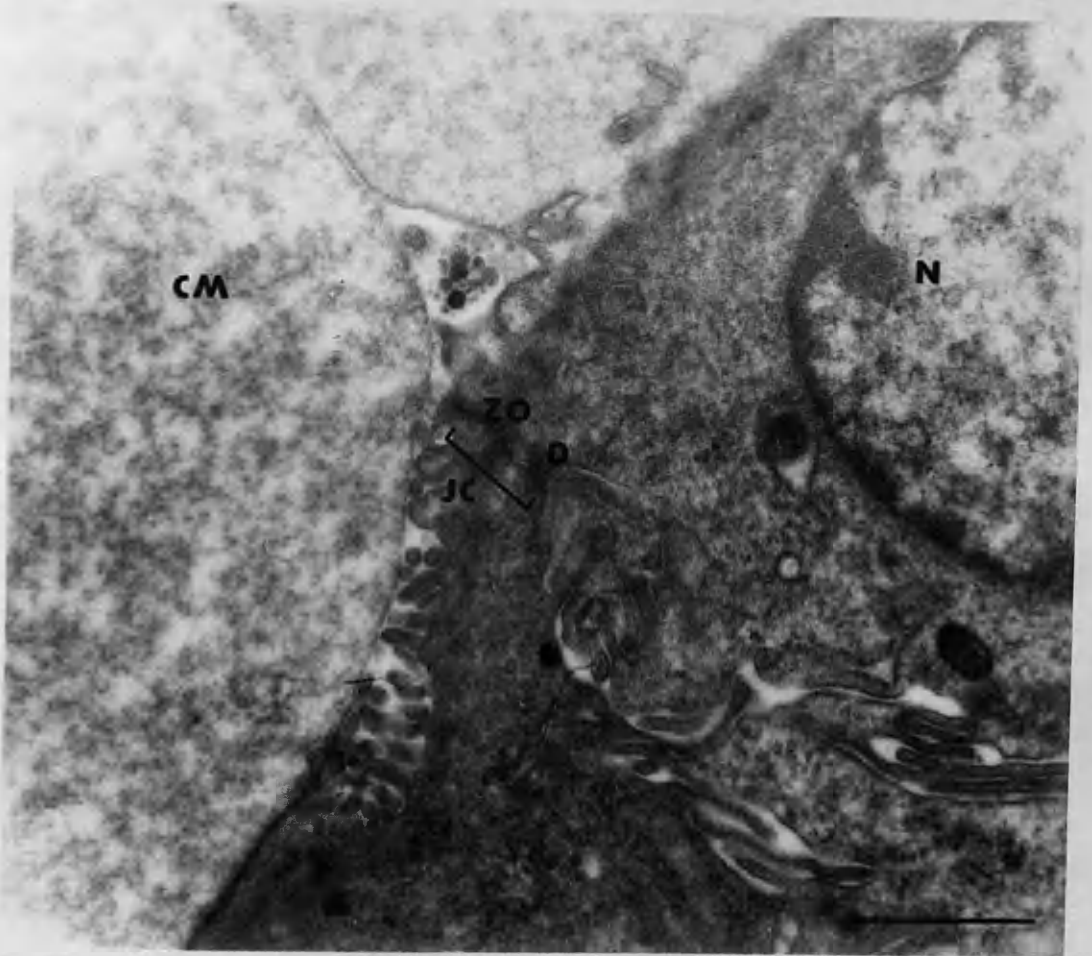
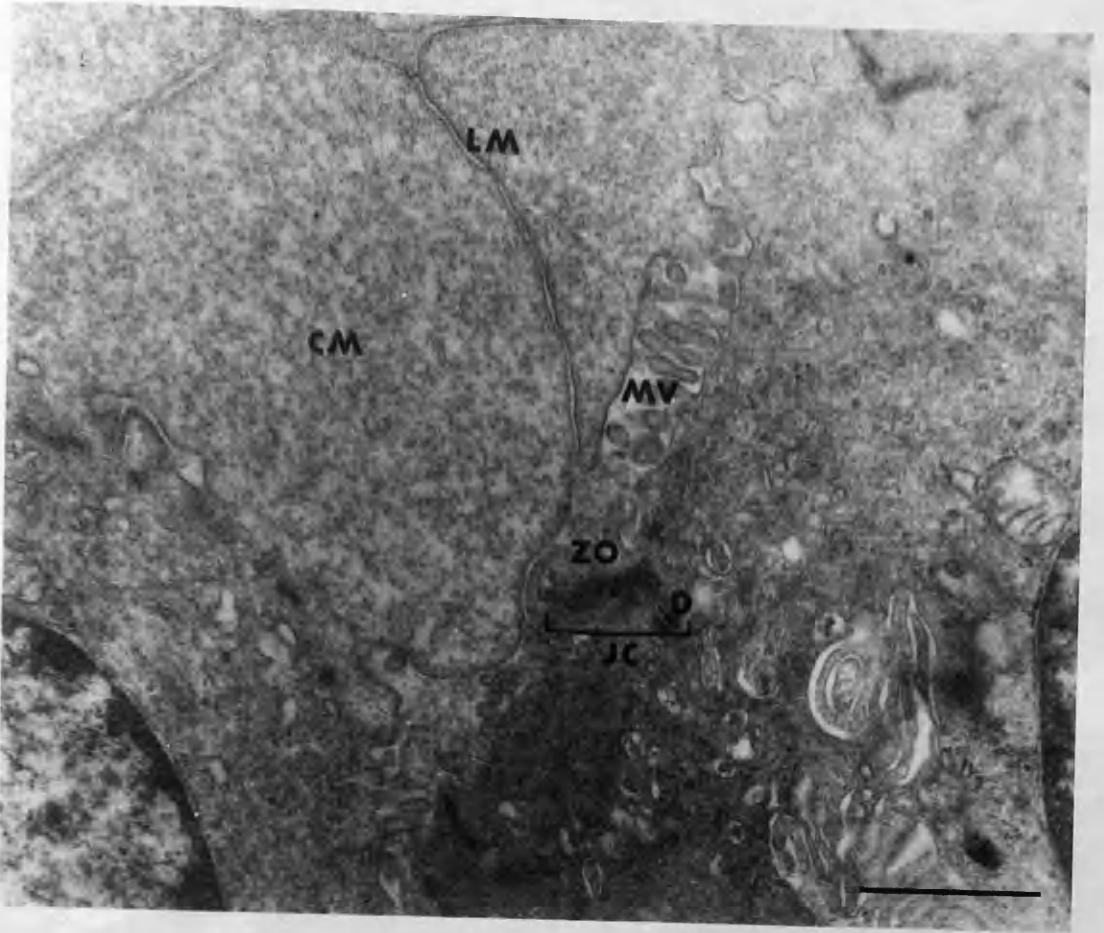


Fig.2.11. During the later stages of pilocarpine stimulation the basolateral interdigitations between secretory cells become more dilated and disorganised. (bar = 1 μ m)

Fig.2.12. Electron micrograph of the apical region of the secretory cells illustrating the "pinching-off" of the extruded cytoplasmic material and the opaque terminal web through which the material is filtered. (bar = 1 μ m)

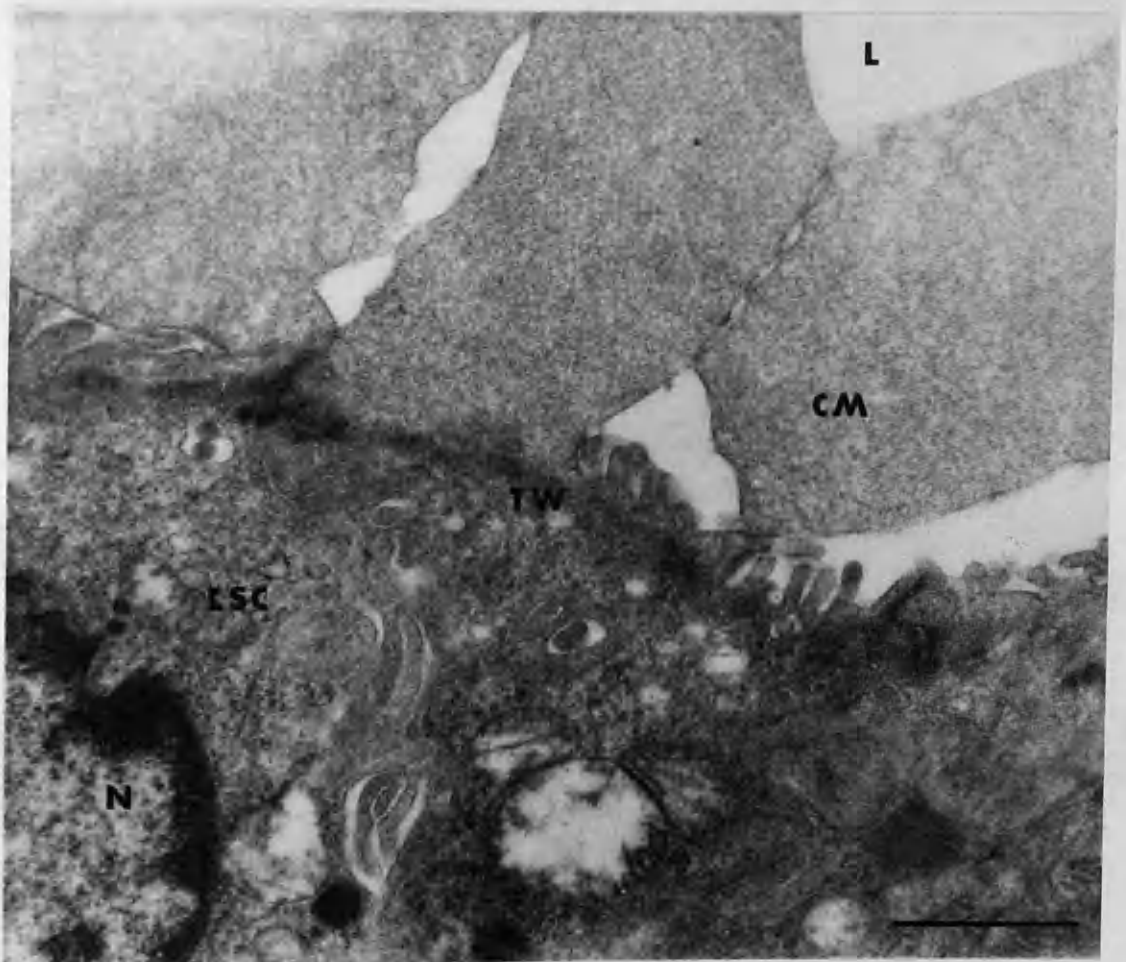
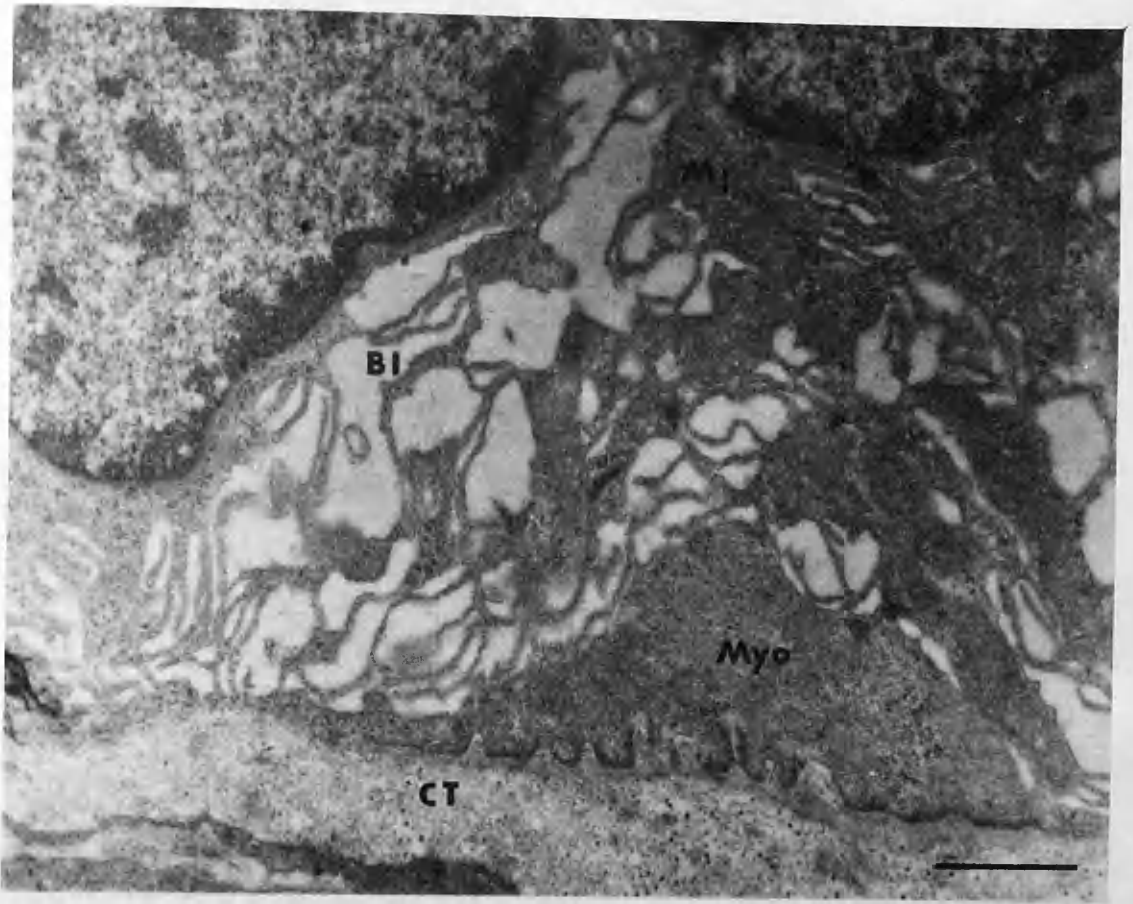


Fig.2.13. After prolonged pilocarpine stimulation the lumen of the fundus dilates and the secretory cells become less columnar. The cytoplasm of these cells is very pale staining and they have an "exhausted" appearance. The myoepithelial cells are still contracted at this late stage. (bar = 1 μ m)

Fig.2.14. Even after prolonged stimulation there are still secretory cells that have a more electron-opaque cytoplasm and which appear to have undergone few changes from the control state. It was not uncommon to find these cells adjacent to the "exhausted" secretory cells. (bar = 1 μ m)

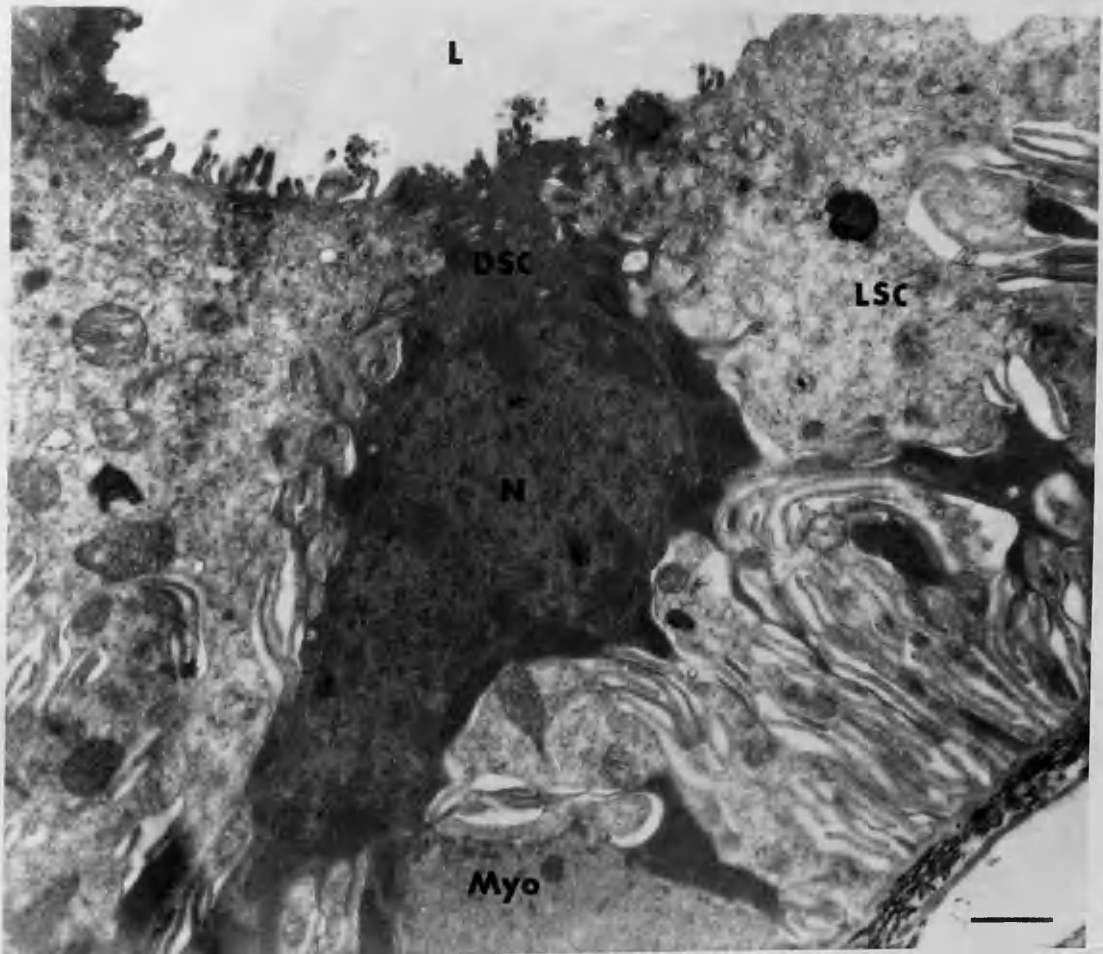
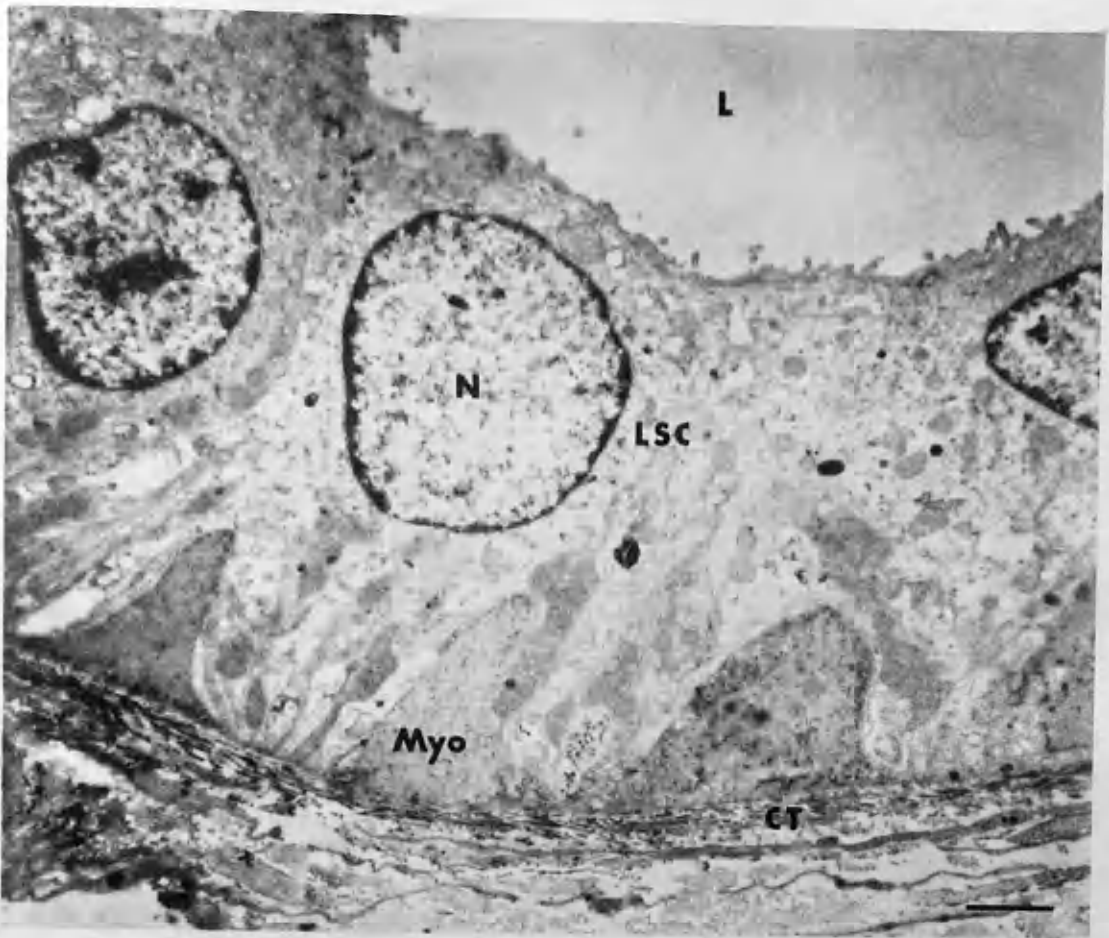
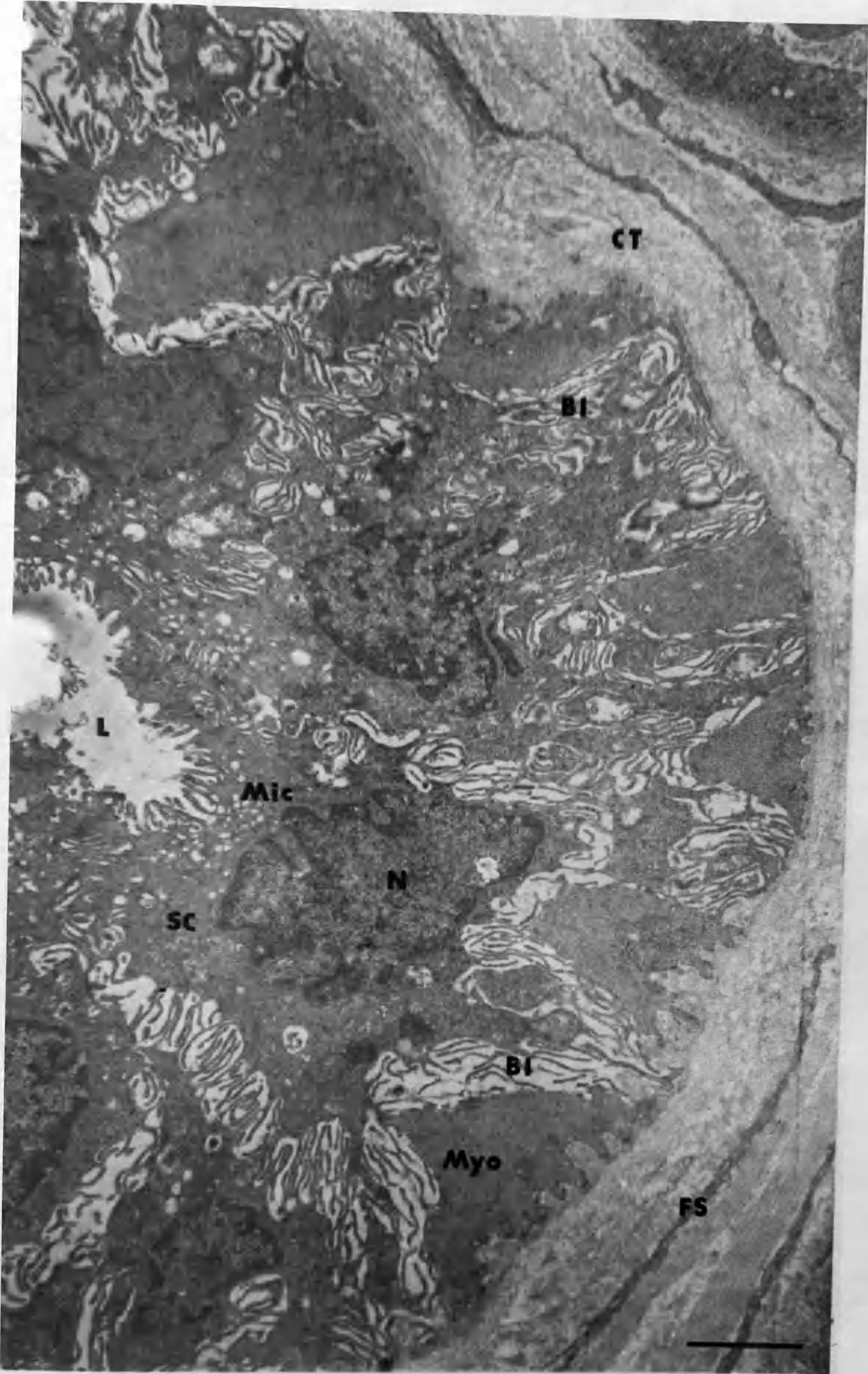


Fig.2.15 An electron micrograph of the fundus after ether anaesthesia. The secretory cells are columnar and the lumen is markedly narrower than in control glands. The myoepithelial cells undergo a pronounced contraction and the intercellular spaces between the basolateral interdigitations are wider than in either unstimulated or pilocarpine stimulated glands. Although the lumen is narrow it is clear and contains no cellular material. In the apical region of the secretory cells there is an increase in the number of microvesicles. (bar = 2 μ m)



**CHAPTER 3 SPECIMEN PREPARATION AND THE PHYSICAL BASIS
OF ELECTRON PROBE X-RAY MICROANALYSIS
(EPXMA).**

3.1. INTRODUCTION

3.2. SPECIMEN PREPARATION

3.2.1. Rapid Freezing (Cryoquenching)

3.3. METHODS AFTER CRYOQUENCHING

3.3.1. Freeze-substitution

3.3.2. Bulk freeze-drying and resin embedding

3.3.3. Cryosectioning

3.3.3.a. Freeze-dried cryosections

3.3.3.b. Frozen-hydrated cryosections

3.4. PREPARATIVE METHODS USED IN THIS THESIS

3.5. PHYSICAL BASIS OF EPXMA

3.6. GENERATION OF X-RAYS

3.6.1. Characteristic X-rays

3.6.2. Background X-rays (bremsstrahlung)

3.6.3. Spatial resolution

3.7. INTERACTIONS OF X-RAYS

3.8. X-RAY DETECTION AND PROCESSING

3.9. QUANTITATION METHODS

3.9.1. Characteristic-alone

3.9.1.a. Advantages and disadvantages

3.9.2. Continuum normalisation

3.9.2.a Advantages and disadvantages

3.9.3. Standards

3.10. CHARACTERISTICS OF THE ELECTRON MICROSCOPE AND QUANTITATION METHODS USED IN THIS WORK

3.10.1. Electron Microscope

3.10.1.a Microscope Modifications

3.10.2. Spectrum Quantitation

3.10.3. Analysis Conditions

3.10.4. Standards

3.1. INTRODUCTION

There are two important stages involved in biological EPXMA i) specimen preparation and ii) specimen analysis. Failure to use the appropriate technique in any part of either stage affects the results adversely (Ingram & Ingram, 1984).

3.2. SPECIMEN PREPARATION

The main objectives of specimen preparation are to process the tissue to the point of microanalysis whilst maintaining it as close as possible to its *in vivo* state so that the elemental distribution can be quantitated with a high degree of spatial resolution. For biological tissues, in general, and for this thesis in particular the important preparative routes are shown in Fig.3.1.

3.2.1. Rapid Freezing (Cryoquenching)

The first step in most, if not all, microanalytical studies is the freezing of the tissue as rapidly as possible, particularly through the temperature range 0 to -120°C, to prevent movement of ions/elements and to inhibit the formation/growth of large ice crystals that would impair both the integrity of the tissue compartments and the spatial resolution of subsequent analysis. Complete vitrification of the surface of cryoquenched rat liver (McDowall *et al.* 1983) and insect flight muscle (Dubochet & McDowall, 1984) has been achieved. However, in most instances the cooling rates of $\sim 1 \times 10^6$ K/s (Franks, 1978) necessary for complete vitrification cannot be achieved. At cooling rates of $\sim 1 \times 10^4$ K/s (Moor, 1971; Bald, 1983), which can be achieved under optimum conditions, it is possible, however, to obtain specimens which contain an outer layer, $\sim 10\mu\text{m}$ thick, in which the ice crystal diameter is below the resolution of the electron microscope and causes little structural disruption or elemental redistribution (Elder *et al.* 1982). The necessary rapid cooling has been produced in three ways: i) direct impingement with liquid sprays (Bachman & Schmitt, 1971; Muller, Meister & Moor, 1980; Knoll, Oebel & Plattner, 1982), ii) slamming into a block of very pure

metal e.g. copper (Heuser *et al* 1979; Escaig, 1982; Bald, 1983) or silver (Van Harreveld & Crowell, 1964; Bald, 1983) cooled to the temperature of liquid nitrogen (Van Harreveld & Crowell, 1964; Bald, 1983) or liquid helium (Heuser *et al* 1979; Escaig, 1982) or iii) rapid immersion in a sub-cooled liquid. The first route has been used virtually exclusively for freeze fracture studies of thin cell layers and has had little use in biological EPXMA. Similarly, the second route, slamming, has not made a significant contribution to biological EPXMA and the major problem appears to be the mechanical distortion of the deeper tissues (Seveus, 1978). However, the surface regions are well preserved (Heuser *et al* 1979) and Escaig (1982) showed excellent cryopreservation to a depth of 25 μ m in liver frozen by freezing against a copper block. The third route is the most commonly used by biologists and there is a great deal of conflicting evidence as to which coolant produces the fastest cooling rates and, therefore, the smallest ice crystals (Elder *et al* 1982). In general, the specimen is either plunged into coolant or held stationary whilst the coolant is brought upwards over the specimen (Barnard, 1982). Coolants used include liquid nitrogen slush (Seveus, 1978; Barnard & Seveus, 1978), Freon 22 (Somlyo, Shuman & Somylo, 1977; Andrews, Mazurkiewicz & Kirk, 1983), Freon 13 (Gupta *et al* 1978; Barnard, 1982), propane (Elder *et al* 1982; Rick *et al* 1979), and ethane (Silvester, Marchese-Ragona & Johnston, 1982). However, the last two have definite safety problems associated with their use (Bald, 1984) and propane also suffers from the disadvantage that its freezing point is several degrees higher than that of liquid nitrogen and may inadvertently freeze during cryoquenching. The latter problem can be overcome by the addition of 20-25% (v/v) isopentane (Bell, 1956; Jehl *et al* 1981) without seriously affecting the cooling rate. Bald (1985) assessed the properties of various liquid coolants and found that at atmospheric pressure ethane or propane was the most efficient coolant depending upon the specimen geometry and nature of the holder. Liquid nitrogen is potentially the best liquid coolant if certain criteria can be satisfied (Bald, 1984) i.e. i) excessive vapour formation is avoided by operating above the critical temperature, ii) entry velocity is high so that the heat transfer coefficient during the plunge is proportional to \sqrt{V} and iii) that the cooling is completed during the plunge whilst the specimen is moving rather than in the stationary

phase after the plunge is completed. It seems highly likely that, in different laboratories using different quenching techniques, different coolants will produce the best cryofixation and it is, therefore, up to the experimenter to assess the individual merits of each. However, Elder *et al.* (1982) suggested nine criteria which, when satisfied, yielded the highest cooling rates and the best cryopreservation with liquid propane. Using liver as a model they found that rather than increasing continuously with depth into the tissue the ice crystal damage reached a maximum at a depth of $\sim 40\text{-}50\mu\text{m}$ and thereafter decreased to a plateau of $<0.3\mu\text{m}$ between $60\text{-}100\mu\text{m}$ from the surface. This has important consequences for EPXMA of deeper tissue regions and implies that analysis may be possible in these regions, without a significant loss in spatial resolution, as long as the probe diameter is greater than the area of the ice crystals present.

3.3. METHODS AFTER CRYOQUENCHING

3.3.1. Freeze-substitution

After cryoquenching, any ice in the specimen is slowly replaced by organic solvent dehydrating agents at low temperatures. Once the ice has been removed (substituted) by the dehydrating agent the specimen is warmed to room temperature and infiltrated with an appropriate embedding medium. The length of time required for the substitution is dependent upon temperature, on the properties of the substituting fluid and on sample size (Morgan, 1980). Using Agar blocks impregnated with Sudan black B, as crude tissue models, Harvey, Hall & Flowers (1976) found that it took 25h for the blocks to clear in acetone as a substituting fluid and 500h in diethyl ether. They subsequently used periods of 3 and 21 days, respectively, for plant tissue substitution. The dangers associated with this route are those of elemental loss and redistribution and, with this in mind, Harvey (1982) recommends that substitution be completed in the shortest possible time. A compromise, however, must be made between the fluids with the most rapid substituting rate and those with the best elemental retention properties. The best substituting fluid found to date, for the retention of diffusible substances, is undoubtedly

diethyl ether with or without acrolein, up to 20%, to improve ultrastructural preservation. Ether, as reported by Harvey *et al* (1976), retains cations at >96% and chloride at 99%. Van Zyl *et al* (1976) recorded 99% elemental retention in root tips and cockroach nerve cord after substitution in ether, although, as mentioned above, complete freeze-substitution with this fluid requires 21 days. Acetone was found by Harvey *et al* (1976) to be a reasonable second choice. Morgan (1980) lists a number of substituting fluids with their respective percent retention rates and it seems clear that with a strict adherence to an anhydrous protocol, for plants at least, the percent retention of elements can be kept to ~95%. The temperature of substitution is normally approximately -80°C and this has been found on an empirical basis to be approximately correct, as it is below both the eutectic point of the salt mixtures present and the recrystallisation temperature (Marshall, 1980). Suitable embedding media should be hydrophobic, be of a low viscosity and preferably contain no elemental peaks that will interfere with EPXMA. The most frequently used media are Spurr's resin (Spurr, 1969) and the low chlorine version of Spurr's resin (Pallaghy, 1973). Lauchli *et al* (1970) has shown that loss of potassium from the tissue to the embedding medium at this stage is negligible. The sections should be dry cut, i.e. without trough liquids, since this is a major source of elemental loss. Harvey, (1982) gives the losses for various elements on different floatation media as between 10-80%.

3.3.2. Bulk Freeze-Drying & Resin Embedding

This represents a technique of increasing popularity as regards X-ray microanalysis (Ingram & Ingram, 1984; Elder *et al* 1985; Roos & Barnard, 1984; 1985; Burovina *et al* 1978; Kuijpers *et al* 1984) presumably as the difficulties in specimen preparation with the cryosection route become apparent. In this method contact with organic solvents is avoided and the water is gradually sublimed from the sample in a vacuum at a temperature between -80° and -100°C. The tissue is infiltrated with embedding media after drying and cut as for freeze-substitution studies. The time taken to freeze-dry samples varies with sample size and the temperature of drying. Drying occurs when the

partial pressure of water at the surface of the specimen is less than the saturation vapour pressure of ice which is proportional to the temperature (Robards, 1974; Robards & Sleytr, 1985). A compromise must be reached between achieving a temperature high enough to allow freeze-drying whilst keeping the specimen below the eutectic point (as for freeze-substitution) and recrystallisation temperature. A range between -80°C to -100°C is normally chosen for drying. The recrystallisation temperature for ice in biological systems is variously estimated at -60°C (Appleton, 1974) and -70°C (Christensen, 1971; Dempsey & Bullivant, 1976a & b). At temperatures colder than -100°C the saturation vapour pressure in the specimen is low and drying would take place at an exceedingly slow rate. Control of the partial pressure of water in the freeze-dryer is tackled by performing the process in a vacuum. However, even in a vacuum of 1×10^{-7} torr, between 10-80% of the residual molecules may be water (Robards, 1974). This problem is normally overcome by placing an anti-contaminator, at liquid nitrogen temperature, within the chamber close to the specimen (Moor, 1969; Ingram & Ingram, 1984). Since the saturation vapour pressure of water at -196°C is 10^{-24} torr this cold surface will avidly attract any remaining water. Additional measures used to reduce the residual water level include physical (molecular sieve) and chemical (P_2O_5) adsorption. In practice, therefore, the partial pressure of water is negligible and the drying rate is essentially a function of temperature.

In the bulk freeze-drying of tissue, vacuums greater than 10^{-3} torr do not seem to markedly improve the drying process (Ingram & Ingram, 1975; Lyon *et al.* 1985) as the diffusion of water from the still frozen tissue core through the already dried outer tissue becomes the rate determining step. In addition to presenting a diffusional barrier to water molecules the thermal characteristics of this dried outer layer are significantly different from ice. In a model system comparing the temperature of a specimen whose properties were initially those of ice but were converted to those of polystyrene (to represent a carbon based compound resembling dried tissue) as it dries, J.N.Chapman & D.Steele, (personal communication) found that, initially, the ice will reach the temperature of the specimen drying stage through conduction. However, as it dries the properties of the polystyrene outer layer are such that it

is a poor thermal conductor and is more affected by radiation from surrounding surfaces. At any time after drying has started it seems likely that the temperature of this insulating layer therefore lies somewhere between the temperature of the drying stage surrounding it and the temperature of the cold stage (-196°C) closely above it. In such circumstances the removal of the remaining ice in the tissue core is likely to be compromised since, as Coulter & Terracio (1977) have shown, the rate of drying of this core is proportional to temperature. Since the mean free path of a water molecule in a vacuum of 10^{-5} torr is $\sim 1000\text{mm}$ (Robards & Sleytr, 1985) it seems unnecessary, and undesirable, to place a cold trap as close to the specimen as is currently supposed and, perhaps, it should be located "out-of-sight" of the specimen (Elder *et al* 1986). Although Lechene *et al* (1979) and Steinbrecht (1984) are disparaging concerning the freeze-drying process, both from the viewpoint of morphological detail and elemental distribution, the work of Coulter & Terracio, (1977) demonstrated excellent morphological preservation and the recent applications (Ingram & Ingram, 1984; Elder *et al* 1985; Roos & Barnard, 1985) have produced meaningful biological results.

For both freeze-substituted and bulk freeze-dried material it appears that the most meaningful results are obtained if the analysis is performed at the cellular level i.e. differences between cells are faithfully preserved. The comparison of subcellular regions is of questionable value (Roos & Barnard, 1985; 1986).

3.3.3. Cryosectioning

The technique of cryoultramicrotomy and the various systems used are discussed in more detail in Chapter 4. Theoretically the cryosection is the ideal specimen, in terms of morphological and spatial resolution, for EPXMA with an energy dispersive detector. All contact with organic solvents and embedding media is avoided and the analysis is far quicker to perform than either of the techniques described in 3.3.1. and 3.3.2. These theoretical advantages are tempered by the practical problems which must be overcome before adequate sections can be produced, including the development of ultramicrotomes capable of functioning at

low temperatures (-120°C for frozen-hydrated sectioning). The relative advantages and disadvantages of freeze-dried and frozen-hydrated sections are given below.

3.3.3.a. Freeze-dried cryosections

Advantages : better peak/background ratio
better contrast
better spatial resolution
easier to prepare than frozen hydrated

Disadvantages : only intracellular elements can be quantitatively measured, although, if there is a dense extracellular matrix, qualitative measurements can be obtained from such regions.

3.3.3.b. Frozen-hydrated cryosections

Advantages : it is the only method for the analysis of fluid-filled spaces and extracellular areas devoid of matrix.

this method enables the water content of subcellular regions to be calculated by comparing the spectrum background in the frozen-hydrated state with that obtained from the same region after the section has been dehydrated.

Disadvantages : the opposite of all the advantageous points given for the freeze-dried cryosections.

3.4. PREPARATIVE METHODS USED IN THIS THESIS

Initially it was proposed to perform the EPXMA study of sweat glands using freeze-dried cryosections since this method is one of the two most reliable in retaining intracellular elemental distributions. A system was developed to prepare freeze-dried cryosections and is described in detail in Chapter 4. However, despite the success of the system in preparing cryosections of a variety of tissues, it was not

possible to use this route for the study of sweat glands due to the difficulties, described in Chapter 4, in locating glands. The alternative route taken to perform the study was a routine bulk freeze-drying and resin embedding method described briefly in Chapter 5. Although, the equipment required for the bulk freeze-drying already existed in the laboratory, a suitable resin for embedding still had to be selected. As discussed in 3.3.1., for freeze-substitution/bulk freeze-drying the ideal resin has a low viscosity (to allow thorough penetration), is hydrophobic (to prevent section rehydration), contains no elements which may interfere with the quantitation and, finally, has good sectioning properties. The normal choice in such instances is the low chlorine version of Spurr's resin (Pallaghy, 1973). However, in practice, the sectioning properties of this resin were too poor to allow regular and routine use. Fig.3.2. shows typical spectra from a variety of commercially available resins used in our laboratory. Experimentation demonstrated that araldite was a suitable alternative, the only contaminant being chlorine. An estimate of the errors that this chlorine introduces to the measurement of chlorine in sections of biological material is described in Appendix 2.

3.5. PHYSICAL BASIS OF ELECTRON PROBE X-RAY MICROANALYSIS

Electron probe X-ray microanalysis (EPXMA) is a means of obtaining quantitative elemental information from highly localised subcellular volumes in material/sections visualised in the electron microscope. The technique can be performed in the scanning, the transmission or the scanning transmission mode and is based on the interaction between a focussed electron beam and the atoms composing the volume of specimen irradiated by the beam. For EPXMA the major requirements are a means of: i) producing a focussed electron beam, ii) visualising the specimen and iii) detecting the emitted X-rays (Moreton, 1981). Extensive reviews of the instrumentation and techniques involved have been given by Hall (1971), Chandler (1977), Russ (1978), Marshall (1980) and Morgan (1985) and only the features relevant to EPXMA using the transmission electron microscope (TEM) equipped with an energy dispersive detector (EDX) are discussed here.

The basic steps in the procedure are: A) the generation of X-rays, B) the interaction of X-rays with the specimen and the surroundings, C) the collection and processing of the X-rays and D) the quantitation of the X-rays.

3.6. GENERATION OF X-RAYS

X-rays are produced when an incident electron is inelastically scattered by an atom and these fall into two categories i) characteristic X-rays and ii) background X-rays (see Fig.3.3).

3.6.1. Characteristic X-rays

An atom is composed of a positively charged nucleus surrounded by negatively charged electrons in orbits within distinct shells, labelled K, L, M, etc. with increasing distance from the nucleus. The innermost (K shell) electrons are the most tightly bound and possess the lowest (potential) energy. Due to the tight binding the K shell electrons are more difficult to remove from their orbits than electrons from the outer shells

and this effect becomes more pronounced as the atomic number (Z), and therefore the charge on the nucleus, increases. If an incident electron collides with an inner orbital electron of an atom and possesses sufficient energy (the critical excitation potential, E_c) it may remove that electron from its orbit. The atom is then in an excited (ionised) and unstable state which lasts ~ 10 ns (Borowitz & Beiser, 1971). In this time an electron from a higher energy orbit refills the vacancy in the inner shell. The excess energy i.e. the difference in potential energy between the initial and final states of this electron, is emitted in the form of an X-ray. These X-rays are named after the shell in which the initial vacancy occurred i.e. K, L, etc. with a subscript α, β, γ , etc. to describe the origin of the electron which filled the vacancy. Since the orbital energies are unique for each element, by measuring the frequency of the emitted X-rays, (ν), the element may be identified or characterised by the equation:

$$\nu = 2.4 (Z-1)^2 \times 10^{15} \quad (\text{Moseley, 1913, 1914}) \quad \text{-----1}$$

The intensity of the emitted X-rays, which is a measure of the number of atoms of that element present in the irradiated volume, varies, and in biological EPXMA the K line is the most easily detected and is used to identify and quantify elements.

There is a possibility that the generated X-ray may not be emitted from the element but may be reabsorbed by an outer electron resulting in a radiationless transition (Auger effect). The likelihood of an X-ray being emitted from an element is called the fluorescent yield and increases with increasing atomic number. The low yield for the low atomic number elements is one of the reasons for the difficulty in accurately measuring them. Green & Cosslett (1961) showed that the efficiency of X-ray production, I_a , (i.e. characteristic intensity/incident electron) from an element is a function of both the fluorescent yield and the ionisation cross-section, (Q), which represents the likelihood of an atom being ionised by an incident electron of energy E_0 .

$$Q = \frac{7.92 \times 10^{-14}}{E_0 E_c} \times \ln \left(\frac{E_0}{E_c} \right) \quad (\text{Roomans, 1980}) \quad \text{-----2}$$

units: [ionisations/electron(cm^2/atom)]

$$\text{Overall } I_a = \omega N/A Q \sigma dz \quad (\text{Russ, 1975})$$

-----3

where : ω = fluorescent yield

N = Avogadro's number

A = atomic weight

σ = density

dz = thickness of specimen

In general, the efficiency of K shell excitation is relatively low e.g. 1 in 1000 (Reed, 1975) but this effect is overcome by the high numbers of incident electrons used in EPXMA.

3.6.2. Background X-rays (Bremsstrahlung; White radiation)

These are also produced from the inelastic scattering of the incident electron beam. In this instance the incoming electrons interact with the nucleus of an atom and undergo a change in direction with the loss of some energy which ranges from 0-100% of their initial energy. The intensity of this background radiation is dependent on the total atomic number of the irradiated volume and can give a measure of the local specimen mass thickness. The intensity of the background radiation, N_c , is given by the equation:

$$N_c(E) = a Z \frac{(E_0 - E)}{E} \quad \text{-----4}$$

where : a = a constant

Z = atomic number

$N_c(E)$ = intensity in photons s^{-1} per unit energy interval per incident electron

According to the Kramers equation (1923) the intensity of the background radiation tends to infinity as the energy of X-rays tends to 0. However, due to absorption of low energy X-rays in the beryllium window, the gold layer and silicon dead layer of the detector, the spectrum has the shape shown in Fig.3.4.

The value E_0/E_c , that occurs in both equations 3 & 4, is called the overvoltage ratio, (U). One of the aims in quantitative EPXMA is to optimise the peak/background (P/B) ratio and plots of the calculated characteristic and continuum X-ray intensity as a function of the overvoltage ratio show that as U increases so does the P/B. By using higher voltages the peak/background ratios are increased and the spatial resolution of the analysis is improved.

3.6.3. Spatial Resolution

As mentioned above, the spatial resolution using high voltages is very good and in a thin specimen depends primarily on the diameter of the incident beam (Goldstein *et al.* 1977):

$$\text{Beam width (cm)} = 6.25 \times 10^{-2} \left(\frac{Z}{E_0} \right) \left(\frac{\sigma}{A} \right)^{1/2} (t)^{3/2} \quad \text{-----5}$$

where : A = atomic weight
 E_0 = accelerating voltage
 t = section thickness
 σ = density
 Z = atomic number

For most biological specimens the mean Z and density are so low that broadening can be ignored (Morgan, 1985). Russ (1972) calculated that for resin embedded and freeze-dried sections 1000Å thick, the lateral spreading of the beam would be 600Å and 200Å respectively. In practice, the theoretical spatial resolution is less of a hindrance than the presence of ice crystal damage which necessitates a large probe diameter.

3.7. INTERACTIONS OF X-RAYS

One of the most important consequences of performing EPXMA at high voltages and on thin specimens is that the correction factors, for atomic number effects (Z), X-ray absorption (A) and for X-ray fluorescence (F) which give rise to the ZAF correction procedure applied

in other, less favourable situations, can be ignored (Hall, 1971). A more important problem in EPXMA, particularly with an EDX detector which accepts X-rays from a wide solid angle, is the possibility of extraneous contributions to the spectra which may include characteristic X-rays and background X-rays from the specimen rod or the microscope and possibly even directly recorded electrons (Nicholson *et al.* 1982). In the TEM this problem is particularly acute since solid structures such as lens polepieces etc. are close to the specimen and detector and may emit X-rays as a consequence of bombardment by elastically scattered electrons and X-rays. The situation is made even worse because the mass of the ultrathin section is so small in comparison with the instrumental mass. To overcome these problems it is important that the EDX detector is well collimated and that as many sources as possible of instrumental radiation are eliminated. Since these factors are of great importance when using the Hall continuum normalisation method of quantitation they will be discussed further below.

3.8. X-RAY DETECTION AND PROCESSING

There are basically two types of detector for X-rays, the wavelength dispersive (WDS) and the energy dispersive. The EDX detector has been available for a much shorter time than the WDS system but has rapidly assumed more widespread use in biological EPXMA (Russ, 1978). Chandler (1977) compared the advantages and disadvantages of each type in detail but the major advantages of the EDX detector are: a) that it can be placed closer to the specimen and, therefore, detect a greater number of X-rays enabling lower probe currents to be used which subsequently reduces specimen damage; b) that it simultaneously detects all characteristic X-rays and the background; c) that it is more sensitive than the WDS detector. Its major disadvantage is that the spectral resolution is poorer than the WDS detector ($\sim 1/10$) and this has important consequences when peak overlap occurs e.g. $K_{k\beta}$ and $Ca_{k\alpha}$. The EDX detector consists of a lithium-drifted silicon crystal (SiLi) which acts as a semi-conductor and converts the incident X-rays to an electrical signal. The signal is processed by computer and multi-channel analyser which

working of the EDX detector requires firstly, that the SiLi crystal be kept under vacuum and a Be window (nominally 8µm) is used to separate the microscope column from the detector and secondly, that a thin layer of gold (~20nm) be applied to the surface of the crystal. The presence of the Be window, gold layer and a dead layer at the surface of the SiLi crystal seriously attenuates soft X-rays from the low atomic number elements e.g. Na.

3.9. QUANTITATION METHODS

Quantitative results can be derived from the original spectrum since the intensity of the characteristic X-rays is proportional to the number of atoms of that element in the irradiated volume (Hall, 1971). Two principal methods have been used to produce quantitative results from thin sections (<1µm) mounted on Formvar-coated mounts (Hall & Gupta, 1984) termed by Hall & Gupta (1982) the characteristic-alone (C-A) (Dörge *et al* 1978; Rick *et al* 1979; Rick, Dörge & Thurau, 1982) and the continuum normalisation (C-N) method (Hall, 1971, 1979; Hall & Gupta, 1982, 1984).

3.9.1. Characteristic-alone

This is normally carried out with a "peripheral" standard, formed by adding albumin (~20g%) to the physiological solution bathing the tissue so that a layer (~10µm) is formed around the tissue after cryoquenching, which is cut and analysed with the specimen. Cell wet weight concentrations are calculated by dividing the characteristic intensities in the cell by the characteristic intensities in the standard and multiplying this ratio by the known wet weight concentration of the element in the standard. e.g.

$$[\text{Na}]_{\text{cell}} = \text{Na INT}_{\text{cell}} / \text{Na INT}_{\text{stan.}} \times [\text{Na}]_{\text{stan.}} \quad \text{-----6}$$

For elements present in low levels in the bathing solution e.g. K and P, the concentrations can be calculated with reference to another element and a correction factor is applied to account for the different fluorescent

yields for the two elements, which have previously been determined from albumin standards. e.g.

$$[K]_{\text{cell}} = K \text{INT}_{\text{cell}} / \text{CI} \text{INT}_{\text{stan.}} \times [\text{CI}]_{\text{stan.}} \times A \quad \text{-----7}$$

3.9.1.a. Advantages and Disadvantages

With peripheral standards, the C-A method gives a direct measure of the amount of element per unit tissue volume at the time of sectioning (Hall & Gupta, 1982). For accurate quantitation two factors need to be taken into consideration:

i) the section must be of uniform thickness or at least be the same thickness in the areas of specimen and standard analysed (Hall & Gupta, 1982; Rick *et al.* 1979). The latter state that small differences in section thickness within individual cryosections might lead to errors but that these can be expected to be minimal if the analysis is performed at a cellular level using serial sections (see discussion in Lechene & Warner, 1979, p528-530). This assumes no discontinuous chipping or cutting during cryosectioning and no differential compression during cutting or retrieval of sections (Hall & Gupta, 1982).

ii) that no differential swelling or shrinkage of the specimen and peripheral standard occurs during processing. Hall & Gupta (1982) state that errors introduced by these problems tend to average out, at least for intracellular elements and if the analysis is performed on numerous sections. The major advantage of this technique is that since it makes no assumptions or use of the background no errors are introduced by this measurement (see C-N method below).

3.9.2. Continuum-normalisation

This method makes use, not only of the proportionality between characteristic intensity and number of atoms of an element, but of a similar relationship between the background intensity and total tissue mass to give a measurement of elemental mass/unit tissue mass (termed the "mass fraction"). Hall (1971) gives the equation in a form which is

applicable to biological specimens where elemental concentrations are <5% as:

$$C_x = R_x A_x G_x \sum_m (C'Z^2/A) \quad \text{-----8}$$

where : C_x = the mass fraction of element x
 R_x = (characteristic counts element x/continuum count)_{spec} / (characteristic counts element x/continuum count)_{stan}
 G_x = $N_x / \sum(NZ^2)$ in the standard for element x
 A_x = atomic weight of element
 $C'Z^2/A$ = a matrix factor to account for the contribution to the background of light elements that do not produce characteristic radiation. See Hall (1971) for the general derivation.

The standards used in this method need to satisfy several criteria. They must: a) contain the element of interest, b) be of known composition, c) be thin i.e. so that measurements will not be affected by X-ray fluorescence and absorption and d) be homogeneous (Hall, Anderson & Appleton, 1973)

Once the standard values (needed for equation 8) for the elements of interest have been calculated the only quantities that need to be measured from the specimen are those in the numerator of the R_x value. The background counts are normally measured in a region of the spectrum free of characteristic peaks. For a worked example see Hall *et al.* (1973).

3.9.2.b. Advantages and Disadvantages

The major advantage of this method is that it is independent of variations in section thickness since the ratio of characteristic/background is simultaneously calculated in the same area. The method is suitable for the quantitative analysis of frozen-hydrated sections and for the calculation of water content, which can be found by measuring the background, first in the frozen-hydrated state, and then in the freeze-dried state (assuming a correction factor for the lateral

sections and for the calculation of water content, which can be found by measuring the background, first in the frozen-hydrated state, and then in the freeze-dried state (assuming a correction factor for the lateral shrinkage that occurs on drying, neglecting the small change in the matrix factor due to the loss of water and assuming that the section was fully hydrated initially). The disadvantages lie in the assumptions made in equation 8 and in the measurement of the background. Firstly, the Kramers equation, used to calculate the total mass of the section from the spectrum, is initially based on a crude assumption. However, although a more accurate theory for background production now exists, the modified Bethe-Heitler (MBH) (Chapman *et al.* 1983; Nicholson & Chapman, 1983), Shuman, Somlyo & Somlyo (1976) calculated that the approximation, (n_w) is proportional to $\sum NZ^2$ (Hall & Gupta, 1984), is adequate at least up to $Z=21$ i.e. the elements of biological interest. Secondly, the matrix correction Z^2A is only an approximation for the elements not measured. In biological material the major elements not measured are C, N and O and Hall (1971) calculated the correction factor for a typical matrix to be 3.28. The variations in Z^2A for different matrices are small (Hall, 1979), except for water (important in analysing frozen-hydrated sections). However, the most important factors that affect the accurate measurement of the specimen background are contamination, mass loss and extraneous contributions from non-specimen regions. Contamination is unlikely to be present in a "clean" microscope system with a good anti-contaminator but, if it were, the effect would be to increase the apparent mass of the section and decrease the P/B and the mass fractions of the characteristic elements. Mass loss, which is generally regarded as a loss of the organic matrix in biological sections, is dependent on i) the composition of the specimen, ii) the electron dose and iii) on the temperature at which analysis is performed:

i) A rapid loss of mass has been reported from gelatin (Stenn & Bahr, 1970), Spurr's resin (Halloran & Kirk, 1979) and dextran (Tormey, 1979). Although Bahr, Johnson, & Zeitler (1965) reported losses of between 10-90%, depending on the composition of the polymers they studied, the mass loss normally found for organic matrices in biological EPXMA is 20-40% (Hall *et al.* 1973; Hall, 1979) under most operating conditions.

ii) Mass loss occurs at electron doses below those usually used for EPXMA (Bahr *et al.* 1965). Hall (1979) calculated that, for biological specimens, mass loss would occur at doses of approximately 1.8×10^{-9} C/ μm^2 , a dose which is exceeded in almost all instances of practical EPXMA. iii) Low temperatures have been used to prevent mass loss (Hall, 1979; Hall & Gupta, 1974) and can reduce the loss to a negligible level, although Egerton (1980) calculated that the resistance to beam damage at low temperature may be no more than 100 fold compared to room temperature analysis. In contrast to the loss of mass from the organic matrix the loss of characteristic counts in biological tissue has only been reported for sulphur in albumin standards (Rick *et al.* 1982) and Ca and P in dentine (Edie & Glick, 1979). For Na, K, and Cl in freeze-dried albumin standards Rick *et al.* (1982) found no loss at room temperature even with a 1000 fold increase in current dose cf. the losses encountered in microdroplet analysis (Roinel & LeRoy, 1980; LeRoy & Roinel, 1983; Morgan & Davies, 1982). Finally, the extraneous contribution to the background is the most hazardous aspect of the C-N method and this can arise from a number of sources. The steps taken to reduce this contribution include the careful collimation of the incident electron beam and the reduction of the mass of solid material above and below the specimen to the minimum mechanically feasible. Constructing these regions from low Z materials also reduces X-ray production (Nicholson *et al.* 1982). There are two approaches which can be taken to reduce the residual extraneous contributions, normally from the specimen rod and the immediate surrounds. The first is to build these regions from a low Z material such as C or Be (Russ, 1977; Saubermann *et al.* 1981; Panessa *et al.* 1978). These materials will, however, leave an unknown background which may be large (Nicholson & Chapman, 1983) and cannot be calculated. The second method is to construct the remaining components of a material which produces a characteristic peak which, with reference to a pure spectrum of that element, can be deducted from the specimen background (Nicholson & Dempster, 1980; Nicholson & Chapman, 1983). The only important consideration with this route is that the material chosen should not produce a characteristic line in a region of interest (Hall, 1971).

3.9.3. Standards

Both techniques require the use of standards to produce quantitative results. The peripheral standard in the C-A method serves as a standard for all the elements of interest (Rick *et al.* 1979) and when used for the C-N method and frozen-hydrated sections can give an indication of the degree of tissue hydration at the time of analysis (Hall & Gupta, 1982; Gupta & Hall, 1979; 1981). A large number of standards have been used for quantitation by the C-N method including; organometallic compounds (Roomans & van Gaal 1977; Spurr, 1975), aminoplastic standard (Roos & Barnard, 1984) and mineral salts (Hall, 1971; Hall *et al.* 1973; Nicholson & Dempster, 1980). Standards that resemble the specimen in terms of matrix composition and mass thickness have been used to eliminate errors in the quantitation due to the Z^2 assumption and because the instrumental contribution to the background will be similar to that from the specimen. Nicholson & Chapman (1983) have shown that where there is no alteration in the mass of the specimen or standard due to radiation damage and contamination the use of such standards is advantageous. However, they also showed that in a well-designed electron microscope with minimal instrumental contribution, which can be quantified, that large differences in mean Z and mass thickness of specimen and standard do not pose any problems and that mineral standards offer the advantage of good counting statistics and stability in the beam.

3.10. CHARACTERISTICS OF THE ELECTRON MICROSCOPE AND QUANTITATION METHODS USED IN THIS WORK

3.10.1. Electron Microscope

A JEOL JEM 100C transmission electron microscope fitted with a Link Systems 290 Analyser and a Kevex energy dispersive SiLi detector (30 mm² crystal, resolution = <160eV at 5.9KeV) was used throughout this study. The quantitation method used in this thesis was based on the Hall continuum normalisation method. As explained in the introduction (3.5.4.b), the Hall continuum-normalisation method of quantitation

requires that the origin and intensity of the background be accurately determined. To reduce the instrumental contribution to the background certain modifications have been made to the microscope used in this study.

3.10.1.a Microscope Modifications

The modifications made to the analysis system have been described in detail elsewhere (Nicholson, Robertson & Chapman, 1977; Nicholson & Dempster, 1980; Nicholson *et al.* 1982) but briefly are as outlined below: i) Any solid material in the vicinity of the specimen that was unnecessary was removed. Any remaining solid structures which produce X-rays and can be "seen" by the detector were constructed from aluminium and any solid materials which contributed only to the scattered electron background were constructed from, or coated with, carbon. ii) The collimation of the incident electron beam was improved by the use of thick condenser apertures (>0.25 mm molybdenum or platinum) to prevent electrons outside the main beam generating X-rays. A lead aperture located in the anti-contaminator ensures that no high energy X-rays generated high in the column reach the specimen. iii) The specimen surrounds were constructed from elements of low atomic number and were modified to increase the solid angle of the free space beneath the specimen. The anti-contaminator was remade in aluminium and the internal surfaces were coated with carbon to reduce scattering. The lower hole in the anti-contaminator was enlarged, the phosphor bronze spray aperture in the lower bore of the objective lens polepiece was removed and a new aluminium guard tube was made to mask the upper part of the lower polepiece. The objective aperture rod was shortened so that it is ~10 mm from the specimen when the aperture mechanism is withdrawn. iv) The specimen rod was remade in aluminium, retaining as little solid material above and below the specimen as possible. The top plate of the rod is the only solid material above the specimen and can be constructed from aluminium, titanium, magnesium or copper depending on the aims of the experiment. v) The X-ray detector collimator was redesigned using lead, coated with carbon, to prevent electrons being scattered onto the detector window and to prevent high energy X-rays

being transmitted through the collimator walls. vi) One hole (0.8 mm diameter) specimen mounts (3 mm diameter) of titanium and copper were used exclusively in place of the conventional mesh grids (Nicholson, 1974).

To reduce mass loss, a specimen rod capable of achieving a tip temperature of $\sim -160^{\circ}\text{C}$ to -170°C was developed (Nicholson, Biddlecombe & Elder, 1982). The rod was made to a similar design to the room temperature rod described above except that the region in which the specimen is held was made from very pure copper rather than aluminium. A new anti-contaminator was designed to replace the commercially available model which could not reach sufficiently low temperatures to prevent contamination of the specimen. The major difference in design was to locate the liquid nitrogen tanks, used to cool the anti-contaminator, inside the microscope column. The region of the new anti-contaminator immediately around the specimen was of a similar construction to the modified commercial model described above. The stability of the rod and the thermal performance of the rod and anti-contaminator have been fully described elsewhere (Nicholson *et al.* 1982).

In the present study the use of low temperatures ($\sim -160^{\circ}\text{C}$) prevented the loss of approximately 16% of the section mass when compared to analysis at room temperature. Whether measurements and analysis at the low temperature represent no organic mass loss or merely a relatively smaller loss compared to room temperature analysis cannot be determined. (See Appendix 3 for experimental details) It appears that, if analysis is performed at room temperature, the organic mass loss will result in a 16% overestimate of the mass fraction which must be taken into consideration when comparing results with those obtained at low temperature.

3.10.2. Spectrum Quantitation

Once the modifications were made to the microscope, any remaining instrumental contribution to background was measured and removed by the method given in Nicholson & Dempster, (1980). A spectrum was recorded from the interfering solid instrumental peak under

identical conditions to those used for analysis of specimens. A "white" window was selected as a region from which to calculate specimen mass, in this study a 5 keV window centred on 12 keV (a region free of characteristic peaks), and the ratio of characteristic counts in the interfering instrumental peak to the number of counts in the "white" window was calculated. With the analytical conditions used in this study it was found that for every 1000 counts in the titanium or copper instrumental peak there were 9.86 and 10.33 counts respectively in the "white" window. These white solid correction factors were incorporated in the quantitation programme. The calculation of the number of characteristic counts in each specimen elemental peak was performed using a straight line background subtraction technique. In spectra from biological specimens the close grouping of the characteristic peaks in the region 1keV to 3keV makes it difficult to place background windows for every peak. The technique described by Nicholson & Dempster, (1980) was used and this involved placing a window (~9 channels) on either side of the group of peaks, phosphorus to chlorine. From plots of typical experimental spectra a factor was calculated for each element which relates the true straight line background, h_2 , to the average straight line background, h_1 , calculated from the two background windows and these were written into the quantitation programme. The number of counts in the characteristic peak is then:

$$\text{peak} = P - \frac{1}{2} (B_1 + B_2) \times k \quad \text{-----9}$$

where : k = correction factor, h_2/h_1

Schematically, both principles are shown in Fig.3.5.

The channel widths (20 eV) used throughout the project were:

Sodium	5
Chlorine	7
Potassium	9
Calcium	9
Titanium	13
Copper	13

The characteristic peak of calcium was deconvoluted by calculating, from a pure potassium standard, the ratio of counts falling in the potassium $k\alpha$ window to the number of counts falling in the calcium $k\alpha$ window, which were due to the potassium $k\beta$ peak. By setting the appropriate background windows this correction factor was calculated and found to be 0.062. This value was also built into the quantitation programme and operated in a similar way to the white solid correction factors above.

3.10.3. Analysis Conditions

Analyses were performed at 80 kV for 100s live time, in the cold specimen rod tilted to 30° from the horizontal, at -160°C for the rat footpad study and at room temperature for the human and horse gland. The modified anti-contaminator was used throughout the study at temperatures of ~-170°C. Beam diameter was typically 200 nm although this varied depending on the ice crystal damage present in the section. Beam current was measured with a collection plate (Nicholson, 1981), accurate to ± 5%, and was found routinely to be about 0.4nA. As explained by Nicholson & Dempster (Discussion pp 529, 1980), provided the specimen can withstand the current focussed into the spot size and the X-ray analysis system is not overloaded with counts, the beam current is relatively unimportant since the characteristic peak is normalised to background and the effects are generated simultaneously. The detector window was placed 30mm from the specimen and the zero and peak calibration were checked prior to each analysis run.

3.10.4. Standards Used in this Study

The various standards that can be used in the Hall method need only be of known composition and thin enough to allow complete transmission of the electron beam. Standards used in this thesis included human enamel (calcium & phosphorus), Jadeite (sodium), solutions of sodium chloride, potassium chloride and potassium dihydrogen phosphate dried on one hole mounts, carbon coated and analysed at -165°C in the cold rod. The most reproducible results were obtained with enamel (for calcium),

Fig.3.1. Diagram showing the most common methods used for the preparation of biological material for EPXMA.

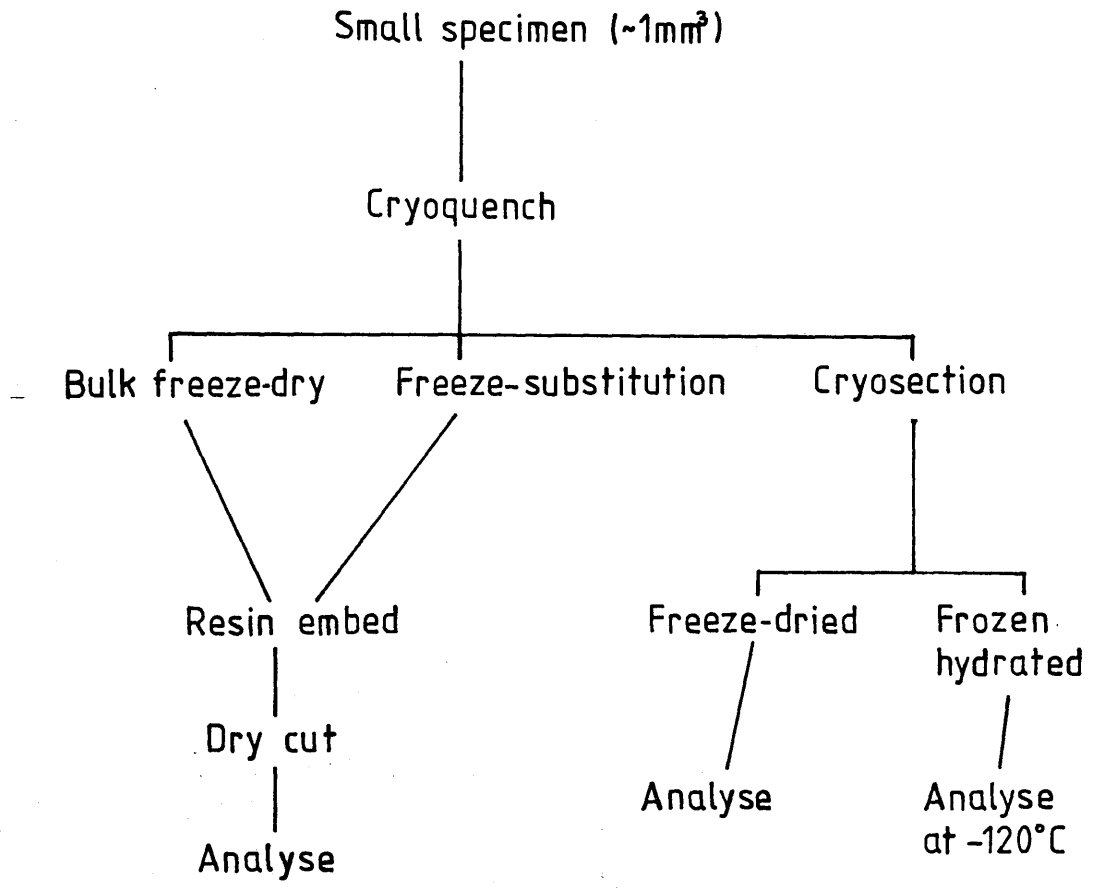
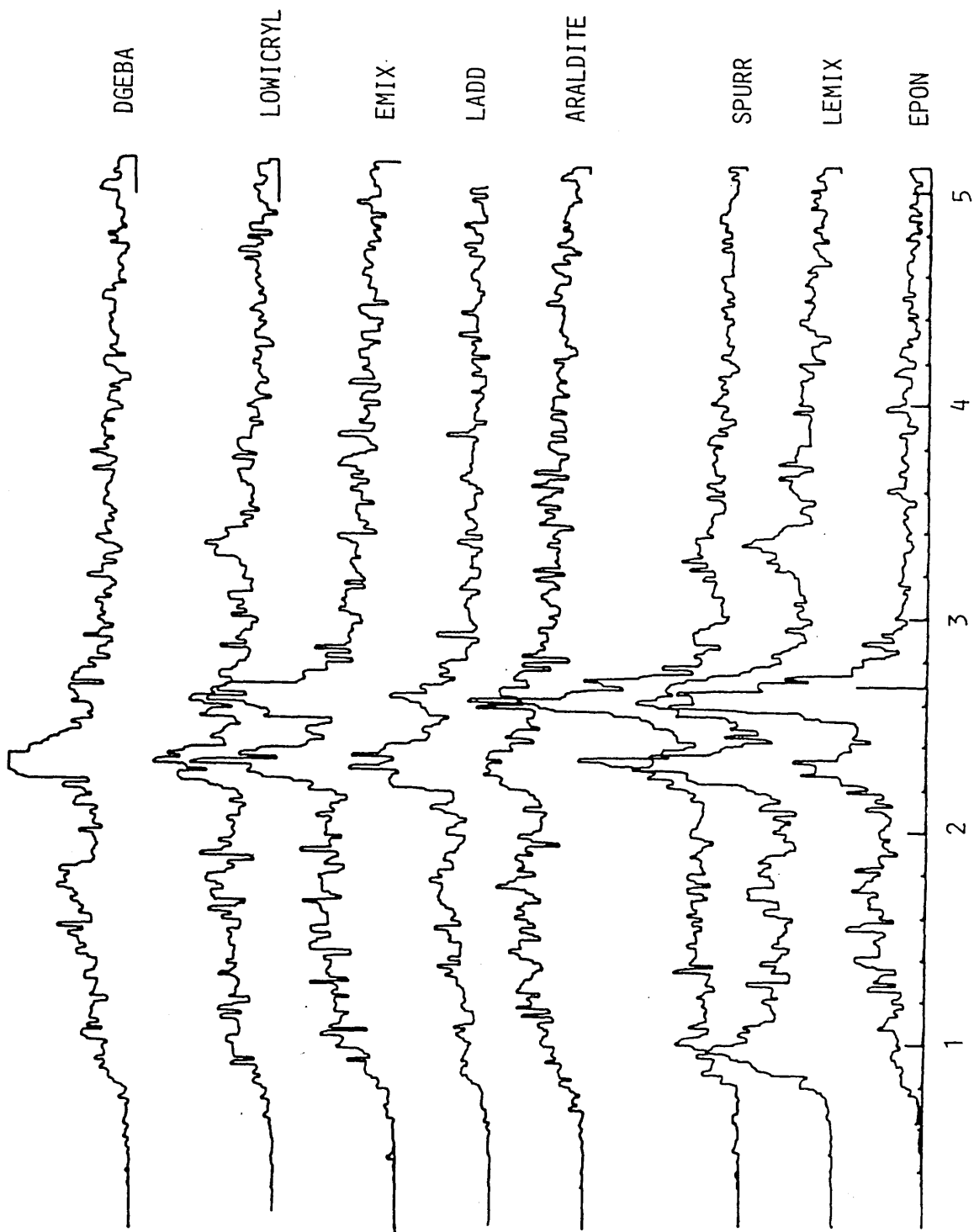


Fig.3.2. X-ray spectra from sections of routine laboratory embedding media showing the elemental composition in the energy range 0keV to 5keV. Araldite has the fewest contaminants and was the embedding medium used for all EPXMA studies in this thesis.



X-ray Energy (keV)

Fig.3.3 Physical basis of X-ray generation in the electron microprobe. Right half of the figure illustrates generation of characteristic X-rays. (1) An electron in the beam impinges on an atom and (2) knocks out an electron in an inner atomic orbit. The incident (3) and the ionised (4) electrons leave the atom, and (5) an electron from an outer orbit "drops" into the vacated orbit. The loss of energy in this transition is emitted as characteristic X-ray quantum. Left half of the diagram illustrates the generation of X-ray continuum. An incident electron (A) is decelerated (B), resulting in the emission of a quantum (C) in the X-ray continuum.

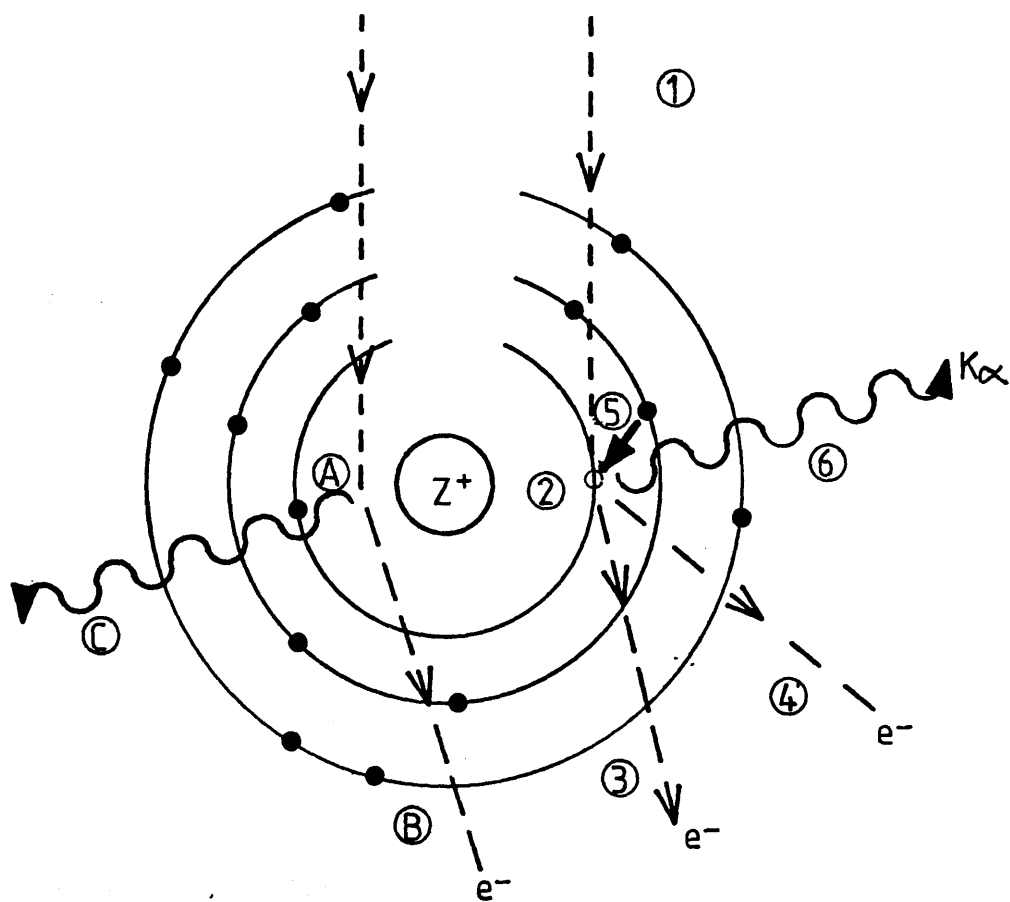


Fig.3.4 A typical spectrum from the sweat gland secretory epithelium, as recorded by the energy-dispersive X-ray spectrometer used in this study, illustrating the characteristic peaks and the background on which they are superimposed.

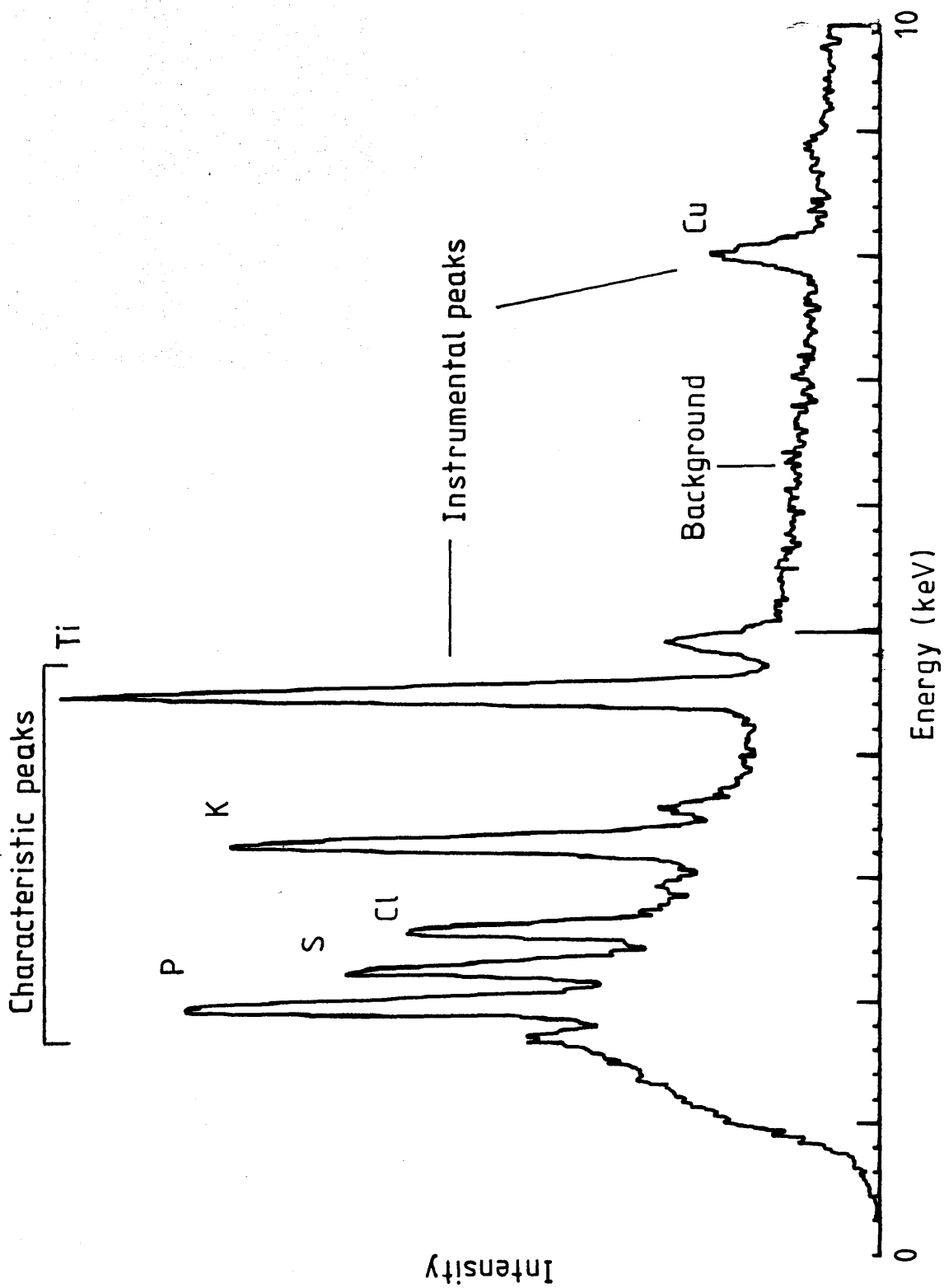
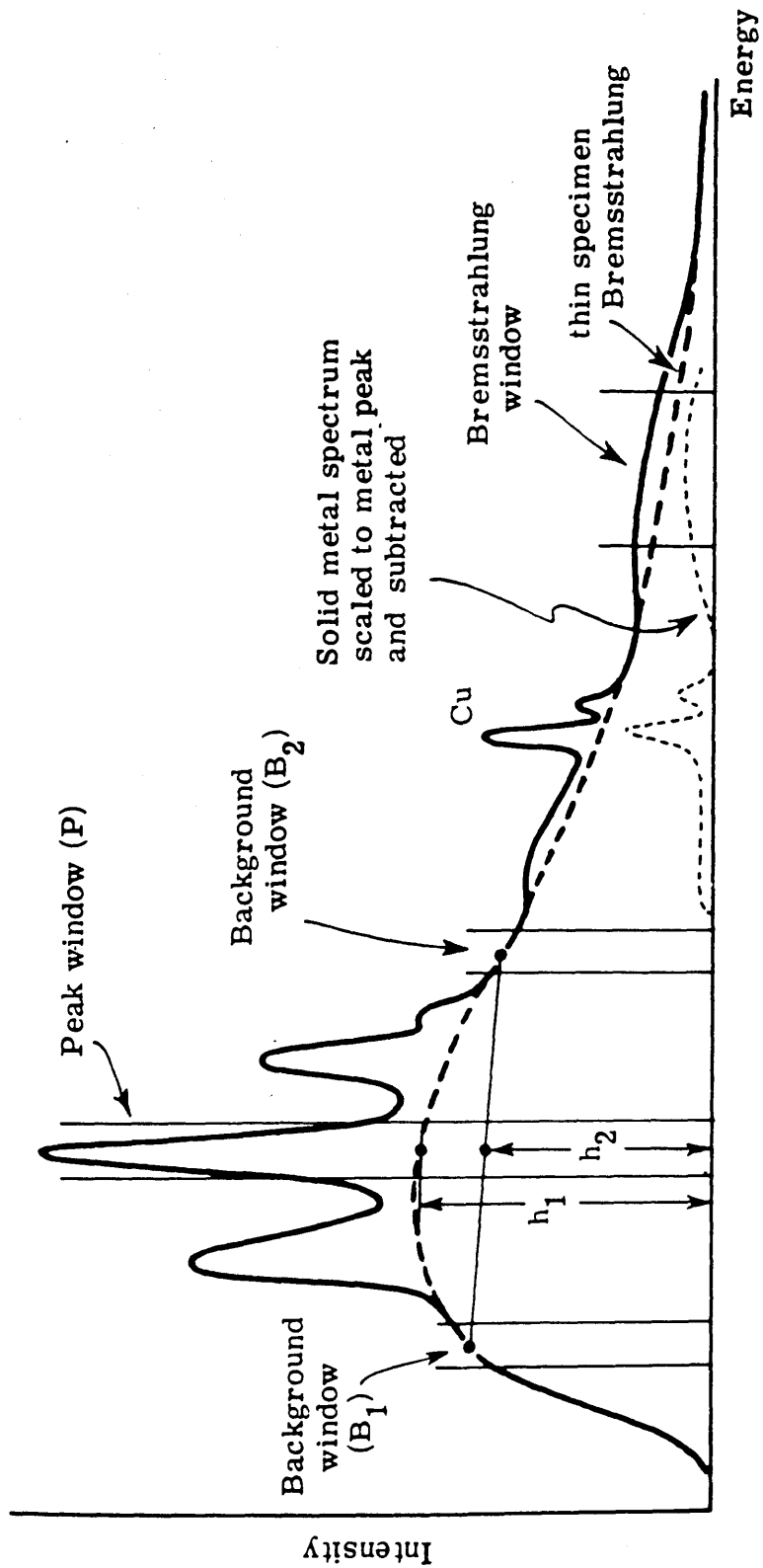


Fig.3.5. Methods for calculating characteristic peak counts and correcting spectra for instrumental background/Bremsstrahlung (Nicholson & Dempster, 1980)



$$\text{Peak} = P - \frac{1}{2}(B_1 + B_2) \times k$$

$$\text{Correction factor, } k = h_1/h_2$$

CHAPTER 4 DEVELOPMENT OF A CRYOULTRAMICROTOME.

4.1. INTRODUCTION

4.1.1. The Ultramicrotome Cryostat

4.1.2. The Ultramicrotome with Cryochamber Attachment

4.2. SPECIFIC PROBLEMS ASSOCIATED WITH THE SORVALL MT2B WITH FTS CRYOATTACHMENT

4.3. METHODS

4.3.1. Reconstruction of Microtome Surrounds

4.3.2. Trimming Assembly

4.4. PERFORMANCE TESTING

4.4.1. Trimming Assembly

4.4.2. Cryochamber

4.4.3. Cantilever Arm

4.4.4. Cryotransfers

4.5. ASSESSMENT OF THE MODIFIED CRYOULTRAMICROTOME

4.6. SECTIONING PROCEDURE

4.7. BIOLOGICAL RESULTS

4.8. DISCUSSION

4.1. INTRODUCTION

The use of cryoultramicrotomy as a preparative method for the electron probe X-ray microanalysis of biological material was first reported in the early 1970's (Davies & Erasmus, 1973). Prior to this date cryosectioning had been used to: i) demonstrate that the appearance of conventionally fixed electron microscopical samples was not artefact (Fernandez-Moran, 1952); ii) enable autoradiographic study of soluble compounds (Appleton, 1977); iii) increase the productivity of histochemical laboratories (Doty, Lee & Banfield, 1974). The specimens used for these purposes were usually chemically pre-fixed and subjected to several other procedures (Bernhard & Leduc, 1967) that would be unacceptable for the preparation of specimens for the EPXMA of diffusible elements. With improved methods of cryofixation an increasing number of investigators turned their attention to the problems of cutting ultrathin, fresh-frozen sections, both to improve its application to the procedures outlined above (Hodson & Marshall, 1969, 1970; Christensen, 1967, 1971) and for X-ray microanalysis (Davies & Erasmus, 1973). These groups, and others, independently developed systems for what had now become known as "ultracryotomy" (Hodson & Marshall, 1970) or more generally as cryoultramicrotomy. The types of microtome used belonged to one of two categories, each with its own advantages and disadvantages.

4.1.1. The Ultramicrotome Cryostat

In this system a cold environment is achieved by the incorporation of a standard ultramicrotome in a low temperature cabinet (Bernhard & Leduc, 1967; Appleton, 1974). These cryostats have good thermal stability and extensive space for manipulations. However, as the ultramicrotome must be adapted to function at low temperatures this method is also expensive, requiring an ultramicrotome dedicated entirely to cryosectioning. The cryostat systems have been used mostly, although not exclusively (Appleton, 1974; 1977) to cut thicker sections at warmer temperatures than those normally employed in cryoultramicrotomy.

4.1.2. The Ultramicrotome With Cryochamber Attachment

In this instrument the cold environment is confined to the region around the specimen and knife. With the cryochamber attachment the knife and specimen may be cooled either separately by their own individual cold gas or liquid nitrogen supply (Seveus, 1978; Dollhopf & Sitte, 1969; Sitte, 1984) or by the cooling of the whole sectioning environment, as in the Sorvall ultramicrotome used in this study (Christensen, 1971). The cryochamber attachment has the advantage that it can easily be fitted to existing ultramicrotomes, but offers cramped conditions (Iglesias, Bernier & Simard, 1971) and, potentially, a less stable thermal environment. Irrespective of the type of microtome used or the route taken to achieve the necessary cooling several well-accepted criteria for successful cryoultramicrotomy now exist. All cryosectioning systems require a cold dry environment (Pearse, 1980), rigid specimen mounting (Appleton, 1974) and stable knife (Saubermann, 1980) and cryochamber temperatures (Doty *et al* 1974).

4.2. SPECIFIC PROBLEMS ASSOCIATED WITH THE SORVALL MT2B AND FTS CRYOATTACHMENT

The specific problems associated with the Sorvall system were: i) condensation of water from the room atmosphere and subsequent ice formation around the rim of the cryochamber and microtome head, resulted in ice crystals falling into the cryochamber. This reduced the duration of cutting and severely impaired freeze-drying; ii) in obtaining a trimmed specimen, which is required for serial sectioning (Appleton, 1974). The cramped conditions within the cryochamber made trimming difficult and while trimming under liquid nitrogen (Christensen, 1971) was an improvement, the bubbling of liquid nitrogen (LN₂) impaired visualisation. This work describes attempts to satisfy the criteria given above and overcome the initial problems found in using the Sorvall system and to then use this modified cryoultramicrotome to cut sections of rapidly frozen biological tissue, particularly sweat glands.

4.3. METHODS

4.3.1. Reconstruction of Microtome Surrounds

The entire microtome, excluding the low temperature controller (LTC), viewing microscope and light source, was encased in a large wooden box sealed at the joins with silicon rubber and heavy duty insulating tape. A perspex front portion enabled viewing of the cryochamber and working areas. All manipulations within this box were performed using long-sleeved rubber gloves fitted to specially designed ports (6 & 7; Fig.4.1.). The microtome on/off switch was transferred to a foot pedal and the remaining ultramicrotome controls, for section thickness and cutting speed, were operated through rubber gloves on ports 1 & 7 (Fig.4.1.). The insulated pipe for cold N₂ gas, from a 25 litre dewar, was channelled through a diaphragm on port 5 (Fig.4.1.). Inlet points for dry N₂ gas, from a cylinder (BOC Ltd.) enabled the box to be flushed with dry gas before and during cryosectioning. A perspex shelf was constructed at the level of the cryochamber base to provide a firm support for the trimming assembly (described below) and a convenient storage area for instruments. Specimens and instruments could be introduced through ports 2, 3 & 4 (Fig.4.1). The temperature sensor (TS) was removed from the microtome head and placed near the cutting edge of the knife (Fig.4.3.).

4.3.2. Trimming Assembly

To enable low temperature trimming of the specimen on its stub within the box a trimming assembly was constructed (Fig.4.2.). The base of the assembly (T; Fig.4.2.) was made of polyset polyurethane (Tufnol Ltd.) and was fastened to the perspex shelf by two wing nuts. A shaped copper block, surrounded by a sheet of expanded polystyrene to increase the insulation, (CB; Fig.4.2.) was screwed firmly to the top of the polyurethane base and was cooled via thick copper braid (CU) immersed in a reservoir (R; Fig.4.2.) of LN₂ filled from the outside via a pipe (I; Fig.4.2.). The microtome head (MH; Fig.4.2.), which fitted precisely into

the copper block, was held in place by a screw (HC; Fig.4.2.) in the side of the assembly. The temperature of a specimen in the microtome head could be adjusted by varying the flow-rate of cold, dry nitrogen gas through a jet (J; Fig.4.2.) cooled by passing through a copper coil (C; Fig.4.2.) immersed in the LN₂ reservoir. The trimming assembly was carefully positioned in the box equidistant with the knife edge from the central pillar of the viewing microscope which could, therefore, be easily swung from one position to the other. In addition, the height of the assembly was accurately determined so that the tip of a specimen on its stub, clamped within the microtome head in the trimming position, was at the same height as the knife edge. The microscope did not, therefore, require refocussing when changing viewing positions. The focal distance of the microscope was increased by a supplementary lens and by the addition of a spacing ring to the microscope central supporting pillar. The illumination of the cryochamber, the trimming assembly and the working areas was improved by the addition of a fibre optic light source (F; Fig.4.1.). An anti-roll plate, constructed from a Teflon-coated sliver of cover-slip, could be positioned above the knife edge using micromanipulators (M; Fig.4.1.) operated through ports 6 & 7 (Fig.4.1.). A modified knife-holder was manufactured to enable sectioning with single-edged steel knives (Schick).

4.4. PERFORMANCE TESTING

To determine the thermal characteristics of this modified system and the temperatures experienced by a "specimen" throughout the procedures involved, a series of thermocouple measurements was undertaken. The measurements were made using copper/constantan thermocouples linked to a ten channel digital thermometer (Comark 5000, Comark Ltd.). This recording system was accurate to one degree and could follow temperature changes of 200K/s. It was calibrated against boiling LN₂, subliming solid carbon dioxide and melting distilled water.

4.4.1. Trimming Assembly

The temperature of the trimming assembly was measured at three points: i) the copper block of the assembly (CB; Fig.4.2.), ii) the microtome head (MH; Fig.4.2.) and iii) in a simulated specimen formed by embedding a thermocouple (diam.~0.4mm) in a drop of polyvinylpyrrolidone (PVP; m.w.=40,000) on a stub. The tip of the thermocouple was bent back until it just protruded from the PVP. Thermal stability was reached at all three regions within 30min of addition of LN₂ to the reservoir irrespective of whether or not the N₂ jet was activated. Fig.4.4. shows the temperatures recorded by the 3 thermocouples at 4 different N₂ flow rates through the jet (readings taken every 30s). Although shown only for 10min periods, the approximate duration of trimming, these stable temperatures could be maintained for upto 1h. The temperature of the specimen was mainly dependent upon the N₂ flow rate and could therefore be set at an appropriate level merely by adjusting the flow rate from the N₂ cylinder and it was important to ensure that the short path from the jet to the specimen was not obstructed. At all flow rates the temperatures of the copper baseplate and the microtome head were very similar except at the highest pressure (15psi), where the microtome head was colder. This was due to the direct influence of the jet which at this pressure produced LN₂ rather than cold N₂ gas. However, the level of LN₂ in the reservoir was also an important feature in maintaining the thermal stability of the entire assembly. If the level fell below 1 inch of the upper lip the temperature rapidly rose and this was most pronounced at the highest flow rate.

4.4.2. Cryochamber

Nine thermocouples were sited in the cryochamber as shown in Fig.4.5. Once a steady temperature had been reached (approx. 30min after transfer of the specimen to the chamber) the readings were recorded at 30s intervals for periods of upto 1h. The figures in Table 4.1. are the means of 60 recordings, taken at 30s intervals, from the nine sites, clearly show that there was a difference of ~40° from the bottom to the

top of the chamber at equilibrium. In addition, the temperature at the same level within the chamber varied by as much as 10°. The outstanding feature, however, was the remarkable stability at all sites, which could be maintained as long as LN₂ supplies permitted. Fig.4.6.a shows the temperature recorded at 5 points within the cryochamber during the cutting stroke of the microtome. At a temperature setting of 193K the knife edge was 9° warmer and the simulated specimen 16° warmer while the temperature of the gas adjacent to the knife was within 4° of the setting. Despite these differences in temperature, the entire arrangement, as for the trimming assembly, was thermally very stable, even during the cutting cycle. Removal of the standard perspex baffle plate (B; Fig.4.3.) from the cryochamber considerably increased the variability of the temperature of the gas at the knife edge. Fig.4.6.b demonstrates the temperature fluctuating regularly by 5-6° corresponding to the switching on and off of the cooling system. Similarly, at control settings of 223K and 153K (Fig.4.7.), the temperatures were warmer than the setting but were still stable throughout the recording period. To obtain the desired temperature within the cryochamber for cutting and freeze-drying, the LTC had to be offset by an amount determined from these experiments/measurements.

4.4.3. Cantilever arm

Fig.4.8. shows the temperature of the cantilever arm measured at the 4 points shown in Fig.4.5., and although a thermal gradient existed along its length this was again very stable with little or no temperature change during the 30min period shown.

4.4.4. Cryo-transfers

The thermal history of the simulated specimen from storage in LN₂, through the trimming procedure, to the cryochamber is shown in Fig.4.9. During the initial transfer from storage into the cooled microtome head the specimen temperature rose rapidly for 5-10s then returned to the preset temperature of the trimming assembly. At no stage was the

temperature warmer than 140K. During trimming there was no significant temperature rise although fluctuations of $\sim 5^\circ$ were observed, especially when loosening the clamping screw to turn the specimen. The second transfer, from the trimming assembly to the cryochamber, was accomplished in <5s using the gloves on ports 6 & 7 (Fig.4.1.). There was a rapid rise in specimen temperature which then equilibrated to the cryochamber temperature over the next 15-30min.

4.5. ASSESSMENT OF THE MODIFIED CRYOULTRAMICROTOME

Encasement of the microtome to provide an environment of dry N_2 gas combined with the evaporation of N_2 from the cryochamber and trimming assembly greatly reduced the frosting originally encountered and, with careful and regular use, the system proved to be completely frost free. The new trimming assembly provided a convenient means of shaping the tissue, and by selecting a temperature at which freeze-drying is minimal i.e. 123K or colder, this step will not compromise subsequent processing, especially in the preparation of frozen-hydrated sections. Trimming, however, was not always deemed necessary, particularly if the "natural" surface of the specimen appeared to be small and suitable for sectioning. This could be achieved for sheets of tissue or for small spindle-shaped tissues by placing them on a shaped specimen stub prior to cryoquenching. Although this was impossible to achieve for irregularly shaped samples such as rat footpad, in which the exact location of the sweat glands to be studied was not known, trimming was rarely performed for reasons explained later. The manipulations involved in section cutting and transfer were not severely impaired by using rubber gloves, particularly when combined with the improved optical arrangements and the on/off pedal for the microtome. The evidence presented here does not support the view that a stable environment cannot be achieved with the commercially available Sorvall system cooled by intermittent gas supply (Saubermann *et al.* 1981). What it does indicate is that most cryochamber systems are likely to have considerable thermal gradients within the region of the specimen. The important points to determine are whether the knife and specimen

temperatures are stable throughout the cutting cycle. In view of the discrepancy between the LTC setting and the knife/specimen temperatures, these should be monitored as close to the specimen as possible, a point also noted by Seveus (1979) and Saubermann (1980). The cantilever arm of the Sorvall is designed in such a way that any thermally induced dimensional changes are likely to occur in the vertical rather than the horizontal direction. This, combined with the stable temperature gradient along the cantilever arm, indicates that alterations in section thickness are unlikely to occur through thermal expansion or contraction of the arm. The theoretical requirements and practical problems outlined in the introduction have been tackled. The modified system is capable of maintaining a stable thermal environment and provision has been made for the trimming of specimens under controlled conditions. The system was then used to cryosection biological material using, firstly, muscle as a model tissue and, secondly, rat footpad sweat gland in a study of the intracellular elemental basis of sweat secretion.

4.6. SECTIONING PROCEDURE

Small pieces of tissue ($<1\text{mm}^3$) were mounted on a small drop of viscous PVP within the conical tip of a brass or steel stub. Alternatively, small, thin sheets of tissue e.g. diaphragm ($4\text{-}6\text{ mm}^2$) were attached to the pyramidal shaped tip of a stub with a thin film of PVP. The stubs, with attached tissue, were rapidly cryoquenched in liquid propane using the method of Elder *et al* (1982) and stored in LN_2 until required. Before use, the microtome box was flushed with dry N_2 gas for approximately 15min. A specimen stub was taken from storage in LN_2 and transferred, in LN_2 within a polystyrene beaker (P; Fig.4.2.), to the microtome box through port 4 (Fig.4.1.). The stub was then rapidly transferred ($<5\text{s}$) to the precooled microtome head, locked in the copper block of the trimming assembly, and held tightly in place with a clamping screw (CS; Fig.4.2.). Trimming was performed with a precooled 4 inch pillar file with an insulated handle (TF; Fig.4.2.). Two sides of the specimen could be trimmed in this position and if a pyramid was required the stub could be loosened, turned through 90° and the remaining two

sides trimmed. The microtome head was then rapidly transferred (<5s) to the cryochamber and locked into place on the microtome arm. After equilibration (~30min) the specimen was manually advanced to the knife edge and the automatic mechanical advance of the microtome arm switched on. Sectioning was performed dry i.e. without a trough liquid, using either a glass, a diamond or a steel knife, precooled within its holder with clearance angles between 2-8°. Sections suitable for EPXMA appeared transparent and cellophane-like with occasional pink/green interference colours. Such sections were collected either with eyelashes on cocktail sticks or precooled dissection pins held in an insulated pin holder and transferred to cold Formvar-coated one hole aluminium, copper or titanium mounts placed on the shelf of the knife holder (Fig.4.3.). The sections were flattened on the Formvar film by placing a second mount on top of the first and gently pressing them together with a cold, polished copper rod. The mounts were then peeled apart and the sections, on the mounts to which they remained attached, left to freeze-dry on the knife shelf for 3h at 193K. The temperature of the shelf was then gradually raised to 213K over the next 30min, the mounts were transferred to a small, precooled dessicator in the cryochamber and warmed to room temperature over the following 60min. The dessicator was constructed from a contact lens case (Contactasol) the upper portion of which contained a copper mesh basket for supporting the mounts while the lower portion contained dessicant (Molecular sieve Type 4A; BDH Ltd.). The mounts were then removed and quickly placed within a vacuum-coating unit (Nanotech 250S) for deposition of a protective carbon film. Coated mounts were stored in a dessicator until required. Using this modified system freeze-dried sections were routinely cut between 0.2 and 0.5 μ m at temperatures between 233K and 153K.

4.7. BIOLOGICAL RESULTS

Sections cut from within the "vitreous" layer, ~0-10 μ m from the surface, showed little sign of ice crystal damage and possessed sufficient contrast to determine morphological detail. Fig.4.10. shows a longitudinal section of rat diaphragm cut from such a region at 193K. Although unfixed in the conventional sense and unstained it is clearly

possible to recognise the striation pattern and associated blood capillaries. Fig.4.11.a. shows the appearance of a section cut from deeper within a tissue block where the cooling rate is slower and ice crystal formation, and hence the danger of elemental redistribution, is greater. The micrograph is from a section of rat footpad sweat gland approximately 20 μ m from the tissue surface where ice crystals of 0.2 μ m diameter were present. The spectra shown in Fig.4.11.b were recorded using standard analysis settings (see 3.10.3.) within the regions shown. The solid line represents a spectrum from inside a cell of the secretory epithelium whilst the dotted line was obtained from the dense collagen surrounding the gland.

4.8. DISCUSSION

The macroscopic and microscopic appearance of the sections cut at 193K using the modified system are in agreement with sections from other workers (Seveus, 1978; McDowell *et al.* 1983). Blocks that did not produce transparent sections were rejected. Presumably this was indicative of poor cryoquenching, especially as it was difficult to cut sections from deeper regions, even within well cryofixed blocks. Once cut, the delicate sections still had to be collected from the knife edge, transferred to the mounts and flattened to obtain good contact with the support film. Although numerous pick-up devices have been developed, including the electrophorus (Hodson & Marshall, 1969), eyelash probes (Christensen, 1971), vacuum tweezers (Appleton, 1974), isopentane droplets (Saubermann, Riley & Echlin, 1977) and electromagnetic rods (Rick *et al.* 1982) it seems, as Sjoström & Valdré (1979) have also reported, that in the hands of the skilled operator, the eyelash probe is as convenient and successful as the more elaborate aids. The fine dissection pins used in this study produced fewer static charging problems but can easily damage the Formvar support. This problem is particularly acute where, for X-ray microanalytical reasons (Nicholson, 1974), single hole mounts with large areas of unsupported film are used. Similarly, the more complex press assemblies (Seveus, 1978) have little advantage over the copper rod method of Christensen (1971) in flattening sections. To date the majority of electron probe X-ray microanalytical studies utilising

cryoultramicrotomy has been performed either on isolated epithelial tissues (Gupta & Hall, 1979; Rick *et al* 1979) or on surface tissues with a repeating structure e.g. muscle (Somlyo, Shuman & Somlyo, 1977; Somlyo, Somlyo & Shuman, 1979). In both instances the specimens benefit from excellent cryofixation and, therefore, minimal ice crystal formation with the accompanying good sectioning properties and minimal danger of redistribution of diffusible elements. The study of structures in regions several 100's of microns from a free surface is bound to be complicated by the presence of ice crystal damage which is unavoidable with the current methods of cryofixation. However, it is still possible to obtain meaningful biological information from sweat glands in deeper regions, as demonstrated in this study, if the probe diameter is kept larger than the "ice crystals" present and the spectra integrated from a large area. The detection of expected Na/K ratios can act as a check on the reliability of the method (Somlyo *et al* 1977) i.e. a higher Na/K ratio extracellularly than intracellularly. In freeze-dried cryosections extracellular measurements are generally unreliable since elements are likely to be lost or translocated over large distances but if, as in this instance, the structure of interest is surrounded by dense connective tissue then such results may be of qualitative significance. This modified system was successfully used on a routine basis to cut cryosections of skeletal muscle and rat footpad. However, in the particular application to the study of diffusible elements in the rat footpad sweat gland a "targeting" problem was encountered. Over a 15 month period the success rate in locating glandular profiles in cryosections of skin reached only 3%. The most likely reasons for this low success rate were: a) the poor sectioning properties of the dense connective tissue which surrounds the glands b) the difficulty in locating a small gland within a relatively massive three-dimensional block. With no means of "targeting" the gland prior to sectioning it was a matter of luck whether a gland was found. It was for this reason that skin blocks were rarely trimmed, since by reducing the area for sectioning the situation could only become worse. It became necessary, therefore, to use a technique which allowed the glands to be spotted prior to ultrathin sectioning without seriously compromising the measurement of the intracellular elemental distribution. In this instance the route chosen was to bulk freeze-dry and

resin embed the tissue blocks and to cut 1 μ m "survey" sections to "spot" the glands prior to ultrathin sectioning on a dry diamond knife.

Fig.4.1. A photograph of the modified Sorvall ultramicrotome and cryoattachment (FTS). The viewing microscope remains outside the box and the controller (C) and digital thermometer (DT) were sited upon it. The trimming device (T) is situated within the box a short distance from the microtome. The inlet ports for the dry nitrogen (N) and the LN₂ supply (R) to the reservoir for the trimming device can be seen. The insulated inlet pipe supplying cold N₂ gas to the cryochamber enters through port 5. Ports 6, 7 and 8 are fitted with rubber gloves through which trimming (7 & 8) or section collection (6 & 7) can be undertaken. Ports 2, 3 and 4 enable transfer of materials to the box and cryochamber and the controls for section thickness can be reached through the rubber diaphragm, 1. A ninth port enables access to the lower regions of the box. The micromanipulator (M) used to operate the Teflon-coated glass antiroll plate at the knife edge can be seen on the left of the cryochamber.

Fig.4.2. (Left) A higher power view of the trimming device. This consists of a polyset polyurethane plastic base (T) and copper block (CB) cooled by thick copper braid (CU) immersed in a reservoir of LN₂ (R) which is filled from the outside through inlet tube, I. The detachable microtome head (MH) of the microtome arm has been fitted into the copper block, which was shaped to take it, and clamped using a copper screw (HC). The specimen on the stub (ST), clamped using a copper screw (CS), is thus cooled by the block and also by a jet of cold N₂ gas (J) played upon it. The gas is cooled by passing it through a copper coil (C) within the LN₂ reservoir. Stubs can be readily transferred from LN₂ in a storage cup (P) to the microtome head using cooled forceps. Trimming is undertaken using a cooled file with an insulated handle (TF).

Fig.4.3. (Right) A photograph showing the interior of the cryochamber. The baffle plate (B) can be seen. One hole mounts lie on the shelf surrounding the knife. The temperature sensor (TS) is situated in the chamber at the same level as the knife.

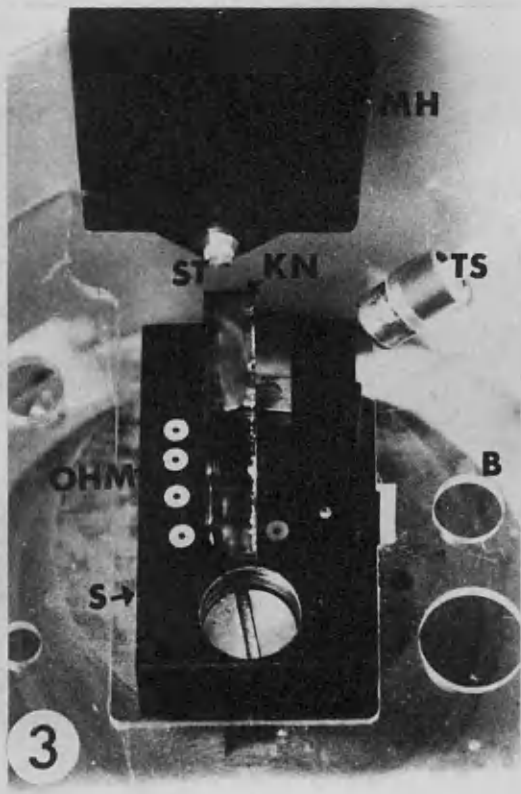
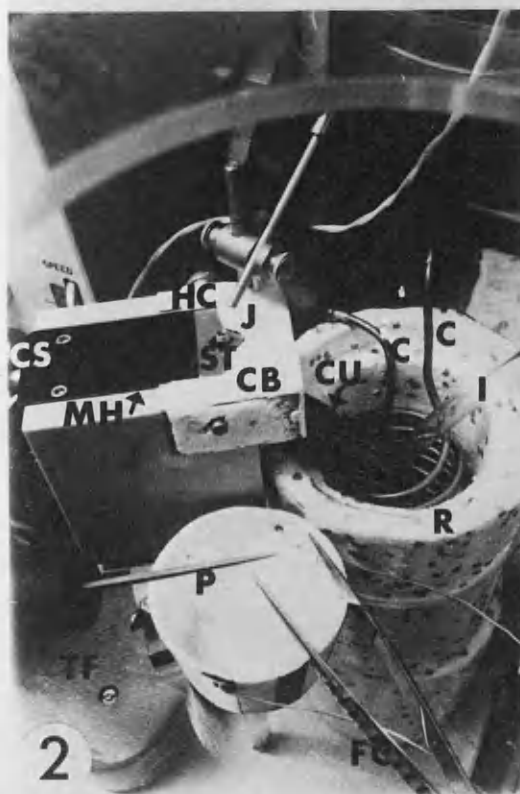
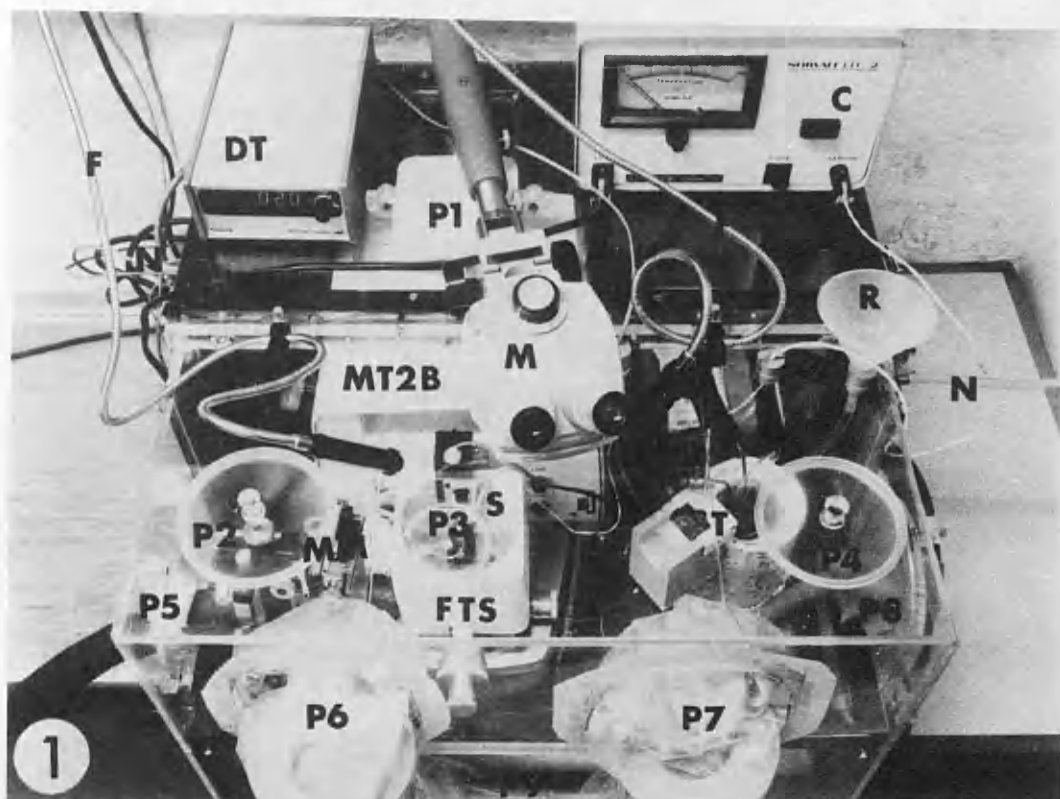


Fig.4.4 Graph illustrating the effect of different flow rates of cold N₂ from the jet on the temperature of the simulated specimen (▲), the copper baseplate (○) and the copper block (●). Temperature recordings were made every 30s.

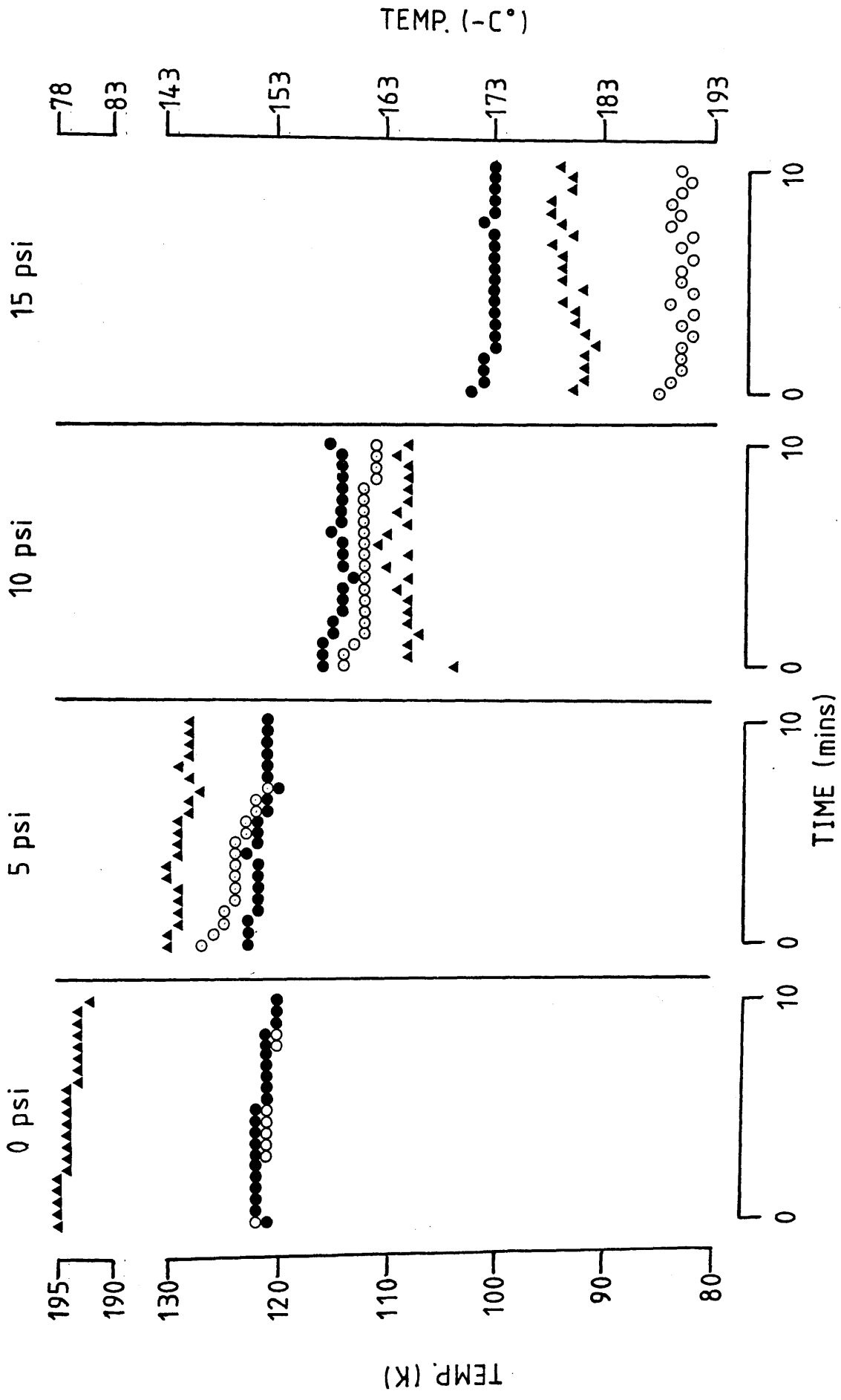
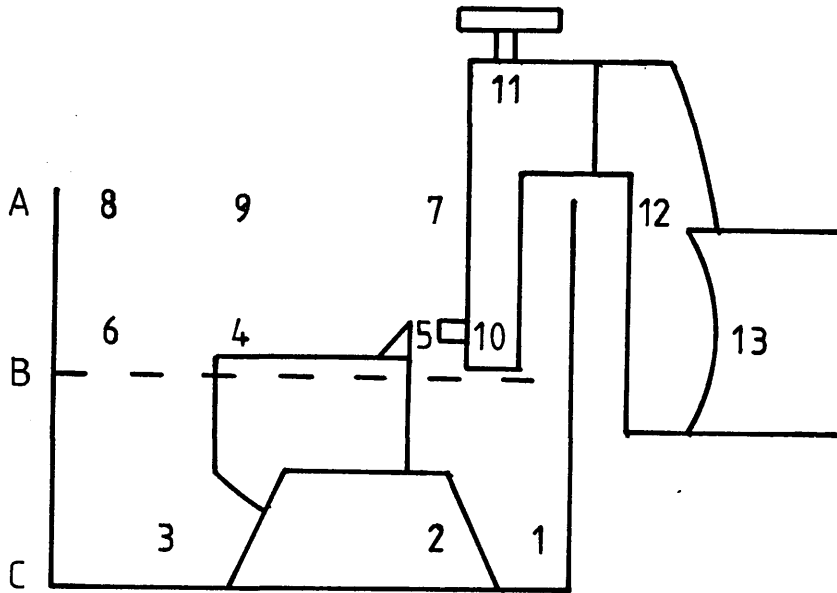


Fig.4.5. A diagram illustrating the levels and sites within the cryochamber from which temperature measurements (in Table 4.1.) were made. The thermocouple points on the microtome arm are also shown.

Table 4.1. Table of the temperatures recorded at the nine sites shown in Fig.4.6. The mean and S.D. were taken of the temperatures recorded every 30s at each site over a 30min period.



Thermocouple	Position in chamber	Temp. (K) $\bar{X} \pm \text{s.d.}$
1	25mm left of knife edge	188.7 ± 0.5
C 2	25mm right of knife edge	180.1 ± 0.3
3	40mm to rear of 2	192.1 ± 0.2
4	directly above 3	191.8 ± 0.4
B 5	next to knife edge	195.4 ± 0.5
6	35mm left of rear of knife holder	200.0 ± 0.1
7	directly above 5	215.8 ± 0.4
A 8	directly above 6	216.9 ± 0.3
9	directly above 3	221.0 ± 0.2

Fig.4.6 a) Recordings of the temperatures of the copper baseplate of the microtome head (Δ), the simulated specimen (\blacktriangle), the cutting edge of the knife (\bullet) and the atmosphere adjacent to the knife edge (\circ) during the cutting stroke, at a controller setting of 193K (-80°C).

b) The temperature of the zone adjacent to the knife edge (\circ) after removal of the baffle plate from the chamber. The greater variation in temperature illustrates the importance of the baffle plate to the stability of the knife.

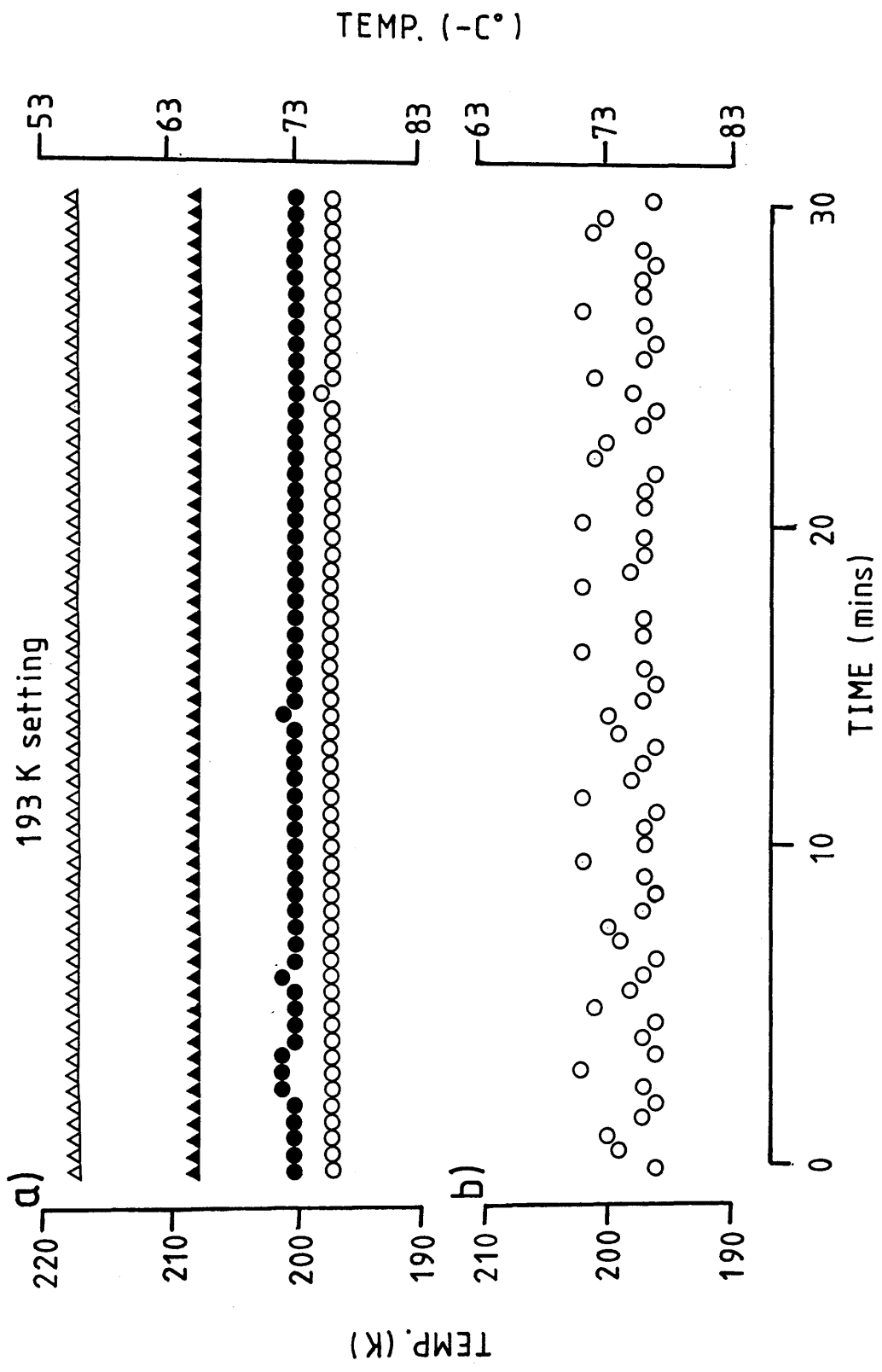


Fig.4.7. Recordings of the temperatures at (upper) 233K (-40°C) and (lower) 153K (-120°C) control settings of the copper baseplate (Δ), the simulated specimen (\blacktriangle) and at the cutting edge of the knife (\bullet).

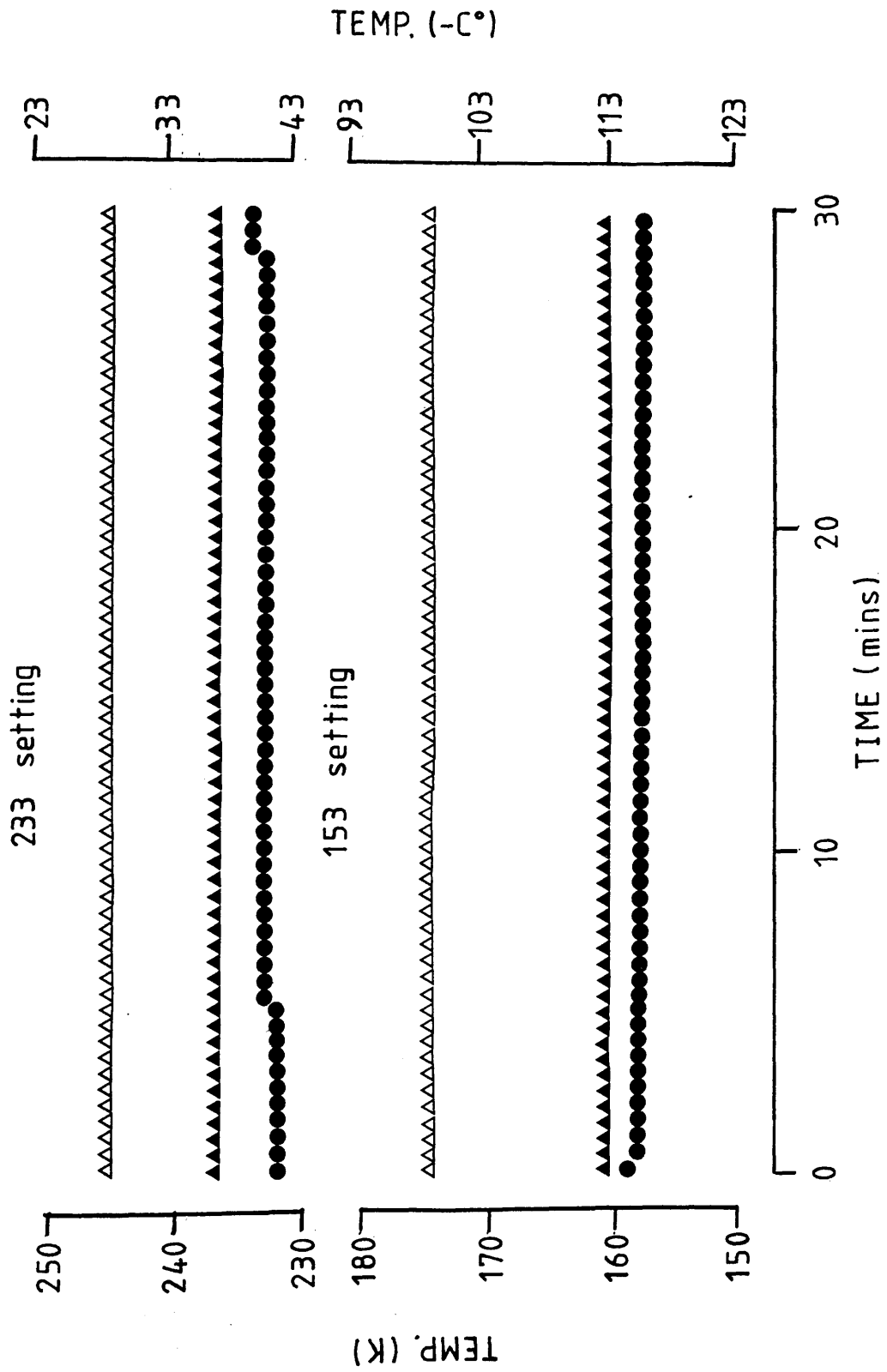


Fig.4.8. Recordings of the temperature of the top of the bridge arm (\blacktriangle), the base of the bridge arm (\triangle), the top of the microtome head (\blacksquare) and the copper baseplate of the microtome head (\square), after a 1h equilibration period.

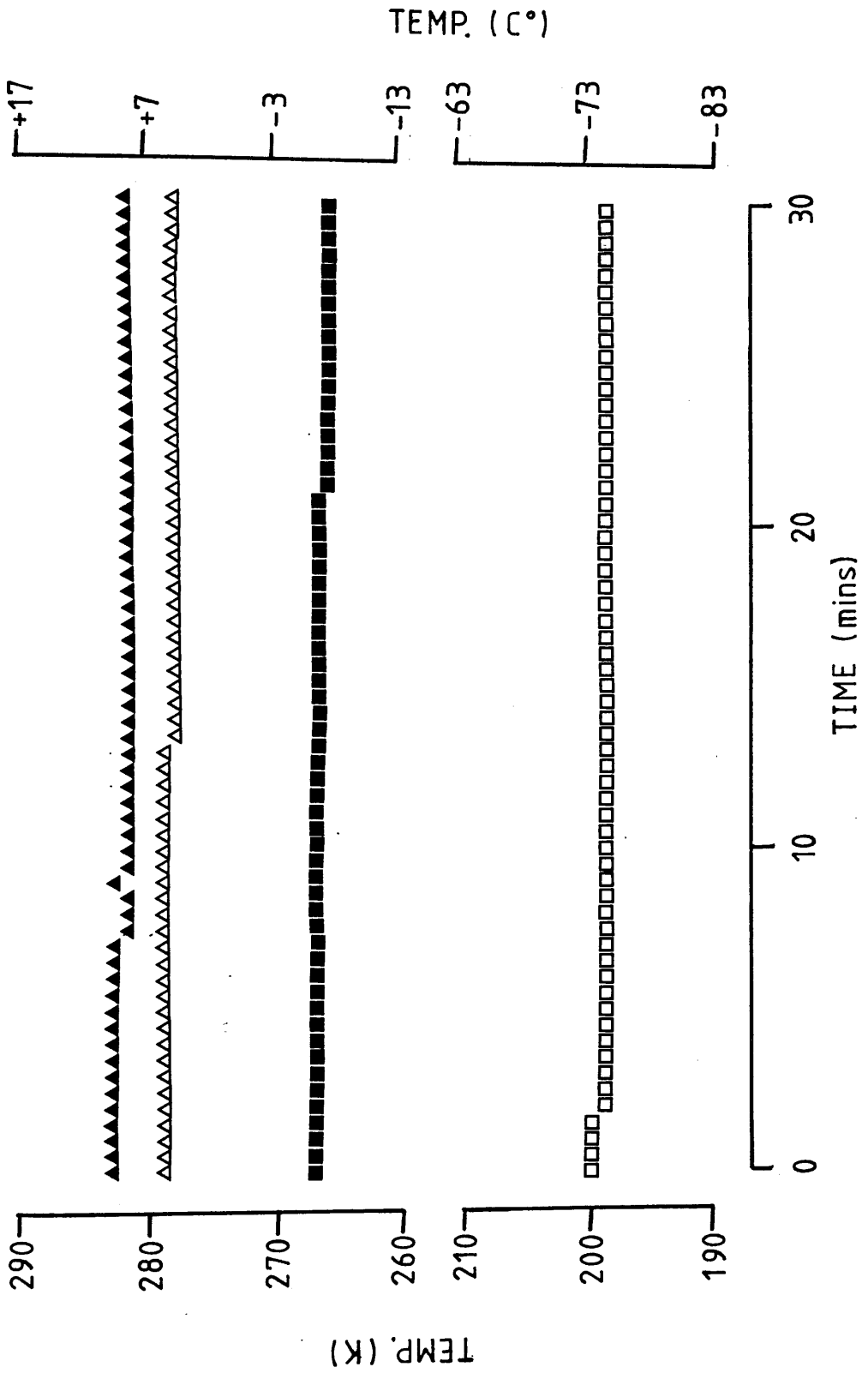


Fig.4.9. A composite graph illustrating the changes in specimen temperature which occur during transfer of a simulated specimen from LN₂ storage, through the trimming process, to the cryochamber. Note that faster recording times were used during the periods of transfer (every 5s).

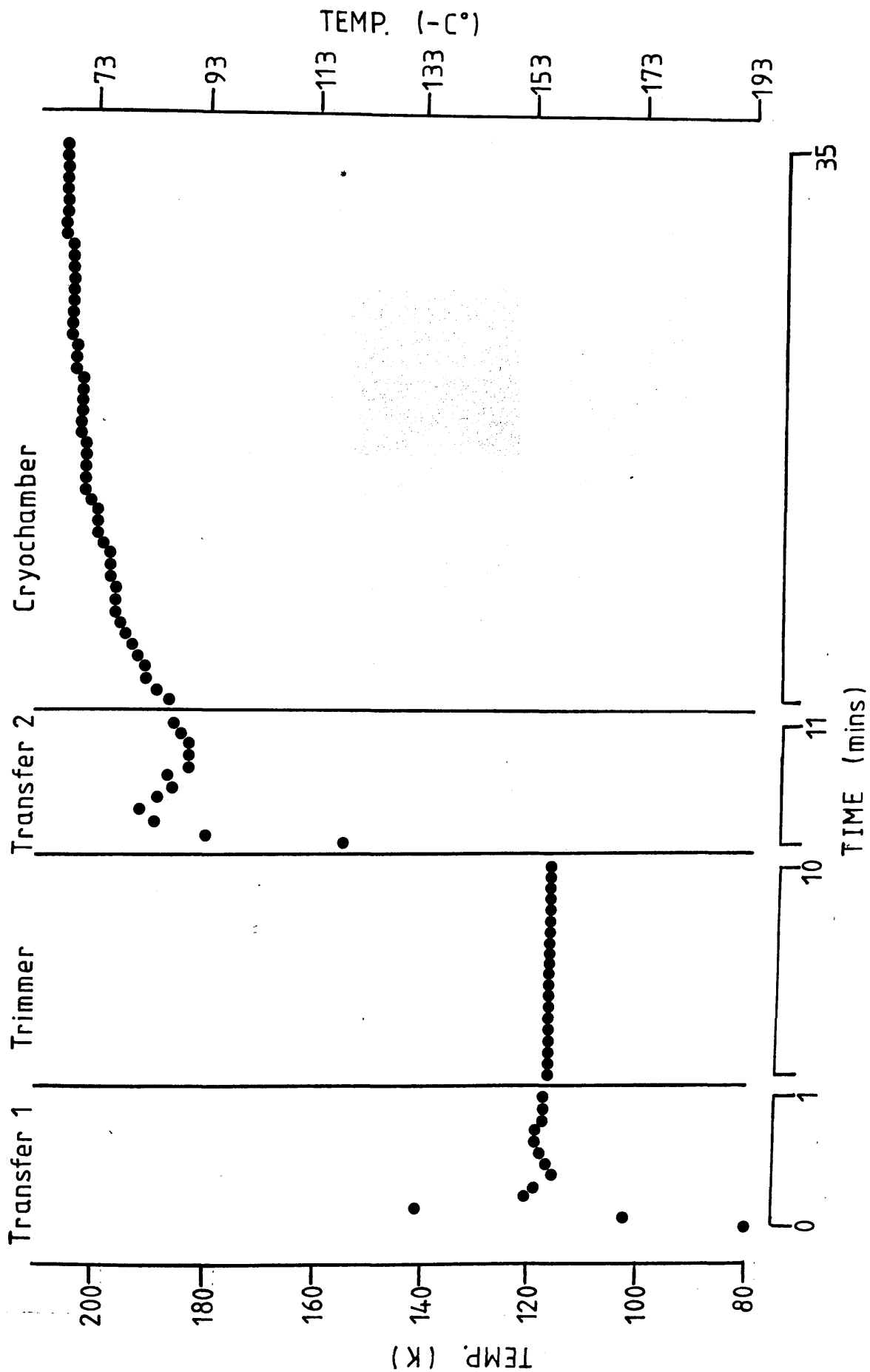


Fig.4.10. An electron micrograph of cryoquenched and cryosectioned skeletal muscle (rat diaphragm) in longitudinal section. Section cut at 200nm thickness, freeze-dried and examined unstained. The striation pattern is clearly visible as is a capillary complete with endothelial cell. A = A band, I = I band, cap = capillary, end = endothelium. (bar = 2 μ m)

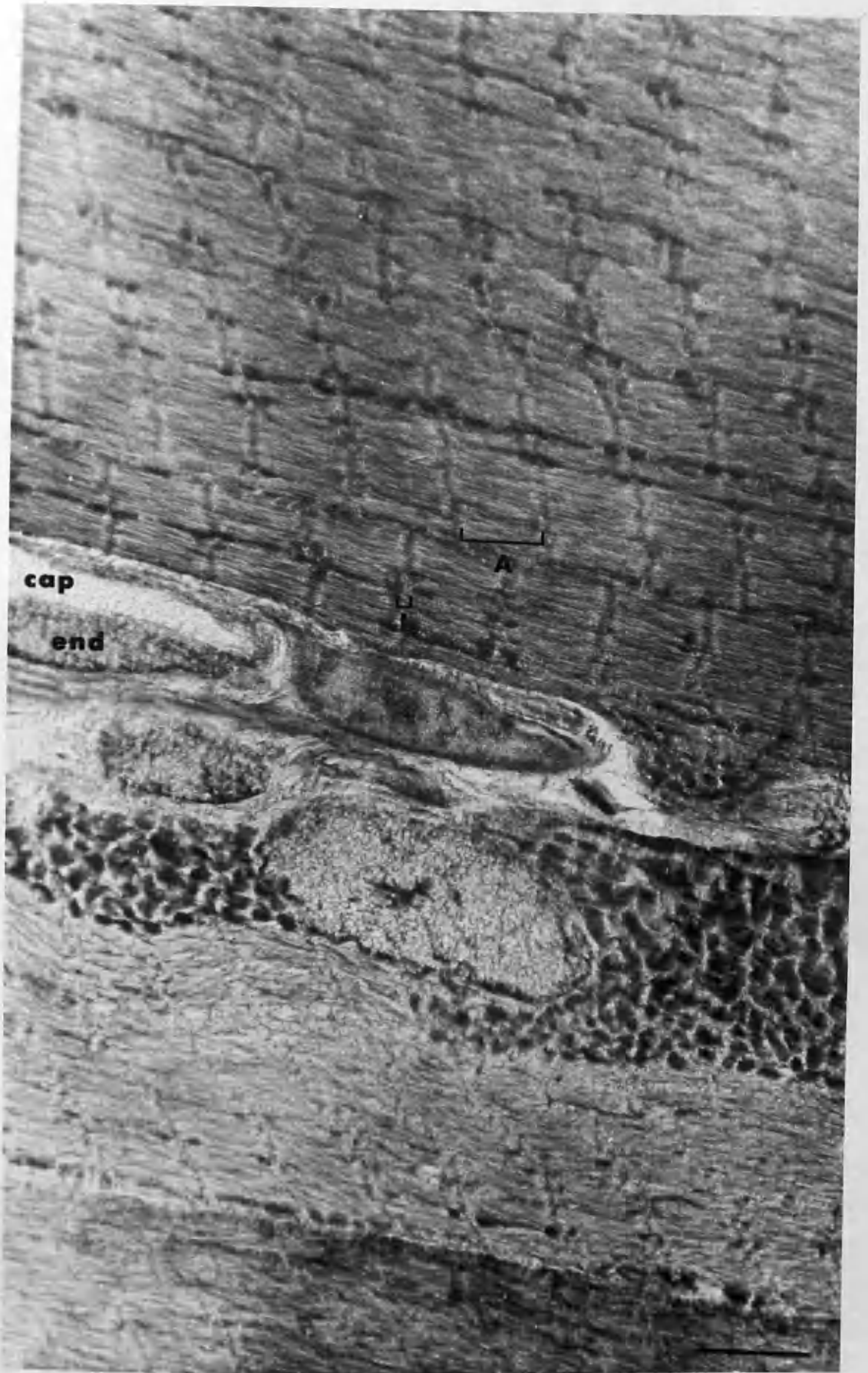
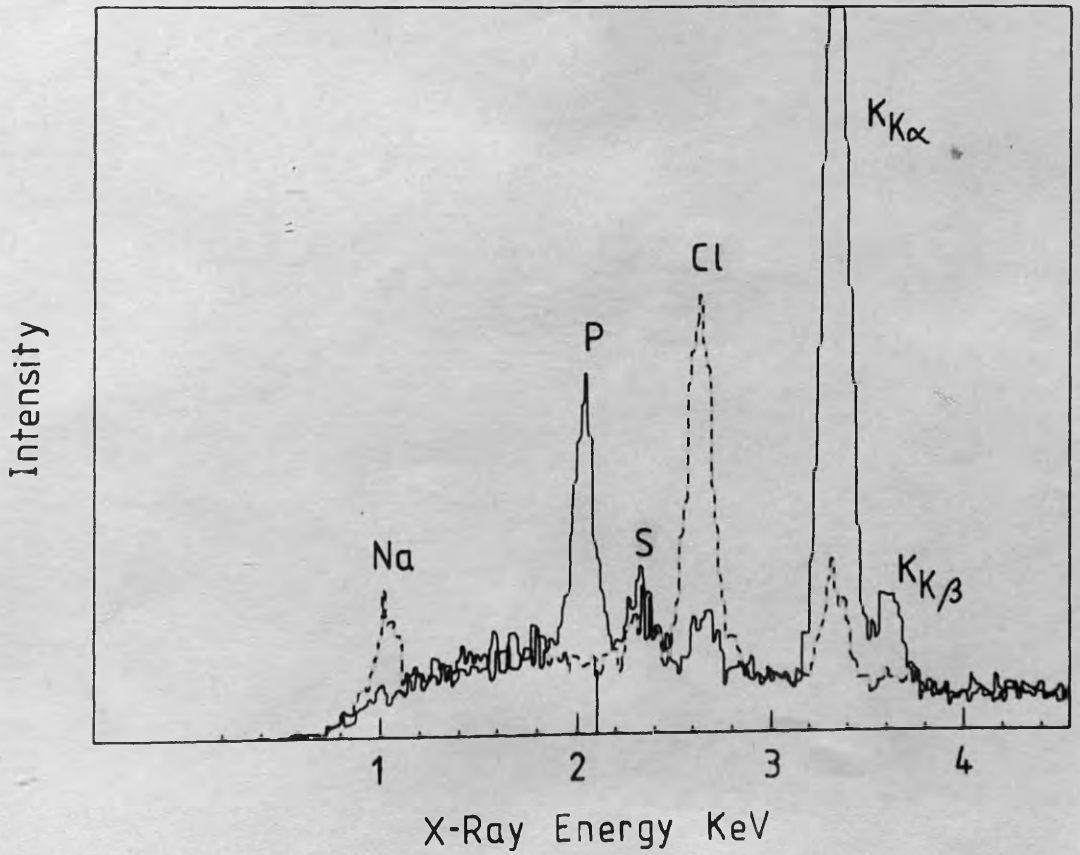
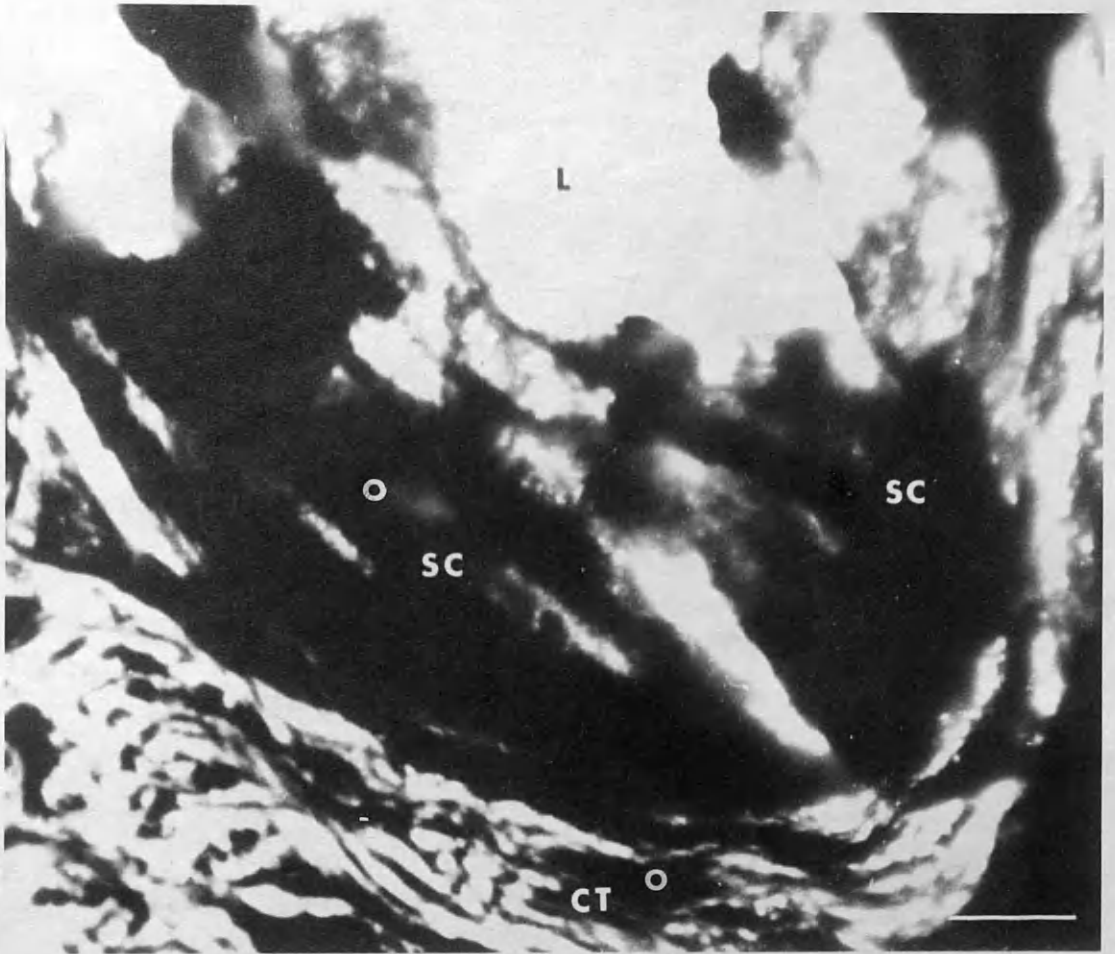


Fig.4.11.a. An electron micrograph of a cryoquenched, cryosectioned, freeze-dried and unstained rat footpad sweat gland ~20 μ m from the cryoquenched surface. Although detail and contrast are poor spectra recorded from the sites circled show clear extracellular/intracellular differences in elemental composition (Fig.4.11.b.). CT = connective tissue, SC = secretory cell, L = lumen. (bar = 2 μ m)

Fig.4.11.b. Energy dispersive X-ray spectra from within the secretory epithelium of rat footpad sweat gland (———) and the surrounding connective tissue (-----). The low Na/K ratio, high P and low Cl contents of the cell contrast with those of the extracellular space.



**CHAPTER 5 EPXMA OF THE INTRACELLULAR ELEMENTS IN THE
RAT FOOTPAD SWEAT GLAND BEFORE AND AFTER
PILOCARPINE STIMULATION.**

5.1. INTRODUCTION

5.2. MATERIALS AND METHODS

5.3. RESULTS

5.4. DISCUSSION

5.1. INTRODUCTION

In Chapter 2 the atrichial glands of the rat footpad have been shown morphologically to conform to the general pattern of sweating described by Montgomery *et al* (1984). The ionic events underlying the fluid transport mechanism, however, have not been well documented. The first description of the composition of rat footpad sweat was given by Quatralle & Laden (1968) and Brusilow *et al* (1968) from secretions collected on the skin surface. These groups studied the effects of pilocarpine stimulation on the glands of anaesthetised rats *in vivo* and the most remarkable features were the hypertonicity of the sweat, ~400mosm., the high K concentration, ~160mM, and the low Na concentration, ~20-50mM. Sato & Sato (1978) induced, pharmacologically, fluid transport in the secretory coils of rat isolated sweat glands and measured, with a micropuncture technique, the concentrations of Na and K in the lumen of the gland at several points. They found that the concentration of the two cations was not dependent on flow rate, as in human sweat glands (Sato, 1977) and in exocrine glands in general (Schneyer, Young & Schneyer, 1972). Moreover, the composition of the sweat collected from the secretory coil was virtually identical to that collected from the *in vivo* skin surface. They concluded from these observations that the secretory coil is the major, if not the sole, site of K and Na secretion in the rat gland. In this respect the rat gland is similar to that of the cat footpad in which the duct is believed to have no active role. Morphological evidence to support this idea was obtained by Matsuzawa & Kurosumi (1963) and Weschler & Fisher (1968) who showed that the duct in the rat footpad is short and rudimentary, as in the cat, and undergoes no notable changes during glandular activity. Sato (1980) attempted to determine whether the high K concentration in rat sweat was due to passive distribution according to the electrochemical potential gradient generated by the active transport of other ions or whether active K transport occurs. In the isolated gland stimulated with ACh he calculated that, based on the K⁺ distribution and transepithelial potential difference profile, the electrochemical gradient for K⁺ across the cells was ~76mV against K⁺ movement. This suggested that K⁺ is either actively transported into the lumen or coupled with

other ions or solutes that are actively transported. The anions accompanying these cations have not been accurately identified or quantitated but lactate is the dominant anion in rat sweat (Thaysen, 1978). Although it is the end product of glycolysis, lactate is distributed against its electrochemical gradient (Sato, 1980) and may have a role in the K secretory mechanism. Brusilow *et al* (1968) have calculated that the large difference between the Cl concentration and the combined K and Na concentrations in rat sweat suggests that anions other than Cl are involved in fluid transport. The present study was undertaken to determine the intracellular distribution of Na, Cl and K in the rat footpad sweat gland before and after pilocarpine stimulation *in vivo* to provide information on ion transport by the glandular fundus. The duct, which apparently plays no active role during activity, was not investigated.

5.2. MATERIALS AND METHODS

The experimental procedures involved in stimulating the rat footpad sweat glands are described in Chapter 2. Small blocks of tissues, ~1-2mm², from the plantar pads were rapidly cryoquenched in liquid propane at -186°C by the method of Elder *et al* (1982) and stored in liquid nitrogen. All specimens were freeze-dried for 3 days at -70°C under a vacuum of 1×10^{-6} torr in the presence of freshly activated molecular sieve (type 3A, BDH). After drying, they were slowly warmed to room temperature (1°/6min) and infiltrated with a de-gassed, non-polar resin whilst still under vacuum. The specimens were removed from the freeze-drier, soaked in resin for a further 48h then polymerised in fresh resin. Light microscope "survey" sections (~1µm), cut parallel to the skin surface starting from the dermis, were used to locate suitable glandular profiles and as an aid to identification in the unfixed and unstained sections used for EPXMA. Sections of sweat gland were cut dry on a diamond knife at 1200Å, mounted on formvar-coated one-hole titanium supports and carbon-coated at ~200Å (Temcarb 500). Samples from animals in the control, saline injection and one and three pilocarpine injection groups were analysed. Poor contrast in the sections restricted gross morphological identification to gland profiles, secretory and myoepithelial cells and to nuclei within these cells. Using the standard

analysis conditions, described in Chapter 3.10.3., 10 spectra were recorded from each of three intracellular sites within the secretory cells: basolateral, perinuclear and juxta-luminal as shown in Fig.5.1. The group means (n=4) and standard deviations were calculated for each treatment and compared by analysis of variance.

5.3. RESULTS

Analyses of variance showed that for Na, K and Cl there were no significant differences between the 3 sites in any one gland. The thirty spectra were subsequently treated as a homogeneous population (n=30). For the 30 spectra from each animal any values lying outside two standard deviations of the mean were rejected as these probably represented spectra recorded from regions with an abnormal, local elemental concentration. The intracellular elemental concentrations of Na, K and Cl for each animal in the four experimental groups are shown in Appendix 4. There was considerable variation for all elements after each procedure, however, when the group means were calculated (Table 5.1.) clear differences were observed. An analysis of variance showed that the measurements from the one and three pilocarpine injected rats represented a single population and the data in these groups were combined to give an estimate of Na, K and Cl in "active" glands (n=8). These results are shown in Table.5.1. and Fig.5.2. together with the values for the control and saline injected animals. Although there were no significant differences between the control and saline injected rats, the values for the latter group lay between those of the control and "active" animals. On the basis of the morphological differences between the control and saline injected animals noted in Chapter 2 these groups were not combined. The secretory cells in the fundus of active glands showed a significant ($p < 0.05$) rise of 139% in the intracellular [Na], a significant ($p < 0.05$) fall of 38% in intracellular [K] and a small decrease in intracellular [Cl] which was not significantly different from the control value. With the exception of Cl, similar changes occurred between the saline injected and "active" groups, although, because of the inter-animal variation, only the fall in K was significant.

5.4. DISCUSSION

The effects of pilocarpine stimulation on the intracellular elemental concentrations were a significant rise in [Na], a significant fall in [K] and no change in [Cl]. These effects were more marked after one pilocarpine injection which suggests that this may be the period of maximum activity. Morphologically, the early stages of sweating were associated with the most extreme signs of activity i.e. "ballooning" of the apical membrane, suggesting that these two findings could be related. The intracellular concentrations of Na and K after saline injection lay between the control and pilocarpine values. Although not significantly different from the control values this suggests that saline injection causes mild activity of the gland and supports the morphological data described in Chapter 2.

Intracytoplasmic elemental gradients have been found by microprobe in cryosections of salt-adapted duckling salt glands (Andrews *et al.*, 1983), rat renal tubules (Beck *et al.* 1980) and rabbit ileum (Gupta, 1979; Gupta & Hall, 1979) and in freeze-dried resin embedded sections of pancreas (Kuijpers *et al.* 1984). The failure to detect gradients in this study could be due to several reasons: i) they do not exist, as Andrews *et al.* (1983) found for much of their work or ii) that infiltration with resin has led to a general redistribution of elements, washed along by the resin front, within the cytoplasm. Ingram & Ingram (1984) have shown that, while the extracellular elemental distribution is disturbed and unnatural in most tissues processed by this route, the elements do not appear to cross membrane boundaries and they claim never to have seen intracellular elemental artefacts. This conclusion has been supported by Roos & Barnard (1985; 1986) who found that, whilst subcellular elemental distributions are perturbed by bulk freeze-drying and resin embedding, the measurements are valid at the cellular level. It is concluded, therefore, that the concentrations calculated in this thesis represent true intracellular measurements although whether the distribution is as it was in "life" cannot be confirmed.

There are several possible reasons for the variation in the concentrations of the elements within every group of animals: 1) In addition to biological variation between the rats all the glands may not

respond to the same extent to the pharmacological stimulus. The responsiveness of glands, even from the same skin region, to a given stimulus is notoriously variable (Hayashi & Nakagawa, 1963; Thaysen, 1978) due to the differences in the periglandular conditions around each gland (Sato, 1977). In this respect it may be significant that the variation (as measured by the Standard Error in Table 5.1.) seems to be less in the unstimulated control animals, where it is more likely that the glands are at a similar level of activity, and hence of more uniform composition, than in the experimental animals. In the future the use of isolated glands, where the level of activity can be accurately determined prior to cryoquenching, would greatly alleviate this problem. 2) Since unstained sections have low contrast, it is possible that subcellular organelles, or regions of abnormal local element concentration, were inadvertently measured. The level of contrast in the TEM image of resin embedded sections is comparable to that in frozen-hydrated cryosections (T.A.Hall, personal communication) however, unlike the situation in frozen-hydrated sections, it is not possible to retrospectively confirm the location of the probe by freeze-drying (Gupta & Hall, 1979; 1981). 3) During freeze-drying it is possible that some of the Na, present in high concentrations in the extracellular fluid, will precipitate onto the outer surface of the basement membrane. Since it is possible that these regions may be analysed and assumed to represent intracellular regions they will introduce an unknown amount of variation in addition to increasing the apparent intracellular Na concentration. Despite these problems the intracellular concentrations calculated in the rat footpad sweat gland in this study showed significant differences between the unstimulated and "active" states. In addition the values calculated by this method are in reasonable agreement with EPXMA studies of other tissues using a variety of preparative methods (see Appendix 5). The consistently larger intracellular values in the present study, and in all EPXMA studies, when compared to known intracellular concentrations are due to the fact that the technique cannot distinguish between the bound and free or ionised and unionised forms of an element. To convert the results in Table 5.1. to more meaningful physiological values they must be multiplied by the appropriate activity coefficients. In the absence of any correlative information on the rat gland these coefficients can only be estimated

from other tissues, see Appendix 6 for appropriate information. The estimated intracellular concentrations, based on the assumptions in Appendix 6 and assuming 75% cell water content, are given in Table 5.2. Using extracellular concentrations of 4mM K⁺, 150mM Na⁺ and 148mM Cl⁻ (cited in Petersen, 1972)) the equilibrium potentials across the basolateral membrane for the three ion species are:

$$E_{Cl} = -44mV$$

$$E_{Na} = +51mV$$

$$E_K = -108mV$$

The physiological significance of these data will be discussed in Chapter 7 and compared with the values calculated for the human and horse sweat glands.

Table 5.1. Intracellular elemental concentrations of Na, K and Cl in the secretory coil of the rat footpad sweat gland before and after saline and pilocarpine injection.

GROUP	n	Na	K	Cl
Control	4	49 ± 16	211 ± 14	44 ± 2
Saline	4	84 ± 26	205 ± 16	37 ± 6
1 Pilo	4	118 ± 20	121 ± 25	39 ± 9
3 Pilo	4	116 ± 28	140 ± 35	38 ± 4
1+3 Pilo	8	117 ± 14	130 ± 20	38 ± 5

Values are the mean ± S.E.M. and the units are mMoles/kg dry wt..Cl values corrected for Cl content of resin.

Table 5.2. Estimated intracellular concentrations of Na⁺, K⁺ and Cl⁻.

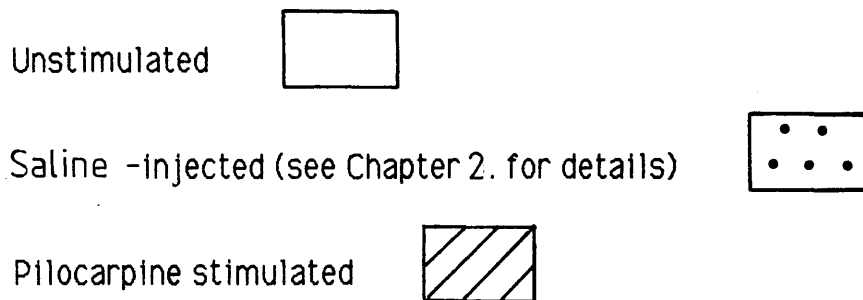
	Na	K	Cl
Control	23	224	29
1 + 3 Pilo	54	138	25

Values are in mM.

Fig.5.1. An electron micrograph of a bulk freeze-dried, resin embedded and unstained rat footpad sweat gland fundus dry cut on a diamond knife at a thickness of 120nm. The areas in which EPXMA was undertaken are shown: 1- juxta-luminal, 2- perinuclear and 3- basolateral. N= Nucleus, L= lumen and BL= basal lamina. SC = secretory cell. (bar = 2 μ m)



Fig.5.2. A histogram showing the elemental concentrations (mMoles/kg dry wt.) of Na, K and Cl (corrected for the Cl content of araldite) in the rat footpad sweat gland fundus.

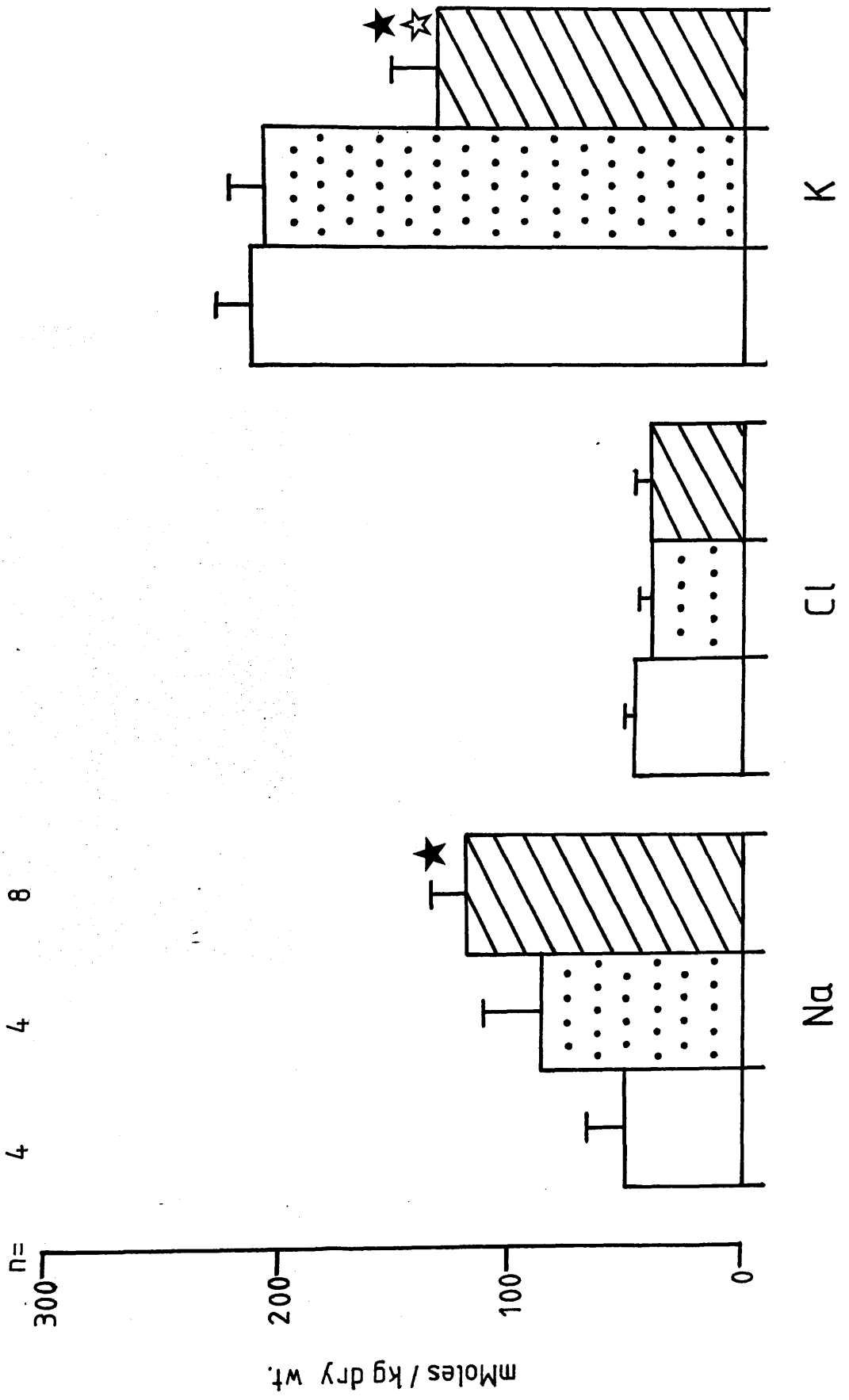


Values are means \pm S.E.M.

n= number of animals

★ = significantly different from unstimulated ($p < 0.05$)

☆ = significantly different from saline ($p < 0.05$)



**CHAPTER 6 EPXMA OF THE INTRACELLULAR ELEMENTS IN THE
HUMAN AND HORSE SWEAT GLANDS BEFORE AND
AFTER THERMAL STIMULATION.**

6.1. INTRODUCTION

6.2. METHODS

6.2.1. Human

6.2.2. Horse

6.3. RESULTS

6.3.1. Human

6.3.2. Horse

6.4. DISCUSSION

6.1. INTRODUCTION

In terms of sweat composition the human atrichial sweat gland behaves differently to the rat sweat gland. The secretory portion produces an initial fluid of plasma-like composition which is modified as it passes along the duct (Schulz, 1969; Sato, 1977). The major site of modification is suggested to be the coiled duct on the basis that there is a greater concentration of Na/K ATPase than in the straight duct (Quinton & Tormey, 1976) and sodium and chlorine are reabsorbed in excess of water to produce a hypotonic final sweat. As in the rat gland, the intracellular elemental changes associated with both processes, the primary secretion and the secondary reabsorption, are not known. Little is known of the ionic content or the mechanism of formation of sweat in the horse epitrichial gland except that the fluid collected at the surface has a relatively high K concentration, approximately 40mM (Snow *et al.* 1982). However, this gland represents an anatomically different sweat gland to the human atrichial gland. It was, therefore, of value to compare elemental levels after thermal stimulation in the two species. This study was undertaken to determine the intracellular elemental distributions and concentrations in the fundus and duct of both species before and after thermal stimulation: i) as part of a larger comparative study of several species to investigate whether there are common elemental changes during activity that parallel the common ultrastructural changes found by Montgomery *et al.* (1984) after stimulation and ii) as a basis for a study of the mechanism of action of aluminium-containing antiperspirants on the human gland. Although the human gland is composed of three distinct regions; the fundus, the coiled duct and the straight duct, because of difficulties in identifying coiled duct profiles in unstained sections, only the fundus and straight duct were analysed.

6.2. METHODS

6.2.1. Human

Twelve healthy adult male volunteers, 20-30 years of age, were placed in a climatic room controlled at 40°C; 50% relative humidity. The

cutaneous evaporative loss from an area of the back was continuously monitored using a ventilated capsule and humidity measuring system (Humitec). The onset of sweating was also assessed by applying a starch/iodine solution to the contralateral side of the back. Skin samples (4mm diameter) were taken by biopsy using a high speed punch, without anaesthetic, at three times: i) prior to entry into the climatic room; these samples were used as controls, ii) at the onset of sweating and iii) 3-4h after sweating had started.

6.2.2. Horse

The experiments were performed on two Shetland mares and two Shetland geldings which received a normal equine diet and had access to grazing. They were exposed to an environment of 40°C and 50% relative humidity in a climatic chamber for 6h and the cutaneous evaporative loss was measured as described by Montgomery *et al* (1982). Skin samples (4mm diameter) were obtained by high speed biopsy punch at 4 times: i) before entering the climatic chamber, ii) at the onset of sweating, iii) after 4h exposure to heat and iv) 24h after entering the chamber.

For both species the samples were quartered longitudinally and rapidly cryoquenched in liquid Freon 22 (Elder *et al* 1982) and bulk freeze-dried and embedded in resin as described in Chapter 5.2. Ultrathin sections were cut dry, carbon-coated and analysed at room temperature in the modified specimen stage under standard conditions (Chapter 3.10.3.). The regions analysed were identical to those studied in the rat sweat gland (Chapter 5) i.e. ~10 spectra were recorded from each of the juxta-luminal, perinuclear and basolateral regions for both the duct and fundus (Figs.6.1. & 6.2.). The intracellular concentrations in the control and stimulated glands were compared by an analysis of variance.

6.3. RESULTS

6.3.1. Human

Analysis of variance showed that there were no consistent significant differences between the measurements at the three sites within each duct or fundus and the values (~ 30) were treated as a homogeneous population (similar to the situation in the rat). Analysis of variance also showed that the data for each element in glands from biopsies ii) and iii) were not significantly different and the mean of these two values was taken as representative of "active" glands. The unstimulated and "active" mean values of the three elements for each individual are shown in Appendix 7. However, the variability between subjects, particularly for stimulated glands, is still obvious and was as much as 3-fold (Subjects 1 and 5 for Na in the "active" fundus). The combined group means and S.E.M. (Table 6.1. and Fig.6.3.) show the effects of thermal stimulation more clearly.

In the fundus, activity caused a 34% fall in K and a 52% elevation in Na both of which were significantly different from the control value ($p < 0.05$) and a small rise in Cl which was not significantly different. In the duct there were no significant changes in Na, K or Cl (Fig.6.4.) Attempts to quantify Ca were largely unsuccessful due to the very low peak/background ratios and the difficulty in deconvoluting the small Ca peak. In the fundus Ca was only detected on 20 occasions in total and there was no increase in detection frequency after stimulation. In 75% of the instances that Ca was detected it was found in the apical region of the cytoplasm and the concentration ranged from 14mM at rest to 18mM during activity in the apical portion and from 2-8mM in the rest of the cell. In the duct Ca could not be detected either before or after stimulation.

6.3.2. Horse

As in both other species studied there were no intracellular elemental gradients and the 30 spectra from each profile were regarded as one group. Similarly, analysis of variance showed that the

concentrations from biopsies i) and iv) represented a single population as did those from biopsies ii) and iii). These values were pooled to give estimates of unstimulated and "active" glands respectively. The means for Na, K and Cl of each horse in the control and "active" groups are shown in Appendix 8. The combined group means for Na, K and Cl are shown in Table 6.2. and Fig.6.5.

In the horse fundus, stimulation caused rises in intracellular Na (58%) and Cl (44%) and a fall in K (16%) all of which were significantly different from the control concentrations ($p < 0.05$). In the duct, thermal stimulation caused a significant ($p < 0.05$) increase in intracellular Cl of 62%. Although the Na and K values in the "active" ducts were not significantly different from control values there was a 42% increase in the former and a 40% decrease in the latter.

6.4. DISCUSSION

The effects of thermal stimulation on the intracellular elemental concentrations in the fundus of the human atrichial sweat gland were a fall in K, a rise in Na and no significant change in Cl. In the duct, activity had no measureable effect on the intracellular concentrations of the three elements. In the fundus of the horse epitrichial sweat gland the intracellular elemental changes found after stimulation were basically the same as in the human fundus i.e. an increase in Na and a fall in K and, in this species, a rise in Cl. In the horse duct stimulation produced the same changes as were found in the fundus, although the small sample size and variability of the results prevented some of these changes reaching significance. In addition to the sources of variability discussed for the rat gland (Chapter 5), which are equally applicable to the human and the horse, the presence of two secretory cell types in the fundus, which could not be distinguished in the unstained sections and which may have separate functions and, therefore, may also have different elemental contents, will add further variation to the results.

When compared to the results from the rat study (Chapter 5), and with the known intracellular elemental composition obtained by other methods, the data for Na and Cl in the human and horse are high. The reason for these discrepancies is unknown; the data were calculated

using identical NaCl crystal standards as were used in the rat study. Unfortunately, time did not permit the re-analysis of the spectra with alternative standards e.g. aminoplastic (Roos & Barnard, 1986) or albumin (Rick *et al* 1982) standards. These discrepancies, between the calculated and "expected" values, render of little value the calculation of cellular parameters such as the resting membrane potential. However, the major objective of this work was to calculate the elemental changes within the sweat gland after activation and this is in no way impaired by the discrepancies, since the results from both unstimulated and "active" glands were obtained in an identical manner. The data for the horse and human will be discussed together with the rat data in Chapter 7.

Table 6.1. Intracellular elemental concentrations of Na, K and Cl in the fundus (A) and duct (B) of the human atrichial sweat gland before and after thermal stimulation.

A) Fundus

Element		Control		Active
Na	(n=8)	151 ± 23	(n=11)	229 ± 14
K	(n=8)	159 ± 11	(n=11)	112 ± 13
Cl	(n=8)	110 ± 13	(n=11)	114 ± 12

B) Duct

Element		Control		Active
Na	(n=6)	256 ± 38	(n=6)	271 ± 53
K	(n=6)	103 ± 24	(n=6)	85 ± 8
Cl	(n=6)	100 ± 9	(n=6)	96 ± 16

Values are means +/- S.E.M. and the units are mMoles/kg dry wt..
Corrected for the Cl content of the resin.

Table 6.2. Intracellular elemental concentrations of Na, K and Cl in the fundus (A) and duct (B) of the horse epitrachial sweat gland before and after thermal stimulation.

A) Fundus

Element	Control	Active
Na	(n=3) 151 ± 9	(n=4) 238 ± 19
K	(n=3) 198 ± 9	(n=4) 167 ± 2
Cl	(n=3) 71 ± 3	(n=4) 102 ± 9

B) Duct

Element	Control	Active
Na	(n=4) 204 ± 32	(n=4) 290 ± 26
K	(n=4) 145 ± 22	(n=4) 87 ± 13
Cl	(n=4) 66 ± 4	(n=4) 107 ± 11

Values are means ± S.E.M. and the units are mMoles/kg dry wt..
Corrected for the Cl content of the resin.



Fig.6.1. An electron micrograph of a bulk freeze-dried resin embedded and unstained human atrichial sweat gland fundus dry cut on a diamond knife at a thickness of 120nm. Nuclei (N), a myoepithelial cell (Myo) and the luminal space can be identified. However, as in the rat study, there is insufficient detail to analyse regions other than 1) juxta-luminal, 2) perinuclear and 3) basolateral. SC = secretory cell. (bar = 4 μ m)



Fig.6.2. An electron micrograph of a typical bulk freeze-dried resin embedded and unstained human atrichial sweat gland duct, again the regions analysed were 1) juxta-luminal, 2) perinuclear and 3) basolateral. DC = duct cell. (bar = 4 μ m)



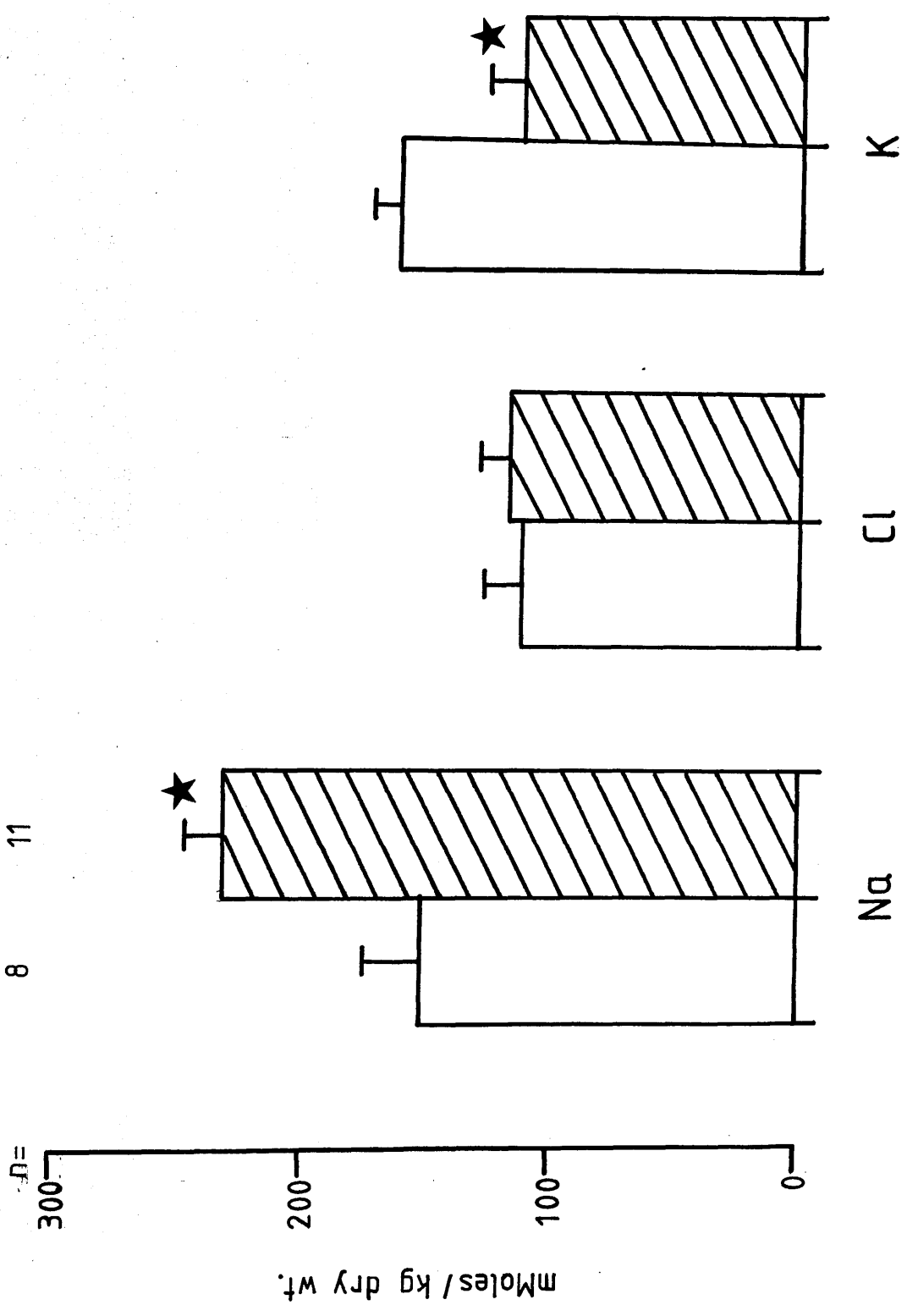
Fig.6.3. A histogram showing the elemental concentrations (mMoles/kg dry wt. corrected for mass loss) of Na, K and Cl (corrected for Cl content of araldite) in the secretory cells of the human atrichial sweat gland fundus.

Unstimulated 
Stimulated 

Values are means \pm S.E.M.


n= number of individuals


★ = significantly different from unstimulated ($p < 0.05$)



8 11

Fig.6.4. A histogram showing the elemental concentrations (mMoles/kg dry wt. corrected for mass loss) of Na, K and Cl (corrected for Cl content of araldite) in the cells of the human atrichial sweat gland straight duct.

Unstimulated 

Stimulated 

Values are means \pm S.E.M.
n= number of individuals

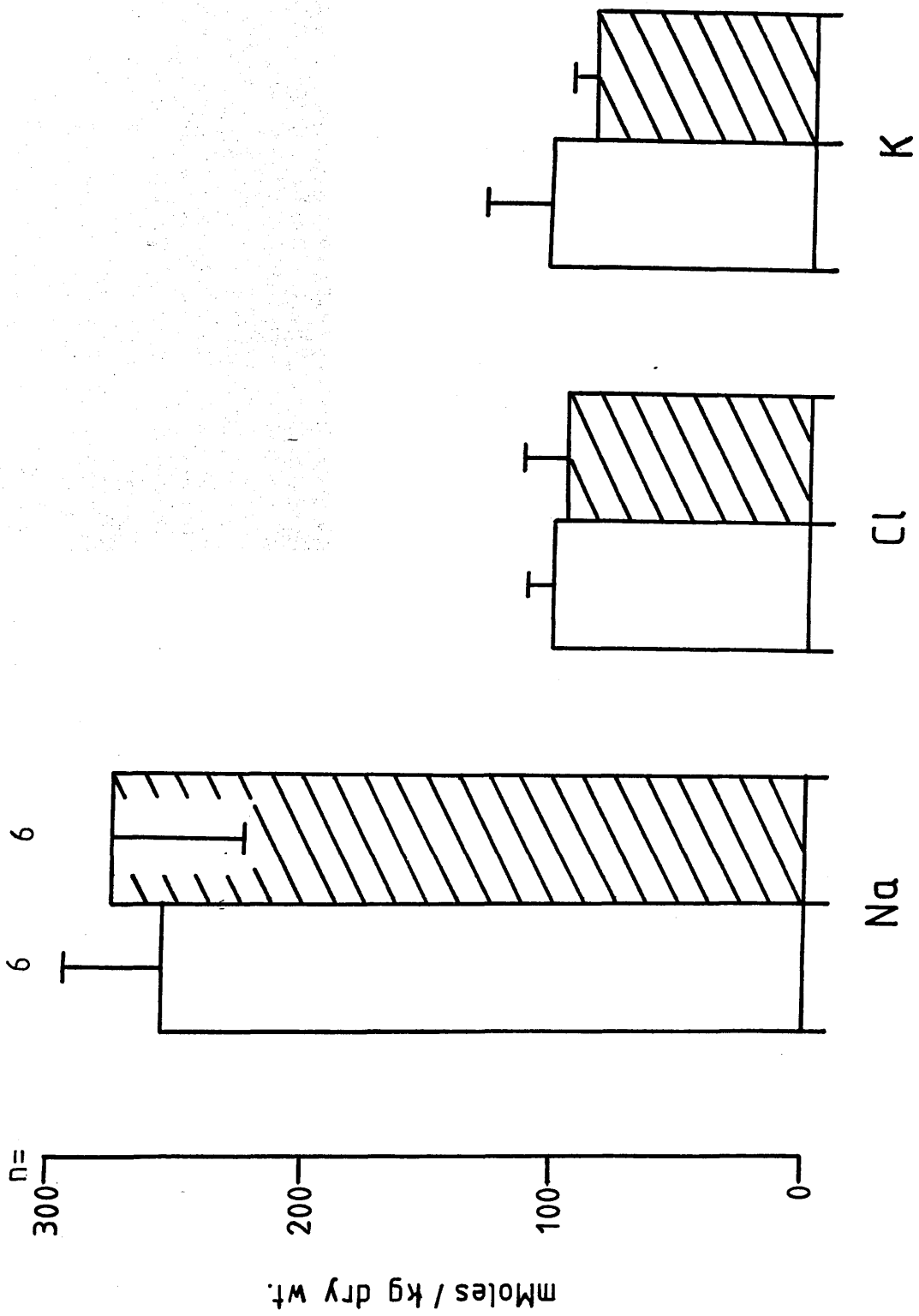




Fig.6.5. A histogram showing the elemental concentrations (mMoles/kg dry wt. corrected for mass loss) of Na, K and Cl (corrected for Cl content of araldite) in the secretory cells of the horse epitrichial sweat gland fundus.

Unstimulated 
Stimulated 

Values are means \pm S.E.M.

n= number of individuals

★ = significantly different from unstimulated ($p < 0.05$)

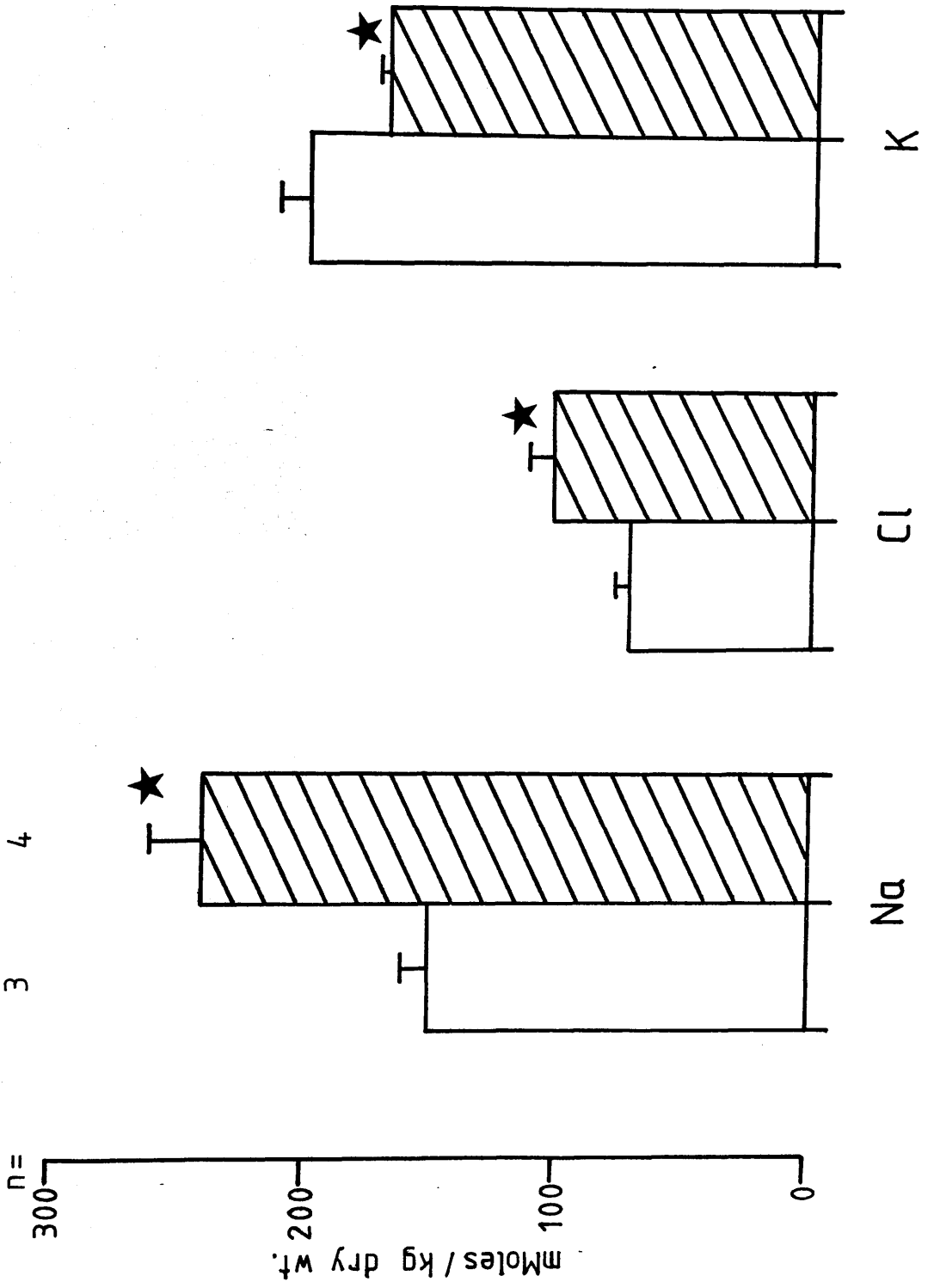




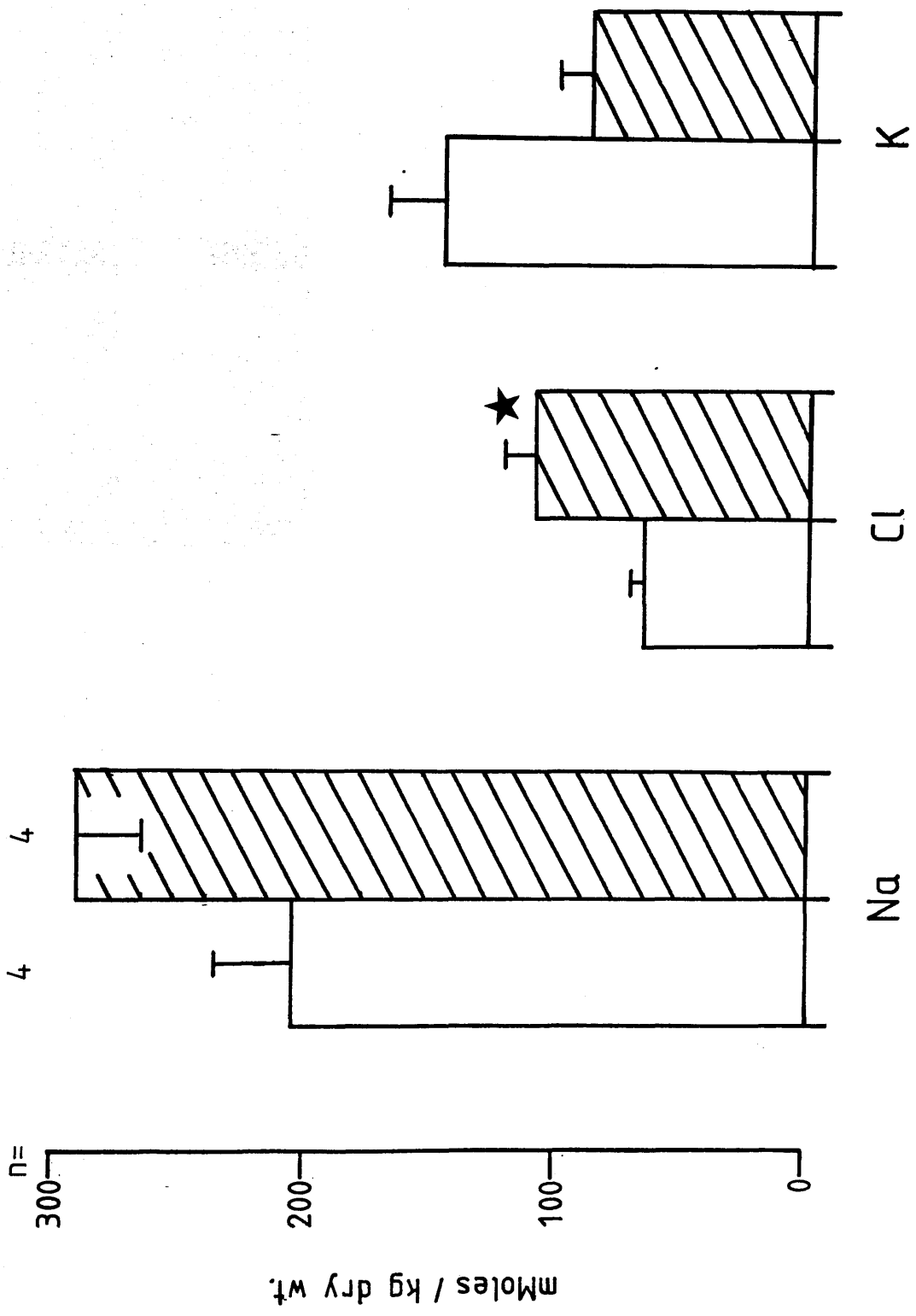
Fig.6.6. A histogram showing the elemental concentrations (mMoles/kg dry wt. corrected for mass loss) of Na, K and Cl (corrected for Cl content of araldite) in the cells of the horse epitrichial sweat gland straight duct.

Unstimulated 
Stimulated 

Values are means \pm S.E.M.

n= number of individuals

★ = significantly different from unstimulated ($p < 0.05$)



CHAPTER 7 GENERAL DISCUSSION.

7.1. GENERAL DISCUSSION

The study of the elemental changes in sweat glands during activity with EPXMA has the advantage over electrophysiological and biochemical methods in that it is possible to accurately measure the elemental concentration with a high degree of spatial resolution. The disadvantage of the method, however, is that with freeze-dried specimens reliable measurements can only be obtained from intracellular locations. In the funduses of the three species studied the common features of glandular activation were, a significant increase in intracellular Na and decrease in intracellular K. In the horse fundus there was also a significant rise in Cl although in the rat and human there were no significant changes in Cl.

In general, the effect of a stimulant on a cell is to increase the permeability of the membrane to one or more ions which have an equilibrium potential different from the resting membrane potential (RMP) resulting in a membrane potential change (secretory potential) (Petersen, 1976). In salivary glands this secretory potential result is normally a hyperpolarisation although in the rat and rabbit (Nishiyama & Kagayama, 1973) and mouse (Petersen, 1973) submaxillary glands the effect of stimulation on the membrane potential depends on the magnitude of the RMP. If the RMP is -50mV or greater the secretory potential is a depolarisation and if the RMP is less than -50mV then the membrane hyperpolarises in response to stimulation. Jones & Kealey (1985) found that the RMP across the basement membrane of the human sweat gland fundus responded to stimulation with ACh in a manner similar to the mouse and cat submaxillary gland i.e. depending on the RMP there was either a depolarisation or a hyperpolarisation. In the rat however, Sato (1980) found that ACh stimulation only caused a depolarisation of $\sim 20\text{mV}$ across the basal membrane.

It is unrealistic to estimate, from the current data, electrical parameters of the glandular cells in either the horse or human fundus in view of the discrepancies between known intracellular concentrations and those calculated in this thesis. In the rat, however, using the values for Na^+ , K^+ and Cl^- shown in Table 5.2. and assuming that the permeability of the basement membrane of the fundus to these ions is the same as in skeletal muscle, then the RMP across the basolateral membrane,

calculated by the Goldman equation, is -63mV . This is in agreement with the -60mV to -80mV range found by Sato (1979) across the same membrane. Similar values have been found in the human fundus (Jones & Kealey, 1985). The electrical effects of stimulation are the result of the movement of ions across the cell membrane. At the ionic level the loss of cellular K has been found in a number of secretory tissues after stimulation (Burgen, 1956; Darke & Smaje, 1972; Schneyer, 1975) and there is little doubt that the secretory potentials, whether depolarising or hyperpolarising, are always associated with a decrease in resistance of the basal cell membrane. The hyperpolarisation is therefore likely to be caused by the efflux of K^+ as determined by the electrochemical gradient. This effect will undoubtedly be modified by changes in the sodium permeability occurring concomitantly with the K^+ efflux leading to Na^+ influx, which if greater than the K^+ efflux will produce a depolarisation. In the rat fundus, assuming a RMP of -63mV and the equilibrium potentials given in Chapter 5 ($E_{\text{Cl}}: -44\text{mV}$, $E_{\text{K}}: -108\text{mV}$, $E_{\text{Na}}: +51\text{mV}$) it is clear that the RMP is close to the equilibrium potential of Cl^- . This is not inconsistent with the passive distribution of Cl^- across the basal membrane according to the electrochemical gradients of the other ions, as in skeletal muscle (Boyle & Conway, 1941) and salivary glands (Petersen, 1976). There are, however, large electrochemical gradients for both K^+ efflux and Na^+ influx. In the unstimulated cell these gradients are probably maintained by an energy requiring mechanism, i.e. Na/K ATPase, that extrudes Na^+ and accumulates K^+ (Petersen, 1972).

The changes in the intracellular elemental concentrations, induced by stimulation, calculated in this study i.e. a decrease in K and increase in Na, are, therefore, consistent with the theory that the initial change after stimulation is an increase in the cation conductance of the basolateral membrane. The intracellular Cl increased in the horse sweat gland fundus and this is consistent with the theory that there is a Na/Cl cotransport system located in the basolateral membrane as in the intestine (Shorofsky, Field & Fozzard, 1982), trachea (Shorofsky *et al.* 1982; Welsh *et al.* 1982) and the shark rectal gland (Silva *et al.* 1977) and that Cl^- is accumulated in the cell against its electrochemical gradient coupled to the influx of Na^+ down its electrochemical gradient. Although the intracellular Cl did not increase in the human or rat funduses it is

still possible that a Cl^- cotransport system is involved in secretion. Two systems will be described to account for the changes in the intracellular elemental levels in the funduses of the three species studied. In the human and horse, which produce isotonic and plasma-like primary secretions, the effects of thermal stimulation can be explained with reference to work on other secretory systems. In the salivary gland there are K^+ selective channels localised in the basolateral membrane and a non-selective cation channel has been postulated in the same membrane (Petersen & Maruyama, 1984). In mouse and rat pancreatic acinar cells there are non-selective cation channels (Petersen & Singh, 1985) and in pig pancreatic acinar cells a similar model has been proposed (Pearson, Flanagan & Petersen, 1984). Both these channels, the K^+ selective and the non-selective cation, are Ca^{++} activated and the sequence after agonist/receptor interaction is thought to involve an increase in intracellular Ca^{++} (Chapter 1) which opens the channels and leads to a depolarisation or a hyperpolarisation depending on the RMP and the individual equilibrium potentials. It seems likely that a similar system operates in the human atrichial and horse epitrichial sweat glands both of which lose potassium after stimulation. The increased concentration of K^+ in the vicinity of the basolateral membrane and in the narrow intercellular clefts is recycled back into the cell by a cotransport with Na^+ and Cl^- (the ratio is thought to be $2\text{Cl}^-/\text{K}^+/\text{Na}^+$ to maintain electroneutrality). The operation of such a cotransport system would explain the elevated intracellular Na and Cl seen in the horse sweat gland. The operation of this cotransport system is dependent on the existence of the Na^+ electrochemical gradient and ultimately on the action of the Na/K ATPase, which would explain the inhibitory effect of ouabain on sweat formation. This theoretical model for the effects of stimulation on human and horse gland is shown in Fig.7.1.

The failure to detect any significant intracellular Ca may seem to be evidence against the involvement of Ca^{++} in the process. However, Petersen (1984) suggested that the increase in Ca^{++} necessary to activate the K^+ channels may be from 50nM to 100-200nM which is below the level of detection in bulk freeze-dried resin embedded sections. This preparative route has also been found "unsuitable for Ca^{++} measurement in rat exocrine pancreas (Roos & Barnard, 1984). The Ca detected in the

present study is probably associated with the secretory granules which have been found to accumulate Ca in the pancreas (Roomans *et al.* 1982; Roos & Barnard, 1984).

The effects at the luminal membrane of secretory epithelia have not been as extensively studied as the effects at the basolateral membrane and are difficult to assess in the presence of low resistance shunt pathways between the cells. The secretion of Cl^- across the luminal membrane in trachea and intestine (Shorofsky *et al.* 1982), after it has been accumulated against its electrochemical gradient in the cell via a Na/Cl transport system, is thought to occur through specific ion conductance pathways for Cl^- , which are also Ca^{++} -activated. Secretagogues stimulate Cl^- secretion in these tissues by increasing the luminal membrane permeability to Cl^- which then diffuses passively from the cell to the lumen. Petersen (1984) and Petersen & Maruyama (1984) have pointed out that such a luminal Cl^- conductance pathway is not incompatible with the model proposed in Fig.7.1. and the increased Cl, detected by EPXMA in the horse, may be expelled into the lumen by such a pathway.

In the rat fundus, although the elemental changes are similar to those found in the human, this epithelium produces a hypertonic and high K primary secretion that is markedly different from that found in the horse or human. It seems unlikely that the model proposed for the other two species can explain the secretory mechanism in the rat. The rat fundus does not, therefore, appear to behave as a classical "leaky" epithelium, most of which produce isotonic fluids (Fromter & Diamond, 1972) with a composition similar to plasma, and presumably this reflects differences in the properties of the paracellular pathways. However, this portion of the rat gland exhibits an ultrastructural change during stimulation that is unique among the sweat gland funduses of the species studied to date i.e. the extreme "ballooning" of the apical membrane. Sato (1980) speculated that some of the K-rich cytoplasmic water is expelled from the cell into the lumen by some exocytotic mechanism to produce a high K sweat. The model put forward to explain the current data concerning the effects of stimulation in the rat fundus is based on the assumption that the paracellular pathway is either impermeable, or has a greatly reduced permeability, to ions and water than in epithelia normally

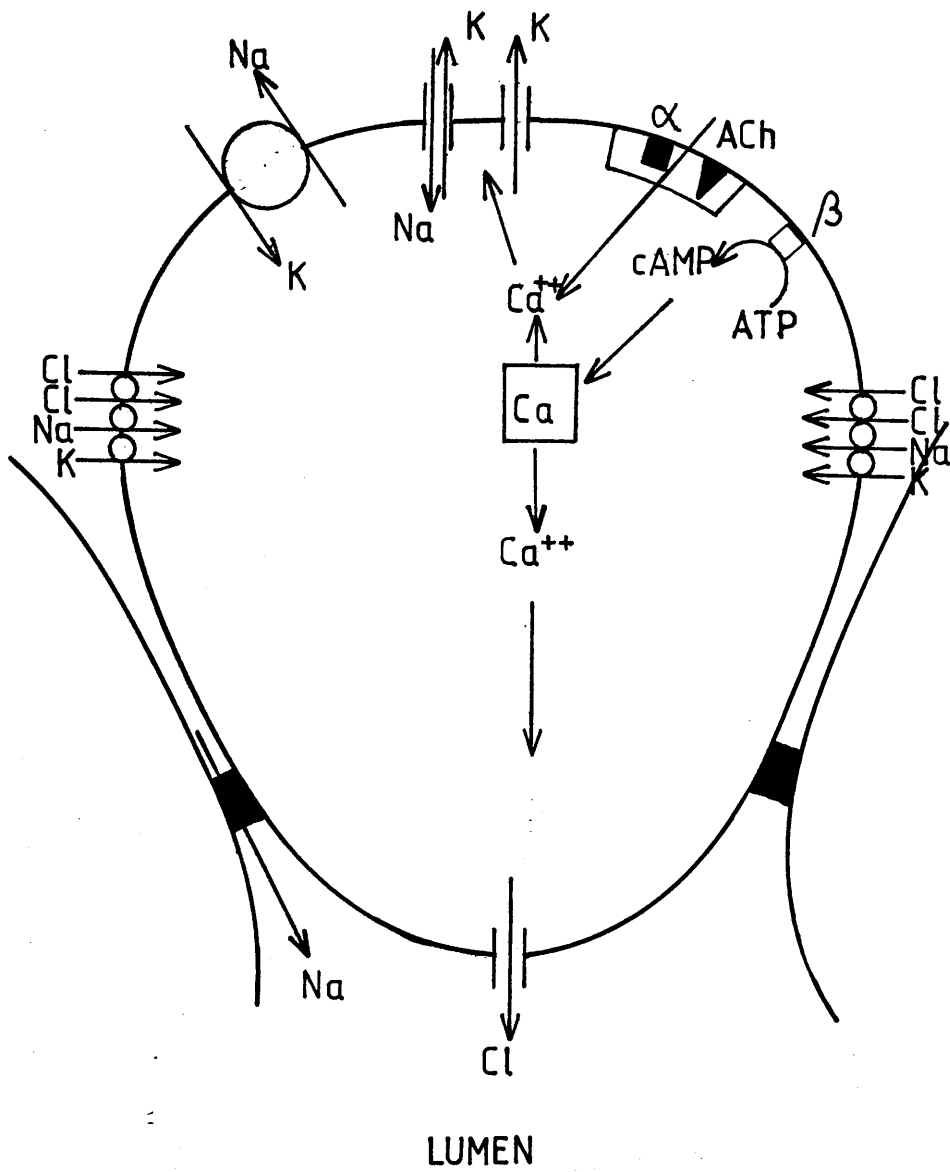
regarded as "leaky". After stimulation, the ionic events (K efflux and Na influx) are initially responsible for creating a hypertonic cytoplasm. Water then enters the cell across the basolateral membrane in an attempt to equilibrate this solution. This results in an increased intracellular volume which ultimately leads to the filtering of the cytoplasm through the terminal web and the expansion of the apical membrane. If the apical membrane separates from the cell before isotonicity is reached the fluid it contains will be both hypertonic and high in K i.e. comparable to the final sweat product.

In the duct of the horse gland, intracellular elemental changes accompanied stimulation/secretion and these were similar to the changes found in the fundus. There is little information on the ductal function of the equine gland although Montgomery *et al.* (1982) found few morphological evidence of activity after thermal stimulation. The coiled duct and, to a much lesser extent, the straight duct of the human gland are thought to be sites of Na and Cl reabsorption and the data for the horse duct are consistent with a similar role. In such a membrane the effects of stimulation are an increase in membrane conductance to Na⁺ (Welsh *et al.* 1982) and the entry of Na⁺ across the luminal membrane down its electrochemical gradient followed by its extrusion across the basolateral membrane. However, horse sweat is slightly hypertonic to plasma and has a [K] of 40-50 mM (Snow *et al.* 1982) and this indicates that the duct may perform a more complex function. The fall in intracellular K in the active duct suggests that this may be the site of K secretion, as in the rat submandibular gland (Schneyer, 1969), although the mechanism remains unclear.

In the human duct the fact that there were no significant changes in the intracellular concentrations of Na, K and Cl provides strong evidence that this region of the gland does not perform an important reabsorptive function. Based on the distribution and density of Na/K ATPase it has been suggested that the coiled duct is the major site of reabsorption and this is borne out by the results presented here. The variability in the intracellular elemental concentration prevented many of the changes found after stimulation reaching significance. Biological variation is undoubtedly partly responsible, however, the greatest source of variability lies in the sampling technique used to obtain glands. The

skin samples were taken from regions in which sweating was definitely occurring and this was confirmed by positive starch/iodine reactions and/or increased cutaneous evaporative loss. However, in view of the known differences in responsiveness of glands to stimulation, even within the same region, it is unlikely that all glands within the sample will be at the same stage of activity and will, therefore, have different elemental concentrations. The use of isolated gland, which can now be obtained without pretreatment (Lee, Jones & Kealey, 1984), would greatly alleviate this problem since the degree of activity of the glands could be more accurately controlled and measured. The use of isolated glands would also overcome the targeting problems encountered in preparing cryosections of skin as described in Chapter 4. The combination of isolated glands and cryosections, particularly frozen-hydrated sections, will provide a great deal more information concerning the secretory process since it would then be possible to measure the concentrations in fluid filled and extracellular spaces and to relate these to the intracellular changes that have been reported in this thesis.

Fig.7.1. Simplified diagram to account for the effects of adrenergic (α and β) and cholinergic agonists on the secretory cells in the fundus of the human atrichial and horse epitrichial sweat glands. Occupation of the β receptor by an agonist stimulates adenylate cyclase within the membrane and there is an increase in the intracellular cAMP concentration. The consequence of the elevated cAMP is an increase in intracellular Ca^{++} from intracellular reservoirs. Similarly, stimulation of the α and ACh receptors leads to an increase in Ca^{++} . The increased Ca^{++} , produced by any of the agonists, opens Ca-activated K^+ selective channels and Ca-activated non-selective cation channels in the basolateral membrane, resulting in an efflux of K^+ and an influx of Na^+ . The K^+ released into the intercellular clefts is recycled back into the cell, partly by a Na, K & Cl cotransport system and partly by an energy-requiring Na/K ATPase, both of which are located in the basolateral membranes. The cotransport is probably electroneutral with a stoichiometry of 1Na, 1K and 2Cl. At the luminal membrane it has been proposed that the elevated internal Ca^{++} stimulates a Ca^{++} -activated Cl^- channel. (Adapted from Petersen & Maruyama, 1984)



CHAPTER 8 MECHANISM OF ACTION OF ALUMINIUM-CONTAINING ANTIPERSPIRANTS.

8.1. INTRODUCTION

- 8.1.1. Action on the Secretory Cell
- 8.1.2. Action on the Reabsorptive Duct
- 8.1.3. Action on the Terminal Duct

8.2. MATERIALS AND METHODS

8.3. RESULTS

- 8.3.1. Sweat Output
- 8.3.2. Ultrastructure
- 8.3.3. Intracellular Elemental Concentrations

8.4. DISCUSSION

- 8.4.1. Rat Study
- 8.4.2. Human Study

8.1. INTRODUCTION

The inhibition of sweating is important in several clinical conditions including hyperhidrosis (excessive sweating, Shelley & Hurley, 1975) and some forms of athlete's foot (Leyden & Kligman, 1975) and is also an important feature of commercially available antiperspirants. The extensive list of the agents that have been used to inhibit sweating (Shelley & Hurley, 1975) fall broadly into two groups: the anti-cholinergic agents and the metal salts. The mechanism of action of the first group, which are unstable and may produce systemic side effects, can be easily explained on the basis of their interference with the nervous control of the gland at the nerve endings, however, the site and mechanism of action of the metal salts have not been conclusively established.

It has been known since 1916 (Stillians) that aluminium chloride hexahydrate effectively inhibits atrichial (eccrine) glands and, despite many attempts to improve the efficacy of the original solution, it remains the most effective and is still the preferred solution in the clinical treatment of certain sweating disorders (Scholes *et al* 1978; Quinton, 1983; Holzle & Braun-Falco, 1984). The irritancy and acidity of this solution made it impractical as a commercial antiperspirant for daily use and Shelley & Hurley (1975) list over 44 aluminium compounds that have been developed as topical antiperspirants, however, most research has been towards consumer acceptance rather than antiperspirant efficacy (Shelley & Hurley, 1975). In the 1940's the chlorhydrated compounds were found to be less problematic, although also less effective, and today two aluminium based compounds, aluminium chlorohydrate (ACH) and the aluminium zirconium chlorohydrate glycine complexes (AZAP) are widely marketed as antiperspirants (Quatrala *et al* 1981b).

The recognition of the site of action is a prime requirement in explaining the mechanism of action and there are three sites where an effect may occur: 1) the fundus (secretory coil), either by interference with the transmission of nerve impulses to the gland, as for the anti-cholinergic agents, or by interfering with the secretory processes,

ii) the reabsorptive duct - possibly by making it leakier to water and/or
iii) the terminal duct portion in the epidermis, by forming an obstructive plug.

8.1.1. Action on the Secretory Coil

To date there is no evidence of an action on the secretory coil. Blank, Jones & Gould (1958) applied concentrated aluminium solutions to excised skin and could find no aluminium in the dermis with chemical analysis. Lyons & Klatz (1958) have shown that aluminium salts bind to human keratinous material, probably to the COOH groups (Shelley & Hurley, 1975), and penetration into the skin is slow. Aluminium has never been observed histologically in the vicinity of the fundus (Quatrala *et al* 1981b) and Papa & Kligman, (1967) found that glycogen depletion, a normal sign of glandular activity, occurred in both the duct and the fundus of glands treated with aluminium and concluded that normal glandular function was not impaired.

8.1.2. Action on the Reabsorptive Duct

An increased permeability of the reabsorptive duct to water was the theory put forward by Papa & Kligman, (1967) to explain their results. In addition to finding evidence of normal glandular function (glycogen depletion) they found that adhesive tape stripping, which restores sweating in cases of miliaria (due to high level ductal blockage; Papa & Kligman, 1966), did not restore sweating to skin made anhidrotic with aluminium salts. They did find an inflammatory infiltration around the duct at the level of the epidermis/dermis junction and took this as evidence that the duct was damaged and that this led to water reabsorption and explained the anhidrotic effect. However, in a TEM study of ACH and AZAP treated glands Quatrala *et al* (1981a & b) could not repeat these findings and reported that the morphological appearance of glands after ACH was identical to that in untreated skin and hence the leaky hose theory has not been universally accepted.

8.1.3. Action on the Terminal Duct

There are equally conflicting data concerning the third possible site. Shelley & Hurley (1975), Gordon & Maibach (1968) and Papa & Kligman (1967) all failed to restore sweating after tape stripping and it was concluded that if a blockage is present it is below the level of the stratum corneum. However, Sulzberger, Zak & Herrman (1949) failed to detect any such blockage. More recently, Quatralè *et al.* (1981a & b) showed that stripping restored sweating to ~50% of the glands made anhidrotic by ACH. It seems likely, as shown by Reller & Luedders (1977), that the blockage can occur as deep as the intradermal duct or as high as the stratum corneum and that this may depend on the nature of the compound. Lansdown (1973) detected aluminium from aluminium chloride but not aluminium from ACH and Quatralè *et al.* (1981c) showed that the blockage formed by ACH occurred at a deeper level than that associated with AZAP. With both compounds, ACH and AZAP, Quatralè *et al.* (1981c) found histological and electron microscopical evidence that they formed an amorphous aluminium-containing electron-opaque mass, predominantly in the stratum corneum but also as deep as the intraepidermal duct at the stratum granulosum layer. Finally, Holzle & Braun-Falco (1984), in a long term study (6-40 months) of the effects of aluminium chloride hexahydrate on the human axilla, concluded that inhibition of sweating was due to a blockage in the distal acrosyringium and that this may eventually lead to atrophy of the secretory coil.

The effects of ACH and aluminium compounds on the epitrichial (apocrine) glands of the axilla, the normal site of application of topical antiperspirants, have not been extensively studied and the results are difficult to interpret since this region contains both atrichial and epitrichial glands. Thus, Rees-Jones & Jenkinson (1978) found neither an antiperspirant effect nor morphological changes induced by aluminium on the epitrichial glands of cattle, whilst Majors & Wild (1974) found a 39% reduction in axillary sweating with ACH. It seems likely, as Rees-Jones & Jenkinson (1978) suggested, that the ACH antiperspirant effect is restricted to atrichial glands, a fact which is supported by the finding that only atrichial glands are affected by treatment of the axilla with

antiperspirants. This would be consistent with an upper ductal blockage mechanism since the tightly spiralling atrichial duct should be easier to block than the duct of the epitrichial gland which opens into the hair canal.

This study was therefore performed on the atrichial sweat glands from the human back to try to identify the glandular site and possible mechanism of action of aluminium-containing antiperspirants. The bases for this study were the comparisons of the morphological changes and of the elemental concentrations within the duct and fundus of sweat glands from skin treated with aluminium-containing antiperspirants with glands from untreated skin, both before and after thermal stimulation. In addition, EPXMA can be used to identify the composition of any "blockage" that might be present.

A preliminary study was also performed on the rat footpad sweat gland to determine the depth of penetration and spread of aluminium, from a commercially available antiperspirant, into the skin, using a freeze-substitution method.

8.2. MATERIALS AND METHODS

8.2.1. Preliminary Rat Study

See Appendix 9 for details of materials and methods.

8.2.2. Human Study

Two areas of skin, each 10 × 15cm, situated between the waist and scapula and 5cm from the mid-dorsal line (Fig.8.1.) were delineated on a total of nine male volunteers aged between 20-30 years.

On five of the subjects, 2ml of a 15% ^{w/v} aqueous aluminium zirconium tetrachlorhydrate complex (Rezal 36) was applied to both areas on six occasions over four days as shown below:

Day 1	Day 2	Day 3	Day 4
a.m.	a.m.	a.m.	a.m.
	p.m.	p.m.	

The solution was applied to the other four subjects on five occasions over two days, three times on the first day and twice on day of the experiment. The aqueous solution of antiperspirant was applied to the prescribed areas of skin from a syringe, spread uniformly with a soft paint brush and allowed to partially dry. Repetition of this procedure allowed the application of 2ml of the solution over a period of 10-15min. These areas were not washed during the experimental period. The final application was made 45min before transferring the subjects to a controlled environment of 40°C;50% relative humidity in a climatic room. In the intervening period all subjects rested in a room at 16°C. Cutaneous evaporative loss was continuously monitored from an adjacent untreated area on the back using a ventilated capsule and humidity measuring system (Humitec). A skin sample (4 mm diameter) was taken from one of the treated areas by biopsy without anaesthetic using a high speed punch before, at the onset of and 3h after sweating occurred on the monitored untreated area. The sweating response on the other treated area was assessed using a starch/iodine mixture. Skin samples from the twelve adult males described in Chapter 6, who had not been given antiperspirant treatment but were otherwise treated identically, served as control tissues. After biopsy, the samples were divided and processed for EPXMA or conventional transmission electron microscopy as described in Chapters 3 and 2 respectively.

For conventional TEM the glands were cut sequentially at 50µm intervals from the epidermis towards the fundus in the deep dermis. The EPXMA was performed as described previously in Chapter 6 and the values in mMoles/kg dry wt. were calculated with corrections applied for mass loss and for the chlorine content of the resin. Statistical comparisons with glands from untreated skin were performed by an analysis of variance.

8.3. RESULTS

8.3.1. Rat Study

See Appendix 10 for results.

8.3.2. Human Study

8.3.2.a. **Sweat Output**

The antiperspirant treated areas exhibited randomly distributed positive starch/iodine reactions within 20-30min of entering the climatic room. By 45min the sweating response was widespread throughout these areas. With reference to the sweating response on the untreated areas it was clear that sweating did not occur simultaneously on both areas but had been slightly delayed in the treated areas.

8.3.2.b. **Ultrastructure**

i) Fundus The ultrastructural appearance of the fundus of unstimulated glands from antiperspirant treated skin (Fig.8.2.) was indistinguishable from that of untreated skin, although the lumen was often narrow in treated glands. The myoepithelial cells and both the granular and non-granular secretory cells appeared normal. Canaliculi were seen between adjacent non-granular cells and the junctional complexes between cells were intact.

Thermal stimulation induced identical changes in the fundus of glands from both treated and untreated skin. In the early stages of sweating (Fig.8.3.) there was evidence of loss of granules from the granular cells, marked dilatation of the spaces between non-granular cells, contraction of the myoepithelial cells and cellular debris was occasionally seen in the lumen. After 3h of continuous sweating (Fig.8.4.) the degranulation was more pronounced and atretic secretory cells were seen in some instances.

ii) Duct Electron microscopy of the ducts of unstimulated glands from treated skin revealed an obstructive electron-opaque mass within the keratinised lining of the duct in the outer epidermis (Fig.8.5.). Similar obstructions were never seen in untreated ducts. Electron probe X-ray microanalysis of the obstructions revealed the presence of aluminium (Fig.8.6.) and although aluminium was occasionally present in lower

concentrations 50 μ m deeper in the duct it was not detected in the intradermal duct at any level. Within the intraepidermal region the only noticeable effect of antiperspirant treatment was a narrowing of the lumen (Fig.8.7.).

At the onset of sweating some ducts in the upper epidermis were still blocked. However, ducts in sections from deeper in the epidermis and just beneath it had an appearance that was identical to those of untreated glands after thermal stimulation (Fig.8.8.). The lumen was enlarged and full of a colloidal material and there was dilatation of the spaces between the cells within the duct wall. After 3h of heat exposure there was no evidence of ductal obstruction (Fig.8.9.) and the ducts were indistinguishable from those in treated skin.

8.3.2.c. Intracellular elemental concentrations

i) Fundus The elemental concentrations in the secretory epithelium of the fundus at rest and after thermal stimulation are shown in Table 8.1., for antiperspirant treated glands, and in Fig.8.10. for glands from both antiperspirant treated and untreated glands (the values calculated for the glands in Chapter 6 were used as the untreated controls). Stimulation produced no significant changes in the intracellular levels of Na, K and Cl in the treated glands. Aluminium itself was never detected in spectra recorded from the fundus.

ii) Duct In the duct, Table 8.2. and Fig.8.11., stimulation caused falls in Na (53%) and Cl (52%) and a rise in K (169%) in glands after antiperspirant treatment. Compared to untreated glands the level of Na in the treated glands was significantly lower after stimulation. Again aluminium was not detected in any of these spectra.

8.4. DISCUSSION

8.4.1. Rat

Application of both substances resulted in the formation of an electron-opaque layer, rich in aluminium, which appeared to be restricted to the outer 2µm of the stratum corneum. This precipitate was also detected within the ducts of the sweat glands in this surface zone after treatment with the aluminium chlorhydrate solution. Aluminium was also present in the lumen of the duct after treatment with "Body Mist", although clear evidence of a precipitate in the duct was not obtained. The precipitate, however, was apparently absent from the stratum corneum in the vicinity of the sweat gland ducts. The evidence thus supports the view that ductal blockage occurs after treatment with aluminium salts.

The presence of aluminium within the duct traversing the living epidermis suggests that the precipitate may well extend to this depth, although this is not immediately visible. The results also indicate the presence of aluminium within the dermis and within the duct and fundus in this region although it was present only in some instances and then only in trace amounts. However, the nature of the preparative method is such that a considerable amount of aluminium may have been lost and the possibility of an action of aluminium on the fundus cannot be completely eliminated.

8.4.2. Human

The results confirm the earlier findings (Reller & Luedders, 1977; Holzle & Kligman, 1979; Quatrala *et al* 1981b & c) that the short-term topical treatment with aluminium salts produces an aluminium-containing obstruction in the duct of the human atrichial sweat gland within the upper epidermis, particularly the stratum corneum. This treatment also caused a constriction of the lumen of both the fundus and duct. The normal ductal response to thermal stimulation did not appear to be affected by the treatment since heat exposure resulted in ultrastructural changes which were indistinguishable from

those which occur during sweating in the untreated duct. Apart from the constriction of the lumen at rest, the ultrastructural appearance of the fundus after antiperspirant treatment was also similar to untreated glands, both before and after stimulation.

The intracellular elemental changes in the fundus and duct suggest that the application of aluminium-containing antiperspirants has an effect in both regions. At rest, comparing the glands from both treated and untreated skin, there were no significant differences in Na, K or Cl. However, after stimulation there were marked differences in the response of the glands in the two groups. Although the small sample size of the treated group necessitates the use of caution in reaching firm conclusions it is clear that the funduses of these glands show no alteration in intracellular concentration of the three elements measured. In the untreated controls there was a significant rise in Na and a decrease in K and it appears that the application of antiperspirants inhibits the normal function of this secretory epithelium. At present there are several possible explanations of this inhibitory effect of aluminium. It has been shown to inhibit the Na/K ATPase in rat brain synaptosomes (Lai *et al* 1980), although this only occurred at relatively high concentrations of aluminium (~ 100mM), which should have been detected by the EPXMA method used in this study. A second, and more likely, explanation is that the aluminium binds to and inhibits calmodulin, as has been shown in bovine brain (Siegel & Haug, 1983). Although the exact mechanism of action of calmodulin is not clear it is thought to modulate cellular processes in which calcium is the second messenger. In view of the importance of calcium in the secretory response of sweat glands, inhibition of calmodulin could have a crucial role. In addition, the aluminium concentration required to inhibit calmodulin is much lower than that required to inhibit Na/K ATPase (i.e. 15µM aluminium produces 50% inhibition of bovine brain calmodulin). This would explain why aluminium was not detected in the fundus.

The effects of stimulation in the duct of antiperspirant treated skin are difficult, if not impossible to explain. In untreated skin there were no significant changes after stimulation. In treated skin there were decreases in Na and Cl and a rise in K, although, because of the small

sample size, these failed to reach significance. There appear to be no circumstances in which the duct cells, presumably high in K and low in Na with respect to plasma and therefore having electrochemical gradients for K efflux and Na influx, would accumulate K and lose Na during activity. The situation is further complicated by the fact that this region is thought to be inactive and clearly further work is required to clarify this situation.

The delay in sweating in treated skin is probably due to the aluminium-containing ductal obstruction in the epidermis and to some impairment of the secretory processes of the fundus. Since the ultrastructure of the treated glands after stimulation is similar to that of untreated glands it suggests that the first factor is the more important and that the delay is caused by the physical obstruction of the outflow of sweat.

The conclusion from both studies is that although aluminium penetrates into the epidermis and dermis to a depth sufficient to produce a pharmacological effect on the secretory fundus the concentration is below the detection limits of the EPXMA method used. The formation of an aluminium-containing obstruction in the upper epidermis is also a component of the antiperspirant action of aluminium salts. Whether this obstruction completely prevents sweat flow to the skin surface or merely delays its appearance is not clear but prolonged sweating is sufficient to completely clear the duct.

Table 8.1. Intracellular elemental concentrations of Na, K and Cl in the fundus of the antiperspirant treated human atrichial sweat gland before and after thermal stimulation.

Element	Rest	Active
Na	154 ± 21	154 ± 17
Cl	72 ± 10	76 ± 11
K	156 ± 18	155 ± 17

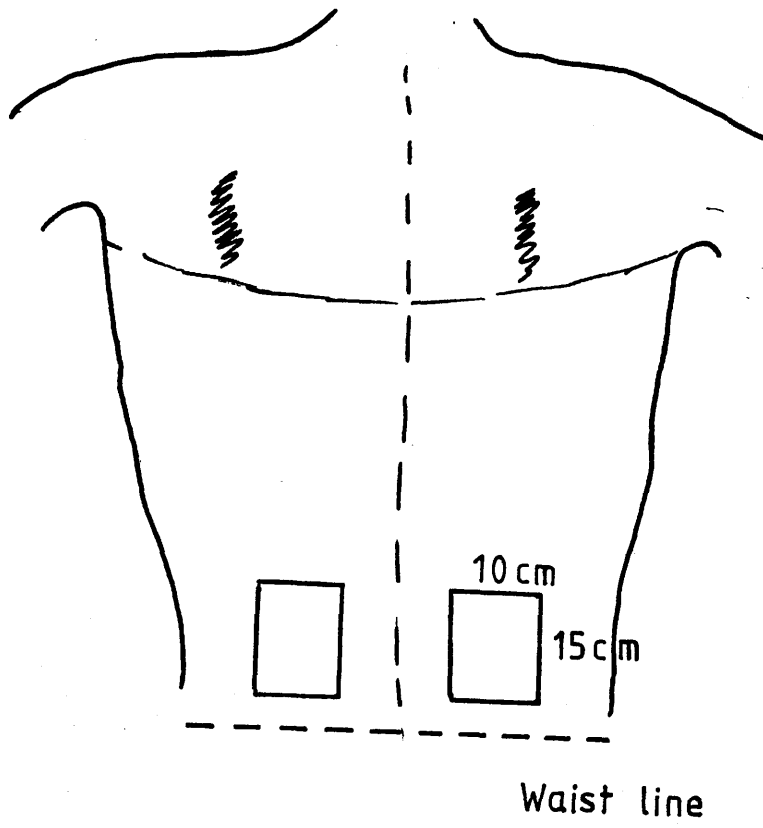
Values are the means ± S.E.M. Units are mMol/kg dry wt..

Table 8.2. Intracellular elemental concentrations of Na, K and Cl in the duct of the antiperspirant treated human atrichial sweat gland before and after thermal stimulation.

Element	Rest	Active
Na	256 ± 54	119 ± 22
Cl	48 ± 16	129 ± 36
K	94 ± 13	45 ± 15

Values are the means ± S.E.M. Units are mMol/kg dry wt..

Fig.8.1. Diagram illustrating the areas of the back that were treated with an aluminium-containing antiperspirant, as described in the text.



Abbreviations used

BI - basolateral interdigitations

Ca - canaliculus

CR - cell remnants

CT - connective tissue

FS - fibrocyte sheath

GC - granular cell

L - lumen

LDC - luminal duct cell

MV - microvilli

Myo - myoepithelial cell

N - nucleus

NGC - non-granular cell

Obs - obstruction

Fig.8.2. An electron micrograph of the fundus of the unstimulated human atrichial fundus after antiperspirant treatment, illustrating the typical appearance of the granular and non-granular cells. The lumen is dilated and the spaces between the basolateral infoldings are narrow. (bar = 2 μ m)

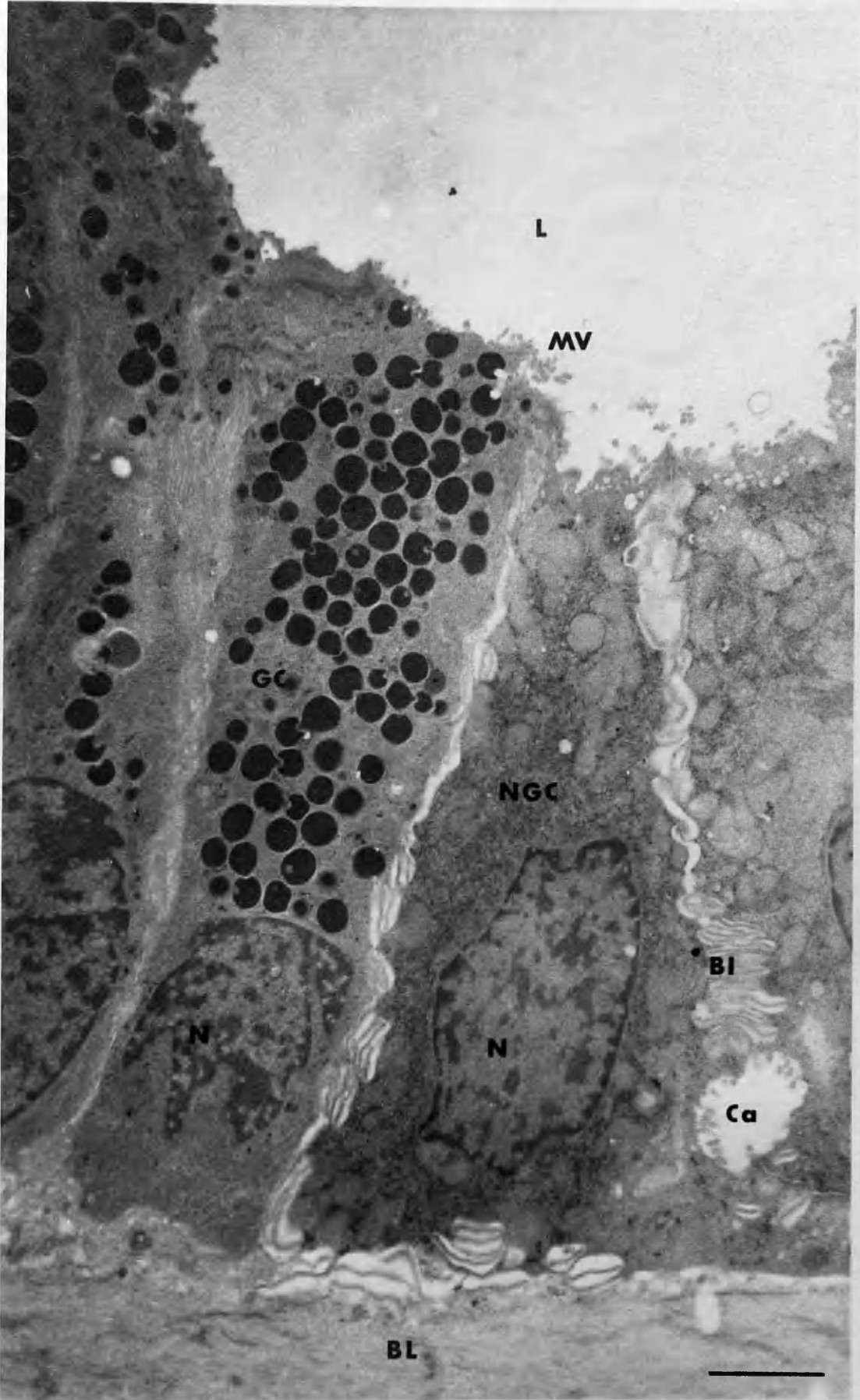


Fig.8.3. An electron micrograph of the early stages of activity in the fundus after antiperspirant treatment. The granules have accumulated at the apical surface of the cells and the cytoplasm of the non-granular cells contains less glycogen and has a foamy appearance. (bar = 4 μ m)

Fig.8.4. After prolonged stimulation of the treated glands the secretory epithelium has become less cuboidal than in the unstimulated state. There is granule depletion and any remaining granules are concentrated in the most apical region of the cells. There is pronounced dilatation of the basolateral spaces and at intervals in the secretory epithelium there are gaps resulting from cell death. (bar = 4 μ m)

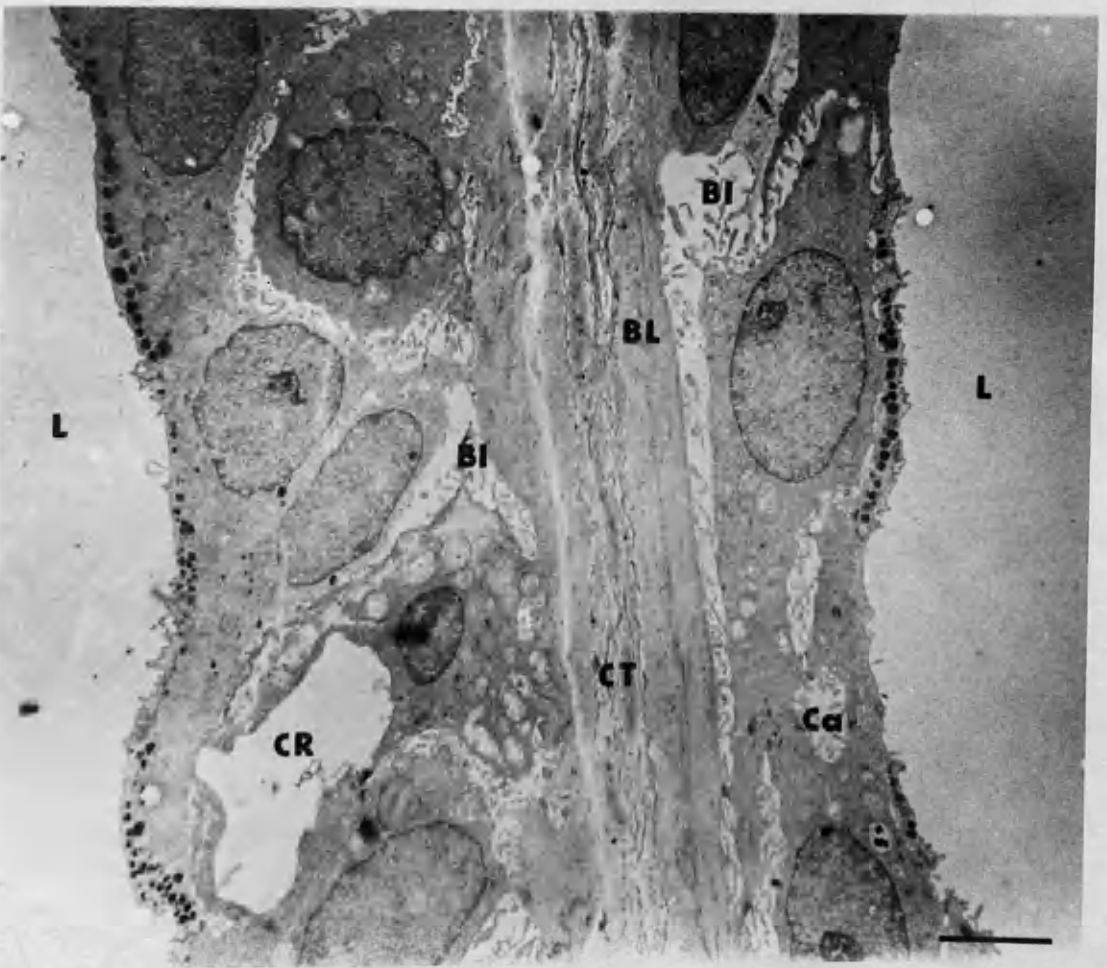
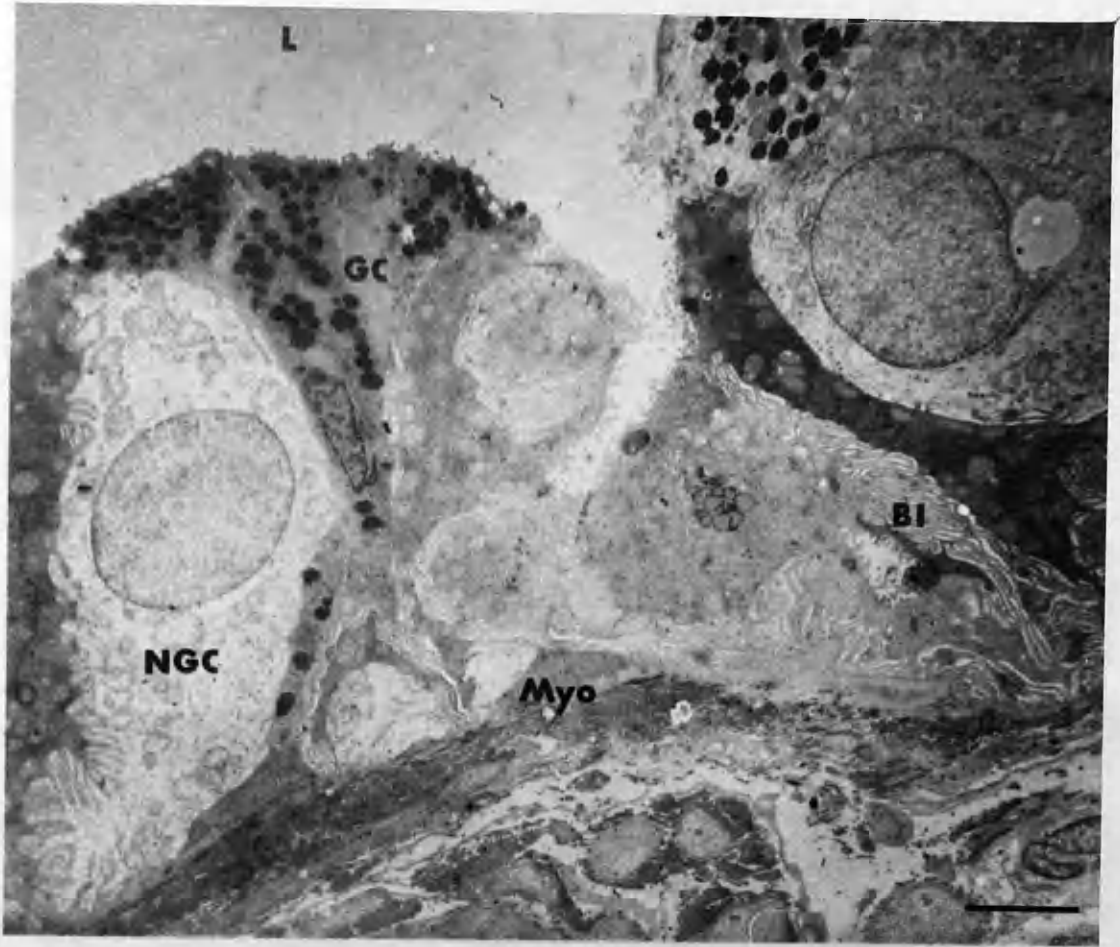


Fig.8.5. An electron micrograph of the intraepidermal region of the human sweat gland duct. The lumen of the gland is narrow and is totally blocked by an electron-opaque precipitate. (bar = 4 μ m)

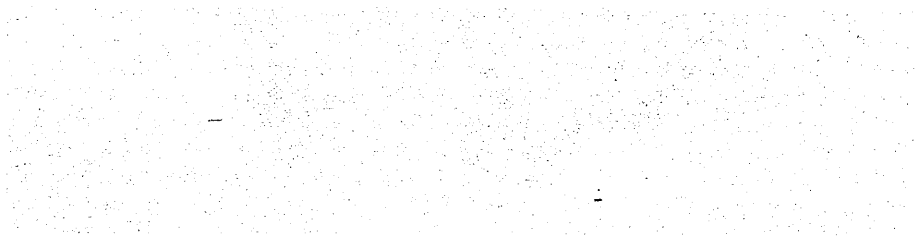


Fig.8.7. An electron micrograph of the unstimulated upper ascending duct in the intraepidermal region. The only noticeable difference between this and untreated ducts is the narrowing of the lumen. (bar = 4 μ m)

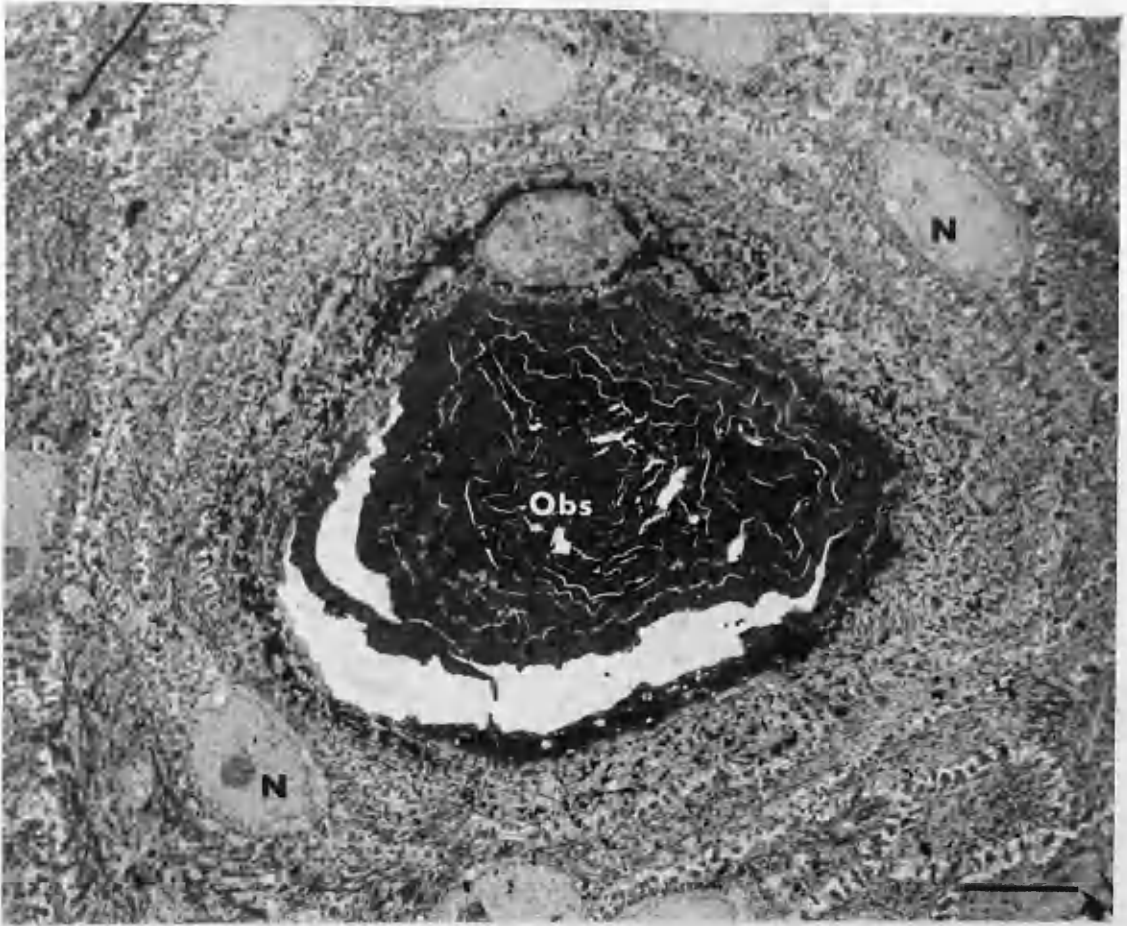


Fig.8.6. X-ray spectra from the duct of the antiperspirant treated gland shown in Fig.8.5. a) from the obstruction within the lumen
b) from the apical edge of the surrounding epithelium
c) from the lumen of the duct 50 μ m deeper than the blockage

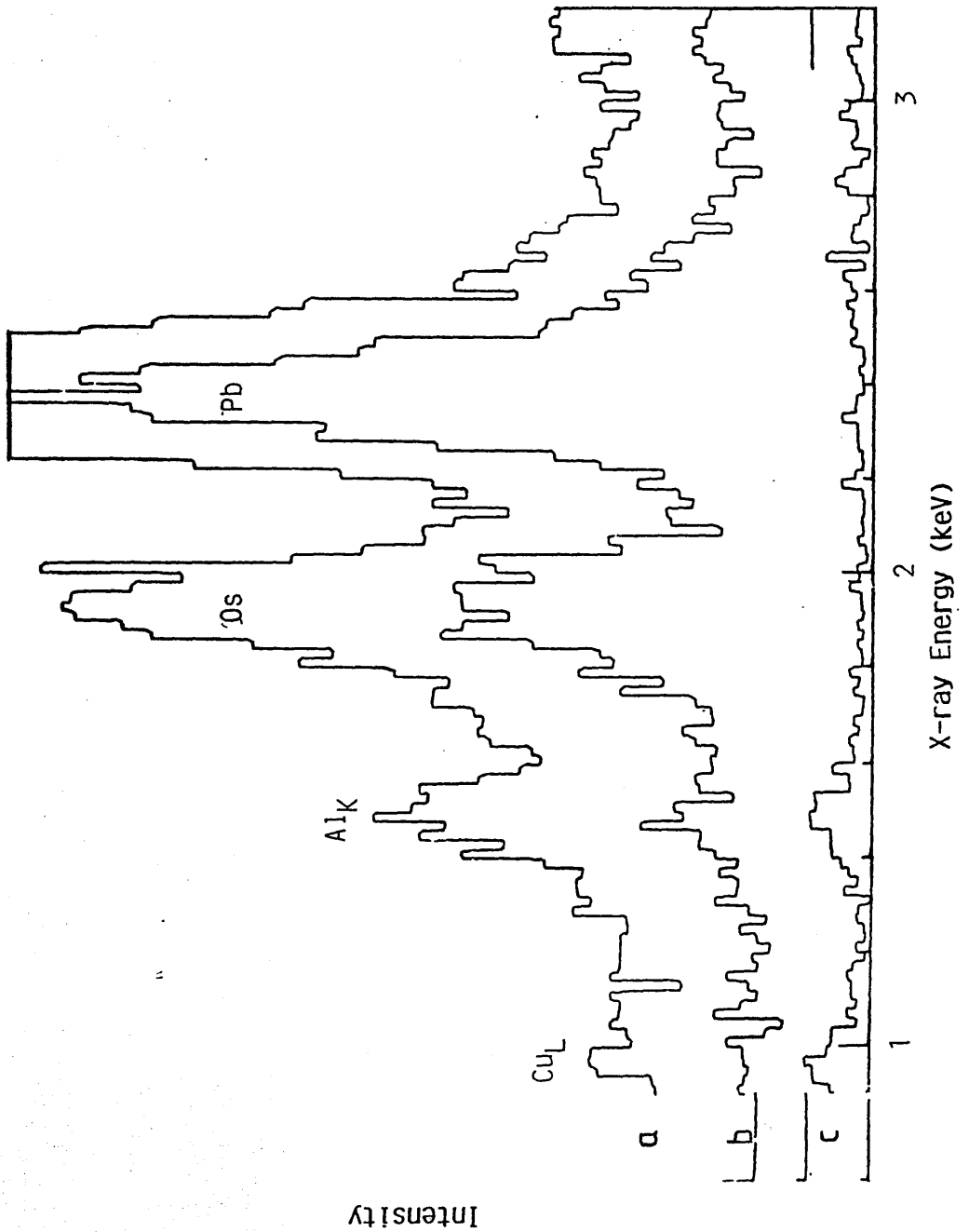


Fig.8.8. In the upper intradermal duct at the onset of stimulation there is a widening of the intercellular spaces and the lumen is full of a colloidal material. (bar = 2 μ m)

Fig.8.9. After prolonged stimulation the appearance of the ascending duct in the epidermis is typical of the active gland. The lumen is clear of any obstruction and is wider than in the unstimulated gland. The basolateral spaces between the duct cells are dilated. (bar = 4 μ m)

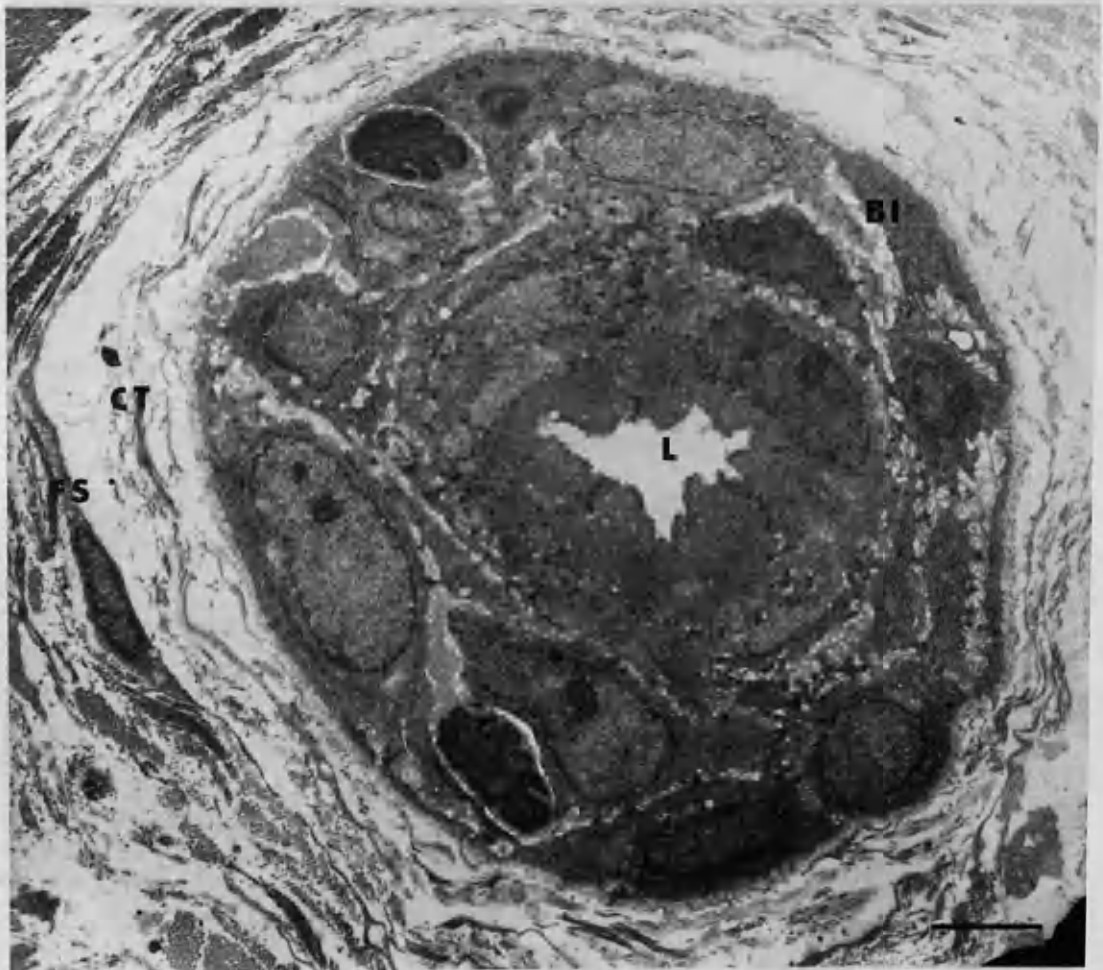
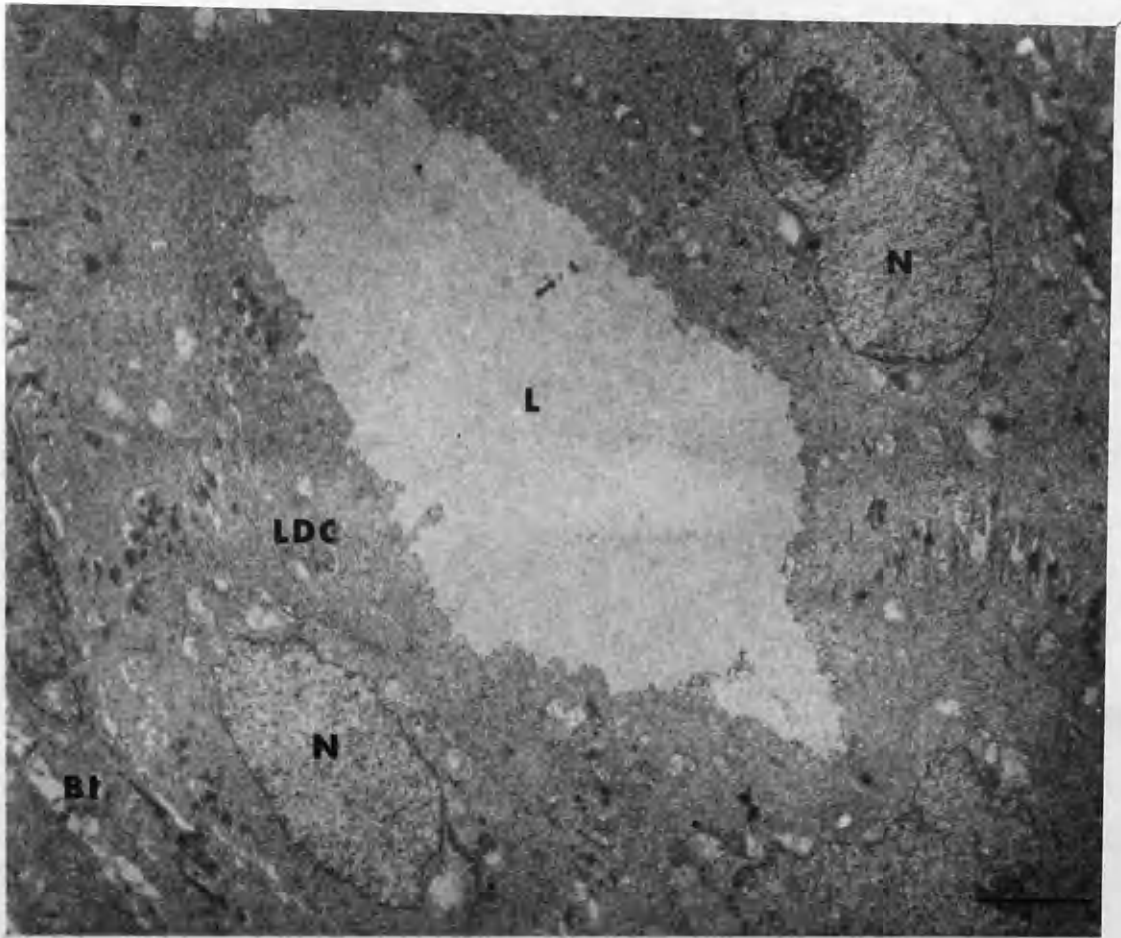

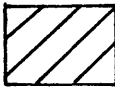


Fig.8.10. A histogram of the elemental concentrations (mMoles/kg dry wt.) of Na, Cl and K in the human sweat gland fundus in the unstimulated and stimulated state before (upper) and after (lower) a course of antiperspirant treatment.

Unstimulated 

Stimulated 

Values are means \pm S.E.M.

n = number of individuals

★ = significantly different from unstimulated ($p < 0.05$)

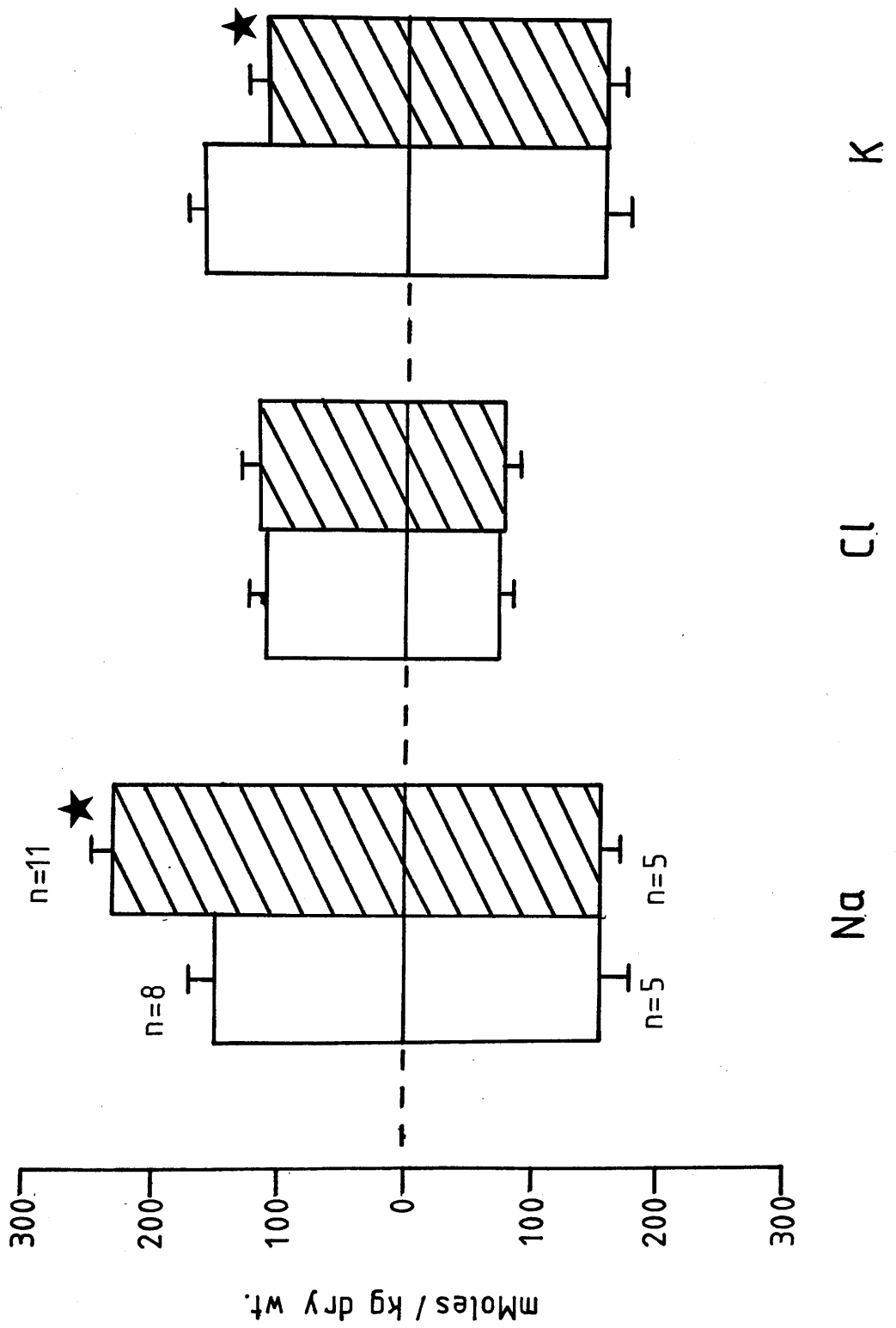
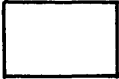



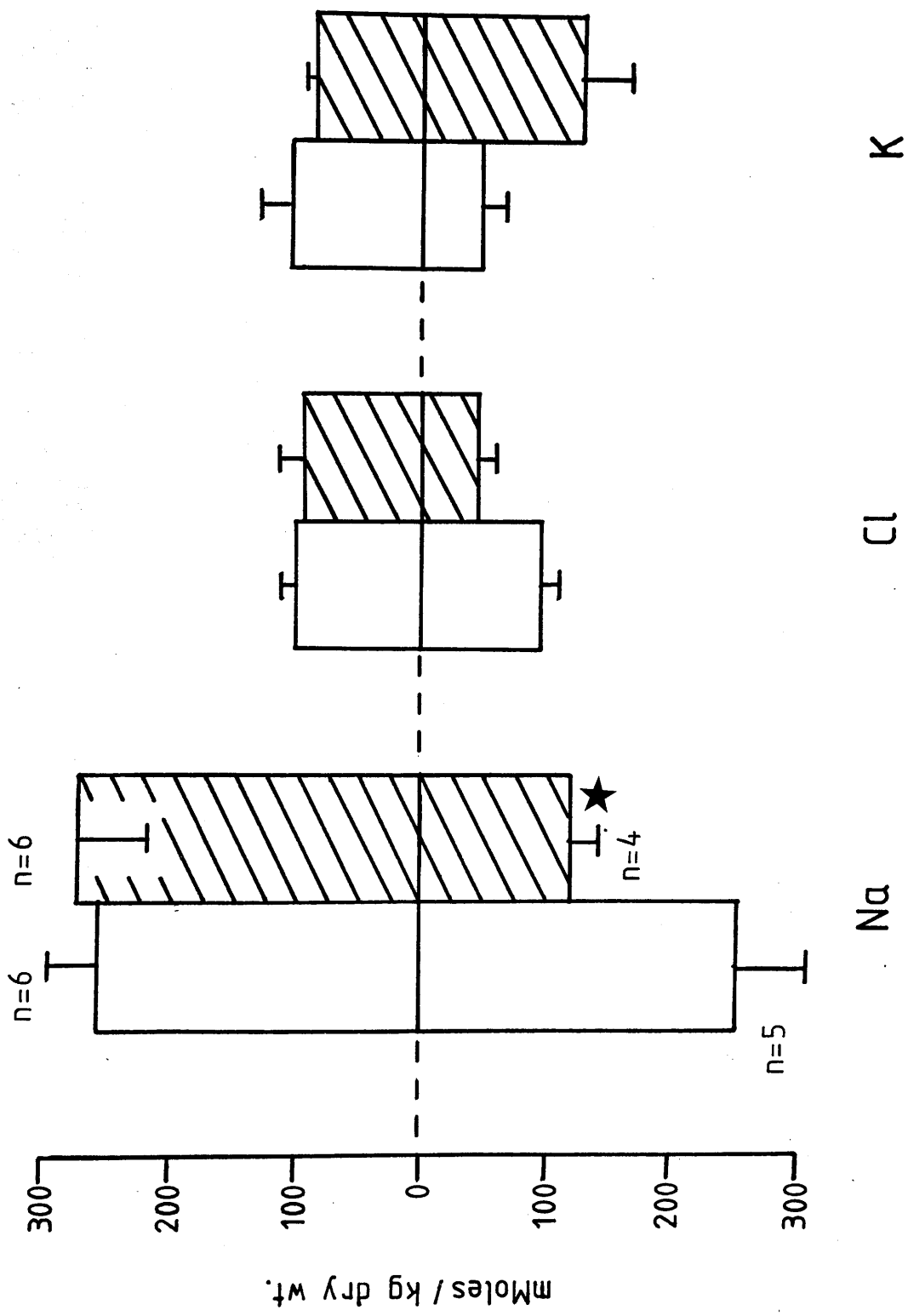
Fig.8.11. A histogram of the elemental concentrations (mMoles/kg dry wt.) of Na, Cl and K in the human sweat gland straight duct in the unstimulated and stimulated state before (upper) and after (lower) a course of antiperspirant treatment.

Unstimulated 
Stimulated 

Values are means \pm S.E.M.

n= number of individuals

★ = significantly different from untreated Δ ($p < 0.05$)



REFERENCES

1. J. H. Duerksen, *Can. J. Microbiol.*, **1975**, **21**, 11-14.

2. J. H. Duerksen, *Can. J. Microbiol.*, **1975**, **21**, 15-18.

3. J. H. Duerksen, *Can. J. Microbiol.*, **1975**, **21**, 19-22.

4. J. H. Duerksen, *Can. J. Microbiol.*, **1975**, **21**, 23-26.

5. J. H. Duerksen, *Can. J. Microbiol.*, **1975**, **21**, 27-30.

- Andrews,S.B., Mazurkiewicz,J.E.& Kirk,R.G. (1983) The distribution of intracellular ions in the avian salt gland. *J.Cell Biol*, **96**, 1389-1399.
- Appleton,T.C. (1974) A cryostat approach to ultrathin "dry" frozen sections for electron microscopy: a morphological and X-ray analytical study. *J.Microsc*, **100**, 49-74.
- Appleton,T.C. (1977) The use of ultrathin frozen sections for X-ray microanalysis of diffusible elements. In: *Analytical and Quantitative Methods in Microscopy* (ed. by G.A.Meek and H.Y.Elder) p.247-268, Cambridge University Press.
- Bachmann,L.& Schmitt,W.W. (1971) Improved cryofixation applicable to freeze-etching. *Proc.Nat.Acad.Sci.USA*, **68**, 2149-2152.
- Bahr,G.F., Johnson,F.B.& Zeitler,E. (1965) The elementary composition of organic objects after electron irradiation. *Lab.Invest*, **14**, 1115-1133.
- Bald,W.B. (1983) Optimising the cooling block for the quick freeze method. *J.Microsc*, **131**, 11-23.
- Bald,W.B. (1984) The relative efficiency of cryogenic fluids used in the rapid quench cooling of biological samples. *J.Microsc*, **134**, 261-270.
- Bald,W.B. (1985) Relative merits of various cooling methods. *J.Microsc*, **140**, 17-40.
- Barnard,T. (1982) Thin frozen-dried cryosections and biological x-ray microanalysis. *J.Microsc*, **126**, 317-332.
- Barnard,T.& Seveus,L. (1978) Preparation of biological material for x-ray microanalysis of diffusible elements. II. Comparison of different methods of drying ultrathin sections cut without a trough liquid. *J.Microsc*, **112**, 281-291.

- Beck,F., Bauer,R., Bauer,U., Mason,J., Dörge,A., Rick,R.& Thurau,K. (1980) Electron microprobe analysis of intracellular elements in the rat kidney. *Kidney Int*, **17**, 756-763.
- Bell,L.G.E. (1956) Freeze-drying. In: *Physical Techniques in Biological Research* (ed. by G.Oster & A.W.Pollister) Vol.III, p.1-27, Academic Press, New York.
- Bernhard,W.& Leduc,E.H. (1967) Ultrathin frozen sections. I. Methods and ultrastructural preservation. *J.Cell Biol*, **34**, 757-771.
- Berridge,M.J. (1975) The interaction of cyclic nucleotides and calcium in the control of cellular activity. *Adv.Cyclic Nucleotide Res*, **6**, 99-136.
- Blank,I.H., Jones,J.L.& Gould,E. (1958) A study of the penetration of aluminium salts into excised human skin. *Pro.Sci.Sect.Toilet Goods Assoc*, **29**, 32-35.
- Bligh,J. (1967) A thesis concerning the processes of secretion and discharge of sweat. *Environmental Research*, **1**, 28-45.
- Borowitz,S.& Beiser,A. (1971) *Essentials of Physics*. Addison-Wesley Publishing Co., Reading, Mass.
- Boyle,P.J.& Conway,E.J. (1941) Potassium accumulation in muscle and associated changes. *J.Physiol*, **100**, 1-63.
- Bruslow,S.W., Ikal,K.& Gordes,E. (1968) Comparative physiological aspects of solute secretion by the eccrine sweat gland of the rat. *Proc.Soc.Exp.Biol.Med*, **129**, 731-732.
- Bundgaard,M., Møller,M.& Poulsen,J.H. (1979) Localisation of sodium and potassium activated ATPase in the pancreas. *J.Physiol*, **295**, 13P.

- Burgen,A.S.V. (1956). The secretion of potassium in the saliva. *J.Physiol.*, **132**, 20-39.
- Burovina,I.V., Gribakin,F.G., Petroysan,A.M., Pivovarova,N.B., Pogorelov,A.G.& Polyanovsky,A.D. (1978) Ultrastructural localisation of potassium and calcium in an insect omnatidium as demonstrated by x-ray microanalysis. *J.comp.Physiol.*, **127**, 245-253.
- Chalmers,T.M.& Keele,C.A. (1951) Physiological significance of the sweat response to adrenaline in man. *J.Physiol.*, **114**, 510-514.
- Chandler, J.A. (1977) Chapter 4 - Specimen Preparation. In: *X-Ray Microanalysis in the Electron Microscope*. In the series Practical Methods in Electron Microscopy (ed. by A.M.Glauert) p.377-423 North-Holland Publishing Co., Amsterdam, New York & Oxford.
- Chapman,J.N., Gray,C.C., Robertson,B.W.& Nicholson,W.A.P. (1983) X-ray production in thin films by electrons with energies between 40 and 100 keV. I. Bremsstrahlung cross-sections. *X-ray Spectrometry*, **12**, 153-162.
- Christensen,A.K. (1967) A simple way to cut frozen thin sections of tissue at liquid nitrogen temperature. *Anat.Rec.*, **157**, 227.
- Christensen,A.K. (1971) Frozen thin sections of fresh tissue for electron microscopy, with a description of pancreas and liver. *J.Cell Biol.*, **51**, 772-804.
- Civan,M.M.,Hall,T.A.& Gupta,B.L. (1980) Microprobe study of toad urinary bladder in absence of serosal K⁺. *JMembr.Biol.*, **55**, 187-202.
- Cohen,P.J. (1975) Chapter 3-Signs and stages of anesthesia. In: *The Pharmacological Basis of Therapeutics* 5th edn. (ed. by L.S.Goodman & A.Gilman) p.60-65, MacMillan Publishing Co., New York.

Coulter,H.D.& Terracio,L. (1977) Preparation of biological tissues for electron microscopy by freeze-drying. *Anat.Rec*, **187**, 477-493

Dale,H.H.& Feldberg,W. (1934) Chemical transmission of secretory impulses to sweat glands of cat. *J.Physiol*, **82**, 121-128.

Darke,A.C.& Smaje,L.H. (1972) Dependence of functional vasodilation in the cat submaxillary gland upon stimulation frequency. *J.Physiol*, **226**, 191-203.

Davies,D.A.& Erasmus,T.W. (1973) Cryo-ultramicrotomy and x-ray microanalysis in the transmission electron microscope. *Sci.Tools*, **20**, 9-13.

Dempsey,G.P.& Bullivant,S. (1976a) A copper block method for freezing non-cryoprotected tissue to produce ice-crystal-free regions for electron microscopy I. Evaluation using freeze-substitution. *J.Microsc.*, **106**, 251-260.

Dempsey,G.P.& Bullivant,S. (1976b) A copper block method for freezing non-cryoprotected tissue to produce ice-crystal-free regions for electron microscopy. II. Evaluation using freeze-fracturing with a cryo-ultramicrotome. *J.Microsc.*, **106**, 261-271.

Dollhopf,F.L.& Sitte,H. (1969) Die Shandon-Reichert Kühleinrichtung FC-150 zum herstellen von Ultradiinn und Feinschnitten bei extrem niederen Temperaturen: I. Geratetechnik. *Mikroskopie*, **25**, 17-32.

Dörge,A., Rick,R., Gehring,K.& Thurau,K. (1978) Preparation of freeze dried cryosections for quantitative x-ray microanalysis of electrolytes in biological soft tissues. *Pflugers Arch*, **373**, 85-97.

Doty,S.B., Lee,C.N.& Banfield,W.G. (1974) A method of obtaining ultrathin frozen sections from fresh or glutaraldehyde-fixed tissues. *Histochemical Journal*, **6**, 383-393.

Dubochet, J. & McDowell, A.W. (1984) Frozen hydrated sections. In: *Science of Biological Specimen Preparation* (ed. by J-P.Revel, T.Barnard & G.H.Haggis) p.147-152, S.E.M. Inc., AMF O'Hare, Ill.

Edie, J.W. & Glick, P.L. (1979) Irradiation effects in the electron microprobe quantitation of mineralised tissues. *J.Microsc.*, **117**, 285-296.

Egerton, R.F. (1980) Chemical measurement of radiation damage in organic samples at and below room temperature. *Ultramicroscopy*, **5**, 521-523.

Elder, H.Y., Gray, C.C., Jardine, A.G., Chapman, J.N. & Biddlecombe, W.H. (1982) Optimum conditions for cryoquenching of small tissue blocks in liquid coolants. *J.Microsc.*, **126**, 45-61.

Elder, H.Y., Jenkinson, D.McEwan, McWilliams, S.A. & Wilson, S.W. (1985) Intracellular concentrations of sodium, phosphorus, chlorine and potassium in the ductal epithelium of unstimulated and active equine sweat glands. *J.Physiol.*, **367**, 74P.

Elder, H.Y., Biddlecombe, W.H., Tetley, L., Wilson, S.M. & Jenkinson, D.McEwan. (1986) Construction of low temperature freeze-driers. *EMSA Bulletin*, **16**, 111-113.

Ellis, R.A. (1962) The fine structure of the eccrine sweat glands. In: *Advances in Biology of Skin*. (ed. by W Montagna, R.A. Ellis & A.F. Silver) Vol.III, p.30-53, Pergamon Press, Oxford.

Ernst, S.A. (1972) Transport adenosine triphosphatase cytochemistry. II. Cytochemical localisation of ouabain-sensitive, potassium-dependent phosphatase activity in the secretory epithelium of the avian salt gland. *J.Histochem.Cytochem.*, **20**, 23-38.

Escaig, J. (1982) New instruments which facilitate rapid freezing at 83K and 6K. *J.Microsc.*, **126**, 221-229.

Fernandez-Moran,H. (1952) The submicroscopic organization of vertebrate nerve fibres. An electron microscope study of myelinated and unmyelinated nerve fibers. *Exp.Cell Res*, **3**, 282-359.

Franks, F. (1978) Biological freezing and cryofixation. *J.Microsc.*, **111**, 3-16.

Foster,K.G., Ginsburg,J.& Weiner,J.S. (1970) Role of circulating catecholamines in human eccrine sweat gland control. *Clinical Science*, **39**, 823-832.

Foster,K.G.& Weiner,J.S. (1970) Effects of cholinergic and adrenergic blocking agents on the activity of the eccrine sweat glands. *J.Physiol.*, **210**, 883-895.

Fromter,E.& Diamond,J.M. (1972) Route of passive ion permeation in epithelia. *Nature*, **235**, 9-13.

Gayton,D.C.& Hinke,J.A.M. (1971) Evidence for the heterogeneous distribution of chloride in the giant barnacle. *Can.J.Physiol.Pharm.*, **49**, 323-330.

Goldberg,N.D.& Haddox,M.K. (1977) Cyclic GMP metabolism and involvement in biological regulation. *Ann.Rev.Biochem.*, **46**, 823-896.

Goldstein,J.I., Costley,J.L., Lorimer,G.W.& Reed,S.J.B. (1977) Quantitative X-ray analysis in the electron microscope. *Scanning Electron Microscopy/1977/1*, p.315-323, SEM Inc., AMF O'Hare, Ill.

Gordon,B.I.& Maibach,H.I. (1968) Studies on the mechanism of aluminium anhidrosis. *J.Invest.Derm.*, **50**, 411-413.

Green,M.& Cosslett,V.E. (1961) The efficiency of production of characteristic x-radiation in thick targets of a pure element. *Proc.Phys.Soc.*, **78**, 1206-1214.

Gupta,B.L. (1979) The electron microprobe x-ray analysis of frozen-hydrated sections with new information on fluid transporting epithelia. In: *Microbeam Analysis in Biology* (ed. by C.P.Lechene & R.R.Warner) p.375-408, Academic Press, New York & London.

Gupta,B.L., Berridge,M.J., Hall,T.A.& Moreton,R.B. (1978) Electron microprobe and ion-selective microelectrode studies of fluid secretion in the salivary glands of calliphora. *J.exp.Biol.*, **72**, 261-284.

Gupta,B.L.& Hall,T.A. (1979) Quantitative electron probe x-ray microanalysis of electrolyte elements within epithelial tissue compartments. *Fed.Proc.*, **38**, 144-153.

Gupta,B.L.& Hall,T.A. (1981) The x-ray microanalysis of frozen-hydrated sections in scanning electron microscopy : An evaluation. *Tissue & Cell*, **13**, 623-643.

Hackenbrock,C.R. (1966) Ultrastructural bases for metabolically linked mechanical activity in mitochondria. I. Reversible ultrastructural changes with change in metabolic state in isolated liver mitochondria. *J.Cell Biol.*, **30**, 269-297.

Hackenbrock,C.R. (1968) Ultrastructurel bases for metabolically linked mechanical activity in mitochondria. II. Electron transport-linked ultrastructural transformations in mitochondria. *J.Cell Biol.*, **37**, 345-369.

Hall,T.A. (1971) Chapter 3. - The microprobe analysis of chemical elements. In: *Physical Techniques in Biological Research*, 2nd edn. (ed by G. Oster) Vol. 1A - Optical Techniques, p.157-275, Academic Press, New York & London.

Hall,T.A. (1979) Problems of the continuum - normalisation method for the quantitative analysis sections of soft tissue. In: *Microbeam Analysis in Biology* (ed. by C.P.Lechene & R.R.Warner) p.185-208, Academic Press, New York & London.

Hall, T.A., Anderson, H.C. & Appleton, T. (1973) The use of thin specimens for X-ray microanalysis in biology. *J. Microsc.*, **99**, 177-182.

Hall, T.A. & Gupta, B.L. (1974) Beam-induced loss of organic mass under electron microprobe conditions. *J. Microsc.*, **100**, 177-188.

Hall, T.A. & Gupta, B.L. (1982) Quantification for the x-ray microanalysis of cryosections. *J. Microsc.*, **126**, 333-346.

Hall, T.A. & Gupta, B.L. (1984) The application of EDXS to the biological sciences. *J. Microsc.*, **136**, 193-208.

Halloran, B.P. & Kirk, R.G. (1979) Quantitative electron probe microanalysis of ultrathin sections. In: *Microbeam Analysis in Biology* (ed. by C.P. Lechene & R.R. Warner) p.571-589, Academic Press, New York & London.

Harvey, D.M.R. (1982) Freeze-substitution. *J. Microsc.*, **127**, 209-221.

Harvey, D.M.R., Hall, J.L. & Flowers, T.J. (1976) The use of freeze substitution in the preparation of plant tissues for ion localisation studies. *J. Microsc.*, **107**, 189-198.

Hashimoto, K., Ogawa, K. & Lever, W.F. (1962) Histochemical studies of the skin. III. The activity of the cholinesterases during the embryonic development of the skin in the rat. *J. Invest. Derm.*, **40**, 15-26.

Hayashi, H. & Nakagawa, T. (1963) Functional activity of the sweat glands of the albino rat. *J. Invest. Derm.*, **41**, 365-367.

Heuser, J.E., Reese, T.S., Dennis, M.J., Jan, Y., Jan, L. & Evans, L. (1979) Synaptic vesicle exocytosis captured by quick freezing and correlated with quantal transmitter release. *J. Cell Biol.*, **81**, 275-300.

Hodson, S. & Marshall, H. (1969) A device for cutting ultra-thin unfixed frozen sections for electron microscopy. *J. Physiol.*, **201**, 63P.

Hodson,S.& Marshall,H. (1970) Ultracryotomy: a technique for cutting ultra-thin sections of unfixed frozen biological tissues for electron microscopy. *J.Microsc.*, **91**, 105-117.

Holzle,E.& Braun-Falco,O. (1984) Structural changes in axillary eccrine glands following long-term treatment with aluminium chloride hexahydrate solution. *Br.J.Derm.*, **110**, 399-403.

Holzle,E.& Kligman,A.M. (1979) Mechanism of anti-perspirant action of aluminium salts. *J.Soc.Cosmet.Chem.*, **30**, 279-295.

Hurley,H.J., Shelley,W.B.& Koelle,G. (1957) The distribution of cholinesterases in human skin, with special reference to eccrine and apocrine sweat glands. *J.Invest.Derm.*, **21**, 139-147.

Iglesias,J.R.,Bernier,R.& Simard,R. (1971) Ultracryotomy: A routine procedure. *J.Ultrastruct.Res.*, **36**, 271-289.

Ingram,F.D., Ingram,M.J.& Hogben,A.M. (1972) Quantitative electron probe analysis of soft biologic tissue for electrolytes. *J.Histochem.Cytochem.*, **20**, 716-722.

Ingram,F.D.& Ingram,M.J. (1975) Quantitative analysis with the freeze-dried, plastic-embedded specimen. *J.Microscopie Biol.Cell.*, **22**, 193-204.

Ingram,F.D.& Ingram,M.J. (1984) Influences of freeze-drying and plastic embedding on electrolyte distributions. In: *Science of Biological Specimen Preparation* (ed. by J-P.Revel, T.Barnard & G.H. Haggis) p.167-174, S.E.M. Inc., AMF O'Hare , Ill.

Jehl,B., Bauer,R., Dörge,A.& Rick,R. (1981) The use of propane/isopentane mixtures for rapid freezing of biological specimens. *J.Microsc.*, **123**, 307-309.

Jenkinson,D.McEwan. (1973) Comparative physiology of sweating. *Br.J.Derm.*, **88**, 397-406.

Jenkinson,D.McEwan, Montgomery,I.& Elder,H.Y. (1978) Studies on the nature of the peripheral sudomotor control mechanism. *J.Anat.*, **125**, 625-638.

Jenkinson,D.McEwan, Montgomery,I.& Elder,H.Y. (1979) The ultrastructure of the sweat glands of the ox, sheep and goat during sweating and recovery. *J.Anat.*, **129**, 117-140.

Jenkinson,D.McEwan, Nimmo,M.C., Jackson,D., McQueen,L., Elder,H.Y., Mackay,D.A.& Montgomery,I. (1983) Comparative studies of the effect of thermal stimulation on the permeability of the luminal cell junctions of the sweat gland to lanthanum. *Tissue & Cell*, **15**, 573-581.

Jones,C.J.& Kealey,T. (1985) Electrophysiological studies on isolated human eccrine sweat glands. *J.Physiol.*, **367**, 73P.

Khuri,R.N. (1979) Chapter 2 - Electrochemistry of the nephron. In: *Membrane Transport in Biology* (ed. by G.Giebisch, D.C.Tosteson & H.H.Ussing) Vol.IV.A p.47-95, Springer-Verlag, Berlin, Heidelberg and New York.

Knoll,G., Oebel,G.& Plattner,H. (1982) A simple sandwich-cryogen-jet procedure with high cooling rates for cryofixation of biological materials in the native state. *Protoplasma*, **111**, 161-176.

Kramers,H.A. (1923) On the theory of x-ray absorption and of the continuous x-ray spectrum. *Phil.Mag.*, **46**, 836-871.

Krause,E-G.& Wollenberger,A. (1977) Chapter 13 - Cyclic nucleotides and heart. In: *Cyclic 3',5' Nucleotides: Mechanism of Action* (ed. by H.Cramer & J.Schultz) p.229-250, John Wiley & Sons, London,New York,Sydney & Toronto.

- Kuijpers,G.A.J., Van Nooy,I.G.P., De Pont,J.J.H.H.M.& Stols,A.L.H. (1984) Determination of intracellular elemental distribution in the exocrine rabbit pancreas by X-ray microanalysis. *Ultramicroscopy*, **14**, 414-415.
- Kurosumi,K.& Kurosumi,U. (1970) Electron microscopy of the mouse plantar eccrine sweat glands. *Arch.Histol.Jap*, **31**, 455-475.
- Kurosumi,K., Kurosumi,U.& Tosaka,H. (1982) Ultrastructure of human eccrine sweat glands with special reference to the transitional portion. *Archivum Histologicum Japonicum*, **45**, 213-238.
- Kurosumi,K., Shibasaki,S.& Ito,T. (1984) Cytology of the secretion in mammalian sweat glands. *Int.Rev.Cytol*, **87**, 253-329.
- Lai,J.C.K., Guest,J.F., Leung,T.K.C., Lim,L.& Davison,A.N. (1980) The effects of cadmium, manganese and aluminium on sodium-potassium-activated and magnesium-activated adenosine triphosphate activity and choline uptake in rat brain synaptosomes. *Biochem. Pharmacol.*, **29**, 141-146.
- Landis,S.C. (1983) Development of cholinergic sympathetic neurons; evidence for transmitter plasticity *in vivo*. *Fed.Proc*, **42**, 1633-1638.
- Lansdown,A.B.G. (1973) Production of epidermal damage in mammalian skin by simple aluminium compounds. *Br.J.Derm*, **89**, 67-76.
- Lauchli,A., Spurr,A.R.& Wittkop,R.W. (1970) Electron probe analysis of freeze-substituted epoxy resin embedded tissue for ion transport studies in plants. *Planta* **95**, 341-350.
- Lechene,C.P., Bonventre,J.V.& Warner,R.R. (1979) Electron probe analysis of frozen-hydrated bulk tissues. In: *Microbeam Analysis in Biology* (ed. by C.P.Lechene & R.R.Warner) p.409-426, Academic Press, New York & London.
- Lechene,C.P.& Warner,R.R. (1979) (Eds.) *Microbeam Analysis in Biology*. Academic Press, New York & London.

- Lee,C.M., Jones,C.J.& Kealey,T. (1984) Biochemical and ultrastructural studies of human eccrine sweat glands by shearing and maintained for seven days. *J.Cell.Sci*, **72**, 259-274.
- Lee,C.O.& Fozzard,H.A. (1975) Activities of K^+ and Na^+ in rabbit heart muscle. *J.Gen.Physiol.*, **65**, 695-708.
- LeRoy,A.F.& Roinel,N. (1983) Radiation damage to lyophilised mineral solutions during electron probe analysis: quantitative study of chlorine loss as a function of beam current-density and sample mass-thickness. *J.Microsc.*, **131**, 97-106. •
- Leyden,J.J.& Kligman,A.M. (1975) Aluminium chloride in the treatment of symptomatic athletes foot. *Arch.Dermatol.*, **111**, 1004-1010.
- Lundberg,J.M., Hedlund,B.& Bartfai,T. (1982) Vasoactive intestinal polypeptide enhances muscarinic ligand binding in cat submandibular salivary gland. *Nature*, **295**, 147-149.
- Lundberg,J.M., Hedlund,B., Anggard,A., Fahrenkrug,J., Hokfelt,T., Tatemoto,K.& Bartfai,T. (1982) Costorage of peptides and classical transmitters in neurons. *Systemic Role of Regulatory Peptides Symposia Medica Hoechst*, **18**, 93-119, Schatlaue Verlag, Stuttgart/New York.
- Lyon,R., Appleton,J., Swindon,K.J., Abbot,J.J.& Chesters,J. (1985) An inexpensive device for freeze-drying and plastic embedding tissues at low temperatures. *J.Microsc.*, **140**, 81-91.
- Lyons,I.& Klatz,I.M. (1958) The interaction of epidermal protein with aluminium salts. *J.Am.Pharm.Assoc.(Scient.Ed.)*, **47**, 509.
- McDowall,A.W., Chang,J.-J., Freeman,R., Lepault,J., Walter,C.A.& Dubochet,J. (1983) Electron microscopy of frozen hydrated sections of vitreous ice and vitrified biological samples. *J.Microsc.*, **131**, 1-9.

- Majors,P.A.& Wild,J.E. (1974) The evaluation of anti-perspirant efficacy - influence of certain variables. *J.Soc.Cosmet.Chem*, **25**, 139-152.
- Marshall,A.T. (1980) Chapter 1.- Principles and Instrumentation. In: *X-Ray Microanalysis in Biology* (ed. by M.A.Hayat) p.1-64, University Park Press, Baltimore.
- Matsuzawa,T.& Kurosumi,K. (1963) The ultrastructure, morphogenesis and histochemistry of the sweat glands in the rat foot pad as revealed by electron microscopy. *J.Electronmicrosc.*, **12**, 175-191.
- Montagna,W, Chase,H.B.& Lobitz,W.C. (1953) Histology and cytochemistry of human skin. IV. The eccrine sweat glands. *J.Invest.Derm*, **20**, 415-423.
- Montgomery,I., Jenkinson,D.McEwan & Elder,H.Y. (1982a) The effects of thermal stimulation on the ultrastructure of the fundus and duct of the equine sweat gland. *J.Anat*, **135**, 13-28.
- Montgomery,I., Jenkinson,D.McEwan & Elder,H.Y. (1982b) The ultrastructure of the sweat gland duct of the ox, sheep and goat before and during sweating. *J.Anat*, **134**, 741-755.
- Montgomery,I., Jenkinson,D.McEwan, Elder,H.Y., Czarnecki,D.& MacKie,R.M. (1984) The effects of thermal stimulation on the ultrastructure of the human atrichial sweat gland. I. The fundus. *Br.J.Derm*, **110**, 385-397.
- Montgomery,I., Jenkinson,D.McEwan & Elder,H.Y., Czarnecki,D.& MacKie,R.M. (1985) The effects of thermal stimulation on the ultrastructure of the human atrichial sweat gland. II. The duct. *Br.J.Derm*, **112**, 165-177.
- Moor,H. (1969) Freeze etching. *Int.Rev.Cytol*, **25**, 391-412.
- Moor,H. (1971) Recent progress in the freeze-etching technique. *Phil.Trans.Roy.Soc.B*, **261**, 121-131.

- Moreton,R.B. (1981) Electron probe X-ray microanalysis: Techniques and recent applications in biology. *Biol.Rev.*, **56**, 409-461.
- Morgan,A.J. (1980) Chapter 2 - Preparation of Specimens. In: *X-Ray Microanalysis in Biology* (ed. by M.A.Hayat) p.65-165, University Park Press, Baltimore.
- Morgan,A.J. (1985) X-ray microanalysis in the electron microscope for biologists. No.5 in the series: *Microscopy Handbooks*, Oxford University Press: Royal Microscopical Society.
- Morgan,A.J.& Davies,T.W. (1982) An electron microprobe study of the influence of beam current density on the stability of detectable elements in mixed-salts (isoatomic) microdroplets. *J.Microsc.*, **125**, 103-116.
- Moseley,H.G.J. (1913) The high frequency spectra of the elements. *Phil.Mag.*, **26**, 1024-1034.
- Moseley,H.G.J. (1914) The high frequency spectra of the elements, Part II. *Phil.Mag.*, **27**, 703-713.
- Muller,M., Meister,N.& Moor,H. (1980) Freezing in a propane jet and its application in freeze-fracturing. *Mikroskopie (Wien)*, **36**, 129-140.
- Munger,B.L.& Brusilow,S.W. (1961) An electron microscopic study of eccrine sweat glands of the cat foot and toe pads - evidence for ductal reabsorption in the human. *J.Biophys.Biochem.Cytol.*, **11**, 403-417.
- Munger,B.L.& Brusilow,S.W. (1971) The histophysiology of rat plantar sweat glands. *Anat.Rec.*, **169**, 1-22.
- Nicholson,W.A.P. (1974) Experience of diffractive and non-diffractive quantitative analysis in the Cameca microprobe. In: *Microprobe Analysis as Applied to Cells and Tissues* (ed. by T.Hall, P.Echlin and R.Kaufmann) p.239-248, Academic Press, New York & London.

Nicholson, W.A.P. (1981) Electron beam current measurement in the electron microscope. *J.Microsc.*, **121**, 141-148.

Nicholson, W.A.P., Biddlecombe, W.H. & Elder, H.Y. (1982) A low x-ray background low temperature specimen stage for biological microanalysis in the TEM. *J.Microsc.*, **121**, 141-148.

Nicholson, W.A.P. & Chapman, J.N. (1983) Bremsstrahlung production in thin specimens and the continuum normalisation method of quantitation. In: *Microbeam Analysis* (ed. by R. Gooley) p.215-220, San Francisco Press.

Nicholson, W.A.P. & Dempster, D.W. (1980) Aspects of microprobe analysis of mineralised tissues. *Scanning Electron Microscopy/1980/II*, p.517-533, SEM Inc., AMF O'Hare, Ill.

Nicholson, W.A.P., Gray, C.C., Chapman, J.N. & Robertson, B.W. (1982) Optimising thin film X-ray spectra for quantitative analysis. *J.Microsc.*, **125**, 25-40.

Nicholson, W.A.P., Robertson, B.W. & Chapman, J.N. (1977) The characterisation of x-ray spectra from thin specimens in the transmission electron microscope. *Inst.Phys.Ser.No.36* (ed. by D. Missel) p.373-376, Institute of Physics, London.

Nishiyama, A. & Kagayama, M. (1973) Biphasic secretory potentials in cat and rabbit submaxillary glands. *Experientia*, **29**, 161-163.

Pallaghy, C.K. (1973) Electron probe microanalysis of potassium and chloride in freeze-substituted leaf sections of *Zea mays*. *Aust.J.Biol.Sci.*, **26**, 1015-1034.

Panessa, B.J., Warren, J.B., Hren, J.J., Zadunaisky, J.A. & Kundrath, M.R. (1978) Beryllium and graphite polymer substrates for reduction of spurious x-ray signal. *Scanning Electron Microscopy/1978/II*, p.1055-1062, SEM, Inc., AMF O'Hare Ill.

- Papa,C.M.& Kligman,A.M. (1966) Mechanism of eccrine anhidrosis. I. High level blockade. *J.Invest.Derm.*, **47**, 1-9.
- Papa,C.M.& Kligman,A.M. (1967). Mechanism of eccrine anhidrosis II. The anti-perspirant effects of aluminium salts. *J.Invest.Derm.*, **49**, 139-145.
- Pearse,A.G.E. (1980) *Histochemistry Theoretical and Applied*. I. *Preparative and Optical Technology*, 4th edn. Churchill Livingstone, Edinburgh.
- Pearson,G.T.,Flanagan,P.M.& Petersen,O.H. (1984) Neural and hormonal control of membrane conductance in the pig pancreatic acinar cell. *Am.J.Physiol.*, **247**, G520-526.
- Petersen,O.H. (1972) Acetylcholine-induced ion transports involved in the formation of saliva. *Acta Physiol.Scand.*, **Suppl.**,**381**, 1-58.
- Petersen,O.H. (1973) Membrane potential measurement in mouse salivary gland cells. *Experientia*, **29**, 160-161.
- Petersen,O.H. (1976) Electrophysiology of mammalian gland cells. *Physiol.Rev.*, **56**, 535-577.
- Petersen,O.H. (1984) The role of Ca⁺⁺ in secretion. In a workshop led by R.M.Case. *Cell Calcium*, **5**, 89-110.
- Petersen,O.H.& Maruyama,Y. (1984) Calcium-activated potassium channels and their role in secretion. *Nature*, **307**, 693-696.
- Petersen,O.H.& Singh,J. (1985) Acetylcholine evoked potassium release in the mouse pancreas. *J.Physiol.*, **365**, 319-329.
- Poulsen,J.H., Bundgaard,M.& Møller,M. (1975) Localisation of (Na⁺ - K⁺)-activated ATPase in "forward" and "backward" epithelia in salivary glands. *The Physiologist*, **18**, 356.

Putney, J.W. (1979) Stimulus-permeability coupling role of calcium in the receptor regulation of membrane permeability. *Pharmacol.Rev.*, **30**, 209-245.

Putney, J.W., Weiss, S.J., Van de Walle, C.M. & Haddas, R.A. (1980) Is phosphatidic acid a calcium ionophore under neurohumoral control? *Nature*, **284**, 345-347.

Quatralo, R.P., Coble, D.W., Stoner, K.L. & Felger, C.B. (1981b) The mechanism of anti-perspirant action by aluminium salts. II. Histological observations of human eccrine sweat glands inhibited by aluminium chlorohydrate. *J.Soc.Cosmet.Chem.*, **32**, 107-136.

Quatralo, R.P., Coble, D.W., Stoner, K.L. & Felger, C.B. (1981c) The mechanism of anti-perspirant action of aluminium salts. III. Histological observations of human eccrine sweat glands inhibited by aluminium zirconium chlorohydrate glycine complex. *J.Soc.Cosmet.Chem.*, **32**, 195-221.

Quatralo, R.P. & Laden, K. (1968) Solute and water secretion by the eccrine sweat glands of the rat. *J.Invest.Derm.*, **51**, 502-504.

Quatralo, R.P., Waldman, A.H., Rogers, J.G. & Felger, C.B. (1981a) The mechanism of antiperspirant action by aluminium salts. I. The effect of cellophane tape stripping on aluminium salt-inhibited eccrine sweat glands. *J.Soc.Cosmet.Chem.*, **32**, 67-73.

Quinton, P.M. (1981) Effects of some ion transport inhibitors on secretion and reabsorption in intact and perfused single human sweat glands. *Pflugers Arch.*, **391**, 309-313.

Quinton, P.M. (1983) Sweating and its disorders. *Ann.Rev.Med.*, **34**, 429-452.

Quinton,P.M.& Tormey,J.McD. (1976) Localisation of Na/K ATPase sites in the secretory and reabsorptive epithelia of perfused eccrine sweat glands; A question to the role of the enzyme in secretion. *J.Membr.Biol.*, **29**, 383-399.

Reed,S.J.B. (1975) *Electron Microprobe Analysis*. Cambridge, London & New York.

Rees-Jones,A.M.& Jenkinson,D.McEwan. (1978) The effect of aluminium chlorhydrate on sweat gland activity in cattle. *J.Invest.Derm.*, **70**, 134-137.

Reller,H.H.& Luedders,W.L. (1977) Pharmacologic and toxicologic effects of topically applied agents on the eccrine sweat glands. II. Mechanism of action of metal salt anti-perspirants. In: *Advances in Modern Toxicology, Dermatotoxicology and Pharmacology* (ed. by F.N.Marzulli & H.I.Maibach) Vol.4, p.18-54, Hemisphere Publishing Co., Washington, London.

Rick,R., Dörge,A., Gehring,K., Bauer,R. & Thurau,K. (1979) Quantitative determination of cellular electrolyte concentrations in thin freeze-dried cryosections using energy dispersive x-ray microanalysis. In: *Microbeam Analysis in Biology* (ed. by C.P.Lechene and R.R.Warner) p.517-534, Academic Press, New York & London.

Rick,R., Dörge,A.& Thurau,K. (1982) Quantitative analysis of electrolytes in frozen dried sections. *J.Microsc.*, **125**, 239-247.

Ring,J.R.& Randall,W.C. (1947) The distribution and histological structure of sweat glands in the albino rat and their response to prolonged nervous stimulation. *Anat.Rec.*, **99**, 7-19.

Robards,A.W. (1974) Ultrastructural methods for looking at frozen cells. *Sci.Prog.*, **61**, 1-40.

Robards,A.W.& Sleytr,U.B. (1985) Low temperature methods in biological electron microscopy. In the series: *Practical Methods in Electron Microscopy* (ed. by A.M.Glauert), Elsevier Science Publishers, Amsterdam, New York & London.

Robertshaw,D.& Taylor,C.R. (1969) Sweat gland function of the donkey (*Equus asinus*) *J.Physiol.*, **205**, 79-89.

Robertshaw,D., Taylor,C.R.& Mazzia,L.M. (1973) Sweating in primates: secretion by adrenal medulla during exercise. *Am.J.Physiol.*, **224**, 678-681.

Roinel,N.& LeRoy,A.F. (1980) Variations in characteristic signals of the elements during microprobe analysis of droplets: a review. In: *Microbeam Analysis 1980* (ed. by D.W.Wittry) p.129-137, San Francisco Press, San Francisco.

Roomans,G.M. (1980) Chapter 10 - Quantitative X-ray microanalysis of thin sections. In: *X-Ray Microanalysis in Biology* (ed. by M.A.Hayat) p.401-453, University Park Press, Baltimore.

Roomans,G.M., van Gaal,H.L. (1977) Organometallic and organometalloid compounds as standards for microprobe analysis of epoxy resin embedded tissue. *J.Microsc.*, **109**, 235-240.

Roomans,G.M., Wei,X., Ceder,O.& Kollberg,H. (1982) The reserpinised rat in the study of cystic fibrosis: X-ray microanalysis of submandibular glands and pancreas. *Ultrastruct.Pathol.*, **3**, 285-293.

Roos,N.& Barnard,T. (1984) Aminoplastic standards for quantitative X-ray microanalysis of thin sections of plastic-embedded biological material. *Ultramicroscopy*, **15**, 277-285.

Roos,N.& Barnard,T. (1985) A comparison of subcellular element concentrations in frozen-dried, plastic-embedded, dry cut sections and frozen-dried cryosections. *Ultramicroscopy*, **17**, 335-344.

Roos,N.& Barnard,T. (1986) Preparation methods for quantitative electron probe X-ray microanalysis (EPXMA) of rat exocrine pancreas: A review. In press.

Russ,J.C. (1972) Resolution and sensitivity of x-ray microanalysis in biological sections by scanning and conventional transmission electron microscopy. *Scanning Electron Microscopy/1972*, p.73, SEM Inc., AMF O'Hare, Ill.

Russ,J.C. (1975) Evaluation of the direct element ratio calculation method. *J.Microscopie Biol.Cell*, **22**, 283-286.

Russ,J.C. (1977) Selecting optimum kV for STEM microanalysis. *Scanning Electron Microscopy/1977/1*, p.335-340, SEM Inc., AMF O'Hare, Ill.

Russ,J.C. (1978) Chapter 2 - Electron probe X-ray microanalysis - principles. In: *Electron Probe Microanalysis in Biology* (ed. by D.A.Erasmus) p.5-36, Chapman & Hall Ltd., London.

Sampson,H.W.& Bowers,D.E. (1982) Intracellular calcium localization in stimulated, non-stimulated and repressed eccrine sweat glands. *J.Anat*, **135**, 565-575.

Sato,F.& Sato,K. (1978) Secretion of a potassium-rich fluid by the secretory coil of the rat paw eccrine sweat gland. *J.Physiol*, **274**, 37-50.

Sato,F., Burgers,M.& Sato,K. (1973) Some characteristics of adrenergic human eccrine sweating. *Experientia* **30**, 40-41.

Sato,K. (1973) Sweat induction from an isolated eccrine sweat gland. *Am.J.Physiol*, **225**, 1147-1152.

Sato,K. (1977) The physiology, pharmacology and biochemistry of the eccrine sweat gland. *Rev.Phys.Biochem.Pharmacol*, **79**, 51-131.

Sato,K. (1978) Does acetylcholine change the electrical resistance of the basal membrane of secretory cells in eccrine sweat gland. *J.Membr.Biol.*, **42**, 123-151.

Sato,K. (1980) Electrochemical driving forces for K⁺ secretion by rat paw eccrine sweat gland. *Am.J.Physiol.*, **239**, C90-97.

Sato,K. (1982) Mechanism of eccrine sweat secretion. In: *Fluid and Electrolyte Abnormalities in Exocrine Glands in Cystic Fibrosis* (ed. by P.M.Quinton, J.R.Martinez & U.Hopfer) p.35-52, San Francisco Press.

Sato,K. (1984) Update on pharmacology of the eccrine sweat gland. *TIPS*, **5**, 391-393.

Sato,K.& Dobson,R.L. (1970) Enzymatic basis for the active transport of sodium in the duct and secretory portion of the eccrine sweat gland. *J.Invest.Derm.*, **55**, 53-56.

Sato,K., Dobson,R.L.& Mali,J.W.H. (1971) Enzymatic basis for the active transport of sodium in the eccrine sweat gland. *J.Invest.Derm.*, **57**, 10-16.

Sato,K., Nishiyama,A. & Kobayashi,M. (1979) Mechanical properties and functions of the myoepithelium in the eccrine sweat gland. *Am.J.Physiol.*, **237**, C177-184.

Sato,K.& Sato,F. (1981a) Pharmacological responsiveness of isolated single eccrine sweat glands. *Am.J.Physiol.*, **240**, R44-51.

Sato,K.& Sato,F. (1981b) Cyclic AMP accumulation in the beta adrenergic mechanism of eccrine sweat secretion. *Pflügers Arch.*, **390**, 49-53.

Sato,K.& Sato,F. (1981c) Role of calcium in cholinergic and adrenergic mechanisms of eccrine sweating. *Am.J.Physiol.*, **241**, C113-120.

- Sato,K.& Sato,F. (1983) Cholinergic potentiation of isoproterenol-induced cAMP level in sweat gland. *Am.J.Physiol.*, **245**, C189-195.
- Sato,K.& Sato,F. (1984) Cyclic GMP accumulation during cholinergic stimulation of eccrine sweat glands. *Am.J.Physiol.*, **247**, C234-239.
- Saubermann,A.J. (1980) Application of cryosectioning to x-ray microanalysis of biological tissue. *Scanning Electron Microscopy/1980/II*, 421-430 & 420, SEM Inc., AMF O'Hare, Ill.
- Saubermann,A.J., Echlin,P., Peters,P.D.& Beeuwkes,R.,III (1981) Application of scanning electron microscopy to x-ray analysis of frozen-hydrated sections. I. Specimen handling techniques. *J.Cell Biol.*, **88**, 257-267.
- Saubermann,A.J., Riley,W.& Echlin,P. (1977) Preparation of frozen hydrated tissue sections for X-ray microanalysis using a satellite vacuum coating and transfer system. *Scanning Electron Microscopy/1977/I*, p.347-356, SEM Inc., AMF O'Hare, Ill.
- Schiefferdecker,P. (1917) Die Hautdrusen des Menschen und der Säugetiere; ihre biologische und rassenanatomische Bedeutung sowie die Muscularis sexualis. *Biologisches Zentralblatt*, **37**, 534-562.
- Schneyer,L.H. (1969) Secretion of potassium by perfused excretory duct of rat submaxillary gland. *Am.J.Physiol.*, **217**, 1324-1329.
- Schneyer,L.H. (1975) Secretion of potassium and fluid by rat submaxillary gland during sympathetic nerve stimulation. *Am.J.Physiol.*, **226**, 821-826.
- Schneyer,L.H., Young,J.A.& Schneyer,C.A. (1972) Salivary secretion of electrolytes. *Phys.Rev.*, **52**, 720-777.

- Scholes,K.T., Crow,K.D., Ellis,J.P., Harman,R.R.& Salhan,E.M. (1978) Axillary hyperhidrosis treated with alcoholic solution of aluminium chloride hexahydrate. *Brit.Med.J.*, **1978(2)**, 84-85.
- Schramm,M.& Selinger,Z. (1975) The function of cyclic AMP and calcium alternative second messengers in parotid gland and pancreas. *J.Cyclic Nucleotide Res.*, **1**, 181-192.
- Schulz,I.J. (1969) Micropuncture studies of the sweat formation in cystic fibrosis patients. *J.Clin.Invest.*, **48**, 1470-1477.
- Schwartz,I.L.& Thaysen,J.H. (1956) Excretion of sodium and potassium in human sweat. *J.Clin.Invest.*, **35**, 114-120.
- Seveus,L. (1978) Preparation of biological material for x-ray microanalysis of diffusible elements. I. Rapid freezing of biological tissue in nitrogen slush and preparation of ultrathin frozen sections in the absence of trough liquid. *J. Microsc.*, **112**, 269-279.
- Seveus,L. (1979) The subcellular distribution of electrolytes. A methodological study using cryoultramicrotomy and x-ray microanalysis. Ph.D. Thesis, University of Stockholm.
- Shelley,W.B.& Hurley,H.J. (1975) Studies on topical anti-perspirant control of axillary hyperhidrosis. *Acta Dermatovener.*, **55**, 241-260.
- Shelton,E.& Mowezko,W.E. (1978) Membrane blisters. A fixation artefact. A study in fixation for scanning electron microscopy. *Scanning*, **1**, 166-173.
- Shorofsky,S.R.,Field,M.& Fozzard,H.A. (1982) The cellular mechanism of active chloride secretion in vertebrate epithelia: studies in intestine and trachea. *Phil.Trans.R.Soc.Lon. B*, **299**, 597-607.

- Shuman,H., Somlyo,A.V.& Somlyo,A.P. (1976) Quantitative electron probe microanalysis of biological thin sections : Methods and validity. *Ultramicroscopy*, **1**, 317-339.
- Siegel,N.& Haug,A. (1983) Aluminum interaction with calmodulin. Evidence for altered structure and function from optical and enzymatic studies. *Biochim.Biophys. Acta*, **744**, 36-45.
- Silva,P., Stopf,J., Field,M., Fine,L., Forrest,J.N.& Epstein,F.H.. (1977) Mechanism of active chloride secretion by shark rectal gland; role of Na/K ATPase in chloride transport. *Am.J.Physiol.*, **233**, F298-306.
- Silvester,N.R., Marchese-Ragona,S.& Johnston,D.N. (1982) The relative efficiency of various fluids in the rapid freezing of protozoa. *J.Microsc.*, **128**, 175-186.
- Sitte,H. (1984) Process of ultrathin sectioning. In: *Science of Biological Specimen Preparation* (ed. by J-P.Revel, T.Barnard & G.H.Haggis) p.97-104, Sem Inc., AMF O'Hare, Ill.
- Sjostrom,M.& Valdré,U. (1979) Freezing of muscle fibers, ultrathin cryocutting and transfer of frozen-hydrated sections. In: *Microbeam Analysis in Biology* (ed. by C. Lechene and R.R.Warner) p.427-444, Academic Press, New York & London.
- Slegers,J.F.G. (1963) The mechanism of eccrine sweat gland function in normal subjects and in patients with mucoviscidosis. *Dermatologica*, **127**, 242-254.
- Snow,D.H., Kerr,M.G., Nimmo,M.A.& Abbott,E.M. (1982) Alterations in blood, sweat, urine and muscle composition during prolonged exercise in the horse. *Vet.Rec.*, **110**, 377-384.
- Somlyo,A.P., Somlyo,A.V.& Shuman,H. (1979) Electron probe analysis of vascular smooth muscle. Composition of mitochondria, nuclei and cytoplasm. *J.Cell Biol.*, **81**, 316-335.

- Somlyo,A.V., Shuman,H.& Somlyo,A.P. (1977) Elemental distribution in striated muscle and the effects of hypertonicity. *J.Cell Biol*, **74**, 828-857.
- Spurr,A.R. (1969) A low-viscosity epoxy resin embedding medium for electron microscopy. *J.Ultrastruct.Res*, **26**, 31-43.
- Spurr,A.R. (1975) Choice and preparation of standards for x-ray microanalysis of biological materials with special reference to macrocyclic polyether complexes. *J.Microscopie Biol.Cell*, **22**, 287-302.
- Steinbrecht,R.A. (1984) Cryofixation and follow-up techniques in biological electron microscopy. *Zeiss Information*, **3**, 9-17.
- Stenn,K.& Bahr,G.F. (1970) Specimen damage caused by the beam of the transmission electron microscope, a correlative reconsideration. *J.Ultrastruct.Res*, **31**, 526-550.
- Stillians,A.W. (1916) The control of localised hyperhidrosis. *J.A.M.A.*, **67**, 2015-2016.
- Sulzberger,M.B., Zak,F.G.& Herrman,F. (1949) Studies of sweating. II. On the mechanism of action of local anti-perspirants. *Arch.Dermatol*, **60**, 404-418.
- Thaysen,J.H. (1978) Chapter 13 - The Sweat Glands. In: *Membrane Transport in Biology* (ed. by G.Giebisch, D.C.Tosteson & H.H.Ussing) Vol.III, p.379-413, Springer-Verlag, Berlin,Heidelberg & New York.
- Tormey,J.McD. (1979) Problems and progress in quantitative localisation of sodium, potassium and chlorine in freeze-dried sections : use of erythrocytes as a model system. In: *Microbeam Analysis in Biology* (ed. by C.P.Lechene & R.R.Warner) p.615-633, Academic Press, New York & London.

Uno,H. (1977) Sympathetic innervation of the sweat glands and piloerector muscles of Macaques and human beings. *J.Invest.Derm.*, **69**, 112-120.

Uno,H.& Montagna,W. (1975) Catecholamine-containing nerve terminals of the eccrine sweat glands of macaques. *Cell Tiss.Res.*, **158**, 1-13.

Ussing,H.H., Erljij,D.& Lassen,U. (1974) Transport pathways in biological membranes. *Ann.Rev.Physiol.*, **36**, 17-50.

Vaalasti,A., Tainio,H.& Rechartd,L. (1985) Vasoactive intestinal polypeptide (VIP)-like immunoreactivity in the nerves of human axillary sweat glands. *J.Invest.Derm.*, **85**, 246-248.

Van Harreveld,A.& Crowell,J. (1964) Electron microscopy after rapid freezing on a metal surface and substitution fixation. *Anat.Rec.*, **149**, 381-385.

Van Zyl,J., Forrest,Q.G., Hocking,C.& Pallaghy,C.K. (1976) Freeze substitution of plant and animal tissue for the localisation of water-soluble compounds by electron probe microanalysis. *Micron*, **7**, 213-224.

Wechsler,H.L.& Fisher,E.R. (1968) Eccrine glands of the rat. *Arch.Derm.*, **97**, 189-201.

Weiner,J.S.& Hellman,K. (1960) The sweat glands. *Biol.Rev.*, **35**, 141-186.

Welsh,M.J., Smith,P.L.& Frizzell,R.A. (1982) Chloride secretion by canine tracheal epithelium. II. The cellular electrical potential profile. *J.Membr.Biol.*, **70**, 227-238.

Young, J.A. & Van Lennep, E.W. (1979) Chapter 12 - Transport in salivary and salt glands (Part 1). In: *Membrane Transport in Biology* (ed. by G.Giebisch, D.C.Tosteson & H.H.Ussing) Vol.IV.B, p.563-674, Springer-Verlag, Berlin, Heidelberg & New York.

Zerahn, K. (1977) Potassium transport in insect midgut. In: *Transport of Ions and Water in Animals* (ed. by B.L.Gupta, R.B.Moreton, J.L.Oschman & B.J.Wall) p.381-401 Academic Press, London & New York.

APPENDICES

APPENDIX

- 1 MATERIALS.
- 2 ESTIMATION OF THE ERROR IN CHLORINE MEASUREMENT.
- 3 ESTIMATION OF THE MASS LOSS DURING ANALYSIS.
- 4 INTRACELLULAR ELEMENTAL CONCENTRATIONS IN THE
FUNDUS OF INDIVIDUAL RAT SWEAT GLANDS.
- 5 BIBLIOGRAPHY OF BIOLOGICAL DATA OBTAINED BY EPXMA FROM
SECTIONS PROCESSED BY DIFFERENT METHODS.
- 6 ESTIMATES OF THE FREE CONCENTRATIONS OF Na AND K.
- 7 INTRACELLULAR ELEMENTAL CONCENTRATIONS IN THE FUNDUS
AND DUCT OF INDIVIDUAL HUMAN SWEAT GLANDS.
- 8 INTRACELLULAR ELEMENTAL CONCENTRATIONS IN THE FUNDUS
AND DUCT OF INDIVIDUAL HORSE SWEAT GLANDS.
- 9 METHODS OF THE PRELIMINARY STUDY OF ANTIPERSPIRANT
ACTION ON THE RAT FOOTPAD.
- 10 RESULTS OF THE PRELIMINARY STUDY OF ANTIPERSPIRANT
ACTION ON THE RAT FOOTPAD.

APPENDIX 1 MATERIALS

Drugs: Pilocarpine hydrochloride (Sigma)

Resins: Araldite, Epon and Lowicryl (Agar Aids)

Lemix and Emix (Emscope)

Ladd and Spurr (Polysciences)

DGEBA (London Resin Co.)

All gases and liquid nitrogen (BOC, Ltd.)

All other chemicals and solutions were standard laboratory reagents of the highest grade.

APPENDIX 2 ESTIMATION OF ERROR IN CHLORINE MEASUREMENT

Spectra were recorded from a number of araldite blocks cut to the same thickness as the biological sections and analysed under standard analysis conditions (Chapter 3.10.3.). The ratio of counts in the chlorine to "white" window were calculated for each spectrum. To estimate the error that the chlorine in resin is likely to introduce to the biological measurements several assumptions and conversions factors are needed. The biological sections will be not be composed entirely of resin and, if the resin is assumed to occupy water space in the original tissue, the counts must be reduced. Gupta *et al.* (1978) estimated water content in Calliphora salivary gland as 75-80% and I have assumed that a value of 75% is representative of the sweat gland. From the average chlorine and "white" counts calculated from representative spectra obtained from rat, human and horse it was estimated that the resin will introduce errors of approximately 40% in the chlorine measurement (range 38-45%). Although this is a retrospective correction factor, it did not influence the statistical significance of any of the Cl measurements.

APPENDIX 3 ESTIMATION OF MASS LOSS DURING ANALYSIS

A series of concentrations (25, 50, 100, 300, & 500 mM) of NaCl, prepared in a 25% (w/v) PVP in distilled water, were frozen by dropping onto a highly polished copper rod cooled to liquid nitrogen temperature. The flattened droplets were freeze-dried and processed by the same method as the biological tissue. Sections were cut at 1200Å and analysed at -160°C using standard conditions (Chapter 3.10.3.), the rod was then warmed to room temperature and adjacent areas of the same section analysed. The characteristic counts in the Na and Cl windows and gross counts in the "white" windows are shown in Table A.3.1. The two sets of data were compared by paired t-test. These results show that there was no significant loss in characteristic counts for Na and Cl during room temperature analysis. There was, however, a consistent and significant ($p < 0.05$) loss of counts in the "white" window (average 16%). This value was then used as a mass loss correction factor for the data obtained by analysis at room temperature i.e. the elemental data from spectra collected at room temperature were reduced by ~16%. To assess the time dependency of this mass loss the following experiment was performed. At -160°C a spectrum was recorded from a Na/Cl PVP droplet under standard analysis conditions. The beam was left on the same spot and successive spectra were recorded at 60s intervals until a total of 5 had been collected. The specimen was warmed to room temperature and the procedure repeated. The results (Table.A.3.2.) show that no loss of "white" counts occurred between the first and last spectrum and suggest that once the initial mass loss occurs the sections are unlikely to lose significant mass thereafter.

Table A.3.1. Characteristic counts in the Na, Cl and gross counts in the "white" windows from standard NaCl mixtures: a) analysed at -160°C
b) analysed at room temperature.

a) Standard	n	Na	Cl	white
1	25	454 ± 72	2352 ± 189	2070 ± 140
2	20	16 ± 14	213 ± 41	1940 ± 162
3	10	68 ± 65	663 ± 223	1693 ± 239
4	20	42 ± 36	339 ± 78	2460 ± 390
5	20	35 ± 22	148 ± 36	1124 ± 248

b) Standard	n	Na	Cl	white
1	25	469 ± 89	2360 ± 152	1600 ± 157
2	20	32 ± 21	230 ± 44	1596 ± 151
3	10	94 ± 65	690 ± 177	1485 ± 165
4	20	51 ± 30	348 ± 67	1981 ± 235
5	20	22 ± 13	142 ± 36	1057 ± 196

Values are the means \pm S.D.

Table A.3.2. Characteristic counts in the Na, Cl and gross counts in the "white" windows: Five repeated spectra (see above for details):

a) analysed -160°C

b) analysed at room temperature.

a) Spectrum	Na	Cl	white
1	387	2490	1903
2	409	2490	1753
3	433	2460	1846
4	366	2450	1894
5	382	2610	1887

b) Spectrum	Na	Cl	white
1	505	2470	1537
2	535	2600	1585
3	610	2640	1574
4	519	2720	1691
5	574	2780	1671

Spectra were recorded from standard 1 (Table A.3.1.)

APPENDIX 4 INTRACELLULAR ELEMENTAL CONCENTRATIONS IN THE
FUNDUS OF INDIVIDUAL RAT SWEAT GLANDS

Number of spectra per group, mean and standard deviation
for the rat sweat gland: a) Na

b) K

c) Cl

a)

GROUP	n	Mean	S.D.
Control 1	20	62	31
2	29	11	15
3	30	73	27
4	27	70	37
<hr/>			
Saline 1	29	163	30
2	30	61	36
3	29	59	35
4	30	62	38
<hr/>			
1 Pilo 1	15	91	30
2	26	118	30
3	27	137	38
4	28	127	23
<hr/>			
3 Pilo 1	30	155	58
2	28	76	30
3	28	61	51
4	29	171	58
<hr/>			

b)

GROUP		n	Mean	S.D.
Control	1	19	241	18
	2	30	178	23
	3	30	224	19
	4	27	201	16

Saline	1	29	251	18
	2	30	183	21
	3	30	188	26
	4	30	198	26

1 Pilo	1	15	80	14
	2	26	106	14
	3	27	193	12
	4	28	101	7

3 Pilo	1	30	242	20
	2	28	87	13
	3	28	115	19
	4	29	117	17

c)

GROUP		n	Mean	S.D.
Control	1	19	72	18
	2	30	78	13
	3	30	63	12
	4	27	79	11
<hr/>				
Saline	1	29	82	10
	2	30	59	14
	3	30	75	18
	4	30	33	17
<hr/>				
1 Pilo	1	15	112	27
	2	26	54	17
	3	27	45	14
	4	28	50	8
<hr/>				
3 Pilo	1	30	85	17
	2	28	55	13
	3	28	52	18
	4	28	60	20
<hr/>				

Values are Mmol/kg dry wt..Chlorine values were corrected for the chlorine content of resin as described in Appendix 2.

APPENDIX 5 BIBLIOGRAPHY OF BIOLOGICAL DATA OBTAINED BY
EPXMA FROM SECTIONS PROCESSED BY DIFFERENT ROUTES

A) Bulk freeze-dried resin embedded sections:

Roos & Barnard, 1984: Exocrine pancreas; mMoles/kg dry wt.

Na = 68 apical cytoplasm 78 basal cytoplasm

K = 148 " " 202 " "

Kuijpers *et al.* 1984: Exocrine pancreas; mMoles/kg wet wt.

Na = 20, K = 150, Cl = 25

Ingram *et al.* 1972: Frog skeletal muscle; mEq/litre

Na = 9.2, K = 122.4, Cl = 10.5

B) Freeze-dried cryosections:

Andrews *et al.* 1982: Duckling salt glands; mMoles/kg dry wt.

Na = 83 apical cytoplasm 125 basal cytoplasm

K = 423 " " 469 " "

Cl = 124 " " 155 " "

Somlyo *et al.* 1977: Striated muscle; mMoles/kg dry wt.

Na = 42, K = 404, Cl = 24

Roomans *et al.* 1982: Rat pancreas; mMoles/kg dry wt.

Na = 135, K = 525, Cl = 99

Rick *et al.* 1982: Frog skin epithelium; mMoles/kg wet wt.

Na = 9.4, K = 118.4

C) Frozen-hydrated cryosections:

Gupta *et al.* 1978: Calliphora salivary glands; mMoles/kg wet wt.

Na = 20, K = 115, Cl = 33

Gupta & Hall, 1979: Rabbit ileum; mMoles/kg wet wt.

Na = ~45, K = ~170, Cl = ~60

The values calculated in this study are not directly comparable with those obtained by methods B) + C) above. For freeze-dried cryosections it should be remembered that the values are mMoles/kg dry wt. in the absence of resin and, assuming a cellular water content of 75%, should be divided by ~4. The frozen-hydrated sections values are in mMoles/kg wet wt. and, again assuming a cell water content of 75%, the values in this study should be multiplied by 100/75.

APPENDIX 6 ESTIMATES OF THE FREE CONCENTRATIONS OF K, Cl AND Na

I) Potassium

Potassium in the intracellular fluid is regarded as being mostly unbound and ionised (Gupta *et al.* 1978). For various tissues the free "active" level of potassium is given as:

<i>Hyalophora cecropia</i> midgut	85%	Zerahn, 1977
Rabbit heart muscle	83%	Lee & Fozzard, 1975
Toad urinary bladder	73%	Civan, Hall & Gupta, 1980
Rabbit ileum	~70%	Gupta & Hall, 1979

The concentrations in Table 5.1. were multiplied by 0.8 (assuming 80% free and ionised)

II) Chloride

A considerable amount of chloride may be bound or compartmentalised (Gupta *et al.* 1979) and not active intracellularly. In barnacle muscle, Gayton & Hinke (1971) calculated that approximately 50% of intracellular chloride is bound. Gupta & Hall (1979) found a similar value in their studies and 50% of the chlorine was assumed to be free and active in the current work.

III) Sodium

Intracellular sodium activity is much lower than that of potassium and calculated free levels for various tissues are given as:

Rabbit heart muscle	21%	Lee & Fozzard, 1975
Rat thigh muscle	36%	Khuri, 1979
Various tissues	50%	Gupta & Hall, 1979

The assumed free and ionised Na level in the present study was 35%.

APPENDIX 7 INTRACELLULAR ELEMENTAL CONCENTRATIONS IN THE
FUNDUS AND DUCT OF INDIVIDUAL HUMAN SWEAT GLANDS

A) Na

B) K

C) Cl

FUNDUS

A) Na	Control	Active
Subject	Mean	Mean
1	185	181
2	197	210
3	228	223
4	187	255
5	198	207
6	152	218
7	113	228
8	126	-
9	-	294
10	-	144
11	-	297
12	-	260

B) K	Control	Active
Subject	Mean	Mean
1	150	98
2	142	136
3	165	111
4	108	113
5	204	47
6	204	147
7	162	155
8	139	-
9	-	154
10	-	152
11	-	39
12	-	79

C) CI Subject	Control Mean	Active Mean
1	127	162
2	165	119
3	136	143
4	118	117
5	119	124
6	69	69
7	58	80
8	86	-
9	-	140
10	-	46
11	-	176
12	-	77

DUCT

A) Na	Control	Active
Subject	Mean	Mean
1	184	273
2	331	429
3	301	421
4	106	-
5	342	212
6	273	171
7	-	120

B) K	Control	Active
Subject	Mean	Mean
1	123	98
2	115	55
3	197	87
4	89	-
5	71	113
6	25	70
7	-	86

C) Cl	Control	Active
Subject	Mean	Mean
1	70	95
2	137	108
3	107	167
4	87	-
5	104	67
6	92	74
7	-	64

Values are mMoles/kg dry wt..The chloride values were corrected for the chlorine content of the resin as explained in Appendix 2.

APPENDIX 8 INTRACELLULAR ELEMENTAL CONCENTRATIONS IN THE
FUNDUS AND DUCT OF INDIVIDUAL HORSE SWEAT GLANDS

A) Na

B) K

C) Cl

FUNDUS

A) Na	Control	Active
Horse	Mean	Mean
1	130	286
2	166	250
3	158	206
4	-	209

B) K	Control	Active
Horse	Mean	Mean
1	218	167
2	181	164
3	196	173
4	-	163

C) Cl	Control	Active
Horse	Mean	Mean
1	67	81
2	76	109
3	69	124
4	-	96

DUCT

A) Na	Control	Active
Horse	Mean	Mean
1	125	234
2	273	322
3	185	260
4	233	345

B) K	Control	Active
Horse	Mean	Mean
1	136	56
2	134	102
3	207	113
4	105	78

C) Cl	Control	Active
Horse	Mean	Mean
1	76	121
2	60	96
3	61	81
4	69	129

Values are mMoles/kg dry wt..

The chloride values were corrected for the chlorine content of the resin as explained in Appendix 2.

APPENDIX 9 METHODS OF THE PRELIMINARY STUDY OF
ANTIPERSPIRANT ACTION ON THE RAT FOOTPAD

One male Wistar rat, 6-8 weeks old, was anaesthetised with "Sagatal" (35mg/kg i.p.) and a solution of "Body Mist" (Beecham Products) was applied to one fore and one hind paw. The solution was applied from a roll-on bottle and, in an attempt to standardise the application, 15 "rolls" were applied. Similarly, an aluminium chlorhydrate solution was applied to the remaining paws. Two-and-a-half hours later a second series of applications of each chemical was administered to the same sites. Twenty four hours after the first application, the procedure of the first day was repeated and, finally, after forty eight hours, repeated again. One hour after the last (6th) application, the rat was killed and samples of footpad were cryoquenched in rapidly-stirred liquid propane and stored in liquid nitrogen until required for freeze-substitution.

All samples were subjected to the same freeze-substitution procedure:

- i) freeze-substitution in acetone/1% OsO₄ at -70°C to -80°C (temp. maintained by dry ice) for three days
- ii) slow warming (~5h) to room temperature
- iii) embedding in araldite
- iv) dry sectioning on conventional ultramicrotomes at 2000Å flattened on one hole copper mounts, carbon-coated and analysed at room temperature in the JEOL JEM 100C.

Sections were cut parallel to the skin surface so that each gland could be examined at different stages along its length (Fig.A.9.1.). Morphological detail in the unstained sections was poor and, combined with the unavoidable ice-crystal damage, made recognition of structures difficult. In all instances where a gland was identified spectra were recorded from the lumen, luminal border, from within the fibrocyte sheath surrounding the dermis (Fig.A.9.1.) and occasionally from the Formvar support film.

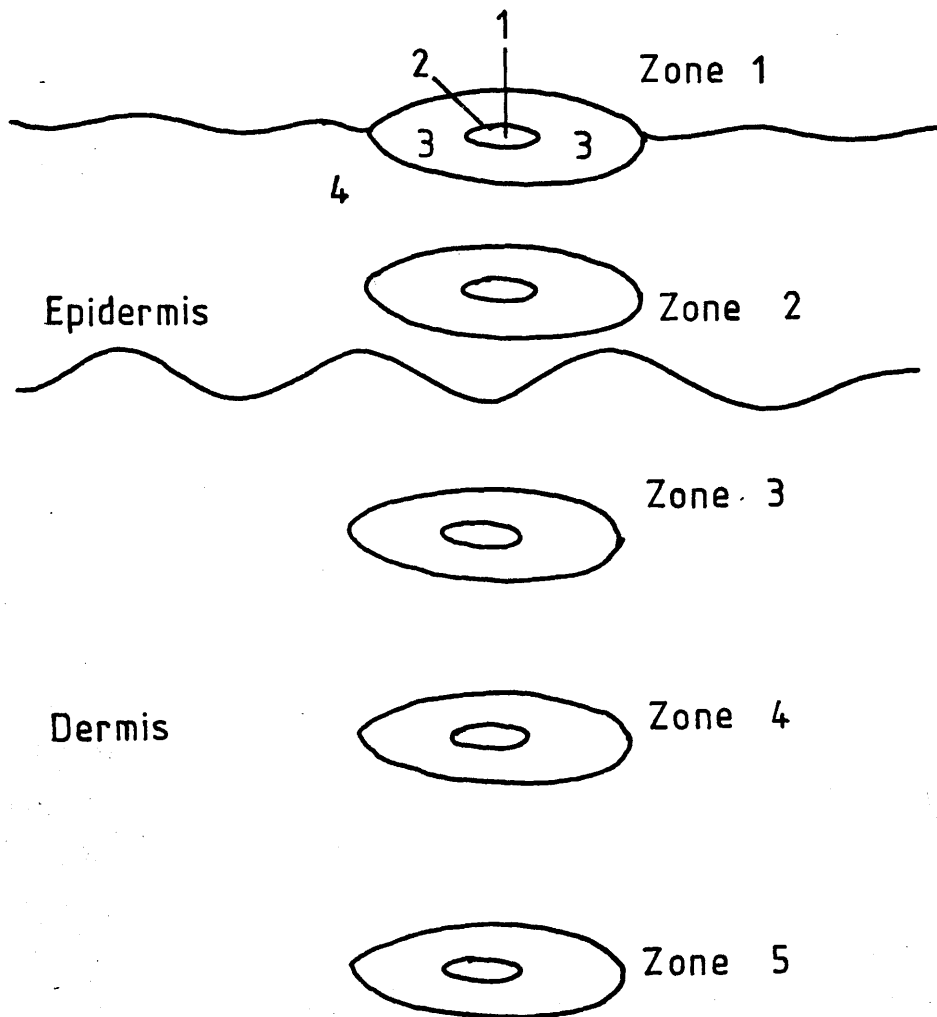
Fig.A.9.1 Schematic diagram showing the 5 levels and 4 regions of the rat footpad sweat gland that were examined by EPXMA after a course of treatment with an aluminium-containing antiperspirant.

Region 1 - luminal contents

2 - luminal edge

3 - cytoplasm

4 - stratum corneum



APPENDIX 10 RESULTS OF THE PRELIMINARY STUDY OF
ANTIPERSPIRANT ACTION ON THE RAT FOOTPAD

With both treatments extensive areas of the pads were covered in a dark electron-opaque "carpet". This "carpet" which must, in view of the method, be a precipitate contained a high concentration of aluminium. Spectra recorded 1 μ m into the stratum corneum demonstrated the presence of aluminium in a lower concentration and at a depth of 2 μ m the level of aluminium was barely above the background (Fig.A.10.1).

The effects of both compounds were essentially identical in all zones where measurements were made.

Zone 1 With both treatments, "Body Mist" and ACH, distinctly measurable quantities of aluminium were recorded at the luminal edge of the gland (Fig.A.10.2.). Some, but not all, ducts treated with ACH contained large electron-opaque deposits, containing appreciable quantities of aluminium (Fig.A.10.2.), lining and almost blocking the lumen which contained. Although no precipitate was detected within the glands after "Body Mist" treatment there was evidence of aluminium in the lumen. Aluminium could not be detected in the fibrocyte sheath of the duct or in the surrounding stratum corneum.

Zone 2 There was no evidence of aluminium in the epidermal cells surrounding the duct and there was no clear evidence of aluminium peaks significantly greater than the background in the fibrocyte sheath. However, aluminium was detected in a low level at the luminal border and occasionally in the lumen.

Zones 3, 4 & 5 In most instances it was impossible to distinguish aluminium peaks from background, however, in a few samples, small but apparently distinct peaks could be obtained from all four regions examined. These peaks were not found during control measurements from the supporting film and suggest the presence of trace amounts of aluminium.

Fig.A.10.1. X-ray spectra recorded from a) the surface, b) 1 μ m from the surface and c) 2 μ m from the surface of the rat footpad after the application of antiperspirant as described in Appendix 9. Note the different y-axis scales.

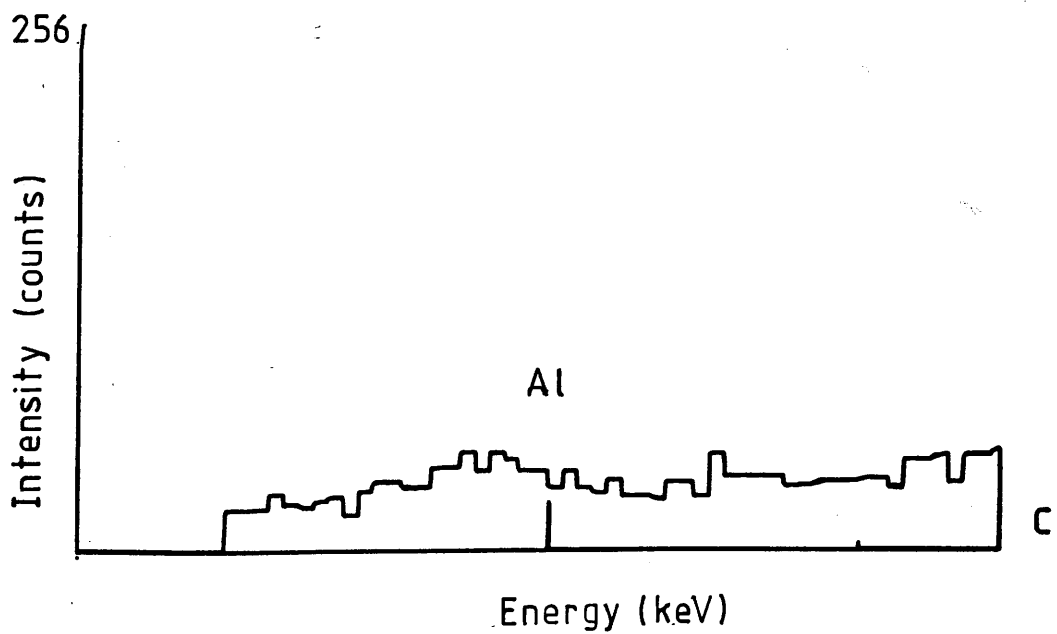
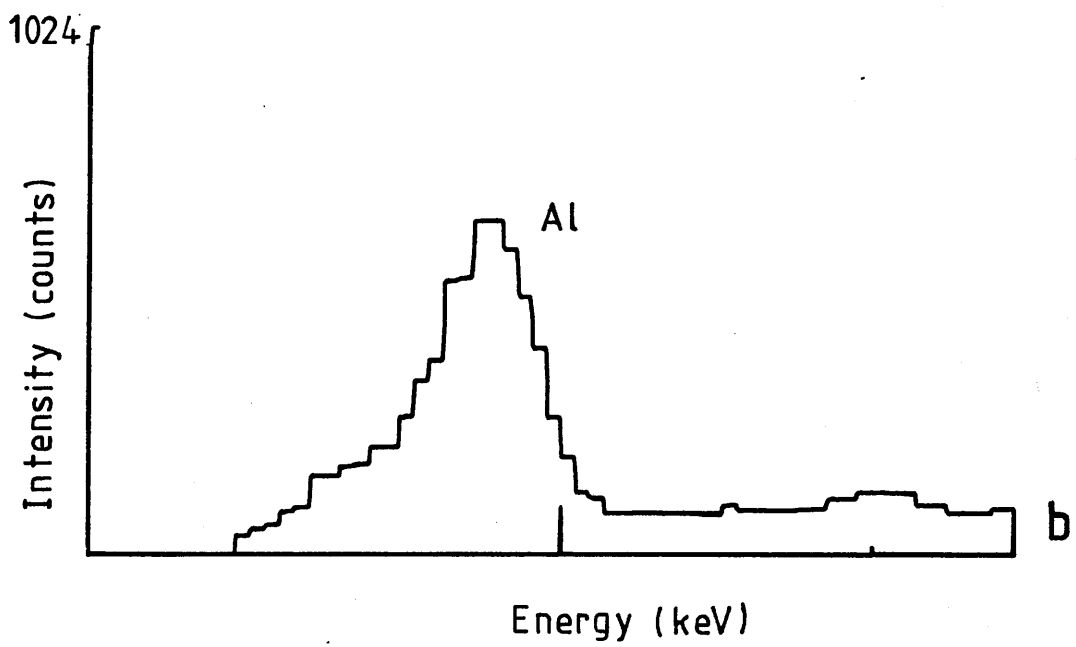
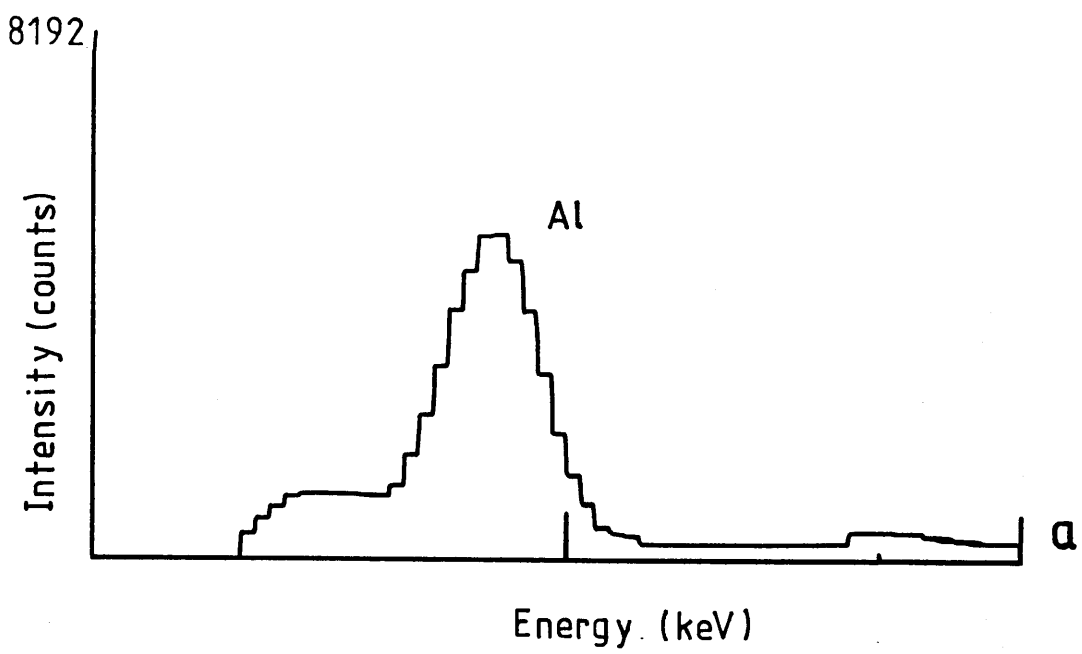
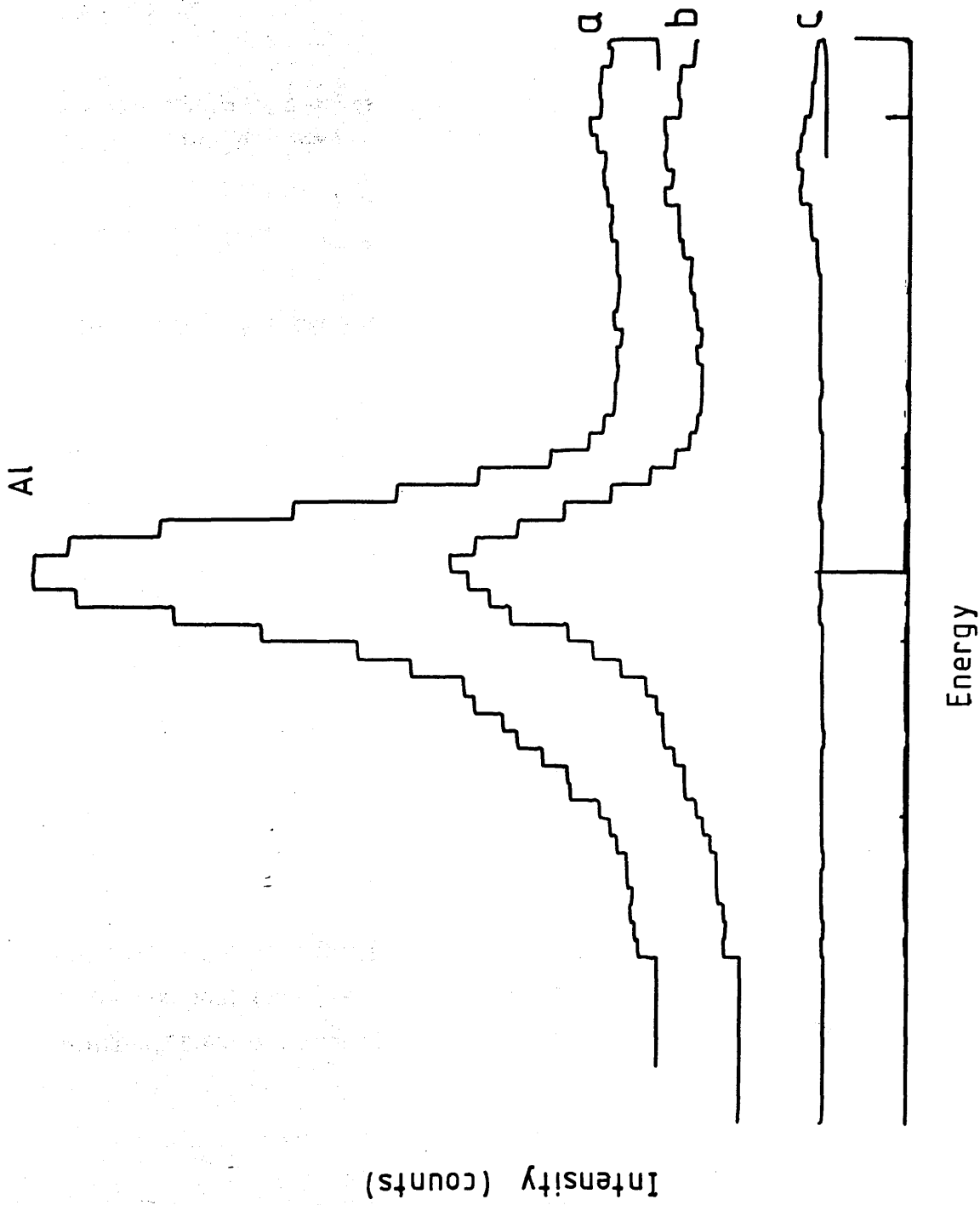


Fig.A.10.2. Typical X-ray spectra recorded from a rat sweat gland in the upper epidermis which contained electron-opaque luminal material. a) luminal contents, b) luminal edge, c) surrounding Formvar film.



Publications

Biddlecombe, W.H., Jenkinson, D.McE., McWilliams, S.A., Nicholson, W.A.P., Elder, H.Y. & Dempster, D.W. (1982) Preparation of cryosections with a modified Sorvall MT2B ultramicrotome and cryoattachment. *J.Microsc.*, **126**, 63-75.

Biddlecombe, W.H., Elder, H.Y., Jenkinson, D.McE., McWilliams, S.A. & Nicholson, W.A.P. (1982) A system for quantitative X-ray microanalysis of diffusible tissue substances in the (scanning) transmission electron microscope. *J.Physiol.*, **329**, 5P.

McWilliams, S.A., Elder, H.Y. & Jenkinson, D.McE. (1984) X-ray microanalytical studies of Na, K and Cl levels in resting and active human sweat glands. *Br.J.Derm.*, **111**, 719.

Elder, H.Y., Jenkinson, D.McE., McWilliams, S.A. & Wilson, S.M. (1985) Intracellular concentrations of sodium, phosphorus, chlorine and potassium in the ductal epithelium of unstimulated and active equine sweat glands. *J.Physiol.*, **367**, 74P.

McWilliams, S.A., Montgomery, I., Elder, H.Y. & Jenkinson, D.McE. (1985) Effects of pilocarpine stimulation on the ultrastructure and intracellular electrolyte composition of rat plantar sweat gland secretory coil. *Br.J.Derm.*, **113**, 792-793.

Elder, H.Y., Jenkinson, D.McE., McWilliams, S.A. & Wilson, S.M. (1986) Changes in the composition of the secretory epithelium of the equine sweat gland which accompany secretion *in vivo*. *J.Physiol.*, **372**, 79P.

SUPPLEMENT

Original data for the three intracellular sites analysed

Data are given as percentage absolute mass fractions \pm S.D.

n= number of spectra

a, b and c denote more than one fundus/duct analysed from each animal

For the 1 Pilo. rat number 1 the subcellular location could not be confirmed and spectra were accumulated from the general cytoplasm.

Example of the derivation of the values given in this thesis

Original data for rat footpad study of the three intracellular sites.

a) Na

Treatment	Juxta-luminal	Perinuclear	Basal
Control 1	.171±.118 (10)	.157±.075 (10)	----
2	.021±.029 (10)	.003±.009 (10)	.069±.036 (9)
3	.167±.066 (10)	.155±.089 (10)	.199±.054 (8)
4	.126±.085 (9)	.164±.095 (10)	.196±.069 (8)
Saline 1	.374±.066 (10)	.337±.07 (10)	.435±.061 (9)
2	.142±.085 (10)	.182±.105 (10)	.122±.085 (10)
3	.186±.06 (10)	.077±.065 (10)	.146±.077 (10)
4	.133±.099 (10)	.129±.076 (10)	.098±.092 (10)
1 Pilo 1	.24±.107 (15)		
2	.279±.071 (10)	.275±.089 (10)	.286±.079 (6)
3	.29±.086 (10)	.282±.128 (10)	.343±.088 (7)
4	.292±.074 (10)	.305±.045 (10)	.286±.048 (8)
3 Pilo 1	.349±.126 (10)	.339±.199 (10)	.348±.113 (10)
2	.202±.067 (10)	.179±.053 (9)	.116±.08 (9)
3	.167±.149 (10)	.16±.113 (10)	.116±.125 (8)
4	.415±.097 (10)	.305±.209 (10)	.378±.163 (9)

b) K

Treatment	Juxta-luminal	Perinuclear	Basal
Control 1	.945±.089 (10)	.932±.04 (9)	----
2	.694±.108 (10)	.749±.136 (10)	.676±.072 (10)
3	.937±.074 (10)	.846±.053 (10)	.86±.086 (10)
4	.824±.071 (9)	.777±.079 (10)	.771±.054 (8)
Saline 1	1.007±.063 (10)	.951±.061 (10)	1.016±.139 (9)
2	.766±.08 (10)	.7±.04 (10)	.619±.125 (10)
3	.774±.128 (10)	.71±.08 (10)	.745±.116 (10)
4	.789±.079 (10)	.813±.114 (10)	.694±.106 (10)
1 Pilo 1	.327±.08 (15)		
2	.41±.062 (10)	.44±.065 (10)	.373±.046 (6)
3	.744±.046 (10)	.783±.063 (10)	.737±.038 (7)
4	.406±.027 (10)	.4±.026 (10)	.37±.02 (8)
3 Pilo 1	.965±.079 (10)	.99±.092 (10)	.878±.065 (10)
2	.384±.034 (10)	.329±.052 (9)	.31±.05 (9)
3	.498±.124 (10)	.446±.043 (10)	.434±.105 (8)
4	.5±.056 (10)	.431±.052 (10)	.413±.083 (9)

c) CI

Control	1	.276± .079 (10)	.239± .058 (9)	----
	2	.28± .038 (10)	.291± .056 (10)	.25± .053 (10)
	3	.202± .057 (10)	.239± .052 (10)	.208± .039 (10)
	4	.29± .046 (9)	.266± .053 (10)	.286± .036 (8)
Saline	1	.27± .024 (10)	.269± .024 (10)	.341± .042 (9)
	2	.194± .046 (10)	.192± .041 (10)	.252± .071 (10)
	3	.279± .05 (10)	.225± .046 (10)	.3± .106 (10)
	4	.104± .054 (10)	.102± .055 (10)	.161± .087 (10)
1 Pilo	1		.406± .12 (15)	
	2	.209± .031 (10)	.148± .06 (10)	.25± .093 (6)
	3	.145± .046 (10)	.141± .04 (10)	.222± .102 (7)
	4	.184± .034 (10)	.168± .028 (10)	.185± .063 (8)
3 Pilo	1	.32± .037 (10)	.275± .034 (10)	.321± .141 (10)
	2	.238± .054 (10)	.155± .032 (9)	.204± .047 (9)
	3	.224± .08 (10)	.164± .079 (10)	.193± .08 (8)
	4	.183± .053 (10)	.186± .043 (9)	.305± .152 (9)

Original data for the human study of three intracellular sites

FUNDUS Unstimulated

a) Na

Subject	Juxta-luminal	Perinuclear	Basal
1	.545±.27 (10)	.481±.235 (10)	.493±.259 (10)
2a	.679±.255 (10)	.755±.459 (10)	.752±.387 (10)
2b	.252±.137 (10)	.431±.182 (10)	.362±.203 (10)
3	.501±.239 (10)	.681±.228 (10)	.523±.208 (8)
4	.358±.256 (10)	.594±.16 (10)	.596±.333 (9)
5	.572±.209 (10)	-----	.512±.171 (10)
6	.437±.055 (10)	.39±.034 (10)	.424±.074 (10)
7	.292±.177 (10)	.25±.155 (10)	.406±.133 (8)
8	.507±.091 (9)	.271±.13 (10)	.2±.122 (8)

b) K

Subject	Juxta-luminal	Perinuclear	Basal
1	.593±.048 (10)	.81±.24 (10)	.692±.154 (10)
2a	.402±.088 (10)	.515±.069 (10)	.597±.158 (10)
2b	.726±.114 (10)	.824±.146 (10)	.885±.063 (10)
3	.71±.097 (10)	.79±.13 (10)	.814±.334 (9)
4	.51±.12 (10)	.467±.06 (10)	.534±.104 (9)
5	.932±.172 (10)	-----	.963±.203 (10)
6	.992±.139 (10)	.926±.087 (10)	.93±.1 (10)
7	.713±.051 (10)	.781±.056 (10)	.774±.08 (10)
8	.561±.044 (10)	.712±.093 (10)	.663±.042 (8)

c) Cl

Subject	Juxta-luminal	Perinuclear	Basal
1	.829±.209 (10)	.796±.322 (10)	.979±.27 (10)
2a	1.078±.222 (10)	1.016±.239 (10)	1.457±.479 (10)
2b	.912±.144 (10)	.924±.147 (10)	1.38±.363 (10)
3	.852±.076 (10)	.893±.213 (10)	1.068±.413 (9)
4	.704±.111 (10)	.733±.124 (10)	.994±.309 (9)
5	.848±.118 (10)	-----	.78±.178 (10)
6	.499±.078 (10)	.452±.027 (10)	.464±.105 (10)
7	.381±.06 (10)	.383±.095 (10)	.44±.139 (10)
8	.571±.09 (10)	.554±.092 (10)	.663±.139 (10)

Original data for the human study of three intracellular sites

FUNDUS Stimulated

a) Na

Subject	Juxta-luminal	Perinuclear	Basal
1a	.33±.087 (10)	-----	.305±.108 (9)
1b	.682±.099 (10)	.87±.272 (10)	.721±.11 (10)
1c	.474±.157 (10)	.329±.158 (10)	.437±.173 (10)
2a	.425±.199 (10)	.47±.179 (9)	.754±.194 (10)
2b	.617±.171 (10)	.545±.179 (10)	.701±.136 (9)
3a	.928±.332 (10)	.868±.265 (10)	.711±.207 (10)
3b	.176±.167 (10)	.414±.196 (10)	.576±.27 (10)
4	.746±.196 (10)	.605±.233 (10)	.742±.142 (9)
5	.67±.233 (10)	-----	.453±.138 (9)
6a	.435±.275 (10)	.481±.279 (10)	.537±.321 (10)
6b	.73±.367 (10)	-----	.694±.272 (10)
7a	.916±.211 (10)	.722±.287 (10)	1.049±.27 (5)
7b	.479±.317 (10)	.253±.18 (10)	.409±.164 (10)
9	.911±.284 (10)	.825±.226 (10)	.677±.224 (10)
10	.473±.132 (10)	.389±.18 (10)	.324±.174 (10)
11	.507±.268 (10)	.844±.22 (6)	1.1±.24 (10)
12a	.781±.189 (10)	-----	.802±.132 (10)
12b	.62±.152 (10)	.655±.193 (10)	.618±.096 (10)

b) K

Subject	Juxta-luminal	Perinuclear	Basal
1a	.223±.026 (10)	-----	.23±.113 (9)
1b	.610±.075 (10)	.762±.147 (10)	.726±.102 (10)
1c	.392±.078 (10)	.463±.044 (10)	.477±.068 (10)
2a	.51±.064 (10)	.651±.155 (10)	.545±.087 (10)
2b	.758±.122 (10)	.659±.076 (10)	.659±.057 (9)
3a	.448±.061 (10)	.473±.063 (10)	.436±.052 (10)
3b	.512±.075 (10)	.664±.155 (10)	.556±.109 (10)
4	.467±.132 (10)	.728±.183 (10)	.375±.259 (9)
5	.263±.089 (10)	-----	.167±.051 (9)
6a	.29±.084 (10)	.327±.086 (10)	.352±.059 (10)
6b	1.01±.25 (10)	-----	1.014±.167 (9)
7a	1.0±.089 (10)	1.096±.226 (10)	1.021±.159 (5)
7b	.41±.099 (10)	.397±.089 (10)	.4±.078 (10)
9	.779±.198 (10)	.651±.097 (10)	.719±.196 (10)
10	.645±.059 (10)	.787±.064 (10)	.691±.062 (10)
11	.181±.034 (10)	.163±.062 (6)	.192±.041 (10)
12a	.307±.076 (10)	-----	.294±.037 (10)
12b	.441±.08 (10)	.452±.07 (10)	.403±.026

Original data for the human study of three intracellular sites

FUNDUS Stimulated

c) C1

Subject	Juxta-luminal	Perinuclear	Basal
1a	.809±.139 (10)	-----	.93±.3 (9)
1b	.959±.187 (10)	1.028±.163 (9)	1.03±.244 (10)
1c	.76±.095 (10)	.699±.187 (10)	1.035±.24 (10)
2a	.733±.082 (10)	.729±.072 (10)	1.066±.165 (10)
2b	.719±.115 (10)	.627±.127 (10)	1.057±.472 (9)
3a	1.078±.217 (10)	1.042±.244 (10)	1.027±.119 (10)
3b	.859±.179 (10)	.859±.106 (10)	.816±.152 (8)
4	.745±.136 (10)	.63±.147 (10)	.959±.161 (8)
5	.835±.182 (9)	-----	.649±.101 (9)
6a	.401±.074 (10)	.403±.092 (10)	.585±.218 (10)
6b	.463±.146 (10)	-----	.504±.173 (10)
7a	.645±.07 (10)	.632±.124 (10)	.691±.046 (5)
7b	.477±.107 (10)	.409±.1 (10)	.482±.092 (10)
9	.965±.139 (10)	.891±.166 (10)	1.037±.136 (10)
10	.291±.061 (10)	.318±.054 (10)	.33±.049 (10)
11	.956±.382 (10)	1.247±.218 (6)	1.35±.254 (9)
12a	.359±.1 (10)	-----	.395±.21 (10)
12b	.576±.105 (10)	.742±.149 (10)	.726±.075 (10)

Original data for the human study of three intracellular sites

Duct Unstimulated

a) Na

Subject	Juxta-luminal	Perinuclear	Basal
1	.523±.074 (10)	.551±.076 (10)	.438±.083 (10)
2	.873±.326 (10)	.757±.39 (10)	1.015±.21 (9)
3	.878±.187 (10)	-----	.768±.274 (10)
4	.293±.15 (10)	.256±.065 (8)	.318±.113 (8)
5	1.047±.286 (10)	.931±.116 (10)	.831±.252 (10)
6	.816±.201 (10)	.72±.205 (10)	.708±.217 (10)

b) K

Subject	Juxta-luminal	Perinuclear	Basal
1	.579±.118 (10)	.539±.082 (10)	.597±.064 (10)
2	.457±.079 (10)	.515±.117 (9)	.566±.125 (10)
3	.984±.191 (10)	-----	.852±.167 (10)
4	.385±.041 (10)	.448±.04 (8)	.41±.022 (8)
5	.326±.062 (10)	.336±.057 (10)	.323±.098 (10)
6	.105±.031 (10)	.142±.026 (10)	.104±.021 (10)

c) Cl

Subject	Juxta-luminal	Perinuclear	Basal
1	.48±.122 (10)	.444±.064 (10)	.513±.042 (10)
2	.902±.145 (10)	.958±.223 (10)	.957±.364 (10)
3	.81±.216 (10)	-----	.652±.216 (10)
4	.556±.102 (10)	.619±.083 (8)	.63±.095 (8)
5	.7±.13 (10)	.711±.097 (10)	.735±.162 (10)
6	.521±.064 (10)	.566±.138 (10)	.809±.12 (10)

Original data for the human study of three intracellular sites

Duct Stimulated

a) Na

Subject	Juxta-luminal	Perinuclear	Basal
1a	.597±.226 (10)	.692±.223 (10)	.748±.126 (9)
1b	.707±.286 (10)	.858±.189 (10)	.713±.234 (10)
2	1.14±.335 (10)	1.238±.281 (10)	1.147±.226 (10)
3a	1.578±.238 (10)	1.384±.477 (10)	1.218±.302 (10)
3b	.987±.242 (10)	.824±.389 (10)	.921±.447 (10)
5a	.701±.233 (10)	.427±.245 (10)	.308±.237 (10)
5b	.735±.277 (10)	-----	.623±.215 (10)
6a	.273±.154 (10)	.25±.169 (10)	.087±.121 (10)
6b	.626±.165 (10)	.822±.15 (10)	.734±.145 (10)
7	.391±.221 (10)	.311±.199 (10)	.251±.198 (5)

b) K

Subject	Juxta-luminal	Perinuclear	Basal
1a	.257±.05 (10)	.326±.155 (9)	.254±.042 (9)
1b	.588±.047 (10)	.581±.059 (10)	.565±.03 (10)
2	.219±.086 (10)	.27±.024 (10)	.274±.045 (10)
3a	.719±.189 (10)	.639±.182 (10)	.485±.06 (10)
3b	.176±.023 (10)	.191±.055 (10)	.222±.096 (10)
5a	.583±.141 (10)	.648±.086 (10)	.632±.157 (10)
5b	.437±.116 (10)	-----	.452±.087 (10)
6a	.595±.049 (10)	.583±.39 (10)	.564±.06 (10)
6b	.069±.031 (10)	.072±.009 (10)	.06±.014 (10)
7	.361±.042 (10)	.43±.05 (10)	.415±.048 (10)

c) Cl

Subject	Juxta-luminal	Perinuclear	Basal
1a	.612±.089 (10)	.693±.17 (10)	.819±.138 (9)
1b	.558±.051 (10)	.518±.076 (10)	.565±.068 (10)
2	.672±.096 (10)	.743±.109 (10)	.796±.113 (10)
3a	1.454±.276 (10)	1.271±.251 (10)	1.184±.136 (10)
3b	.954±.118 (10)	.942±.193 (10)	1.052±.258 (10)
5a	.326±.063 (10)	.319±.108 (10)	.443±.087 (10)
6a	.344±.061 (10)	.323±.046 (10)	.332±.093 (10)
6b	.667±.067 (10)	.695±.09 (10)	.699±.098 (10)
7	.481±.07 (10)	.413±.041 (10)	.403±.118 (5)

Specimen calculation

The expanded form of the quantitation equation used in this thesis is shown below.

$$C_x = A_x \frac{(n_x/n_w)_{\text{spec}}}{(n_x/n_w)_{\text{stan}}} \frac{N_x}{NZ^2_{\text{stan}}} (Z^2/A)_{\text{spec}}$$

Where C_x = concentration of element x as a mass fraction of the analysed volume

A_x = atomic wt.

The ratios n_x/n_w are the peak to background ratios for the element in the specimen and standard

Using the standard data given in Table 3.1 and using a Z^2/A value of 3.28 (approx. biological tissue) the equation only requires the peak to background ratio for the specimen.

For potassium a typical peak to background ratio was 0.28, calculated as described in Chapter 3. this gives an absolute mass fraction of element of .0039 or .39%.

To calculate the mMol/kg concentrations it is assumed that the resin replaces the water originally in the specimen. It therefore follows that .39% potassium is equivalent to 3.9grams per 1000grams of analysed tissue i.e. approximately 100mMoles per kg dry weight. It should be remembered that the dry weight is composed of approx. 25% biological tissue and 75% embedding medium. The appropriate correction factor for mass loss can then be applied as described in Appendix 3

GLASGOW
UNIVERSITY
LIBRARY